# MICRORNA-REGULATED MOLECULAR MECHANISMS IN CEREBRAL ISCHEMIA

**TAN JUN RONG**

**NATIONAL UNIVERSITY OF**

**SINGAPORE**

**2015**

# MICRORNA-REGULATED MOLECULAR MECHANISMS IN CEREBRAL ISCHEMIA

**TAN JUN RONG**

(*B.Sc(Hons), NUS*)

**A THESIS SUBMITTED**

**FOR THE DEGREE OF DOCTOR OF PHILOSOPHY**

**DEPARTMENT OF BIOCHEMISTRY**

**NATIONAL UNIVERSITY OF SINGAPORE**

**2015**

**DECLARATION**

I hereby declare that this thesis is my original work and it has been written by me in its entirety. I have duly acknowledged all the sources of information which have been used in the thesis.

This thesis has also not been submitted for any degree in any university previously.

_____

TAN JUN RONG

09 March 2015

**Acknowledgement**

Firstly, I would like to thank my main supervisor, Professor Kandiah Jeyaseelan for his support, patience and guidance throughout these years. I am very grateful for his timely advice during the course of my study. I have obtained much knowledge from my interaction with him and I would not have come thus far if not for his tutelage and support.

I would also like to thank my co-supervisor, Professor Peter Wong for his support and assistance throughout my PhD program. His gracious assistance and timely advice through the years are very much appreciated.

I am thankful to Dr Arunmozhiarasi Armugam for her guidance and encouragement throughout the course of my study. I am very grateful for her encouragement and help rendered at the critical periods of my project. I have learnt invaluable skills and gained extensive experience from her, which I am very grateful for.

I would like to extend my gratitude to Professor Tan Kay Sin, Professor Wang Chee Woon and Ms Yong Fung Lin for the patient samples obtained from UMMC, that contributed substantially to my project. I would also like to thank Professor Tan Kay Sin for his fruitful discussions and suggestions to compile and interpret the clinical data presented in this thesis.

Not forgetting the past and present members of the laboratory, from whom I have learnt various skills. I would like to thank Dr Lim Kai Ying and Dr Liu Fujia for their indispensible help with the animal model experiments. I would also like to thank Ms Chai Siaw Ching for helping me to get accustom to the laboratory when I first came. I would also like to thank other members of the laboratory, Dr Sugunavathi Sepramaniam, Dr Karolina Dwi Setyowati, Mr Karthikeyan Chandrasekaran, Ms Priyadharshni Swaminathan, Ms Prameet Kaur and Mr Silambarasan Maskomani for their constant help and support throughout my candidature.

I will also like to thank my good friends who have been with me since the beginning of my candidature, and for their encouragement whenever I am faced with difficulties in moving forward with my research.

Finally I would like to dedicate this work for my parents who allowed me to embark on this journey. They have silently supported me throughout this study and cared for me whenever I am down. They have sacrificed much for me throughout this study and I am eternally grateful to have my parents' understanding and support.

"No man is an island"

John Donne, Meditation XVII

## Table of Contents

**Summary**

Stroke is a major cause of death and disability worldwide, of which ischemic stroke accounts for 87% of all stroke cases. Its impact on society and economy is extensive and profound. This drives translational stroke research discoveries for new biomarkers and treatments. However, translational stroke research is still in its infancy and requires greater understanding of the pathophysiology and pathogenesis of ischemic stroke. Circulating miRNAs were used as a surrogate marker to study mechanisms in ischemic stroke patients. Changes in miRNA expression were studied in rat MCAo model and in ischemic stroke patients. miRNA microarray was used as a high-throughput method to screen the entire microRNome for dysregulated miRNAs in the shortest possible time.

miRNA profiles obtained were analysed to identify ischemic stroke specific miRNAs as well as miRNAs that were specific for ischemic stroke subtype. These clusters contained known associated miRNAs as well as novel miRNAs. Furthermore, pathway analysis revealed biological pathways associated with inflammation, cell death, vascular maintenance, metabolism and neuronal signaling and development were dysregulated during ischemic stroke in patients and animal model. These biological pathways included ones previously reported, and also new pathways thath were never shown any association with ischemic stroke till now. It was inferred from the results that neuroinflammation is a critical process in the pathophysiology of ischemic stroke and in the pathogenesis of ischemic stroke subtypes. Among the biological pathways, complement and coagulation cascades were identified to be specific for cardioembolic stroke, a stroke subtype with high mortality rate. *CD46*, an inhibitor of complement activation, was previously reported to be

able to distinguish cardioembolic stroke from large artery stroke. Using bioinformatics and experimental data, miR-19a, -20a, -185 and -374b were predicted to target *CD46*, which were verified using Luciferase assay. These miRNAs were shown to have differential expression between cardioembolic stroke vs large artery and small vessel stroke. Thus, demonstating the new miRNAs interacting with *CD46* may act as potential biomarkers for cardioembolic stroke. In addition, chemokine signaling pathway, also associated with neuroinflammation was found to be highly ranked in all the pathway analysis. Chemokine *CCL2* previously reported to be dysregulated in ischemic stroke was studied. mRNA expression in rat correlated with infarct volume, and protein expression in human patients showed positive correlation with outcome. Hence, searching for miRNA targeting *CCL2* may also be useful as biomarkers or therapeutic targets in stroke.

Hence, this study discovered the crucial mechanisms underlying ischemic stroke pathophysiology and highlighted clusters of miRNAs which may act as potential biomarkers for ischemic stroke diagnosis as well as stroke subtype diagnosis.

422 words

## List of tables

## List of figures

## Abbreviations

| | |
|---|---|
| A&E | accident and emergency |
| APS | Ammonium persulfate |
| bp | base pair |
| CCL2 | chemokine CC motif ligand 2 |
| CCL5 | chemokine CC motif ligand 5 |
| CD46 | cluster of differentiation 46 |
| cDNA | complementary deoxyribonucleic acid |
| CE | cardioembolic stroke |
| CIP | calf intestinal phosphatase |
| CXCL1 | chemokine CXC motif ligand 1 |
| CT | computed tomography |
| DMEM | Dulbecco's modified eagle medium |
| DMSO | Dimethyl sulfoxide |
| DNase I | deoxyribonuclease I |
| dNTP | deoxy-nucleotide-tri phosphate |
| *E. coli* | *Escherichia coli* |
| EDTA | Ethylenediaminetetraacetic aicd |
| FDR | false discovery rate |
| g | gram |
| HbA1c | haemoglobin A1c |
| HCL | hierarchical clustering |
| HDL | high density lipoprotein |
| hr | hour |
| L | liter |
| LA | large artery stroke |
| LDL | low density lipoprotein |
| LNA | locked-nucleic-acid |
| M | molar |

| | |
|---|---|
| MCAo | middle cerebral artery occlusion |
| $MgCl_2$ | Magnesium chloride |
| mg | milligram |
| ml | milliliter |
| min | minute |
| µg | microgram |
| µl | microliter |
| miRNA(s) | microRNA(s) |
| mM | millimolar |
| mmHg | millimetre of mercury |
| mmol | millimole |
| MOPS | morpholinopropanesulphonic acid |
| MRI | magnetic resonance imaging |
| mRNA | messenger RNA |
| mRS | modified Rankin score |
| NaCl | Sodium chloride |
| ND | not detected |
| ng | nanogram |
| nM | nanomolar |
| OD | optical density |
| PAGE | polyacrylamide gel electrophoresis |
| PBS | phosphate buffered saline |
| PCA | principal component analysis |
| PCR | polymerase chain reaction |
| RISC | RNA-induced silencing complex |
| RNA | ribonucleic acid |
| Rnase | ribonuclease |
| rpm | revolutions per minute |
| RT | reverse transcription |

| | |
|---|---|
| SD | standard deviation |
| SDS | Sodium dodecyl sulphate |
| SEM | standard error of mean |
| SLR | signal logarithm ratio |
| SV | small vessel stroke |
| TEMED | N,N,N’,N’-Tetramethylethylenediamine |
| Tris | hydroxymethylaminomethane |
| TTC | 2,3,5-triphenyltetrazolium chloride |
| U | unit(s) |
| UTR | untranslated region |
| V | volt |

## List of publications

1. **Tan JR**, Tan KS, Koo YX, Yong FL, Wang CW, Armugam A, Jeyaseelan K. Blood microRNAs in Low or No Risk Ischemic Stroke Patients. *Int J Mol Sci*. 2013, **14**(1):2072-2084. doi: 10.3390/ijms14012072.

2. **Tan JR**, Koo YX, Kaur P, Liu F, Armugam A, Wong PT, Jeyaseelan K. microRNAs in stroke pathogenesis. *Curr Mol Med*. 2011, **11**(2):76-92. Review

3. Sepramaniam S, **Tan JR**, Tan KS, DeSilva DA, Tavintharan S, Woon FP, Wang CW, Yong FL, Karolina DS, Kaur P, Liu FJ, Lim KY, Armugam A, Jeyaseelan K. Circulating microRNAs as biomarkers of acute stroke. *Int J Mol Sci*. 2014, **15**(1):1418-1432. doi: 10.3390/ijms15011418.

4. Kaur P, Liu F, **Tan JR**, Lim KY, Sepramaniam S, Karolina DS, Armugam A, Jeyaseelan K. Non-Coding RNAs as Potential Neuroprotectants against Ischemic Brain Injury. *Brain Sci*. 2013, **3**(1):360-395. doi: 10.3390/brainsci3010360. Review

5. Lim KY, Chua JH, **Tan JR**, Swaminathan P, Sepramaniam S, Armugam A, Wong PT, Jeyaseelan K. MicroRNAs in Cerebral Ischemia. *Transl Stroke Res*. 2010, **1**(4):287-303. doi: 10.1007/s12975-010-0035-3.

6. Sepramaniam S, Armugam A, Lim KY, Karolina DS, Swaminathan P, **Tan JR**, Jeyaseelan K. MicroRNA 320a functions as a novel endogenous modulator of aquaporins 1 and 4 as well as a potential therapeutic target in cerebral ischemia. *J Biol Chem*. 2010, **285**(38):29223-29230. doi: 10.1074/jbc.M110.144576.

## List of conference abstracts

1. **Tan JR**, Lim KY, Karolina DS, Sepramaniam S, Armugam A, Wong TH, Jeyaseelan K. MicroRNAs Regulating Inflammatory Pathways in Ischemic Stroke. Poster session presented at: Gordon Research Conference. 2013 Jun 2-7; University of New England, Biddeford, ME, US

2. **Tan JR**, Sepramaniam S, Armugam A, Jeyaseelan K. Blood MicroRNA Expression during Acute Phase of Ischemic Stroke. Poster session presented at: Biochemistry 5th Student Symposium. 2012 Sep 27; National University of Singapore, Singapore

3. Jeyaseelan k, Lim KY, Armugam A, **Tan JR**, Koo YX, Tan KS, Wang CW, Seet RC, Chan BP, Sharma VK, Teoh HL, Venketasubramanian Ramani N, Chen CL, Yim EK, Ong WY, Chuang KH, Wong PT. MicroRNAs as Biomarkers in Stroke Pathogenesis. Poster session presented at: 14th Congress of the European Federation of Neurological Societies. 2010 Sep 25-28; Geneva, Switzerland

# Chapter 1

# Introduction

## 1.1 Stroke

Stroke is the second leading cause of death and the leading cause of disability worldwide [1, 2]. In 2005, it was estimated that 16 million cases of first-time stroke and 5.7 million deaths resulting from stroke [3]. In past decade, the annual mortality due to stroke has been on the rise. In 2000, stroke accounts for 5.6 million deaths worldwide, by 2011, the number had risen to 6.2 million, which contributes to 11.4% of deaths worldwide in 2011 [3].

Stroke has a profound effect on the socioeconomic status of the patients, the immediate families and even the world. Stroke patients suffer from disabilities and become dependent on their immediate families. In addition, the medical cost is an immense burden on the family. In the United States of America, the average lifetime cost for stroke is USD$140,048 and in 2010 the total cost of stroke was a massive USD$36.5 billion [4].

Stroke is a disorder resulting from an occlusion or rupture in the cerebral artery, that caused a lack of perfusion to affected area of the brain, manifesting as deficit in cerebral function [5]. Stroke can be classified into ischemic stroke (cerebral ischemia) or hemorrhagic stroke. Ischemic stroke accounts for 87% of all stroke cases while hemorrhagic stroke makes up the remaining 13% (Figure 1.1) [6, 7]. Ischemic stroke and hemorrhagic stroke can be further sub-classified into more subtypes based on the location or cause of the stroke. Ischemic stroke cases are generally classified according to the Trial of Org 10172 in Acute Stroke Treatment (TOAST) classification, where ischemic stroke cases can be classified as large artery atherosclerosis, cardioembolic, small-vessel occlusion or lacunar, other determined etiology and undetermined etiology [8]. As for hemorrhagic stroke cases, they are generally classified

intracerebral hemorrhage and subarachnoid hemorrhage [9]. Given that ischemic stroke contributes the majority of stroke cases, this project focuses on investigating ischemic stroke.

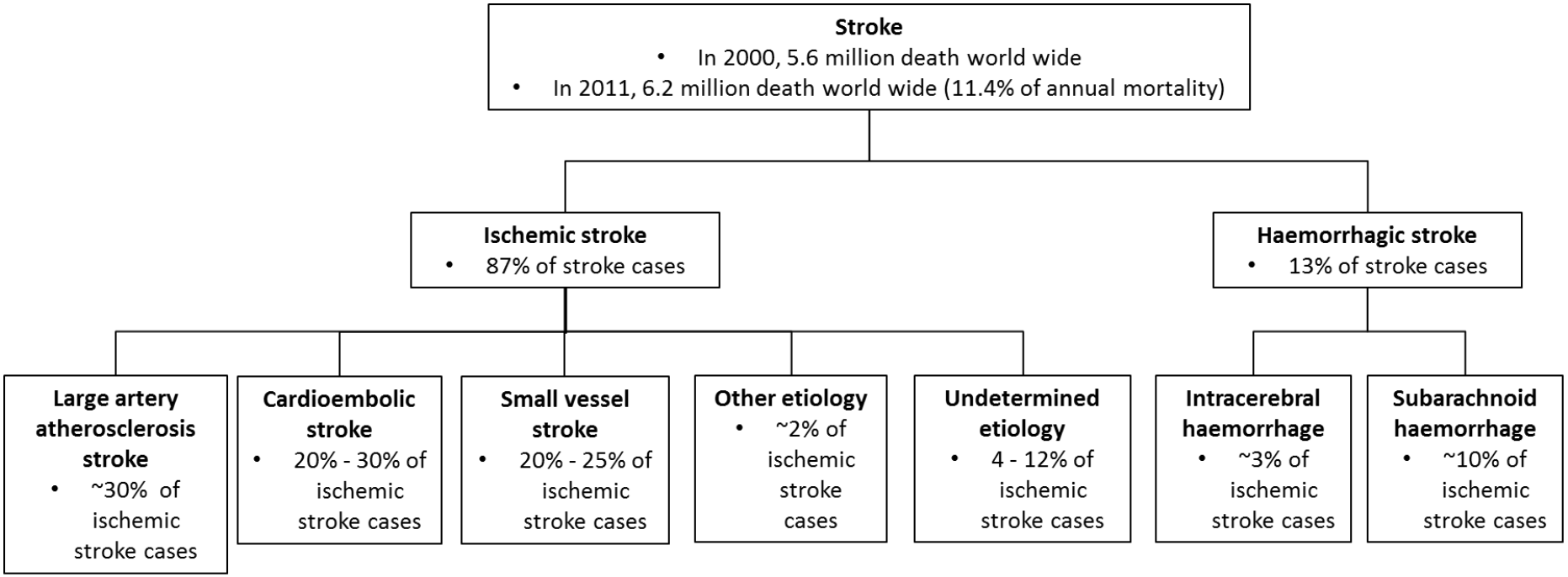


**Figure 1.1:** Stroke subtype and prevalence of each stroke subtype.

### 1.1.1 Ischemic stroke

Ischemic stroke is the disruption of blood flow to a part of the brain as a result of a blockage in cerebral vasculature [5]. The consequence of this is a devastating injury to the affected part of the brain as the blood supplying oxygen and glucose is cut off. Hence, the cells (mainly astrocytes and neurons) in the affected region die in response to the insult. The effect of this is manifested in the clinical presentation of symptoms such as decreasing level of consciousness, vomiting, seizures and weakness in limbs, all of which signify a decrease in cerebral function [9].

### 1.1.2 Ischemic stroke subtypes

The pathophysiology and pathogenesis of ischemic stroke are complex and heterogeneous. There can be more than 150 causes for ischemic stroke [10]. In general, ischemic stroke cases are classified according to the TOAST classification [8]. Some of the common ischemic stroke subtypes observed are large artery stroke (accounts for 30% - 50% of ischemic stroke in Asians and 10% of ischemic stroke in Caucasians), cardioembolic stroke (makes up 20% - 30% of ischemic stroke cases) and small vessel stroke (attributes to 20% - 25% of ischemic stroke cases; Figure 1.1). Large artery stroke is clinically defined as having major artery or branch cortical artery with >50% stenosis, with infarct ≥ 15mm in diameter and no cardioembolic source [8, 10]. Cardioembolic stroke can be characterized with patient having a cardioembolic source for blood clot with no atherosclerotic thromboembolic source [8, 10]. Small vessel stroke is determined as a traditional lacunar syndrome with no evidence of cerebral cortical dysfunction and with infarct <

15mm [8, 10]. The prevalent underlying pathologies that contribute to ischemic stroke onset are atherosclerosis and heart ailments [8, 9].

#### 1.1.2.1 Large artery and small vessel stroke

In large artery stroke and small vessel stroke, the blood clot typically originates from an atherosclerotic plaque present in the major cerebral artery or carotid artery [11]. Atherogenesis is the progressive buildup of atherosclerotic plaque, which is characterized by lipid accumulation in the tunica intima, inflammatory cell recruitment, smooth muscle cell proliferation and migration [12-14]. The atherosclerotic plaque develops and overtime stenosis of the blood vessel ensues [13, 14]. The atherosclerotic plaque can also become unstable and ruptures, which causes blood clotting to take place [15]. The blood clot formed can move along the circulation and obstructs any part of the cerebral circulation, resulting in cerebral infarction [15].

#### 1.1.2.2 Cardioembolic stroke

In the case of cardioembolic stroke, blood clot occluding cerebral circulation is of cardiac origins. Underlying cardiac ailments can result in the formation of blood clot in the heart which can be channeled to the brain, causing a blockage in cerebral circulation [16-17].

The most common cardiac comorbidity that results in ischemic stroke is atrial fibrillation, accounting for 50% of all cardioembolic stroke cases [16]. Atrial fibrillation is a form of cardiac arrhythmia, where the atria (upper chambers of the heart) contract in a rapid and irregular manner [18]. This disrupts the proper pumping of blood from the atria to the ventricles (lower chambers of

the heart), resulting in pooling of blood in the atria [19]. Blood stasis provides the condition for blood clot to form.

Other heart ailments contributing to cardioembolic stroke includes myocardial infarction. dilated cardiomyopathy and mitral valve stenosis [16]. Myocardial infarction is commonly known as heart attack that occurs when the coronary artery which supplies the heart becomes occluded, leading to cardiac injury due to lack of oxygen [20]. Dilated cardiomyopathy is a condition where the heart becomes enlarged and unable to pump blood efficiently [21]. This is due to previous damage to myocardium resulting in cardiac remodeling and heart enlargement [21]. Mitral valve stenosis is the narrowing of the mitral valve opening [22]. All these conditions result in areas of the heart having stagnant pool of blood which promote blood clotting [16]. Blood clot formed in the heart gets pumped into circulation reaching the brain, causing an obstruction in cerebral blood flow and ischemic stroke ensues.

### 1.1.3 Risk factors of ischemic stroke

Ischemic stroke is usually seen as a severe disease resulting from other pre-existing disorders. These other disorders are typically: hypertension, dyslipidemia and type 2 diabetes, which are considered to be risk factors for ischemic stroke, as they predispose an individual to ischemic stroke [23].

#### 1.1.3.1 Hypertension

Hypertension is defined as diastolic blood pressure >90 mmHg or systolic blood pressure >140 mmHg when measured at 2 or more times independently [24]. The increased blood pressure acting on the vessel wall triggered

hypertrophy in the vessel wall [25]. This leads to the stiffening and thickening of vessel wall, resulting the narrowing of the lumen. It has also been reported that hypertensive patients have decreased vascular tone due to the deficiency in endothelial nitric oxide (NO) production [26]. In addition, endothelial cells becomes activated from the increased blood pressure, resulting in the increased expression of cell adhesion molecules such as vascular cell adhesion molecule 1 (VCAM-1), intracellular adhesion molecule 1 (ICAM-1), P- and E-selectins [27]. This can aid in the monocytes and leukocytes to infiltrate the intima layer. These conditions pave the way for development of atherosclerotic plaque and ultimately ischemic stroke.

Similarly, hypertension also stresses on the cardiac muscles, this in turn causes the development of atrial fibrillation, a major cause of cardioembolic stroke [28, 29]. The stress brought about by hypertension causes structural remodeling of the heart and affects atrial electrical properties [30-32]. This causes the atrium to contract prematurely, resulting in atrial fibrillation.

#### 1.1.3.2 Dyslipidaemia

Dyslipidaemia is defined as having total cholesterol $\geq$ 5.2 mmol/L, triglyceride level $\geq$ 1.8 mmol/L, high density lipoprotein (HDL) $\leq$ 1.0 mmol/L and low density lipoprotein (LDL) $\geq$ 3.4 mmol/L [33]. With excess lipid in circulation, there is increase in lipid deposition within the blood vessels [34]. Low density lipoprotein (LDL) is a lipoprotein that functions as a transport of cholesterol from liver to peripheral tissue and LDL can infiltrate into the intima of blood vessels [35]. The infiltrated LDL undergoes oxidation to form oxidized LDL (oxLDL) [36]. oxLDL induces endothelial cell activation which brings about

infiltration of monocytes [37]. oxLDL also triggers the production of chemokines (chemotactic molecules) to aid in the migration of leukocytes pass the endothelium and into the tunica intima [38]. The monocytes in the intima differentiate into macrophages and these macrophages will uptake the oxLDL forming foam cells [39]. This is the initial phase of atherosclerosis where fatty streak (accumulation of leukocytes, oxLDL and foam cells) is observed in the vascular wall [14]. Dyslipidemia together with other risk factors will enhance the progression of atherosclerosis and leads to atherosclerotic plaque formation. If the plaque occurs in the coronary artery, myocardial infarction will occur and myocardial infarction is a pre-condition for cardioembolic stroke. The progression of atherosclerosis will ultimately result in plaque rupture and hence large artery or small vessel stroke will ensue.

#### 1.1.3.3 Type 2 diabetes

Type 2 diabetes is a disease characterized by hyperglycemia and insulin resistance. Clinically, it is diagnosed by having fasting glucose > 6.1 mmol/L and HbA1c ≥ 7% [40, 41]. During hyperglycemic condition, the proteins and lipids present in circulation gets glycosylated forming advanced glycation end-products (AGEs) [42, 43]. AGE by itself can affect the extracellular matrix by forming crosslinks with proteins such as type I collagen and elastin, causing stiffness of the vessel [44, 45]. AGEs can also act through binding to receptor for AGE (RAGE) and thus mediate multiple processes [46, 47]. Generally, RAGE signaling triggers inflammation, coagulation, increase smooth muscle cell proliferation and increase vascular permeability [48-50]. RAGE signaling in endothelial cells causes the increase expression of cell adhesion molecules

such as vascular cell adhesion molecule 1 (VCAM-1), intracellular adhesion molecule 1 (ICAM-1), P- and E-selectins [51, 52]. These molecules aid in the recruitment and infiltration of leukocytes into the intima layer of the vessels. AGEs affects the vascular tone by reducing the bioavailability of nitric oxide (NO), an important vasodilator, through inhibiting the activity of NO producing enzyme, endothelial nitric oxide synthase (eNOS) [53, 54]. Furthermore, RAGE signaling triggers an increase in endothelial permeability and induces the expression of cytokines, enhancing immune cell infiltration into the vessel [55]. RAGE also induces platelet activation, promoting a pro-coagulation state [56]. All of which promotes the formation and development of atherosclerosis.

Type 2 diabetes can also induce atrial fibrillation. Type 2 diabetes can affect blood flow to the nerves involved in atrium contraction, resulting in cardiac autonomic neuropathy [57]. This can further develop into atrial fibrillation [58]. Type 2 diabetes also causes electrical and structural remodelling of the heart [59-62]. This is usually characterized by hypertrophy, interstitial fibrosis and impaired myocardial contractile reserve [63]. Thus, individuals with type 2 diabetes are more prone to suffer from atrial fibrillation.

### 1.1.4 Ischemic stroke pathophysiology

Even though the source of the occlusion may arise from different pathologies and comorbidities, the resulting trauma to the brain is similar. The occluded region in the brain undergoes similar pathology and forms the ischemic lesion [64].

The ischemic lesion can be segregated into two distinct regions: ischemic core and penumbra [64]. Upon ischemic onset, the tissue proximal to the occlusion suffers from oxygen and nutrient deficiency. The extreme condition inflicts tremendous stress in the cells of this region [65]. These cells succumb to cell death via necrosis. This region is known as the ischemic core [65]. The damage on the ischemic core is permanent and the cells are beyond rescue.

The region distal from the occlusion and adjacent to the ischemic core forms the penumbra. This region consists of cells that are dysfunction but viable. In 1977, Astrup *et al* [66] first characterized ischemic penumbra as the zone surrounding the ischemic core with diminished cerebral blood flow and no electrical activity, while exhibiting limited energy and ion pump failure. The cells in this region though viable, are still faced with the possibility of cell death overtime. Hence, the penumbra is the target of therapy due to the undetermined fate of the cells in this region.

### 1.2 Ischemic cascade

Having looked at the clinical aspect of ischemic stroke, next is to focus on the molecular processes underlying the pathophysiology of ischemic stroke. The molecular processes in ischemic stroke can be described as a cascade, aptly known as the ischemic cascade (Figure 1.2) [67].

In brief, the ischemia cascade begins due to occlusion in blood vessel resulting in a deficit in glucose and oxygen. This brings about energetic failure leading to the depolarization of the membrane, resulting in the release of excitotoxic neurotransmitter, glutamate [68]. Glutamate binds to the respective glutamate receptors that trigger influx of calcium, inducing excitotoxicity [69].

Concurrently, the sudden deprivation of oxygen and glucose results in the derangement of the metabolic processes such as oxidative phosphorylation [70]. Mitochondria dysfunction ensues, triggering apoptosis by the release of cytochrome c from mitochondria [71, 72].

Also, the onset of hypoxia induces the expression of detrimental genes including inflammatory molecules, all of which are mediated primarily by transcription factor, hypoxia inducible factor-1 (*HIF-1*) [73-75]. Cells within the infarcted region also responds which include astrocytes and microglia that become reactive, and endothelial cells that start to express cell adhesion molecule and secrete cytokines and chemokine [76, 77]. These actions bring about an uncontrolled inflammatory response that is detrimental to the cells and the patient.

All of these processes though described in a cascade are in fact occurring simultaneously which ultimately leads to cells dying in the infarct lesion. Within the ischemic cascade, there are 4 key molecular processes occurring, cell death, excitotoxicity, inflammation and oxidative damage, which will be described below in detail.

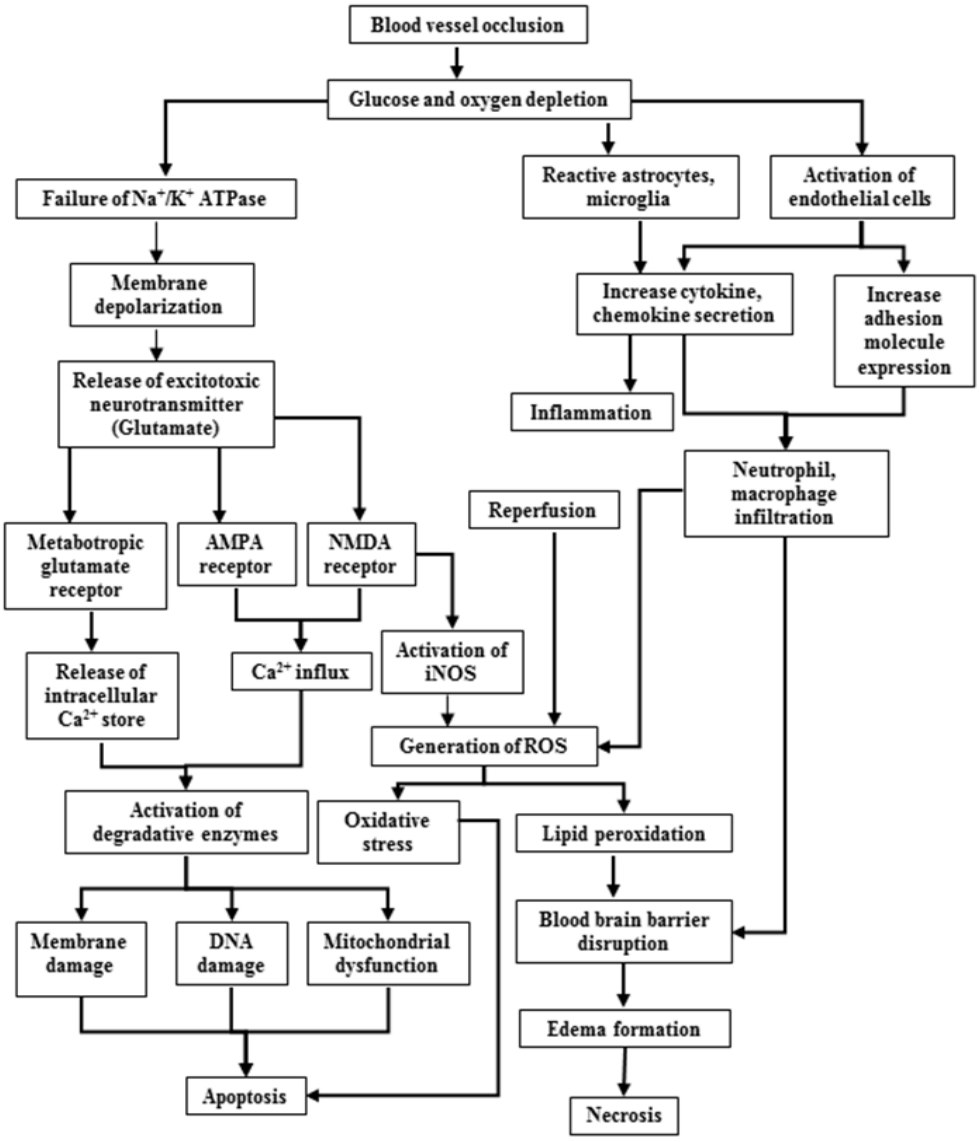


**Figure 1.2:** Diagram of ischemic cascade. Adapted from Ly *et al* [67]

### 1.2.1 Excitotoxicity

Excitotoxicity is characterized by the accumulation of calcium ions in neurons due to over-stimulation of excitatory neurotransmitter receptors by an excess of excitotoxic neurotransmitter (glutamate) [78]. Glutamate is a major excitatory neurotransmitter in the central nervous system [79]. It is involved in cell to cell communication between neurons by initiating excitatory post-synaptic potential (EPSP) at adjacent neuron [80]. Glutamate is stored in vesicles at the axon terminal, which are released during membrane depolarization [79].

During ischemia, the decrease of blood flow causes the depletion of the ATP store in the neurons due to the absence of oxygen and glucose for generation of ATP [70]. The metabolic dysfunction causes failure maintenance of ionic balance in neuron due to failure of $Na^+/K^+$ ATPase [64]. Subsequently, the membrane depolarizes and releases all the glutamate stored in the vesicles. The glutamate diffuses across the synaptic cleft and bind to the glutamate receptors at the postsynaptic membrane. There are three main types of glutamate receptors in the central nervous system, α-Amino-3-hydroxy-5-methyl-isoxazole-4-propionate (AMPA) receptor, N-methyl-D-aspartate (NMDA) receptor and metabotropic glutamate receptor (mGluR) [81-83]. When glutamate binds to AMPA receptors and NMDA receptors, the receptors form open channels to allow the influx of calcium ions into neuron [81, 82]. The interaction between glutamate and mGluR will result in the release of internal calcium ion store from the endoplasmic reticulum [84]. The net effect of glutamate binding to the glutamate receptor is the influx of calcium ion and the accumulation of calcium ion in the soma of the neuron.

The accumulation of calcium ion is detrimental to the survival of neurons as this activates a number of calcium dependent proteases, lipases and endonucleases, which can disrupt cell membrane, digest important protein and nucleic acids [85-87].

It has been reported that NMDA receptor activation leads to the activation of neuron specific calpain I (Figure 1.3) [88, 89]. Calpain then inactivates $Na^{+}/Ca^{2+}$ exchanger (NCX3) which is an important ion exchanger for maintaining $Ca^{2+}$ homeostasis (Figure 1.3) [90]. This potentiates on calcium overload during excitotoxicity.

Mitochondria play an important role in $Ca^{2+}$ homeostasis [91]. During $Ca^{2+}$ overload, mitochondria act as a temporary store for excess $Ca^{2+}$ [91]. However, during excitotoxicity, the excessive $Ca^{2+}$ in the mitochondria causes mitochondrial dysfunction, leading to release of cytochrome c and ultimately apoptosis (Figure 1.3) [92].

Activation of NMDA receptors also couples to inducible nitric oxide synthase (iNOS), producing nitric oxide (NO) which reacts to form reactive oxygen species (ROS), and increasing oxidative stress (Figure 1.3) [93]. Thus, excitotoxicity decrease the viability of cells in the penumbra by promoting oxidative stress, activating endogenous endonucleases and proteases; all of which promote neuronal cell death.

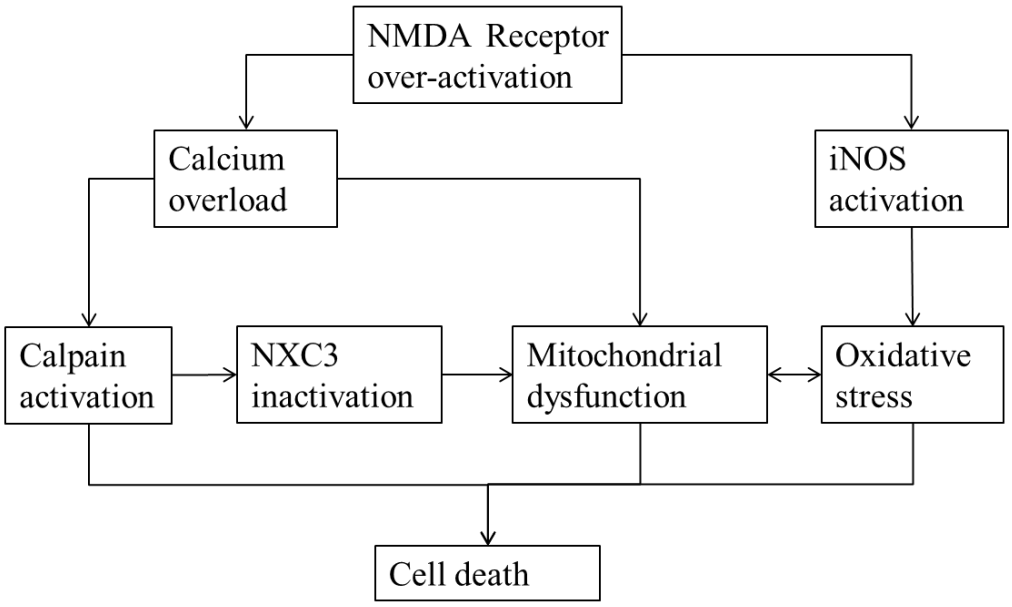


**Figure 1.3:** Excitotoxicity during ischemic stroke.

### 1.2.2 Oxidative damage

The brain utilizes more than 20% of total oxygen consumption, making it susceptible to oxidative damage, especially during ischemic stroke [94]. Oxidative damage is the event where the over-production of reactive oxygen species (ROS) overwhelms the anti-oxidant defenses in the cell and causes damage to biologically important macromolecules such as nucleic acid, protein and lipids [95].

The brain is especially susceptible to oxidative damage due to its high lipid content, and so it will have a greater extent of lipid peroxidation under oxidative stress [96]. During cerebral ischemia, the activation of glutamate receptors can be coupled to molecular processes that increase oxidative stress in neurons [93]. iNOS is triggered during glutamate receptor activation to produce NO which drives ROS production (Figure 1.4) [93]. NO readily reacts with superoxide radical ($O_2^-$) to produce peroxynitrite radical ($ONOO^-$) which is a potent radical that results in lipid peroxidation [95]. The product from lipid peroxidation, 4-hydroxynonenal (4-HNE) is neurotoxic, which aggravates the neuronal damage brought on by ischemia and reperfusion (Figure 1.4) [97, 98].

During ischemia, the deficit in oxygen and glucose causes disruption in the electron transport chain (ETC) in the mitochondria. Due to the lack of oxygen, there is an accumulation of activated complex along the ETC which results in electron leakage [99, 100]. This causes the generation of ROS and leads to mitochondrial dysfunction and ultimately cell death.

Under ischemic condition, xanthine dehydrogenase (enzyme involved in the metabolism of hypoxanthine) transmutes to xanthine oxidase (XO) [99]. XO

can generate superoxide anions which increases the ROS load (Figure 1.4). Similarly, NADPH oxidase (NOX), an enzyme generating ROS in phagocytes as a form of defense against pathogens, was found to contribute to ischemic/reperfusion injury [101]. NOX generates superoxide radical ($O_2^-$) which reacts with water to form hydroxyl radical (•HO) and forms peroxynitrite radical ($ONOO^-$) when reacting with NO (Figure 1.4) [101].

Activation of phospholipase A2 ($PLA_2$) also contributes to oxidative damage in cerebral ischemia. The product, arachedonic acid undergoes further oxidation which generates more ROS (Figure 1.4) [102]. ROS generated during ischemia results in direct modification of important macromolecules such as proteins, lipids and nucleic acids. This triggers apoptosis via p53 pathway, resulting in neuronal cell death [103].

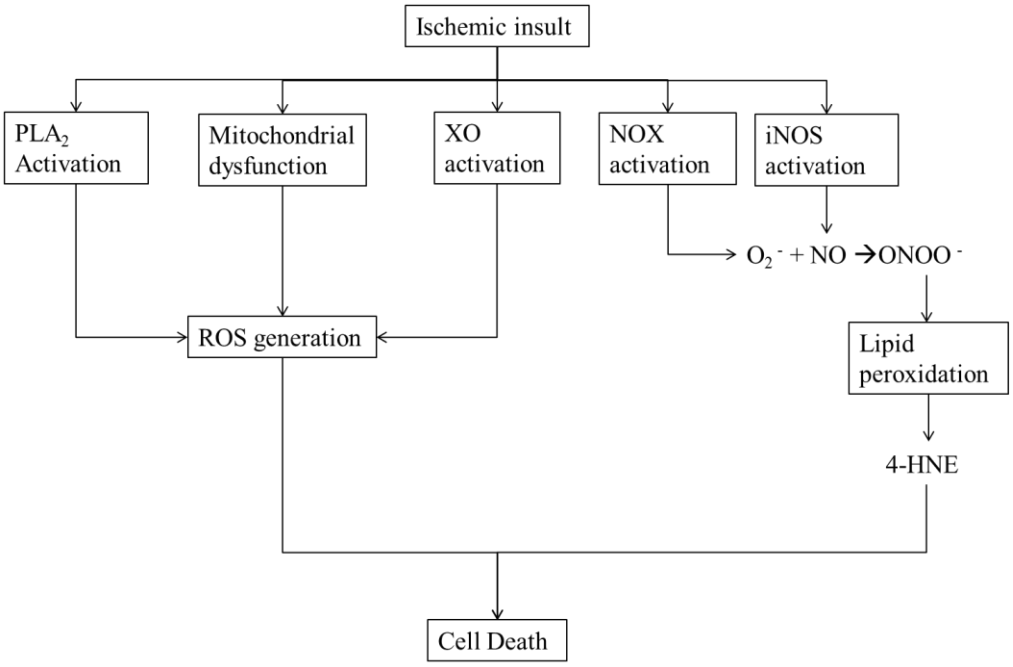


**Figure 1.4:** Oxidative damage during cerebral ischemia

### 1.2.3 Apoptosis

Apoptosis is synonymous to programmed cell death. The weakened neurons in the penumbra undergo apoptosis after the onset of cerebral ischemia. Apoptosis is triggered by lack of neurotropic factors, oxidative damage, DNA damage and mitochondrial dysfunction [104]. Apoptosis can be induced by two pathways: Intrinsic pathway and extrinsic pathway [105].

Intrinsic pathway is activated by mitochondrial damage during ischemic stroke. During cerebral ischemia, there is an increase in oxidative stress and the mitochondria are damaged by free radicals [106]. In addition, the disruption of blood causes depletion of glucose and oxygen which results in energy depletion. All of which leads to mitochondrial dysfunction [71, 72]. Mitochondria are a store for multitude of pro-apoptotic proteins such as cytochrome c, endonuclease G, caspases, AIF and second mitochondria-derived activator of caspases/direct IAP-binding protein with low p (SMAC/DIABLO) (Figure 1.5A) [107]. When mitochondria are damaged, the apoptogenic proteins leak into the cytosol which induces apoptosis.

In addition, ROS signaling also triggers cell death via p53 signaling pathway [103, 108]. p53 can mediate the release of cytochrome c from mitochondria and up-regulate the expression of pro-apoptotic protein such as Bcl-2 associated X protein (Bax), BH3 interacting-domain death agonist (Bid) and p53 upregulated modulator of apoptosis (PUMA) to bring about apoptosis [109]. Also, the influx of calcium ions also activates calpains which are calcium dependent proteases that cleave Bid forming tBid that promotes the release of pro-apoptotic proteins from mitochondria [110].

Cytochrome c released from mitochondria, together with apoptotic protease activating factor 1 (Apaf-1) and caspase 9, assembles into an apoptosome which activates the caspase 3 (Figure 1.5A) [111, 112]. Caspase 3 cleaves many important proteins which are crucial for cell survival, including poly (ADP-ribose) polymerase (PARP) [113]. PARP inactivation prevents DNA repair and leads to cell death (Figure 1.5A) [114].

External triggers can also induce apoptosis (extrinsic pathway) through the death receptor. Ligands such as TNF-α and Fas ligand (FasL) bind to Fas receptor (FasR) and induce formation of death inducing signaling complex (DISC) which consists of FasL, FasR, Fas-associated death domain protein (FADD) and procaspase 8 (Figure 1.5B) [115]. DISC will activate caspase 8 which initiates down-stream activation of caspase 3, leading to cell death [111].

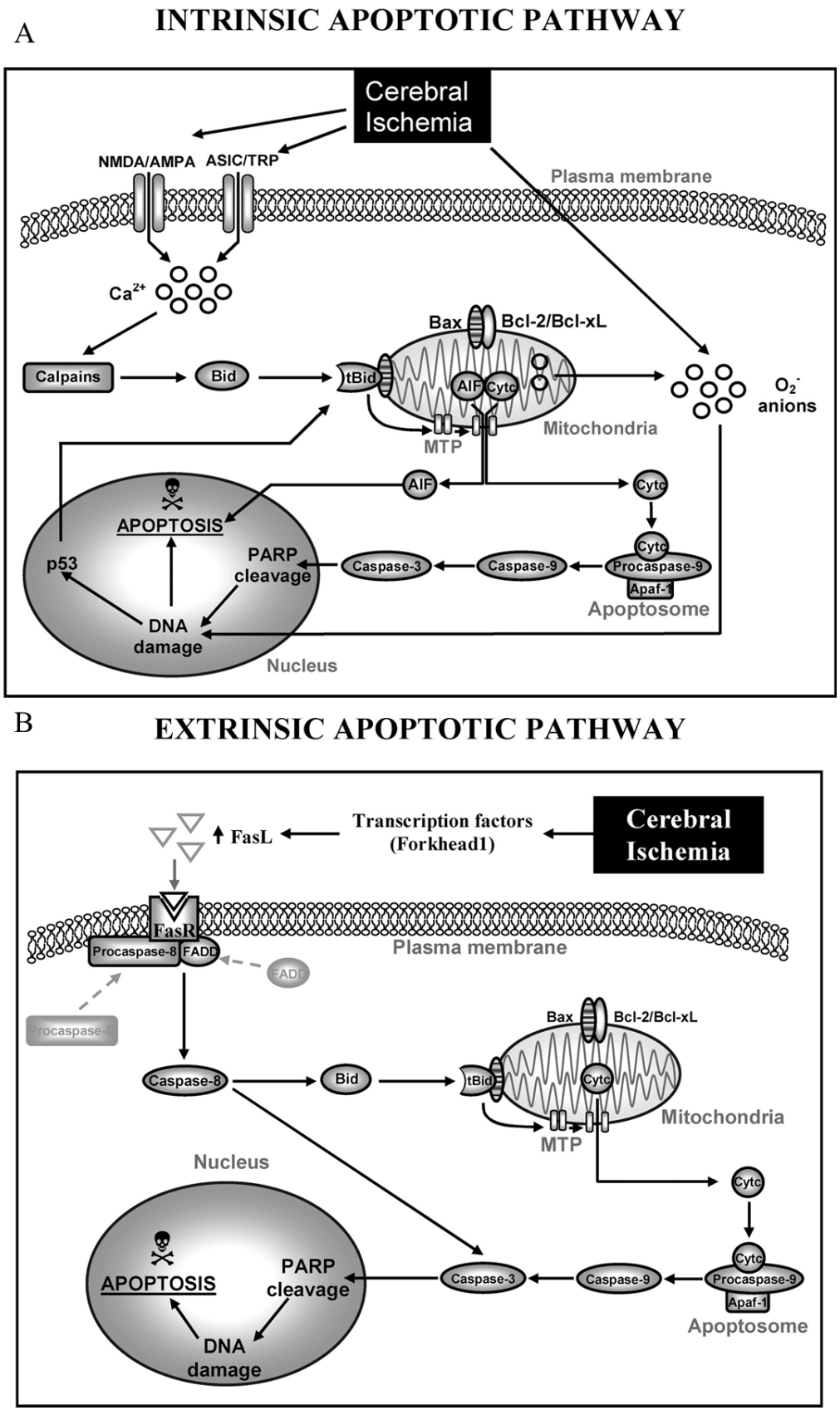


**Figure 1.5:** Apoptosis during cerebral ischemia. **A.** Intrinsic pathway. **B.** Extrinsic pathway. Adapted from Broughton *et al* [105].

### 1.2.4 Inflammation

Inflammation is another important biochemical process that is involved in cerebral ischemia. Inflammation occurs a few hours after the onset of stroke. It is mediated by cells (immune cells and local cells) and protein molecules (cytokine and complement) [116-119].

Inflammation involves the activation of endothelial cells, astrocytes and microglial cells (local immune cell) [120]. Under the ischemic condition, astrocytes and microglial cells are activated and start producing cytokines and chemokines, which are potent mediators of inflammatory response (Figure 1.6) [121]. Cytokines are molecular mediators of inflammation; they generally induce macrophage activation, B-cell and T-cell maturation [118]. Chemokines are chemicals that help in the localization of inflammatory cells to the site of injury [119, 122]. In response to injury, the endothelial cells lining the blood vessel are also activated and start to express vascular cell adhesion molecule 1 (VCAM1), which helps in the adhesion of inflammatory cells such as monocytes and neutrophil; to facilitate localization of inflammatory cells to site of injury [122]. Chemokines are secreted by microglial cells and astrocytes, which form a chemical gradient that attracts monocytes to site of injury [119]. Endothelial cells also express intracellular adhesion molecular 1 (ICAM1) causes the immune cells to tether along the lumen side of the endothelial cells [123]. Among these modulators, chemokine C-C motif ligand 2 (*CCL2*) has been shown to be involved in the pathophysiology of ischemic stroke. In animal models, *Ccl2* has been demonstrated to be involved in blood brain barrier disruption [124]. Furthermore, animals with CCL2 or its receptor CCR2 knockout have smaller

infarct following middle cerebral artery occlusion (MCAo) as compared with wild-type [125, 126]. Monocytes will extravasate from the blood and move towards the area of ischemic injury down the chemokine gradient. Therefore, the increase in chemokine secretion will result in increasing localization of inflammatory cells.

In order for the monocytes to enter into the brain parenchyma, they have to pass through the blood brain barrier (BBB; Figure 1.6). Cytokines secreted by microglial cells, astrocytes and neurons, such as interleukin 6 (IL-6), interleukin 8 (IL-8) and tumor necrosis factor alpha (TNF-α) [120, 121]. IL 8 induces neutrophils and monocytes to secrete matrix metalloproteinase 9 (MMP9) which breaks down the BBB to allow the infiltration of inflammatory cells to reach the site of injury [127]. The breakdown of BBB is an undesirable event as this will lead to edema and hemorrhage. The secretion of pro-inflammatory cytokines (IL-6, TNF-α) will induce respiratory burst in the macrophages present at the site of infarct (Figure 1.6) [122]. This in turn leads to an increase in oxidative stress.

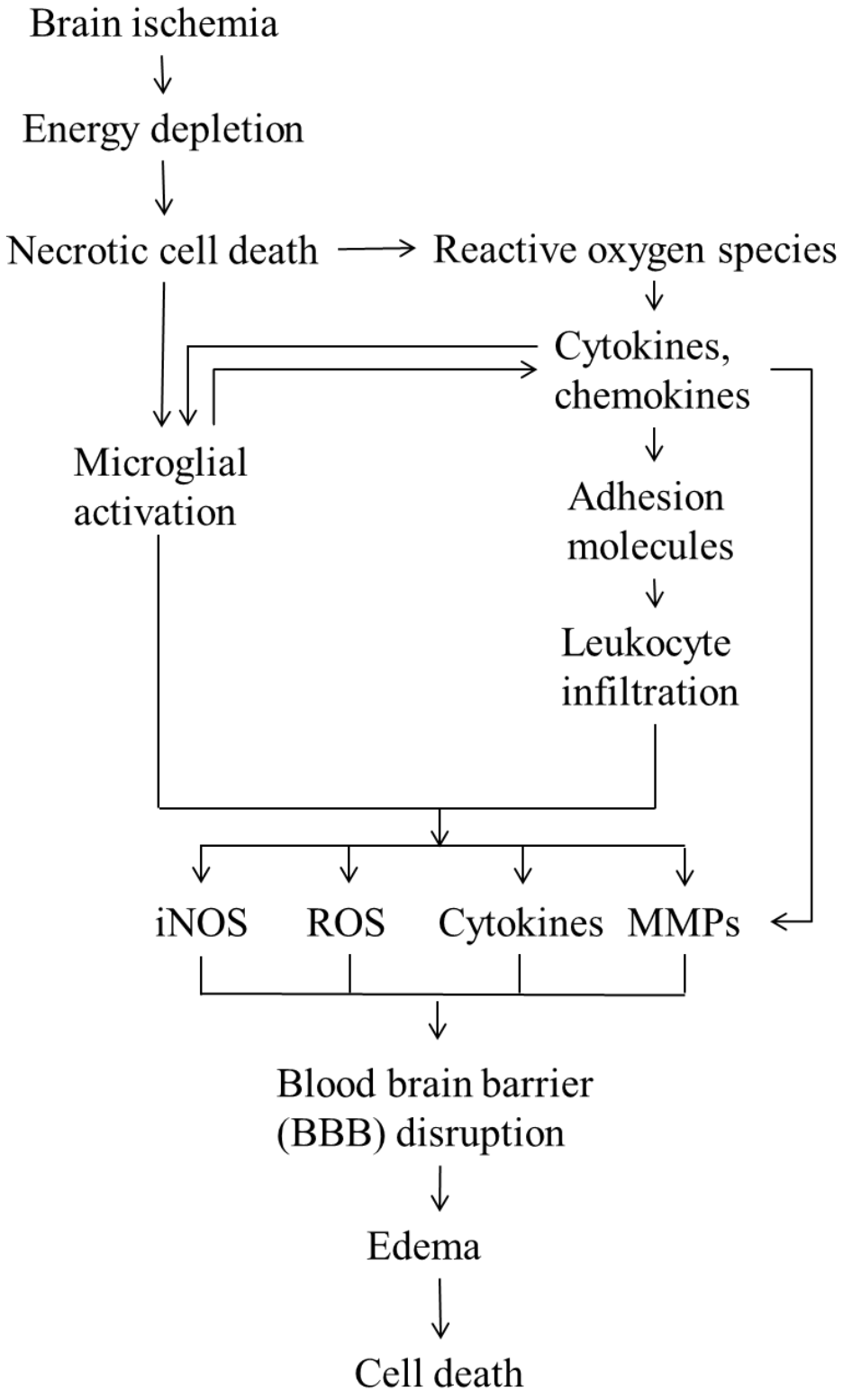


**Figure 1.6:** Inflammation during cerebral ischemia.

Complement is a component of innate immunity, which responds to pathogen during infection, and in pathological state, complement can cause damage to self-tissue [128]. Complement is present as zymogens synthesized in the liver and becomes activated via proteolytic cleavage by protein components early in the complement cascade [128]. Complement activation occurs via 3 pathways namely: classical pathway, alternative pathway and lectin pathway (Figure 1.7) [128]. These 3 pathways converge on the formation of C5 convertase [128]. C5 convertase cleaves C5 into C5a and C5b. C5b is responsible for the formation of membrane-attack complex (MAC) which is the effector for clearing infected cells and pathogens [128].

Components of the complement cascade had been reported to be elevated in the serum of ischemic stroke patients. Mannose-binding lectin (MBL; component in the lectin pathway of complement activation) was found to be elevated in serum of ischemic stroke patients and the level of MBL had been shown to be associated with outcome of ischemic stroke [129-131]. The MBL level also acted as a possible predictor for the outcome of ischemic stroke patients, whereby higher level of MBL correlated with worse outcome [129, 130]. Complement component 3 and 4 (C3 and C4) were found to be in high level in young ischemic stroke patients and also pose as a possible predictor for outcome similar to MBL [132]. Another study demonstrated strong activation of complement, quantified by high level of C4d and soluble terminal complex (SC5b-9), was associated with poor outcome in ischemic stroke patients [133]. Current literature also highlights possible effects of complement activation that could account for having poor outcome in patients. Complement activation during ischemic stroke triggered an inflammatory

response which aggravated the pathological condition leading to worse outcome. Hypo-perfusion performed in mice showed increase in complement component 5 (C5) in the brain resulting in increased inflammation in terms of increased numbers of reactive astrocytes and microglia [134]. Furthermore, C5a (a cleaved fragment of C5) was found to be increased in neurons subjected to ischemia and C5a was shown to be responsible for neuronal apoptosis during ischemia [135]. In addition, MBL has been demonstrated to induce local microvascular thrombosis after ischemia performed in mice [136]. Hence, complement activation during ischemic stroke brings about detrimental effects which enhance inflammation and cell death.

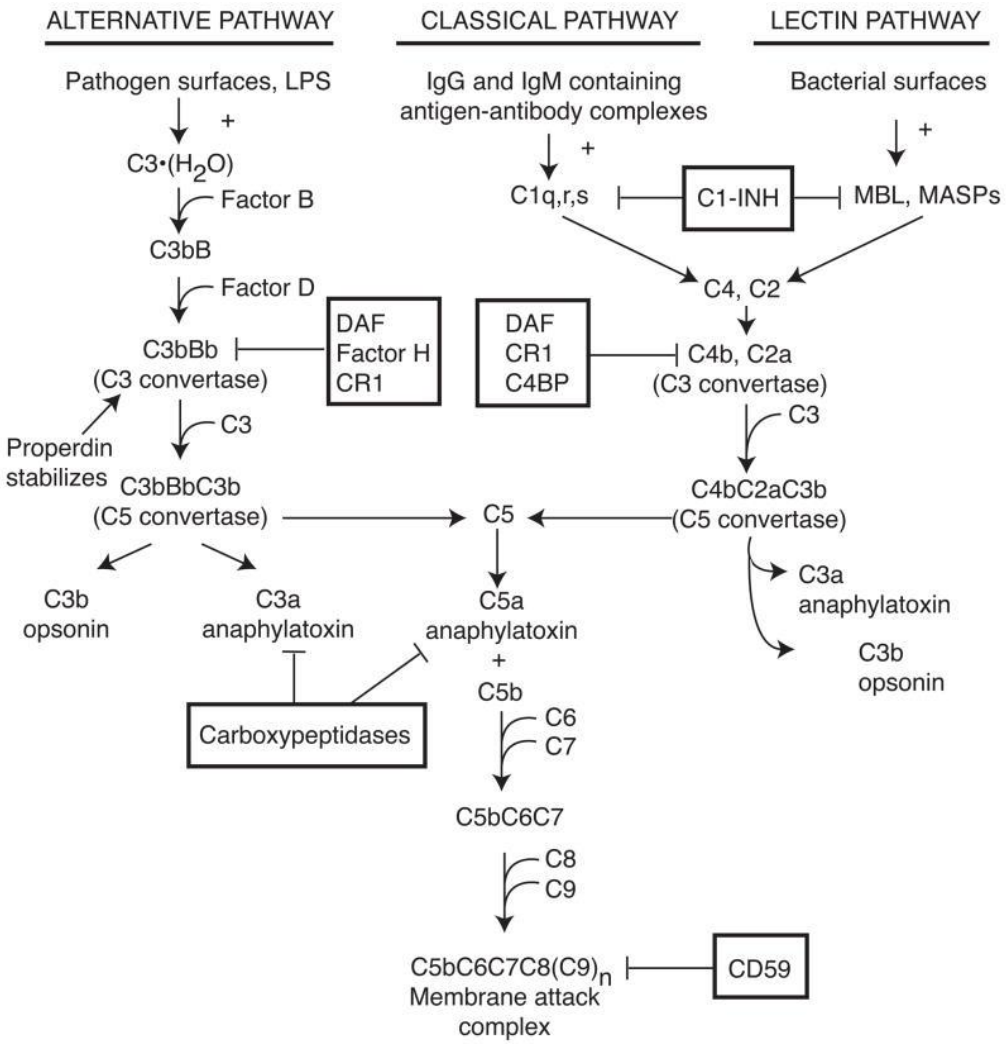


**Figure 1.7:** Complement activation. Adapted from Sarma and Ward [128]

### 1.3 microRNA (miRNA)

For a long time, RNA was thought to play the role of a passive role in the transition from genetic code to protein peptide. It was in 1993 that Victor Ambros, Rosalind Lee and Rhonda Feinbaum [137] discovered the first miRNA, *lin-4*, which target lin-14 in the regulation of *Caenorhabditis elegans* (*C. elegans*) development. The second miRNA was discovered in 2000 where *let-7* RNA was found to target *lin-41* in *C. elegans* [138]. It was soon found that *let-7* is conserved in many species. miRNAs are a class of short (18 to 22 nucleotides), endogenous, non-coding RNAs [137, 139].

#### 1.3.1 Biogenesis

miRNAs are found within both intragenic and intergenic regions in the genome [140] and they can be transcribed as individual miRNAs or as a cluster of miRNAs. miRNAs are usually transcribed by RNA polymerase II to produce primary-miRNAs (pri-miRNA; Figure 1.8) [141]. Pri-miRNAs usually several thousand bases long forming several hairpin loops and contain the 7-methylguanosine cap and a poly(A) tail [141-142]. Pri-miRNAs are processed by Drosha and Pasha (RNase III endonuclease) in the nucleus to produce ~60 to 70 nucleotides long stem-loop structures known as precursor miRNAs (pre-miRNAs; Figure 1.8) [143]. Pre-miRNAs are exported out of the nucleus by Exportin 5, a nuclear exporting protein [144]. Pre-miRNAs are processed by Dicer (RNase III enzyme) to produce miRNA:miRNA* duplex with a 2 nucleotides overhang at the 3' end (Figure 1.8) [139, 145]. miRNA:miRNA* duplex forms a pre-complex with RNA-induced silencing complex (RISC; Figure 1.8). Only one strand of the miRNA, the guide, which

is having the low internal stability at the 5′ end, is incorporated into the miRNA-RISC complex. [145-147].

### 1.3.2 RNA interference (RNAi)

miRNA-RISC will recognize the 3’ un-translated region of messenger RNA (mRNA) that is perfectly complementary to miRNA sequence. This will trigger mRNA degradation which results in post-transcriptional silencing of the target gene (Figure 1.8). In the event of partial complementary base-pairing, the mRNA will be targeted for storage in P-bodies which represses the expression of the mRNA (Figure 1.8). The mRNA within the P-bodies may be sent for degradation. This process is RNA interference (RNAi) [148]. A single miRNA can have multiple binding sites on the same target mRNA and it can also target multiple mRNAs. Usually, a single miRNA is estimated to target about 200 different transcripts [149].

### 1.3.3 RNA activation (RNAa)

Alternatively, microRNA can also enhance gene expression by RNA activation [150]. miRNA can be shuttled back into the nucleus and modulate gene expression by binding to promoter regions, which have been shown to both activate gene expression (Figure 1.8) [151-152]. Gene activation is believed to take place via the interaction of miRNAs and their target genes at the 5‟ non-coding regulatory regions. Janowski *et al* [152] showed that transfection of short double stranded RNAs which were complementary to the progesterone receptor promoter, increased mRNA and protein expression of the progesterone protein in breast cancer cells.

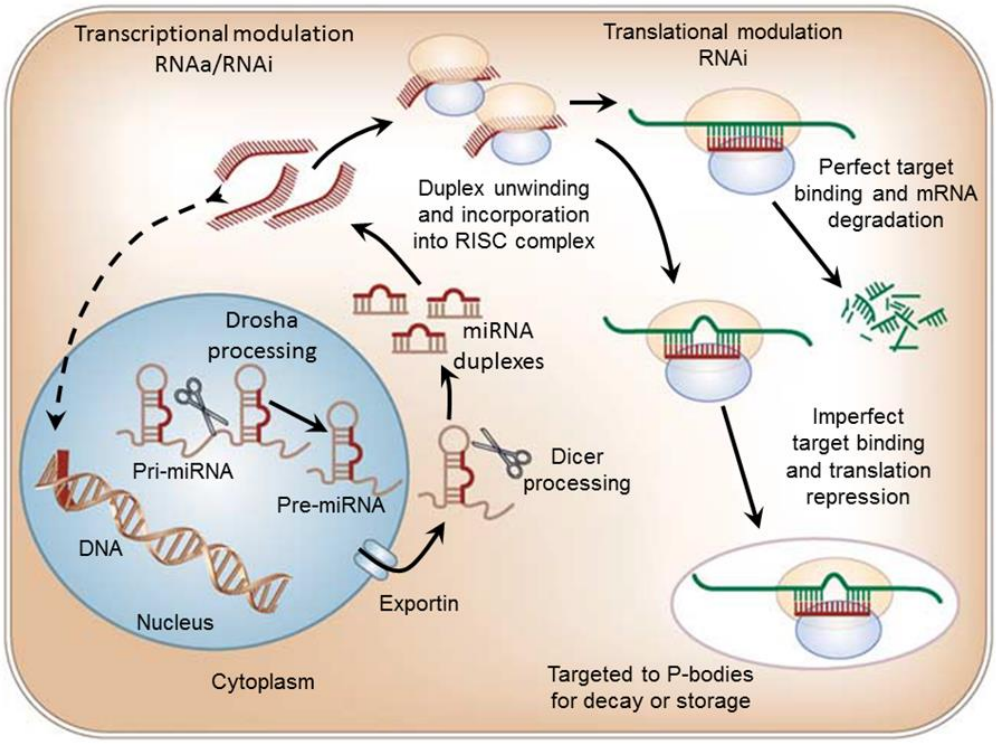


**Figure 1.8:** miRNA biosynthesis and function. Adapted from Chandrasekaran *et al* [153].

### 1.3.4 Bioinformatics prediction

Since the discovery of RNAi, multiple online platforms have been developed to exploit the large computing capacity to make prediction for miRNA-mRNA target pairs. Most of the prediction algorithms based the concept of seed-region, which consists of the first 2 to 8 nucleotides on the 5' end of the miRNA [154]. If the 5' end of the miRNA pairs sufficiently well with the 3' UTR then the pairing at the 3' end of miRNA to the target is not essential [155]. Most of the prediction databases use sequence alignment, thermodynamic calculations and statistical testing to shortlist the possible miRNA-mRNA target pairs. Using multiple databases to obtain consensus can ensure a more accurate prediction for miRNA-mRNA target pairs.

### 1.3.5 miRNA prediction databases

Currently, there are quite a number of databases present for making predictions. Each database will have different criteria for selection. Some of the most common miRNA prediction databases are: Targetscan version 6.2 (www.targetscan.org) [156-159], miRanda August 2010 release (www.microRNA.org) [160-163], microcosm version 5 (www.ebi.ac.uk/enright-srv/microcosm/htdocs/targets/v5/) [163-165], DIANA microT version 3 (http://diana.cslab.ece.ntua.gr/microT/) [166, 167], miRDB version 4 (mirdb.org/) [168, 169], miRWalk March 2011 update (www.umm.uni-heidelberg.de/apps/zmf/mirwalk/) [170], PITA 2007 release (genie.weizmann.ac.il/pubs/mir07/mir07_prediction.html) [171], RepTar version 1.2 (reptar.ekmd.huji.ac.il/) [172] and StarBase version 2 (starbase.sysu.edu.cn/) [173, 174].

Targetscan takes into account various aspects of the seed region when it comes to prediction. The length of the seed region is taken into account as it affects the binding strength (8 nucleotide site > 7 nucleotide site > 6 nucleotide site) [158, 175]. The TargetscanS algorithm picks up targets with 6 nucleotide seed region [156]. As for microRNA.org and microcosm, both uses miRanda algorithm [162]. It gives an alignment score which is a weighted sum of match and mismatch scores for base pairs and gap penalties [162, 163]. An estimate of free energy of binding was calculated using Vienna package [176]. Similarly, DIANA microT algorithm takes into account 7 to 9 nucleotides of 5' end of miRNA that form Watson–Crick base pairing nucleotides with target mRNA [167]. As for miRDB, mRNA sequences were obtained from NCBI databases and genome-wide miRNA target prediction was performed using MirTarget2 algorithm [177, 178]. miRWalk algorithm 'walks' along complete sequence of a gene identifying multiple consecutive Watson–Crick complementary subsequences between miRNA and gene sequences [170]. The probability distribution of the pairing was calculated using Poisson distribution [179]. RepTar database uses RepTar algorithm which search for statistically significant repetitive motifs in each 3' UTR, represented in the form of hidden Markov model [172]. The thermodynamic stability was evaluated using Vienna package RNA cofold program [180]. PITA looks for perfect miRNA target seeds 6 to 8 bases long, disallowing G:U wobbles, mismatches or loops [171]. Similarly, the free energy of miRNA-mRNA duplex was also calculated using Vienna RNA package [180]. StarBase uses ClipSearch program to search for 6–8-mers in CLIP-Seq sequence data sets from 8 studies [173, 174, 181-188]. Using results from all these databases, the

consensus miRNA-mRNA target pair will be more accurate as it has taken into account multiple variables using different methodologies.

### 1.3.6 miRNAs and ischemic stroke

Being important regulators of gene expression, during disease states, miRNAs also becomes dysregulated. miRNAs have been reported to be dysregulated in diseases. It has been demonstrated that miRNAs are dysregulated during cerebral ischemia, shown in animal model [189]. Subsequently, circulating miRNAs in ischemic stroke patients were also found to be dysregulated [190]. Following which, other groups have reported more on the miRNA dysregulation in animal models [191-196] as well as in patients [197-205]. Since miRNA dysregulation can be studied in human patients, it is plausible to elucidate the mechanisms underlying ischemic stroke pathology and to validate experimentally.

## 1.4 Hypothesis and objectives

Since miRNA dysregulation have been demonstrated to be involved in ischemic stroke clinically and experimentally, it is possible to study the dysregulated miRNA both in patients and animal models, as well as to study the underlying mechanisms of ischemic stroke pathology. The hypothesis of this study is that through miRNA profiling and analysis, it is possible to identify miRNAs that are specific for ischemic stroke and various stroke subtypes. By studying these miRNAs and the processes that they regulate, there can be better understanding of the mechanisms underlying the pathogenesis and pathophysiology of ischemic stroke. These miRNAs can also

become potential markers and therapeutic targets in cerebral ischemia where expression of these miRNAs can be manipulated by using anti-miRNAs or miRNA mimics.

The objectives of this study are as follows:

1. Identify ischemic stroke specific miRNAs from a comparative analysis of miRNA profiles between ischemic stroke patients with and without risk factors, and highlight the biological pathways regulated by these miRNAs
2. Identify stroke subtype specific miRNAs by comparing miRNA profiles of each stroke subtypes and highlight the biological pathways regulated by these miRNAs
3. Create middle cerebral artery occlusion (MCAo) models in rats at various stages or time-points (12, 24, 48, 72, 120 and 168 hours) in cerebral ischemia
4. Identify miRNAs that correlate with infarct volume in miRNA profile of rats subjected to MCAo
5. Identify biological pathways commonly dysregulated among animal models and ischemic stroke patients and subsequently study the effects of regulating the genes in these biological pathways using anti-miRNA and miRNA mimics

# Chapter 2

# Materials and methods

## 2. Materials and methods

### 2.1.1 Reagents animal procedure and anaesthesia

#### 2.1.1.1 Animal

Male Wistar (~250 to 300g) rats were obtained from the Laboratory Animal Centre (National University of Singapore, Singapore) and maintained on an ad libitum intake of standard laboratory chow and drinking water. All animals were handled according to the guidelines given by the Council for International Organization of Medical Sciences on animal experimentation (WHO, Geneva, Switzerland) and the National University of Singapore (IACUC/NUS) guidelines for handling laboratory animals.

#### 2.1.1.2 Saline, NaCl 0.9% w/v

| | |
|---|---|
| NaCl | 9g |
| Deionised water | 1L |

#### 2.1.1.3 Anesthesia

| | |
|---|---|
| Ketamine | 75mg/kg |
| Xylazine | 10mg/kg |

Ketamine and xylazine were dissolved in sterile saline (NaCl 0.9%) and used to anesthetize the rats.

#### 2.1.1.4 2,3,5-triphenyltetrazolium chloride (TTC) 2% w/v

| | |
|---|---|
| 2, 3, 5-triphenyltetrazolium chloride | 1g |
| NaCl 0.9% w/v | 50ml |

### 2.1.2 Reagents for RNA isolation from brain tissues

#### 2.1.2.1 Ethanol 75% v/v

| | |
|---|---|
| Absolute ethanol | 37.5ml |
| Autoclaved water | 12.5ml |

Stored at 4°C.

### 2.1.3 Reagents for RNA isolation from whole blood

#### 2.1.3.1 NaCl (5M)

| | |
|---|---|
| NaCl | 2.922g |
| Autoclaved water | 10ml |

#### 2.1.3.2 Wash 1: Ethanol (70%):Denaturation Solution (30%)

| | |
|---|---|
| Absolute ethanol (100%) | 24.5ml |
| Denaturation solution | 10.5ml |

#### 2.1.3.3 Wash 2: Ethanol (80%):NaCl (50mM)

| | |
|---|---|
| Absolute ethanol (100%) | 56ml |
| NaCl (5M) | 0.7ml |
| Autoclaved water | 13.3ml |

### 2.1.4 Reagents for RNA agarose gel electrophoresis

#### 2.1.4.1 10X MOPS running buffer

| | |
|---|---|
| Morpholinopropanesulfonic acid (MOPS, pH7.0) | 0.4M |
| Sodium acetate | 0.1M |
| EDTA (pH 8.0) | 10mM |

10X MOPS was prepared using autoclaved water and sterile-filtered with a 0.22μm filter. The solution was diluted with deionised water to 1X MOPS for gel running.

#### 2.1.4.2 Deionised formamide

Formamide (500ml) was stirred with 500mg Dowex XG8 resin for 1 hr and filtered through Whatman No.1 paper. Deionised formamide was stored at room temperature in the dark.

#### 2.1.4.3 Ethidium bromide (10mg/ml)

| | |
|---|---|
| Ethidium bromide | 10mg |
| Autoclaved water | 1ml |

Store at room temperature in dark.

#### 2.1.4.4 RNA loading buffer

| | |
|---|---|
| Glycerol | 50% (v/v) |
| Bromophenol blue | 0.4% (w/v) |
| EDTA (pH8.0) | 1mM |

#### 2.1.4.5 RNA sample buffer (per sample)

| | |
|---|---|
| Deionised formamide | 10μl |
| 37% formaldehyde | 3.5μl |
| 10X MOPS | 2μl |
| RNA loading buffer | 2μl |

**2.1.4.6 RNA agarose gel (1%)**

| | |
|---|---|
| Electrophoresis grade agarose | 0.5g |
| Deionised water | 43.5ml |
| 37% formaldehyde | 1.5ml |
| 10X MOPS | 5ml |
| Ethidium bromide (10mg/ml) | 1ul |

Powdered agarose was mixed with water and heated to 100°C, to dissolve completely. It was then cooled to about 60°C before the addition of 37% formaldehyde, 10X MOPS and ethidium bromide

**2.1.5 Reagents for RNA polyacrylamide gel electrophoresis**

**2.1.5.1 Ammonium persulfate (APS) 10% w/v**

| | |
|---|---|
| Ammonium persulfate | 100mg |
| Autoclaved water | 10ml |

**2.1.5.2 10X Tris-Borate-EDTA (TBE) buffer**

| | |
|---|---|
| Tris base | 108g |
| Boric acid | 55g |
| 0.5M EDTA (pH 8.0) | 40ml |
| Deionised water | 960ml |

Tris base and boric acid was dissolved in 960ml of deionised water before addiing of 40ml of EDTA, pH 8.0.

**2.1.5.3 Denaturing polyacrylamide gel (15%)**

| | |
|---|---|
| Urea | 7.2g |

| | |
|---|---|
| 40% Acrylamide | 5.63ml |
| 10X TBE Buffer | 1.5ml |
| Deionised water | 0.95ml |
| TEMED | 7.5µl |
| 10% APS | 37µl |

Acrylamide, urea and 10X TBE buffer were heated to 60°C. Once urea was dissolved, deionised water, TEMED and APS were added to the mixture and the gel was cast immediately.

#### 2.1.5.4 RNA sample buffer (per sample)

| | |
|---|---|
| 10X TBE Buffer | 2µl |
| Deionised Formamide | 10µl |
| RNA Loading Buffer | 3µl |
| Ethidium bromide (10mg/ml) | 1ul |

### 2.1.6 Reagents for cell culture

#### 2.1.6.1 Cell lines

Human umbilical vein endothelial cells (HUVEC, CRL-1730™) and HeLa cells (CCL-2™) were obtained from the American Type Cell Culture (ATCC, USA).

#### 2.1.6.2 1X Phosphate-buffered saline (PBS)

| | |
|---|---|
| NaCl | 8g |
| KCl | 0.2g |
| $Na_2HPO_4.2H_2O$ | 1.4g |

| | |
|---|---|
| $KH_2PO_4$ | 0.24g |
| Deionised water | 1L |

The solution was adjusted to pH7.4 and autoclaved.

### 2.1.6.3 Trypsin

10X trypsin was diluted to 1X with 1X PBS and stored at -20°C

### 2.1.6.4 Basal Dulbecco's Modified Eagle Medium (DMEM, 1L)

| | |
|---|---|
| DMEM | 16.2g |
| L-glutamine | 0.4g |
| Sodium bicarbonate | 1.74g |
| Penicillin-streptomycin (50U-50mg/ml) | 1% |
| Deionised water | 1L |

The solution was adjusted to pH7.4 and filtered sterilized. Stored at 4°C.

### 2.1.6.5 Complete DMEM (1L)

| | |
|---|---|
| Basal DMEM | 900ml |
| Fetal bovine serum (FBS) | 100ml |

### 2.1.6.6 Freezing medium (100ml)

| | |
|---|---|
| Basal DMEM | 30ml |
| Fetal bovine serum (FBS) | 70ml |

Cells were stocked with freezing medium and 5% sterile DMSO and kept in -80°C.

### 2.1.7 Reagents for reverse transcription (RT)

#### 2.1.7.1 RT mixture for mRNA

| | |
|---|---|
| 10X Taqman RT buffer | 1µl |
| 25mM $MgCl_2$ | 2.2µl |
| DeoxyNTPs mixture | 2µl |
| 50µM Random hexamers | 0.6µl |
| 20 U/µl RNase inhibitor | 0.2µl |
| 50 U/µl MultiScribe™ Reverse transcriptase | 0.25µl |
| Autoclaved water | 1.75µl |

The individual components were obtained from Taqman RT Reagents kit (Applied Biosystems, Carlsbad, CA, USA.).

#### 2.1.7.2 RT mixture for miRNA

| | |
|---|---|
| 10X RT buffer | 1.5µl |
| 100mM DeoxyNTPs mixture | 0.15µl |
| 20 U/µl RNase inhibitor | 0.19µl |
| 50 U/µl MultiScribe™ Reverse transcriptase | 1µl |
| Autoclaved water | 4.16µl |

The individual components for the miRNA RT mixture were obtained from Taqman miRNA RT kit (Applied Biosystems, Carlsbad, CA, USA).

### 2.1.8 Reagents for quantitative real-time polymerase chain reaction (PCR)

#### 2.1.8.1 SYBR green assay for mRNA

| | |
|---|---|
| 2X SYBR Green PCR Master Mixture | 10µl |
| Forward primer | 0.6µl (300nM) |

| | |
|---|---|
| Reverse primer | 0.6µl (300nM) |
| RT product | 5 µl |
| Autoclaved water | 3.8µl |

**2.1.8.2 SYBR green assay for mRNA/miRNA**

| | |
|---|---|
| 2X SYBR Green PCR Master Mixture | 10µl |
| Forward primer | 0.6µl (300nM) |
| Reverse primer | 0.6µl (300nM) |
| RT product | 1µl |
| Autoclaved water | 7.8µl |

The real-time PCR master mixture reagents and primer-probes were obtained from Applied Biosystems (Carlsbad, CA, USA.). Gene specific forward and reverse primers for Sybr Green assays were purchased from 1st Base (Singapore) or Integrated DNA Technologies (IDT, Singapore).

**2.1.8.3 Taqman assay for miRNA**

| | |
|---|---|
| 2X TaqMan Universal PCR Master Mixture | 10µl |
| Taqman miRNA probe | 1µl |
| RT product | 1.33µl |
| Autoclaved water | 7.67µl |

The TaqMan Universal PCR Master Mixture reagent was obtained from the Applied Biosystems (Carlsbad, CA, USA.).

**2.1.9 Reagents for Cloning**

**2.1.9.1 Reverse Transcription (RT)**

| | |
|---|---|
| Random hexamer | 1µl (100pmol) |

| | |
|---|---|
| 5X Reaction Buffer | 4µl |
| RiboLock™ RNase Inhibitor | 1µl (20U/µl) |
| dNTP Mixture, 10 mM each | 2µl |
| RevertAid™ Reverse Transcriptase | 1µl (200U/µl) |
| RNase free water | Top up to 20µl |

The individual components for the RT mixture were obtained from the RevertAid™ H Minus First Strand cDNA Synthesis Kit (Fermentas, Lithuania).

**2.1.9.2 Polymerase chain reaction (PCR)**

| | |
|---|---|
| 10X Taq buffer with $MgCl_2$ | 2.5µl |
| dNTP mixture | 2.5µl |
| Forward Primer (1 OD stock) | 2.5µl |
| Reverse Primer (1 OD stock) | 2.5µl |
| Taq DNA Polymerase (2 units/µl) | 1µl |
| Nuclease free water | Top up to 25µl |

**2.1.9.3 DNA agarose gel (1%)**

| | |
|---|---|
| Electrophoresis grade agarose | 0.5g |
| 1X TBE Buffer | 50ml |
| Ethidium bromide (10mg/ml) | 1ul |

Powdered agarose was mixed with 1X TBE buffer and heated to 100°C. It was then cooled to about 60◦C prior to the addition of ethidium bromide.

**2.1.9.4 Ligation**

#### 2.1.9.4.1 Ligation of TA cloning vector

| | |
|---|---|
| TOPO® vector | 1µl |
| Salt Solution | 1µl |
| Autoclaved water | Top up to 6µl |

The individual components for TA ligation were obtained from TOPO® TA Cloning Kit for Sequencing (Invitrogen, USA).

#### 2.1.9.4.2 Ligation of luciferase vector

| | |
|---|---|
| 2X DNA Ligation buffer | 5µl |
| T4 DNA Ligase (5U/µl) | 1µl |
| Autoclaved water | Top up to 10µl |

The individual components for ligation were obtained from Rapid DNA ligation kit (Roche, Germany).

### 2.1.9.5 Luciferase vectors

The various luciferase vectors used in this study are as follows:

pRL-CMV Vector (Promega, Madison, USA)

pMIR-REPORT™ Luciferase miRNA Expression Reporter Vector (Ambion, USA)

### 2.1.9.6 Competent cells

50µl of chemically competent TOP10 *E. coli* cells were used for each transformation procedure (Invitrogen, USA).

### 2.1.9.7 Ampicillin

Powdered ampicillin (Sigma, USA) was dissolved in autoclaved water to make concentrated stocks of 100mg/ml. The stocks were aliquoted into small volumes and stored at -20°C. Working concentration for ampicilin was 100µg/µl.

#### 2.1.9.8 Lysogeny broth (LB)

| | |
|---|---|
| Tryptone | 1% (w/v) |
| NaCl | 1% (w/v) |
| Yeast Extract | 0.5% (w/v) |

The pH of the LB Broth was adjusted to 7.0 prior to autoclaving. The LB broth was stored at 4°C.

#### 2.1.9.9 LB agar plates

Powdered agar (Gibco, Carlsbad, CA, US) 1.3% (w/v)

Agar was mixed with the LB broth and autoclaved. The mixture was cooled to approximately 55°C prior to the addition of the antibiotic ampicillin. 20ml of the molten agar was poured into each 90mm sterile petri dish and allowed to set at room temperature. The LB agar plates were sealed using parafilm and stored at 4°C in an inverted position. All plates were pre-warmed at 37°C for 1 hour before use.

### 2.1.10 Reagents for plasmid isolation

#### 2.1.10.1 Resuspension buffer

| | |
|---|---|
| Glucose | 50mM |
| Tris-HCL (pH 8.0) | 25mM |

EDTA (pH 8.0) 10mM

The resuspension buffer without glucose was sterilised by autoclaving and cooled to room temperature. Filter sterilised glucose was later added to the buffer and stored at 4°C.

**2.1.10.2 Lysis buffer**

NaOH 0.2M

SDS 1% (w/v)

Freshly prepared lysis buffer was used for plasmid extraction.

**2.1.10.3 Precipitation buffer**

Potassium acetate 3M

Glacial acetic acid 1.5% (w/v)

Precipitation buffer was stored at 4°C.

**2.1.10.4 RNase**

Powdered RNase dissolved in sterile nuclease free water at 10mg/ml. The solution was heated to 60°C and stored at - 20°C.

**2.1.11 Reagents for restriction enzyme digestion**

10X Restriction Enzyme Buffer 2µl

Autoclaved water Top up to 20µl

Restriction Enzyme 1 U

The restriction enzymes used in this study were purchased from Roche (USA).

For each reaction, the respective compatible buffers with 100% activity were used.

### 2.1.12 Reagents for sequencing

#### 2.1.12.1 Cycle sequencing reaction

| | |
|---|---|
| Terminator Ready Reaction Mixture | 4µl |
| Sequencing Buffer | 4µl |
| Primer (5 OD) | 1µl |
| Autoclaved water | Top up to 20µl |

#### 2.1.12.2 Purification of extension products reaction

| | |
|---|---|
| 3M Sodium acetate (pH 4) | 3µl |
| 95% Ethanol | 62.5µl |
| Nuclease free water | 14.5µl |

### 2.1.13 Reagents for miRNA array

#### 2.1.13.1 Calf intestinal phosphatase (CIP) master mix (per sample)

| | |
|---|---|
| Spike –in miRNA | 1µl |
| CIP Buffer | 0.5µl |
| CIP Enzyme | 0.5µl |

#### 2.1.13.2 miRNA labelling master mix (per sample)

| | |
|---|---|
| Labelling buffer | 3µl |
| $Hy_3$ Fluorescent label | 1.5µl |
| DMSO | 2µl |
| Labelling Enzyme | 2µl |

**2.1.13.3 Wash buffers**

**2.1.13.3.1 Wash buffer A**

| | |
|---|---|
| 20X Salt buffer | 60ml |
| 10% Detergent solution | 12ml |
| Sterile water | 528ml |

Wash buffer A together with two containers was pre warmed overnight to 56°C prior to use.

**2.1.13.3.2 Wash buffer B**

| | |
|---|---|
| 20X Salt buffer | 20ml |
| Sterile water | 380ml |

**2.1.13.3.3 Wash buffer C**

| | |
|---|---|
| 20X Salt buffer | 2ml |
| Sterile water | 198ml |

**2.1.14 Reagents for luciferase assay**

**2.1.14.1 Passive lysis buffer**

| | |
|---|---|
| 5X Passive lysis buffer | 1ml |
| Autoclaved water | 4ml |

Freshly prepared lysis buffer was used for luciferase assay

**2.1.14.2 Stop and Glo™ reagent**

| | |
|---|---|
| Stop and Glo™ substrate | 18µl |
| Stop and Glo™ buffer | 882µl |

### 2.1.15 Reagents for milliplex assay

#### 2.1.15.1 Antibody-immobilized beads

| | |
|---|---|
| Antibody beads | 60µl each |
| Bead diluent | Top up to 3ml |

#### 2.1.15.2 Wash buffer

| | |
|---|---|
| 10X Wash buffer | 30ml |
| Autoclaved water | 270ml |

#### 2.1.15.3 Standard

Reconstitute lysophilized rat cytokine standard with 250µl of autoclaved water. Serial dilution with assay buffer for the following dilution ratio: 1:4, 1:16, 1:64, 1:256, 1:1,024, and 1:4,096.

#### 2.1.15.4 Serum Matrix

Reconstitute lysophilized serum matrix with 1ml autoclaved water and 4ml assay buffer.

### 2.1.16 Reagents for CCL2 ELISA

#### 2.1.16.1 Substrate solution

Colour reagent A and B mixed together in equal volume within 15 min of use.

#### 2.1.16.2 Wash buffer

| | |
|---|---|
| 25X Wash buffer | 20ml |
| Autoclaved water | 420ml |

#### 2.1.16.3 Standard

Reconstitute the CCL2 Standard with 5.0 mL of Calibrator Diluent RD6Q. Serial dilution with Calibrator Diluent RD6Q for the following dilution ratio: 1:2, 1:4, 1:8, 1:16, 1:32, and 1:64.

## 2.2 Methods

### 2.2.1 Animal models

#### 2.2.1.1 Transient focal middle cerebral artery occlusion (intraluminal filaments or suture method)

Adult male Wistar rats were anesthetized with 200µl/100g weight of ketamine and xylazine (section 2.1.1.3) intraperitoneally. The animal was considered sufficiently anesthetized when there was a complete loss of pedal reflex. The body temperature of the animal was maintained by placing the animal on the Right Temp Homeothermic Warming System set at 37 ± 0.5°C (Kent Scientific Corporation, Torrington, CT).

The left Middle Cerebral Artery (MCA) was temporarily occluded using a 4/0 silicon rubber-coated monofilament (Doccol Corporation, CA, USA) as described by Longa *et al.* [206] (Figure 2.1). In brief, region around the neck of rat was shaved and cleaned with betadine™. A skin incision was made from the petrous bone to the scapula and the neck muscles were dissected to gain access to the common carotid artery (CCA). The CCA, the origin of internal carotid artery (ICA), the external carotid artery (ECA), the occipital artery (OA), and the superior thyroid artery (STA) were then exposed. OA and STA were cauterized using Aura 20 watt bipolar electrosurgical coagulator (Kirwan

Surgical Products, Inc., Marshfield, MA, US). The ICA and its bifurcation were dissected carefully as close to its entrance to the skull as possible. The pterygopalatine artery (PPA) that is proximal to the skull was ligated using 5/0 Silk Black, (B.Braun, Melsungen, Germany). The ECA was also ligated as proximal as possible. Microvascular clips (World Precision Instruments, Inc. Sarasota, FL, US) were applied to the proximal side of CCA and ICA.

The origin of the ECA was tied loosely with 5/0 Silk Black, and an incision was made on the ECA to allow access to the lumen. A 4/0 silicon rubber-coated monofilament was carefully inserted into the lumen of ECA, the stump of ECA was tightened together with the monofilament inside and the clip on ICA was removed. The monofilament was further introduced carefully into ICA until it reached the origin of middle cerebral artery (MCA), which is about 17mm from the bifurcation and the clip on CCA was released. After 60min, a clip was applied to CCA again and the suture was gently removed (to allow reperfusion to take place) and the ligation on ECA stump tightened and the incision was closed using 3/0 Silkam Black suture (B.Braun, Melsungen, Germany).

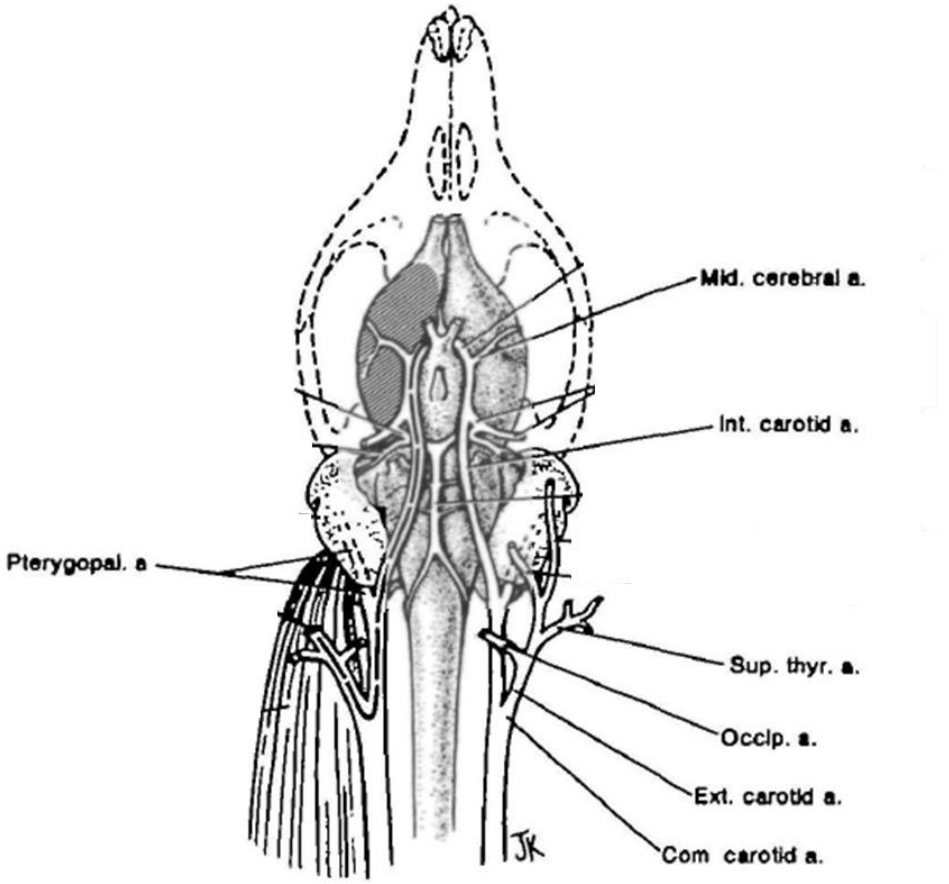


**Figure 2.1**: Diagram of vessels exploited in the middle cerebral artery occlusion (MCAo) in rat. Mid cerebral a: middle cerebral artery. Int. carotid a: internal carotid artery. Pterygopal. a: pterygopalatine artery. Sup. thyr. a: Superior thyroid artery. Occip. a: occipital artery. Ext. carotid a: external carotid artery. Com. carotid a: common carotid artery. Adapted from Longa *et al* [206].

#### 2.2.1.2 Laser-doppler flowmetry

To evaluate the cerebral blood flow (CBF) reduction in the MCA during occlusion, cerebral cortical perfusion was monitored by laser-doppler flowmetry (OxyFlo, Oxford Optronix, UK) during pre-occlusion, immediately post occlusion, at the time of reperfusion and before the end point of the experiments. CBF was expressed as a percentage relative to pre-occlusion baseline levels. CBF reduction of more than 80% was observed upon occlusion.

The area around the frontal bone of the skull was shaved and cleaned with betadine™. An incision was made in the midline of the scalp. The temporal muscle was dissected from the bone. The skull of the animal was thinned (1mm in diameter) at 2mm posterior and 6mm lateral to the bregma using a high speed micro-drill (Fine-Science Tool, USA). The tubing of Terumo® Surflo® Winged Infusion Set (Terumo Corporation, Tokyo, Japan) was cut into 5mm in length, glued on the hole using Krazy Glue All Purpose (Elmer's Products, Inc, Columbus, OH, USA) and fixed using ZAP Zip Kicker PT-29 CA Accelerator (Pacer Technology, CA, USA) to allow placement of a 5mm LDF probe (OxyFlo XP Probe, UK) for the measurement of CBF. The signals of CBF were digitized using a 4 channel Powerlab 4SP (ML760) and recordings were displayed with Chart 5 software (AD Instruments Pty Ltd, Australia).

#### 2.2.1.3 Neurological measurement for animal models

The neurological status of each rat was assessed as described by Bederson *et al.* [207]. The neurological examination was carried out for 5min. In brief, each rat was evaluated carefully at the following time-points 24, 72 and 120

hours post occlusion and graded according to the Bederson score (Table 2.1) [207].

Firstly, rats were held gently and carefully by the tail, suspended about a meter above the floor, and examined for any forelimb flexion. Rats that extended both forelimbs toward the floor with no other neurological deficit were graded 0. Rats that exhibited any extent of consistent forelimb flexion without any other abnormal behaviour were assigned grade 1.

Subsequently, rats were put on to a large sheet of soft, plastic coated paper (counter protection paper, Kimberly Clarke). While holding the tail of rats, lateral pressure was applied gently at the back of the rat's shoulder until the forelimbs slid for several inches and the same way of examination was repeated several times at different directions. Rats with severe neurological dysfunction exhibited minimal or no resistance consistently to lateral push toward the paretic side, and were assigned grade 2.

This group of rats was then permitted to move without any restriction and were examined for any circling behaviour. Grade 3 was given to rats which circled toward the paretic side consistently.

**Table 2.1**: Bederson score. Adapted from Bederson *et al* [207]

| **Severity** | **Grade** | **Observation** |
|---|---|---|
| Normal | 0 | No observable deficit |
| Moderate | 1 | Decrease forelimb flexion |
| Severe | 2 | Decrease forelimb flexion and resistance to lateral push |
| Very Severe | 3 | Same as grade 2 with circling |

#### 2.2.1.4 Histological analysis of brain infarct volume

At the end of different reperfusion time points (12, 24, 48, 72, 120 and 168 hours), the rats were sacrificed and their whole brains were sectioned coronally into 2mm slices using an Alto SA-2160 brain-sectioning matrix (Roboz, Gaithersburg, MD, USA). The slices were incubated in 2% TTC (section 2.1.1.4) and stained for 30min and photographed. The infarcted region was left unstained while the surrounding (surviving) area were stained red. The infarct volume was quantified using Image J (http://rsbweb.nih.gov/ij/) and calculated according to an indirect method [208] and expressed in $mm^3$, as below:

$$VI = \Sigma(CA - IA) \times \text{Thickness of slice} / (\text{conversion from pixel to } mm^2)$$

where VI = Infarct Volume

CA = Contralateral Area

IA = Ipsilateral Area

#### 2.2.1.5 Collection of brain slices

Ipsilateral and contralateral brain tissue samples (2nd to 5th slices) were immediately snap-frozen and stored at -80°C until use.

### 2.2.2 Patient recruitment

This study was approved by the Medical Ethics Committee of the University of Malaya Medical Centre (UMMC), Kuala Lumpur, Malaysia and the Institutional Review Board of the National University of Singapore (NUS). The patients were recruited from University Malaya Medical Centre (UMMC), Kuala Lumpur, Malaysia. The patients were admitted into UMMC via the

Neurology service and Accident and Emergency (A&E) department. Ischemic stroke in patients were diagnosed through either magnetic resonance imaging (MRI) or computed tomography (CT) scan. For acute samples, the patients' blood samples were collected between admission and 24 hours after (Day 1), between 24 hours to 48 hours (Day 2) and on seventh day after admission (Day 7). For the low or no risk ischemic stroke samples, blood was collected after patient discharge during their follow-up at outpatient clinics (3 months onwards). For healthy control samples, blood was collected from healthy volunteers for this study. The whole blood was stored in RNAlater™ (Ambion, Life Technology, Carlsbad, CA, USA) according to manufacturer's protocol and stored at -80°C until required.

### 2.2.3 Total RNA (include miRNAs) isolation

#### 2.2.3.1 Total RNA isolation from brain tissue/cells

100mg of rat brain was weighed out and placed in 1ml of TRIzol® reagent (Invitrogen, USA). The sample was homogenised until a fine consistency with no visible pieces were achieved. For cell culture, upon completion of a treatment, medium from 24-well plates was removed and washed with 1X PBS (section 2.1.6.2) twice. 1ml of TRIzol® reagent was added into three wells of a 24-well plate. The reagent was pipetted up and down to mix and lyse the cells before they were collected into a 1.5ml eppendorf tube. This was then used for RNA extraction according to manufacturer's protocol. Briefly, add 200µl of saturated chloroform to each sample and mixed vigorously before it was centrifuged at 12,000g for 15min at 4°C. The aqueous phase was transferred to a new tube. DNase I (3µl) was added to the aqueous phase and it

was incubated at 37°C for 20min, followed by the addition of 500µl of isopropanol. The mixture was mixed vigorously and left overnight at -80°C. Total RNA was pelleted by centrifuging at 12,000g for 10min at 4°C. The pellet was washed by centrifuging it with 1ml of ice-cold 75% ethanol (section 2.1.2.1) at 7,500g for 5min at 4°C. The supernatant was removed and the pellet was air dried before it was solubilised in 20µl of autoclaved water at 50°C for 5min. RNA concentration and integrity were determined by Nanodrop™ N2000C spectrophotometer (Thermo Scientific™, Rockford, IL, USA) and RNA gel electrophoresis. The presence of small RNA species was verified using denaturing gel (15% polyacrylamide) electrophoresis..

#### 2.2.3.2 Total RNA isolation from blood

Total RNA (including small RNA) from blood was isolated using Ambion Ribopure™ blood extraction kit according to manufacturer's protocol (Ambion, Texas, USA). Briefly, the sample was centrifuged at 14,500rpm for 5min. The supernatant was discarded and 1ml of lysis solution was added and vortexed vigorously to obtain a clear solution.

10µl acetic acid was added to each sample and incubated on ice for 5min. 400µl of Acid-Phenol: Chloroform was added and each sample was vortexed vigorously and centrifuged at 14,500rpm for 5min. The aqueous phase (~1.2ml) was transferred to fresh 15ml tube. 1ml of denaturation solution was added and vortexed thoroughly. 2.7ml of 100% ethanol was added and vortexed until the mixture became clear. 700µl of this solution was filtered through filter cartridge followed by a short spin (~7sec). This step was repeated until all solution went through the filter cartridge. The filter cartridge

was washed once with 700µl of Wash 1 (section 2.1.3.2) followed by a short spin (~7sec). Wash 2 (section 2.1.3.3) was used to wash through the filter cartridge twice 700µl each and centrifuged at 14,500rpm for 2min. The filter cartridge was transferred into a new labelled collection tube. 75µl of preheated (75°C) elution solution was added to the filter cartridge and incubated at room temperature for 2min and centrifuged at 14,500rpm for 2min. This step was repeated again. The concentration and integrity of RNA concentration were determined using Nanodrop™ N2000C spectrophotometer (Thermo Scientific™, Rockford, IL, USA and RNA gel electrophoresis. The presence of small RNA species was verified using denaturing gel (15% polyacrylamide) electrophoresis.

### 2.2.4 RNA gel electrophoresis

#### 2.2.4.1 Denaturing agarose (1%) gel electrophoresis

RNA was separated by electrophoresis in denaturing agarose gels containing formaldehyde. This is necessary to determine the integrity of the RNA isolated. Molten RNA gel (section 2.1.4.6) was poured into a horizontal gel-casting tray and an appropriate "comb" was inserted immediately to create wells for sample loading. Once the gel solidified, the "comb" was removed and the gel was placed into the electrophoresis tank containing 1X MOPS running buffer. RNA samples (0.4-1.0µg) were mixed with the sample buffer (section 2.1.4.5) and incubated for 10min at 65°C prior to loading into the gel. Electrophoresis was carried out at 80V for about 30 min and the migration of the bands was viewed using a UV transilluminator (Cell Biosciences, Santa Clara, CA, USA).

#### 2.2.4.2 Denaturing polyacrylamide (15%) gel electrophoresis (PAGE)

Denaturing polyacrylamide gel electrophoresis was used to analyse the presence and integrity of small RNAs. Molten PAGE gel was poured into a vertical gel casting tray and an appropriate "comb" was inserted immediately to create wells for sample loading. Once the gel solidified, the "comb" was removed and the gel was placed into the electrophoresis tank containing 1X TBE running buffer. The gel was pre-ran for 30min at 100V. Meanwhile the RNA samples (5-10μg) were mixed with the sample buffer (section 2.1.5.2) and heated up to 95°C for 5min. Samples were chilled immediately and pulse down prior to loading into the gel. Electrophoresis was carried out at 100V for about 1.5 hours and the migration of bands was visualized using a UV transilluminator (Cell Biosciences, Santa Clara, CA, USA).

### 2.2.5 LNA-based miRCURY LNA™ arrays

LNA-modified oligonucleotide (Exiqon, Denmark) probes for human, mouse and rat miRNAs annotated in based on miRBase version 11.0 and 12.0 annotations (http://www.miRBase.org) were used in the microarray [165].

#### 2.2.5.1 miRCURY LNA™ miRNA power labelling

All the components were thawed on ice. 500ng of total RNA (included miRNA) were used on each array which contains over 1769 capture probes that are complementary to human, rat, mouse and related viral sequences from miRBase version 11.0 and 12.0. Total RNAs were 3'-end-labelled with Hy3 dye using miRCURY LNA™ Power Labelling Kit (Exiqon, Vedbaek, Denmark).

Firstly, the master mix for CIP reaction (section 2.1.13.1) was prepared The CIP master mix was pulsed down and 2µl of CIP master mix was aliquoted into 0.5ml PCR tubes containing 2µl of total RNA (500ng). The tubes were pulsed down briefly and the mixture was incubated at 37°C for 30min and then at 95°C for 5min on PCR cycler (GeneAmp®, PCR System 9700, Applied Biosystems, CA, USA). The tubes were then snapped cool on ice to stop the reaction.

Secondly, master mix for labelling reaction was prepared (section 2.1.13.2) and pulsed down. 8.5µl of labelling master mix was added into each PCR tubes containing the 4µl CIP reaction. Following this step, all the samples had to be kept in the dark due to the use of fluorophores. The labelling reactions were pulsed down and incubated at 16°C for 90min followed by 65°C for 15min on PCR cycler.

#### 2.2.5.2 Array preparation for hybridization

Hybridization was performed on the MAUI® Hybridization system according to manufacturer's protocol (Exiqon, Vedbaek, Denmark). MAUI hybridization chamber was switched on and set at 56°C. The arrays were placed on the pre-heated block for 5min. The SL mixer was aligned and adhered carefully onto the array slide in the jig with the tab facing away from the barcode. MAUI® Gasket brayer was used to press the mixer-slide with moderate pressure to ensure complete adhesion. The mixer-slide assembly was then removed from the jig and placed back onto the 56°C heated block with the mixer side up. Samples must be loaded to the mixer-slide assembly within 30min.

### 2.2.5.3 Reagents preparation for hybridization

12.5µl of RNase free water was added into each labelled reaction products to bring the sample volume to 25µl. 25µl of 2X Hyb buffer was added into the sample, vortexed to mix and followed by pulsing down. Subsequently, the samples (labelled sample Hyb buffer, 50µl) were denatured at 95°C for 2min using PCR cycler with heated lid and then snapped cool on ice for 2 to 15min. The samples were spun briefly and heated to 56°C for 5min. Another 25µl of 2X Hyb buffer with 25µl of RNase free water was prepared and incubated at 56°C for wetting the tips prior to loading the samples to the mixer-slide assembly.

### 2.2.5.4 Hybridization of samples

The pipette tips were pre-wetted with (Hyb + RNase free water) solution. 45µl of sample was aspirated (avoid bubbles formation) and loaded carefully. The pipette tip was removed from the vent with the plunger depressed and surface of SL-mixer + array was wiped for any excess amount of samples. Adhesive port seals were placed directly over both the ports with forcep and pressed down simultaneously to seal the ports effectively. The loaded slide-mixer was then placed back onto the bay of MAUI mixer (pre-heated at 56°C) and loaded into the chamber slot. The bay was covered up with pre-wet humidity chamber and the lid was closed. The mixing chamber was switched on to mode B and the slides were incubated for 16hr at 56°C.

### 2.2.5.5 Washing of array chips

After 16hr of hybridization, the slide-mixer assembly was removed from MAUI and the slides were washed gently using 400ml of pre-warmed (56°C) buffer A (section 2.1.13.3.1) for 2min. The slides were then transferred to 200ml of buffer B (section 2.1.13.3.2) at room temperature for about 2min twice. Subsequently, they were washed with 200ml of buffer C (section 2.1.13.3.3) and slides were washed by gentle plunging of the rack for 2min. Finally, the slides were dipped in 99% ethanol for about 1min and dried by centrifugation (AllegraTM X-12R Centrifuge, eckman Coulter, CA, USA) at 800rpm, 25 C for 5min. before proceeding with scanning at 532nm (Hy3) in an InnoScan 700, microarray scanner (Innopsys, Carbonne, France) and analysed on Mapix® Version 4.3 software (Innopsys, France).

#### 2.2.5.6 Scanning of miRNA array chips and data anlaysis

Scanning of the miRNA array chips was performed using the InnoScan 700 Microarray scanner (Innopsys, Carbonne, France) and the signal intensity was quantified using Mapix® Version 4.3 software (Innopsys, Carbonne, France). Background subtraction and normalisation were performed on the raw signal intensity data using the internal controls inherent in the chips. Signal values lower than 300 were omitted from the analysis. For comparison purposes, the data was expressed as relative fold change with respect to controls. Statistical comparisons between controls and test samples are performed using Student's *t*-test and ANOVA. False discovery rate (FDR) was obtained, where FDR < 0.05 was considered to be statistically significant. Hierarchical clustering plot was generated using TIGR multiple experimental viewer software (http://www.tm4.org/mev/) [209].

### 2.2.6 Reverse Transcription (RT)

#### 2.2.6.1 RT of mRNA

200ng of total RNA (100ng/µl) was reverse transcribed using 8µl of RT mixture (section 2.1.7.1) to generate 10µl of first strand complementary DNA (cDNA). Synthesis of cDNA was carried out in a PCR machine (Perkin-Elmer, Germany) at 25°C for 10min; 37°C for 60min followed by 95°C for 5min.

#### 2.2.6.2 RT of miRNA

10ng of total RNA (2ng/µl) was reverse transcribed using 7µl of miRNA RT mixture (section 2.1.7.2) and 3ul of miRNA specific primers to generate 15µl of RT product. Synthesis was carried out using a PCR machine (Perkin-Elmer, Germany) at 16°C for 30min; 42°C for 30min followed by 85°C for 5min. The miRNA specific primers were purchased as MicroRNA Assay kits (Applied Biosystems, Carlsbad, CA, USA.).

### 2.2.7 Quantitative real-time PCR (qRT-PCR)

#### 2.2.7.1 qPCR (mRNA)

Gene expression was quantified using real-time PCR technology. SYBR green assay uses two (forward and reverse) gene specific primers and a DNA intercalating dye (SYBR). Sequences for gene specific primers were designed using the PrimerExpress 2.0 software and the respective mRNA strands. The primers were designed to yield amplicons of about 200bp. GAPDH was used as an internal calibrator. 15µl of the SYBR green assay master mix (section 2.1.8.1) was mixed with 5µl of RT product (section 2.2.6.1) and loaded into 96

well optical plates. The plates were sealed with a clear plastic cover and the PCR reaction was carried out on ABI PRISM 7900 cycler with thermal cycling conditions of 50°C for 2min, 95°C for 10min followed by 40 cycles at 94°C for 15sec and 60°C for 1min per cycle. All reagents and consumables needed for the PCR reaction were purchased from Applied Biosystems, Carlsbad, CA, USA.

#### 2.2.7.2 qPCR (stem-loop)

18.67µl of the Taqman miRNA mixture (section 2.1.8.2) was mixed with 1.33µl of miRNA RT product (section 2.2.6.2) and loaded into 96 well optical plates. The plates were sealed with a clear plastic cover and the PCR reaction was carried out on ABI PRISM 7900 cycler with thermal cycling conditions of 95°C for 10min followed by 40 cycles at 94°C for 15s and 60°C for 1min per cycle. All reagents and consumables needed for the PCR reaction was purchased from Applied Biosystems, USA. The miRNA specific primers were purchased as MicroRNA Assay kits (Applied Biosystems, Carlsbad, CA, USA).

### 2.2.8 First strand cDNA synthesis for cloning

Total RNA from rat brain or patient blood sample were used to reverse transcribe all expressed mRNAs. Briefly, the individual components of the Fermentas RevertAid™ H Minus First Strand cDNA Synthesis Kit (section 2.1.9.1) were thawed on ice. 1µg of total RNA and 1µl (100 pmol) of random hexamers were aliquoted into a sterile PCR tube containing RNase free water. The volume was adjusted to 12µl. The contents in the tube were mixed gently,

centrifuged briefly and incubated at 65°C for 5min. The tube was then chilled on ice. The remaining components of the Fermentas RevertAid™ H Minus First Strand cDNA Synthesis Kit were added to the tube. The contents were mixed and centrifuged briefly. The PCR tube was incubated at 25°C for 10min followed by 60min at 42°C. The reaction was terminated by heating at 70°C for 5min.

### 2.2.9 Polymerase chain reaction (PCR)

The PCR reaction was prepared in 0.2ml PCR tubes on ice according to section 2.1.9.2. 2.5µl of the cDNA (section 2.2.8) was directly used to perform PCR in a 25µl volume and the mixture in the PCR tubes were pulsed down. The PCR cycling conditions were set depending on the melting temperatures (Tm) of the primers used and the size of the product amplified. Typically the annealing temperature was set 5°C below the primer Tm for 45s while the extension temperature was kept at 72°C. At the end of the run, 10µl of the product was analysed on a 1% DNA agarose gel.

### 2.2.10 DNA agarose (1%) gel electrophoresis

Nucleic acids were separated by electrophoresis in 1% agarose gels. This is necessary to determine the integrity of the DNA isolated as well as to analyse PCR products. Molten DNA gel (section 2.1.9.3) was poured into a horizontal gel-casting tray and an appropriate "comb" was inserted immediately to create wells for sample loading. Once the gel solidified, the "comb" was removed and the gel was submerged into the electrophoresis tank containing 1X TBE running buffer. DNA samples were mixed with the 6X loading buffer (Thermo

Fisher Scientific, Fermentas, Waltham, MA, US) prior to loading into the gel. 100 basepairs or 1 kilo basepair markers (Thermo Fisher Scientific, Fermentas, Waltham, MA, US) were used according to the requirement. Electrophoresis was carried out at 90V for about 60min and the migration of the bands was viewed using a UV illuminator (Cell Biosciences, Santa Clara, CA, USA). Once the desired fragment size was obtained, the fragment was excised out with a clean, sharp scalpel for further processing.

### 2.2.11 DNA gel extraction

The excised DNA/PCR fragment from the agarose gel was weighed and QG buffer, (Qiagen, Hilden, Germany), volume equivalent to 3 times the weight of the gel was added. The gel and buffer mixture was incubated at 50°C for 10min. Once the gel fragment had completely dissolved, 1 gel volume of isopropanol was added and mixed. The sample was put through QIAquick spin column 700µl each time and centrifuged at 10,000rpm for 1min. The flow-through was discarded and the column was washed with 700µl of PE buffer (Qiagen, Hilden, Germany) twice and centrifuged at 10,000rpm for 1min each time. The QIAquick column was transferred into a clean 1.5ml microcentrifuge tube and the DNA was eluted with 20µl of autoclaved water by centrifuging for 2min at 13,000rpm. 2µl of the DNA was loaded onto a 1% agarose gel to check its integrity. The remaining DNA extract was used directly for cloning or stored at –20°C.

### 2.2.12 Ligation and transformation

Ligation reactions were carried out with a vector: insert molar ratio of approximately 1:3 to increase the ligation efficiency. Generally 50ng of plasmid vector was used for each reaction (section 2.1.9.4). The reaction mixture was incubated at room temperature for 30min before the addition of competent cells. Competent cells (Invitrogen, USA) stored in -80°C were thawed on ice. The ligation mixture was added to 50µl of the competent cells and mixed gently. The tube was kept in ice for 1 hour. The cells were then heat-shocked at 42°C for 90s, transferred to a 15ml falcon tube with 250µl SOC medium (Invitrogen, USA). The cells were incubated for 1 hour at 37°C before plating them on LB-agar plates (section 2.1.9.9) containing ampicillin (section 2.1.9.7). The plates were left at 37°C for about 18 hours to allow for the colonies to grow. Single colonies were then picked using sterile toothpicks and re-grown for 18 hours in 1.5ml LB broth (section 2.1.9.8) containing ampicillin.

### 2.2.13 Plasmid extraction

Plasmid extraction was necessary for further analysis of cloned fragments. 1.5ml of individually grown colonies were transferred into an eppendorf tube and centrifuged at maximum speed for 2min to pellet the cells. The supernatant was aspirated and the pellet was resuspended in 100µl of cold resuspension buffer (section 2.1.10.1). The tube was vortexed vigorously to resuspend the cells. 200µl of freshly prepared lysis buffer (section 2.1.10.2) was added and the tube was inverted 5-6 times to mix the contents. Following which, 150µl of cold precipitation buffer (section 2.1.10.3) was added to the tube and also mixed by inversion (5-6 times). The tube was incubated in ice

for 10min and centrifuged at maximum speed for 20min. The supernatant was transferred to a new tube. 3µl of RNase solution (section 2.1.10.4) was added to the supernatant and incubated at 60 °C for 20min. The tube was then cooled on ice and the plasmid was precipitated with addition of 450µl isopropanol and kept at -80°C for 1 hour. After which, the tube was spun at maximum speed for 30min. The supernatant was discarded and 200µl of 70% ethanol was added for wash. The sample was centrifuged at maximum speed for 30min. The supernatant was removed and the pellet was air dried before being resuspended in 20µl of autoclaved water.

### 2.2.14 Restriction enzyme digestion

To check for the presence of the cloned fragment in the vector, restriction enzyme digestion was carried out. About 1µg of the plasmid (section 2.2.13) was added to the restriction enzyme mixture (section 2.1.11). The final volume was adjusted to 20µl and the tubes were incubated at 37°C overnight. For double digests, buffers compatible to both enzymes were used, where the buffer and enzyme with low salt content were added first and incubated at 37°C for 6 hours, followed by addition of buffer and enzyme with high salt content and incubation at 37°C overnight. The digested products were analyzed on a 1% DNA agarose gel (section 2.2.10). If the digested fragment was needed for further sub-cloning, the fragment was excised out with a clean, sharp scalpel and the fragment would proceed with DNA gel extraction (section 2.2.11).

### 2.2.15 Sequencing

### 2.2.15.1 Cycle sequencing reaction

The PCR reaction was prepared in 0.2ml PCR tubes on ice according to section 2.1.12.1, with 1µl of plasmid template (section 2.2.13) and primer specific for the plasmid. The mixtures in the PCR tubes were pulsed down. The thermal cycling conditions were 96°C for 30sec, 50°C for 15sec followed by 60°C for 4min for 25 cycles. The product was kept on ice for further purification.

### 2.2.15.2 Purification of extension products and sequencing

80µl of reaction mix for purification of extension products (section 2.1.12.2) was added to each PCR tube and the mixture was transferred to 1.5ml eppendoff tube. The mixture was vortexed briefly and incubated on ice for 15min. After which, samples were centrifuged at maximum speed for 30min. The supernatant was aspirated and 500µl of 75% ethanol was added. The samples were centrifuged for 20min and the ethanol was removed. The pellet was dried by Hetovac (Heto lab equipment, Denmark). The pellet was resuspended in 10µl Hi-Di™ formamide and vortexed for 1min followed by a short pulse. The resuspended pellet was transferred to 96 well plate. The plate was sealed and heated at 95°C for 2min. The plate was loaded into ABI PRISM® 3100 genetic analyser (Applied Biosystems, Carlsbad, CA, USA). All reagents and consumables were purchased from Applied Biosystems, Carlsbad, CA, USA.

## 2.2.16 Cell culture

HeLa and HUVEC cell lines were cultured using complete DMEM (section 2.1.6.6). All cells were cultured in T-75 flasks and maintained in a 37°C incubator with 5% $CO_2$.

### 2.2.17 Transfection

#### 2.2.17.1 miRNA transfection

SiPORT NeoFX transfection reagent (Ambion, Carlsbad, CA, US) and Opti-MEM (Gibco, Carlsbad, CA, US) was complexed at a ratio of 1:49µl and incubated for 10min at room temperature. The miRNA (Ambion, Carlsbad, CA, US) was diluted to the appropriate concentration in 50µl Opti-MEM. The diluted transfection reagent and the miRNA were then mixed at a ratio of 1:1 and incubated at room temperature for another 20min. HUVECs were seeded at density of 3 x $10^4$per well in 24-well plates. 100µl of miRNA-transfection reagent mixture was added dropwise to the wells. After 24 hrs of incubation, 500µl of complete medium was added to the wells. Transfection was stopped at 48 hrs. Wells treated with negative control (Ambion, Carlsbad, CA, US), composed of scrambled miRNA fragments, were used to analyse the percentage of gene knockdown in the miRNA treated wells.

#### 2.2.17.2 miRNA and reporter plasmid transfection

For miRNA target interaction studies, anti-miRNA or miRNA mimic was co-transfected with luciferase reporter plasmids containing the target recognition sites. For miRNA transfection, lipofectamine transfection reagent (Invitrogen, Carlsbad, CA, US) and Opti-MEM (Gibco, Carlsbad, CA, US) was complexed at a ratio of 1.5:150µl and incubated for 10min at room temperature. The anti-

miRNA or miRNA mimic (Ambion, Carlsbad, CA, US) was diluted to a concentration of 50nM in 150µl Opti-MEM. The diluted transfection reagent and the miRNA complex were then mixed at a ratio of 1:1 and incubated at room temperature for further 20min. Cells were pre-seeded 24 hrs earlier at a density of 7 x $10^4$/per well in 24-well plates. The wells were washed with 300µl of Opti-MEM twice followed by the addition of 300µl of the miRNA-transfection reagent mixture. The cells were left in the 37°C $CO_2$ incubator for 3 hours. After which, preparation for plasmid transfection was done. For plasmid transfection, lipofectamine transfection reagent and Opti-MEM was complexed at a ratio of 3:150µl and incubated for 10min at room temperature. The luciferase plasmid (section 2.1.9.5) was diluted to a concentration of 200nM in 150µl Opti-MEM. 10ng of pRL-CMV (Promega, Madison, WI, USA) vector was used to determine transfection efficiency. The diluted transfection reagent and the plasmids were then mixed at a ratio of 1:1 and incubated at room temperature for further 20min. At the end of the 3 hours incubation the cells, the medium was aspirated and the cells were washed again with Opti-MEM. 300µl of the plasmid - transfection reagent mixture was then added to the cells. The cells were left in the 37°C $CO_2$ incubator for another 3 hrs. At the end of the 3 hours, the medium was replaced with complete medium (DMEM) and the cells were left to grow for 48 hrs, following which luciferase assays were performed.

### 2.2.18 Luciferase assay

To study the miRNA and its target gene interaction, the Dual-Luciferase® Reporter (DLR) assay system was used (Promega, Madison, WI, USA). This

assay allows the simultaneous expression and measurement of two individual reporter enzymes within a single system. The *Firefly* luciferase expression is used to correlate the effect of miRNA and its target interaction, while the activity of the co-transfected *Renilla* luciferase provides an internal control that serves as the baseline response. *Firefly* and *Renilla* luciferases, because of their distinct evolutionary origins, have dissimilar enzyme structures and substrate requirements. These differences make it possible to selectively discriminate between their respective bioluminescent reactions. 48 hours after transfection, the medium was aspirated and the cells were washed with 1X PBS (section 2.1.6.2). 100µl of passive lysis buffer was added to each well and the cells were left on IKA MS 3 basic (IKA, Wilmington, NC, US) for 10min with gentle agitation. The cells were then collected and centrifuged at maximum speed for 5min. The cell lysate was transferred into a separate tube. 25µl of the cell lysate was transferred into a white optical plate in a luminometer. Upon addition of 50µl Dual-Glo™ Luciferase substrate, the firefly luciferase activity was measured. To quench the *firefly* luciferase activity and read the *Renilla* luciferase activity, 50µl of Stop & Glo™ reagent was added and the luminescence measured.

### 2.2.19 Milliplex cytokine assay

Serum samples were obtained from rats subjected MCAo. Whole blood was collected and left to clot at 4°C for at least 2 hours and centrifuged at 1000 X g for 10 min. Serum was collected and stored in -80°C until required. Serum samples were diluted by five folds using serum matrix (section 2.1.15.4). The wells were pre-wetted with 200µl of assay buffer and placed on IKA MS 3

basic (IKA, Wilmington, NC, US) shaking for 10min at room temperature. Assay buffer was removed by vacuum. Add 25µl of standard or samples into each well. Add 25µl of serum matrix to standard wells and add 25µl of assay buffer to sample wells. Add 25µl of mixed beads (section 2.1.15.1) to each wells. The plate was sealed with a plate sealer and placed on IKA MS 3 basic (IKA, Wilmington, NC, US) shaking for overnight (18-20 hours) at 4°C. Remove fluid by vacuum and wash wells with 200µl of wash buffer (section 2.1.15.2) per well twice. Following that, add 25µl of detection antibody per well and place on IKA MS 3 basic (IKA, Wilmington, NC, US) shaking for 2 hours at room temperature. After which, add 25µl of Streptavidin-Phycoerythrin to each well. The plate was sealed and covered with lid, which was placed on shaker for another 30min at room temperature. The contents in wells were removed by vacuum and washed twice with 200µl of wash buffer per well. 150µl of sheath fluid was added to each well and placed on shaker for 5min to resuspend beads. The plate was placed in Luminex 100™ system (Luminex Corporation, Austin, TX, US) for detection and analysis. All reagents and consumables were purchased from Merck Millipore, Billerica, MA, US.

### 2.2.20 CCL2 ELISA

Serum samples were obtained from ischemic stroke patients. Samples were obtained in BD Vacutainer ® (Becton, Dickinson and Company, New Jersey, US) at Day 1, 2 and 7 upon admission. They were left for at least 30 minutes to allow clotting and subsequently, spun down and aliquot for storage at -80°C until required. To each well, add 50µl of Assay Diluent RD1-83 and 200µl of

standard (section 2.1.16.3) or sample. After which, covered the plate with adhesive strip and incubated at room temperature for 2 hours. Aspire each well and wash each well with 400µl of wash buffer (section 2.1.16.2) three times. Following that, 250µl of CCL2-conjugate was added to each well, covered with new adhesion strip and incubate at room temperature for 2 hours. Subsequently, the content of each well was removed and washed with 400µl of wash buffer per well thrice. 200µl of substrate solution (section 2.1.16.1) was added to each well and incubated for 30min at room temperature. To stop the reaction, 50µl of stop solution was added. Optical density at 450nm of each well was determined using Spectramax 190 microplate reader (Molecular Devices, US). Readings were corrected by subtracting optical density at 570nm. All reagents and consumables were purchased from R&D systems, Minneapolis, MN, US.

### 2.2.21 Statistical analysis

Statistical analysis was performed using two-tailed t-test for case-control comparison. For multiple comparisons, One-way ANOVA was used. For testing dichotomized parameters between stroke subtypes, chi-square test was performed on SPSS version 16. The significance level was kept at p value $< 0.05$. Pearson correlation was used to test correlation between 2 variables where Pearson correlation coefficient (R) $> \pm 0.9$ indicates strong correlation between the variables.

# Chapter 3

# Expression of circulating miRNAs in ischemic stroke patients and their possible roles in biological processes

### 3.1 miRNAs and ischemic stroke

miRNAs are endogenous, short (18-22 nucleotides), non-coding RNA that act as ribo-regulators for gene expression [137]. miRNA expression was first demonstrated to be dysregulated in rat animal model for ischemic stroke by Jeyaseelan *et al* [189], where blood and brain miRNA profile between control rats and rats subjected to middle cerebral artery occlusion (MCAo) was compared and found to be different. This implied that miRNAs had roles to play in the pathophysiology of ischemic stroke.

Subsequently, blood miRNAs were profiled in young ischemic stroke patients by Tan *et al* [190]. Following that, more data were published with regards to miRNAs and ischemic stroke. In 2014, Sepramanium *et al* [197] and Jickling *et al* [198] reported on miRNA profiles in ischemic stroke patients, both highlighting groups of miRNAs as potential ischemic stroke specific miRNAs.

Others published that miRNAs were potential diagnostic markers for ischemic stroke. miR-210 was reported to be down-regulated in blood of ischemic stroke patients and showed correlation with outcome of patients where good outcome correlated with higher miR-210 expression [199, 200]. In addition, miR-210 together with miR-21 (up-regulated in ischemic stroke), were shown to be potential biomarkers for atherosclerosis and stroke. [201]. miR-145 had been reported to have increased expression in ischemic stroke patients [202], though it was later shown by Tsai *et al* [201] that miR-145 expression between ischemic stroke patients and healthy controls were not statistically different. Other circulating miRNAs such as let-7b, miR-16, -30a, -124-3p, -126 and -233 have also been reported as potential biomarkers for ischemic

stroke [203-205]. miR-30a and miR-126 were shown to be down-regulated in ischemic stroke patients while let-7b showed down-regulation in large artery stroke patients and up-regulation in other stroke subtypes [203]. Circulating miR-223 level was reported to be increased in ischemic stroke patients by Wang *et al* [204]. As for miR-16 and -124-3p, they were described as markers to distinguish between haemorrhagic and ischemic stroke, where miR-16 concentration was higher and miR-124-3p concentration was lower in ischemic stroke patients and vice versa for haemorrhagic stroke patients [205].

Interestingly, miR-146aG allele and miR-146aG/-149T/-196a2C/-499G allele combination polymorphisms of miRNAs have also been found to predispose individual to ischemic stroke, with ischemic stroke occurrence [210].

Among the recent reports published, only Tan *et al* [190] and Jickling *et al* [198] highlighted a few biological pathways involved in ischemic stroke. More information on the processes taking place during ischemic stroke is still unknown. This study seeks to conduct an in-depth analysis of biological pathways involved in ischemic stroke and possibly identify the crucial processes influencing ischemic stroke pathophysiology and pathogenesis.

### 3.2 Patient recruitment and sample collection

The patients for this study were recruited from University Malaya Medical Centre (UMMC), Kuala Lumpur, Malaysia. The patients were admitted into UMMC via the Neurology service and Accident and Emergency (A&E) department. Ischemic stroke patients were diagnosed through either magnetic

resonance imaging (MRI) or computed tomography (CT) scan. The patients' peripheral blood samples were collected between admission and 24 hours after (Day 1), between 24 hours to 48 hours (Day 2) and on seventh day after admission (Day 7). Blood was collected on various timepoints during the acute phase of ischemic stroke. The whole blood was stored in RNAlater™ (Ambion, Life Technology, Carlsbad, CA, USA) according to manufacturer's protocol and stored at -80°C until required. The patients were classified into the different stroke subtypes according to the Trial of Org 10172 in Acute Stroke Treatment (TOAST) classification [8], based on clinical symptoms and upon further investigation. Majority of the ischemic stroke cases were cardioembolic, large-artery and small vessel occlusion (lacunar). The patients' clinical data was separated according to the respective ischemic stroke subtype (TOAST classification).

The outcomes of the patients were assessed using the modified Rankin scale (mRS) [211]. mRS scores patient outcome on a scale of 0 to 6, where 0 signify no symptoms and 6 represents the patient is dead (Table 3.1). The patients' outcomes were usually assessed a week after admission. For clinical purposes, mRS was dichotomized into good and poor outcome. In general, mRS $< 2$ was denoted as good outcome, while mRS $\geq 2$ indicated poor outcome. Clinical data were collected from the patients and used for further analysis.

For healthy control samples, healthy volunteers were recruited for this study. Exclusion criteria included hypertension, dyslipidaemia, diabetes, cardiac ailments, previous stroke, cancer and other inflammatory diseases.

**Table 3.1:** Grading of modified Rankin scale (mRS). Adapted from Farrell *et al* [211].

| **Modified Rankin Scale (mRS)** | **Description** |
|---|---|
| 0 | No symptoms |
| 1 | No significant disability despite some symptoms; able to carry out usual activities |
| 2 | Slight disability; unable to carry out all previous activities; able to look after own affairs without assistance |
| 3 | Moderate disability; require some help; able to walk without assistance |
| 4 | Moderately severe disability; unable to attend to bodily needs without assistance; unable to walk without assistance |
| 5 | Severe disability; bedridden and incontinent; requires constant nursing care and attention |
| 6 | Dead |

There were a total of 48 acute ischemic stroke patients recruited for this study. They constituted 14 large artery stroke patients, 20 cardioembolic stroke patients and 14 small vessel stroke patients (Table 3.2). Various parameters of the patients were dichotomized; Chi-square test was used for statistical testing performed on SPSS version 16.

Age (p-value = 0.215) and gender proportion (p-value = 0.708) were found to be similar among the stroke subtypes (Table 3.2). As for risk factors, incidence of hypertension (p-value = 0.188), dyslipidaemia (p-value = 0.849), type 2 diabetes (p-value = 0.285) and alcohol consumption (p-value = 0.289) were shown to be similar among the stroke subtypes, while there were more smokers (p-value = 0.024; 4 patients; 28.5%) in small vessel stroke patients (Table 3.2). As for comorbidities, number of patients with ischemic heart disease (p-value = 0.267), aortic stenosis (p-value = 0.489) and previous stroke (p-value = 0.074) were similar among the stroke subtypes (Table 3.2). There was significantly higher number of cardioembolic stroke patients with atrial fibrillation (p-value < 0.001; 16 patients; 80.0%) as compared with large artery stroke and small vessel stroke patients (Table 3.2). There were also greater numbers of patients with good outcome (p-value = 0.029; 5 patients; 35.7%) in small vessel stroke as compared with large artery stroke and cardioembolic stroke (Table 3.2).

**Table 3.2:** Patient demographics of acute ischemic stroke patients.

| | Large-artery (n=14) | Cardioembolic (n=20) | Small vessel (n=14) | p-value |
|---|---|---|---|---|
| Age, mean ± standard deviation | 62.3 ± 11.3 | 66.8 ± 15.2 | 64.4 ± 11.6 | 0.215 |
| Gender, Male, n (%) | 8 (57.1%) | 10 (50.0%) | 9 (64.3%) | 0.708 |
| Gender, Female, n (%) | 6 (42.9%) | 10 (50.0%) | 5 (35.7%) | |
| **Risk Factors** | | | | |
| Hypertension, n (%) | 11 (78.5%) | 10 (50.0%) | 10 (71.4%) | 0.188 |
| Dyslipidaemia, n (%) | 11 (78.5%) | 14 (70.0%) | 10 (71.4%) | 0.849 |
| Type 2 diabetes, n (%) | 6 (42.8%) | 6 (30.0%) | 8 (57.1%) | 0.285 |
| Smoking, n (%) | 1 (7.1%) | 0 (0.0%) | 4 (28.5%) | 0.024 |
| Alcohol consumption, n (%) | 1 (7.1%) | 0 (0.0%) | 0 (0.0%) | 0.289 |
| **Comorbidities** | | | | |
| Ischemic heart disease, n (%) | 2 (14.2%) | 8 (40.0%) | 4 (28.5%) | 0.267 |
| Atrial fibrillation, n (%) | 0 (0.0%) | 16 (80.0%) | 0 (0.0%) | <0.001 |
| Aortic stenosis, n (%) | 0 (0.0%) | 1 (5.0%) | 0 (0.0%) | 0.489 |
| Previous stroke, n (%) | 4 (28.5%) | 6 (30.0%) | 0 (0.0%) | 0.074 |
| **Functional outcome (mRS)** | | | | |
| Good outcome, mRS <2, n (%) | 1 (7.1%) | 1 (5.0%) | 5 (35.7%) | 0.029 |
| Poor outcome, mRS ≥2, n (%) | 13 (92.9%) | 19 (95.0%) | 9 (64.3%) | |

### 3.3 miRNA profiles in ischemic stroke patients

Total RNA (including small RNAs) was isolated from the peripheral blood using Ribopure™ Blood RNA purification kit (Ambion, Life Technology, Carlsbad, CA, USA) according to manufacturer's protocol. The concentration and integrity of the RNA was determined using Nanodrop™ N2000C spectrophotometer (Thermo Scientific™, Rockford, IL, USA) and RNA gel electrophoresis (1% agarose). The presence and integrity of small RNA species (less than 200 nucleotides) were verified using denaturing polyacrylamide gel electrophoresis (15% polyacrylamide).

The isolated RNA was used for miRNA microarray that was performed on miRCURY LNA miRNA array (version 11.0) platform, based on miRBase version 11.0 and 12.0 annotations [165]. The samples were pooled according to stroke subtype and time-point for each array chip. All probes with positive raw signal intensities were analysed and statistical testing was performed to obtain false discovery rate (FDR), where miRNAs with FDR <0.05 were selected. The profiles were visualised using TIGR multiple experiment viewer (TMEV) [209].

In total, 352 miRNAs were detected in this study (Supplementary Table 1). Using these 352 miRNAs, hierarchical clustering (HCL) was performed on the samples. HCL demonstrated that the control samples segregated away from the patients' samples, signifying there was a difference in miRNA profile between healthy controls and ischemic stroke patients (Figure 3.1).

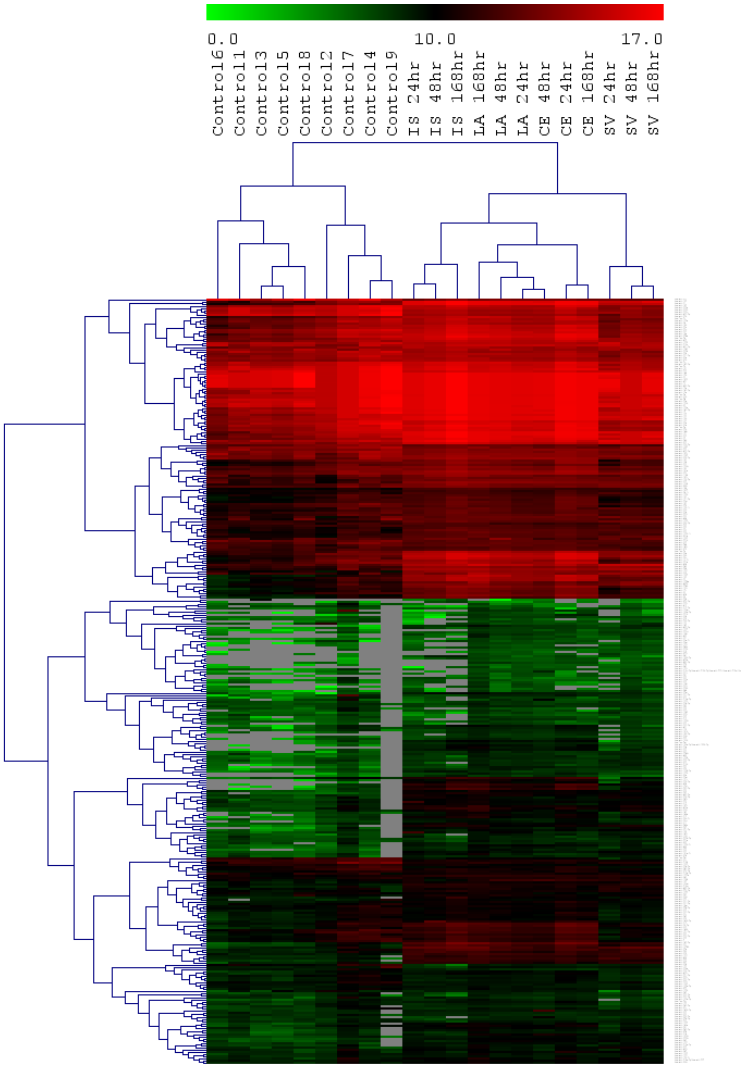


**Figure 3.1:** Hierarchical clustering analysis of 352 miRNAs in ischemic stroke patients and healthy controls. The miRNA expression were expressed logarithm of raw intensity. Green represents low signal intensity. Red represents high signal intensity. Grey represents absence. Patient samples were named according to their respective stroke subtype (IS: ischemic stroke; LA: large artery; CE: cardioembolic; SV: small vessel) and their respective time-points.

Further analysis was performed where HCL of miRNA expression values in the patient samples were converted to signal log ratio (SLR; Figure 3.2). SLR was obtained by logarithm of fold change with respect to control samples. The samples showed the segregation according to stroke subtypes (Large artery: LA, cardioembolic: CE and small vessel: SV). This signified that the miRNA profiles during acute phase of ischemic stroke could be correlated with underlying etiology of the stroke subtypes. Hence this information could be used to uncover the mechanism for the pathogenesis of each subtype.

### 3.4 miRNAs with similar expression in all acute ischemic stroke samples

From the miRNA profiling, there were 147 miRNAs that showed similar expression in all the samples (Table 3.3). Among these 147 miRNAs, 22 miRNAs were down-regulated in all samples while the remaining 125 miRNAs were up-regulated in all samples.

miR-21 and -223 which were previously reported to be increased in ischemic stroke patients were also detected in this study as increased in all acute ischemic stroke samples [201, 204]. Thus, suggesting that possible biomarkers for ischemic stroke can be found among these 147 miRNAs.

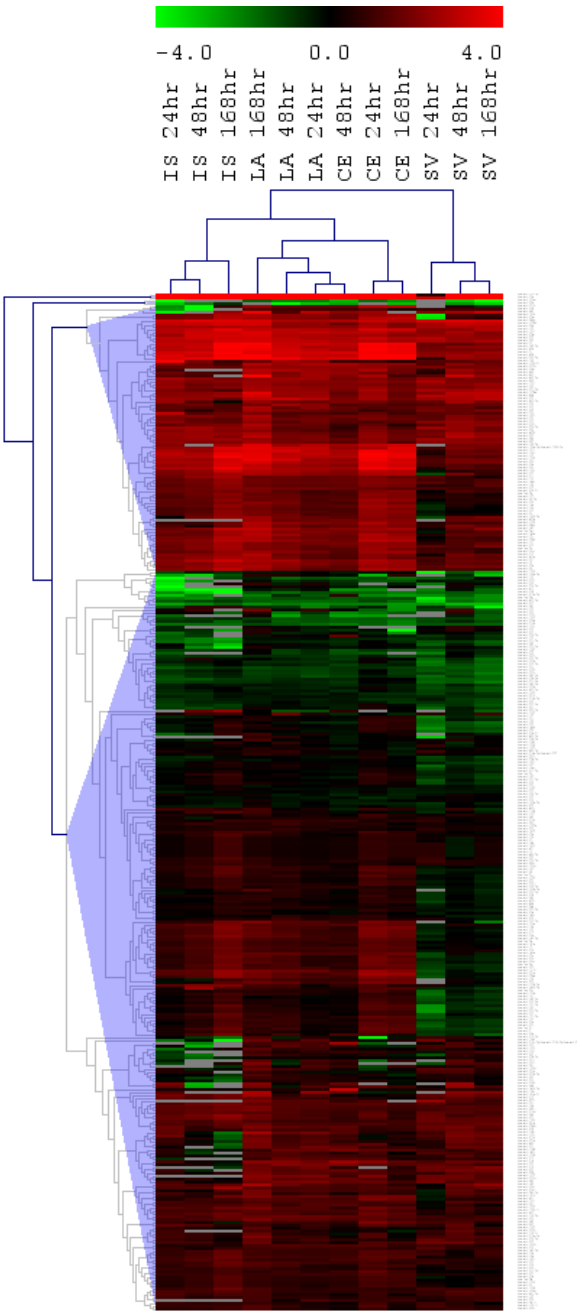


**Figure 3.2:** Hierarchical clustering analysis of 352 miRNAs in ischemic stroke patients. The miRNA expression were expressed as signal log ratio (SLR) with respect to control samples. Green represents down-regulation. Red represents up-regulation. Grey represents absence. Samples from cohort 1 were named according to their respective stroke subtype (IS: ischemic stroke; LA: large artery; CE: cardioembolic; SV: small vessel) and their respective time-points.

**Table 3.3**: Expression of 147 miRNAs showing similar expression in acute ischemic stroke sample. miRNAs were expressed as fold change with respect to healthy controls. LA: large artery stroke. CE: cardioembolic stroke. SV: small vessel stroke.

| Hsa-miRNA | IS 24hr | IS 48hr | IS 168hr | LA 24hr | LA 48hr | LA 168hr | CE 24hr | CE 48hr | CE 168hr | SV 24hr | SV 48hr | SV 168hr |
|---|---|---|---|---|---|---|---|---|---|---|---|---|
| Let-7d* | -3.70 | -4.75 | -2.51 | -2.20 | -2.26 | -2.94 | -2.35 | -2.69 | -2.16 | -13.00 | -3.86 | -4.65 |
| Let-7e | 3.19 | 4.00 | 5.81 | 2.72 | 3.83 | 4.08 | 5.41 | 2.60 | 3.91 | 1.99 | 2.08 | 1.67 |
| Let-7f | 1.49 | 1.79 | 2.57 | 1.54 | 1.60 | 1.77 | 2.21 | 1.62 | 2.01 | 1.01 | 1.00 | 1.31 |
| miR-15a | 1.73 | 2.08 | 2.97 | 1.79 | 1.85 | 2.05 | 2.57 | 1.88 | 2.33 | 2.06 | 1.16 | 1.98 |
| miR-15b* | 7.81 | 6.55 | 13.07 | 8.24 | 7.56 | 12.53 | 16.42 | 6.38 | 13.15 | 1.40 | 3.21 | 3.22 |
| miR-17 | 1.92 | 2.31 | 3.31 | 1.99 | 2.06 | 2.28 | 2.85 | 2.09 | 2.59 | 1.05 | 1.22 | 1.07 |
| miR-19a | 1.87 | 2.25 | 3.22 | 1.93 | 2.00 | 2.02 | 2.77 | 2.03 | 2.52 | 1.26 | 1.25 | 1.75 |
| miR-19b | 2.63 | 3.16 | 4.53 | 2.72 | 2.82 | 3.12 | 3.91 | 2.87 | 3.54 | 1.57 | 1.77 | 2.69 |
| miR-20b* | 2.35 | 2.50 | 5.94 | 2.34 | 2.08 | 2.66 | 2.40 | 1.99 | 2.16 | 1.18 | 2.68 | 3.14 |
| miR-21 | 9.73 | 11.03 | 17.18 | 10.09 | 10.67 | 11.82 | 14.79 | 10.70 | 13.42 | 4.53 | 4.76 | 5.56 |
| miR-23a | 1.19 | 1.69 | 2.50 | 1.17 | 1.48 | 1.68 | 1.67 | 1.06 | 1.71 | 1.16 | 1.24 | 1.09 |
| miR-23b | 1.61 | 2.06 | 2.85 | 1.41 | 2.12 | 2.39 | 2.33 | 1.39 | 2.07 | 1.24 | 1.53 | 1.23 |
| miR-25 | 4.21 | 4.10 | 6.48 | 4.11 | 4.98 | 5.71 | 6.01 | 3.41 | 5.39 | 2.21 | 3.07 | 2.81 |
| miR-25* | 2.45 | 3.33 | 3.82 | 2.40 | 2.53 | 2.96 | 2.70 | 2.50 | 2.12 | 2.48 | 1.93 | 2.00 |
| miR-27a | 3.57 | 4.71 | 6.53 | 3.34 | 4.63 | 6.61 | 5.13 | 2.84 | 5.06 | 2.69 | 3.80 | 3.59 |
| miR-27a* | 5.55 | 9.92 | 10.23 | 6.69 | 6.86 | 10.87 | 6.06 | 6.03 | 4.55 | 5.05 | 5.34 | 4.35 |
| miR-29a | 5.14 | 5.53 | 10.72 | 5.14 | 5.59 | 8.00 | 12.14 | 4.38 | 9.52 | 2.16 | 2.63 | 2.21 |
| miR-29b | 6.35 | 6.27 | 10.99 | 5.81 | 6.99 | 10.71 | 12.16 | 5.62 | 10.81 | 2.41 | 3.65 | 3.82 |
| miR-29b-2* | 3.14 | 3.24 | 3.64 | 2.01 | 2.67 | 3.65 | 4.08 | 2.35 | 4.25 | 1.04 | 2.34 | 1.95 |
| miR-29c | 6.39 | 6.61 | 13.48 | 5.94 | 6.08 | 8.74 | 14.80 | 5.69 | 12.56 | 1.35 | 2.74 | 2.29 |
| miR-29c* | 2.91 | 3.21 | 4.85 | 3.68 | 4.43 | 5.45 | 5.51 | 2.60 | 5.69 | 2.02 | 2.54 | 1.73 |
| miR-32 | 8.39 | 8.49 | 17.49 | 9.18 | 8.92 | 15.90 | 20.00 | 8.16 | 14.20 | 3.00 | 2.82 | 3.58 |
| miR-32* | -2.64 | -1.98 | -1.63 | -1.99 | -1.92 | -2.27 | -1.62 | -1.72 | -1.95 | -2.43 | -2.59 | -3.01 |

| Hsa-miRNA | IS 24hr | IS 48hr | IS 168hr | LA 24hr | LA 48hr | LA 168hr | CE 24hr | CE 48hr | CE 168hr | SV 24hr | SV 48hr | SV 168hr |
|---|---|---|---|---|---|---|---|---|---|---|---|---|
| miR-33a | 38.94 | 37.02 | 100.04 | 50.54 | 44.51 | 121.51 | 68.33 | 43.26 | 80.84 | 8.92 | 23.92 | 43.69 |
| miR-34b | 2.82 | 3.46 | 4.94 | 2.12 | 2.34 | 3.36 | 2.92 | 1.89 | 1.77 | 3.09 | 1.93 | 2.36 |
| miR-92b | 1.85 | 1.63 | 2.15 | 1.52 | 1.62 | 1.98 | 2.01 | 1.35 | 1.50 | 1.01 | 1.57 | 1.37 |
| miR-98 | 4.24 | 5.09 | 8.60 | 2.57 | 3.99 | 5.81 | 7.10 | 2.76 | 6.19 | 2.44 | 2.38 | 2.37 |
| miR-99b* | 1.55 | 1.59 | 1.89 | 1.44 | 1.58 | 2.44 | 1.85 | 1.15 | 1.18 | 1.69 | 1.87 | 1.54 |
| miR-101 | 3.45 | 4.15 | 5.94 | 3.57 | 3.54 | 4.09 | 5.12 | 3.75 | 4.64 | 1.59 | 2.32 | 3.02 |
| miR-101* | 6.52 | 5.19 | 10.22 | 7.76 | 10.59 | 11.79 | 13.72 | 6.18 | 11.12 | 1.52 | 3.22 | 2.84 |
| miR-103 | 2.83 | 3.40 | 4.87 | 2.92 | 3.03 | 3.35 | 4.19 | 3.08 | 3.81 | 2.13 | 1.90 | 2.34 |
| miR-107 | 2.34 | 2.98 | 4.03 | 2.44 | 3.12 | 3.35 | 4.40 | 2.46 | 3.99 | 1.48 | 1.66 | 1.41 |
| miR-125b | -2.21 | -1.34 | -1.65 | -1.02 | -1.25 | -1.23 | -1.21 | -1.34 | -1.11 | -27.06 | -2.51 | -6.13 |
| miR-125b-1* | 2.05 | 2.11 | 2.44 | 2.27 | 2.23 | 2.84 | 2.81 | 2.16 | 2.10 | 1.42 | 2.11 | 1.44 |
| miR-125b-2* | 4.19 | 3.06 | 2.25 | 6.58 | 5.48 | 7.20 | 5.01 | 6.17 | 4.69 | 2.44 | 4.62 | 3.34 |
| miR-129-5p | 2.48 | 2.09 | 3.15 | 3.20 | 3.29 | 3.18 | 2.75 | 2.90 | 2.53 | 2.00 | 1.76 | 2.05 |
| miR-135b | 1.90 | 1.96 | 3.39 | 3.87 | 4.88 | 7.02 | 6.78 | 3.62 | 4.58 | 1.58 | 2.21 | 2.07 |
| miR-138-1* | 1.74 | 1.82 | 1.91 | 1.35 | 1.83 | 2.41 | 2.50 | 1.30 | 1.24 | 2.18 | 1.70 | 1.43 |
| miR-140-5p | 7.27 | 9.12 | 17.60 | 6.50 | 9.30 | 14.93 | 15.41 | 7.08 | 13.24 | 3.44 | 4.52 | 4.63 |
| miR-142-3p | 1.73 | 2.07 | 2.97 | 1.78 | 1.85 | 2.04 | 2.56 | 1.88 | 2.32 | 1.80 | 1.16 | 1.97 |
| miR-143 | 3.08 | 4.00 | 8.47 | 3.75 | 5.36 | 8.24 | 5.52 | 4.47 | 6.23 | 1.15 | 2.88 | 4.83 |
| miR-144* | 2.93 | 3.52 | 5.05 | 3.03 | 3.14 | 3.47 | 4.35 | 3.19 | 3.95 | 2.76 | 1.97 | 2.59 |
| miR-146b-3p | 1.30 | 1.38 | 1.19 | 1.61 | 1.45 | 1.63 | 1.25 | 9.76 | 1.32 | 1.49 | 1.72 | 1.50 |
| miR-148a | 2.82 | 3.30 | 5.75 | 3.61 | 5.59 | 7.38 | 6.90 | 3.30 | 5.06 | 1.42 | 2.85 | 2.77 |
| miR-150 | -2.76 | -3.97 | -5.90 | -1.11 | -1.18 | -1.15 | -1.48 | -1.47 | -1.80 | -1.46 | -1.15 | -1.62 |
| miR-181a-2* | 3.58 | 2.67 | 3.60 | 2.47 | 1.65 | 6.07 | 1.02 | 1.17 | 1.29 | 2.85 | 3.75 | 3.02 |
| miR-183* | 1.96 | 2.46 | 2.86 | 1.75 | 1.77 | 1.90 | 2.42 | 2.19 | 1.80 | 1.83 | 1.59 | 1.43 |
| miR-184 | 2.71 | 2.86 | 3.31 | 2.42 | 2.50 | 3.71 | 2.08 | 2.20 | 1.93 | 2.17 | 2.56 | 2.36 |
| miR-187* | 3.92 | 4.40 | 3.55 | 3.21 | 2.68 | 6.70 | 3.59 | 3.44 | 2.80 | 2.65 | 4.10 | 3.53 |

| Hsa-miRNA | IS 24hr | IS 48hr | IS 168hr | LA 24hr | LA 48hr | LA 168hr | CE 24hr | CE 48hr | CE 168hr | SV 24hr | SV 48hr | SV 168hr |
|---|---|---|---|---|---|---|---|---|---|---|---|---|
| miR-190 | 6.71 | 7.13 | 15.10 | 7.27 | 8.35 | 12.52 | 15.48 | 7.11 | 13.34 | 2.06 | 2.71 | 2.47 |
| miR-193b* | 1.44 | 1.47 | 1.37 | 2.29 | 2.54 | 2.18 | 2.53 | 2.40 | 1.72 | 2.08 | 1.71 | 1.45 |
| miR-195 | 7.30 | 8.76 | 12.37 | 7.26 | 7.71 | 8.64 | 10.62 | 6.25 | 9.82 | 4.59 | 4.90 | 7.18 |
| miR-196a* | 2.34 | 2.09 | 2.50 | 1.67 | 1.70 | 2.20 | 1.85 | 1.65 | 1.62 | 1.84 | 2.51 | 2.17 |
| miR-197 | 2.00 | 1.45 | 1.76 | 1.67 | 1.64 | 2.08 | 1.80 | 1.42 | 1.65 | 1.49 | 1.86 | 1.94 |
| miR-198 | 19.03 | 3.93 | 1.75 | 4.79 | 5.72 | 3.01 | 1.87 | 1.75 | 1.38 | 2.60 | 2.49 | 3.03 |
| miR-199a-3p | 5.15 | 5.18 | 11.12 | 8.32 | 9.04 | 12.31 | 6.43 | 5.05 | 11.54 | 2.13 | 3.94 | 3.56 |
| miR-200b* | 2.99 | 3.44 | 2.97 | 4.99 | 4.92 | 5.23 | 4.88 | 5.16 | 3.74 | 3.89 | 3.54 | 3.70 |
| miR-206 | 3.87 | 2.88 | 2.59 | 3.51 | 3.33 | 5.77 | 3.83 | 2.74 | 3.09 | 2.60 | 4.33 | 3.27 |
| miR-208a | -1.73 | -1.67 | -2.89 | -2.47 | -2.72 | -1.52 | -2.82 | -2.79 | -4.08 | -2.14 | -1.44 | -2.23 |
| miR-210 | 4.26 | 4.16 | 5.48 | 2.69 | 3.33 | 7.09 | 4.50 | 2.44 | 3.76 | 1.21 | 3.56 | 2.91 |
| miR-221 | 4.30 | 6.46 | 9.19 | 3.95 | 6.20 | 6.28 | 6.77 | 3.62 | 5.51 | 1.99 | 3.24 | 3.14 |
| miR-223 | 3.19 | 4.17 | 6.18 | 2.86 | 3.84 | 4.21 | 5.16 | 3.24 | 4.76 | 2.77 | 2.41 | 3.89 |
| miR-300 | 1.85 | 1.93 | 3.10 | 2.06 | 2.23 | 2.51 | 2.17 | 1.83 | 1.62 | 1.95 | 1.44 | 1.42 |
| miR-302c* | 1.31 | 1.68 | 1.01 | 2.98 | 2.77 | 4.08 | 2.63 | 3.08 | 1.45 | 3.28 | 3.17 | 2.44 |
| miR-320b | -1.68 | -1.36 | -1.18 | -2.05 | -1.82 | -1.89 | -1.00 | -1.74 | -1.81 | -2.71 | -2.19 | -3.08 |
| miR-320c | -1.81 | -1.57 | -1.32 | -2.12 | -1.86 | -2.03 | -1.08 | -1.82 | -1.91 | -1.94 | -2.44 | -3.78 |
| miR-326 | 1.71 | 1.26 | 1.87 | 1.89 | 2.05 | 2.02 | 1.79 | 2.00 | 1.57 | 2.57 | 1.63 | 1.77 |
| miR-331-5p | -3.24 | -4.12 | -4.88 | -1.53 | -1.42 | -1.35 | -1.00 | -1.65 | -1.63 | -2.54 | -1.82 | -2.88 |
| miR-338-3p | 29.70 | 25.30 | 51.57 | 18.54 | 28.16 | 44.69 | 23.43 | 19.01 | 27.81 | 1.40 | 16.28 | 27.43 |
| miR-339-5p | -1.86 | -1.43 | -1.05 | -1.50 | -1.32 | -1.40 | -1.49 | -2.01 | -1.33 | -3.39 | -2.28 | -3.20 |
| miR-340* | 2.64 | 2.87 | 3.44 | 2.21 | 2.47 | 3.78 | 2.20 | 2.05 | 1.83 | 2.08 | 2.39 | 2.33 |
| miR-342-3p | -2.23 | -1.59 | -1.40 | -2.46 | -1.73 | -1.86 | -1.35 | -1.99 | -1.63 | -3.27 | -1.93 | -2.92 |
| miR-342-5p | -1.43 | -1.14 | -1.33 | -1.41 | -1.28 | -1.17 | -1.15 | -1.61 | -1.36 | -2.15 | -1.35 | -2.00 |
| miR-374b | 3.86 | 4.47 | 7.53 | 3.93 | 5.08 | 6.87 | 7.94 | 3.25 | 6.87 | 1.27 | 2.39 | 2.13 |
| miR-374b* | 3.07 | 1.69 | 2.52 | 2.48 | 2.75 | 3.93 | 1.77 | 2.77 | 1.88 | 3.18 | 3.67 | 2.63 |

| Hsa-miRNA | IS 24hr | IS 48hr | IS 168hr | LA 24hr | LA 48hr | LA 168hr | CE 24hr | CE 48hr | CE 168hr | SV 24hr | SV 48hr | SV 168hr |
|---|---|---|---|---|---|---|---|---|---|---|---|---|
| miR-422a | 3.74 | 4.82 | 6.30 | 2.65 | 3.86 | 5.90 | 4.56 | 2.32 | 3.11 | 2.28 | 3.05 | 2.66 |
| miR-423-3p | -1.53 | -1.35 | -1.02 | -1.23 | -1.25 | -1.28 | -1.01 | -1.63 | -1.25 | -2.00 | -1.78 | -2.37 |
| miR-423-5p | -2.68 | -2.31 | -1.84 | -3.05 | -2.96 | -2.72 | -2.18 | -2.98 | -3.16 | -9.16 | -3.24 | -4.24 |
| miR-424 | 7.62 | 7.99 | 15.14 | 8.46 | 9.98 | 13.43 | 17.95 | 6.57 | 13.59 | 3.59 | 3.66 | 3.83 |
| miR-425 | 2.30 | 2.58 | 3.21 | 1.94 | 2.54 | 2.56 | 3.44 | 1.92 | 2.71 | 1.38 | 1.72 | 1.32 |
| miR-454 | 11.57 | 8.54 | 14.74 | 8.77 | 10.33 | 16.37 | 20.18 | 8.58 | 17.87 | 4.63 | 5.88 | 4.80 |
| miR-483-5p | 6.28 | 4.93 | 3.69 | 5.65 | 5.48 | 4.90 | 4.23 | 3.65 | 3.10 | 5.04 | 3.77 | 3.57 |
| miR-487b | 5.03 | 5.30 | 5.00 | 3.41 | 3.51 | 6.35 | 4.73 | 2.41 | 3.03 | 3.81 | 6.50 | 4.89 |
| miR-488 | 3.30 | 2.34 | 2.19 | 5.81 | 3.88 | 6.71 | 3.72 | 5.18 | 3.14 | 1.47 | 4.71 | 3.65 |
| miR-491-3p | 2.35 | 1.75 | 2.25 | 1.45 | 1.39 | 2.19 | 1.90 | 1.12 | 1.15 | 1.79 | 2.24 | 2.02 |
| miR-494 | 4.69 | 4.92 | 5.60 | 5.61 | 5.31 | 9.56 | 5.73 | 3.39 | 3.19 | 7.13 | 7.05 | 7.61 |
| miR-498 | 4.89 | 4.00 | 4.62 | 4.45 | 5.05 | 5.42 | 4.90 | 4.16 | 3.72 | 6.50 | 4.04 | 3.98 |
| miR-508-5p | 5.39 | 5.79 | 4.54 | 2.80 | 2.71 | 5.57 | 3.68 | 1.67 | 2.30 | 5.72 | 5.02 | 3.26 |
| miR-513a-5p | -1.74 | -1.58 | -1.33 | -1.39 | -1.24 | -1.33 | -1.74 | -1.26 | -1.70 | -1.27 | -1.84 | -2.16 |
| miR-519d | -3.40 | -3.27 | -3.28 | -3.18 | -2.62 | -2.25 | -2.89 | -3.96 | -4.33 | -2.58 | -2.63 | -2.98 |
| miR-519e | 1.31 | 1.16 | 1.87 | 1.65 | 1.87 | 1.84 | 1.34 | 1.84 | 1.56 | 1.72 | 1.00 | 1.23 |
| miR-519e* | 2.51 | 2.90 | 2.86 | 2.11 | 2.41 | 2.67 | 2.59 | 1.83 | 1.54 | 2.95 | 2.54 | 2.09 |
| miR-525-5p | 1.92 | 1.63 | 1.18 | 2.17 | 1.71 | 2.87 | 1.53 | 1.67 | 1.30 | 2.98 | 2.43 | 2.00 |
| miR-548e | 9.89 | 11.85 | 11.59 | 6.09 | 6.40 | 10.86 | 9.10 | 7.02 | 7.51 | 10.74 | 11.50 | 11.05 |
| miR-548n | 2.39 | 1.34 | 2.97 | 2.63 | 3.57 | 6.37 | 4.82 | 3.12 | 3.99 | 1.62 | 3.75 | 3.04 |
| miR-549 | 4.61 | 5.16 | 5.61 | 3.90 | 3.53 | 5.08 | 4.38 | 3.11 | 3.27 | 5.75 | 4.77 | 4.11 |
| miR-551b | -1.36 | -1.53 | -1.14 | -1.14 | -1.15 | -1.29 | -1.38 | -1.23 | -1.42 | -1.42 | -1.63 | -1.62 |
| miR-552 | 8.49 | 2.55 | 3.28 | 2.46 | 2.40 | 3.90 | 3.09 | 2.09 | 2.06 | 2.70 | 2.94 | 2.53 |
| miR-557 | 7.70 | 9.44 | 9.67 | 6.61 | 7.83 | 9.85 | 8.89 | 6.43 | 6.49 | 7.42 | 5.11 | 4.93 |
| miR-576-3p | 1.46 | 1.61 | 2.17 | 1.29 | 1.42 | 1.64 | 1.51 | 1.54 | 1.29 | 2.06 | 1.46 | 1.42 |
| miR-583 | 1.41 | 1.89 | 1.58 | 1.55 | 2.02 | 1.57 | 1.57 | 1.43 | 1.07 | 1.34 | 1.15 | 1.10 |

| Hsa-miRNA | IS 24hr | IS 48hr | IS 168hr | LA 24hr | LA 48hr | LA 168hr | CE 24hr | CE 48hr | CE 168hr | SV 24hr | SV 48hr | SV 168hr |
|---|---|---|---|---|---|---|---|---|---|---|---|---|
| miR-584 | 6.31 | 6.02 | 6.70 | 4.79 | 4.56 | 7.33 | 6.67 | 4.75 | 4.20 | 6.33 | 6.66 | 6.85 |
| miR-585 | 7.40 | 7.55 | 10.33 | 7.70 | 8.16 | 10.01 | 7.48 | 6.67 | 5.91 | 6.77 | 5.40 | 6.37 |
| miR-589 | 4.32 | 5.46 | 4.30 | 2.46 | 2.75 | 4.51 | 4.02 | 1.95 | 2.96 | 3.22 | 4.64 | 3.33 |
| miR-590-5p | 10.78 | 12.65 | 25.93 | 10.18 | 14.47 | 21.69 | 25.69 | 11.58 | 19.80 | 1.65 | 5.47 | 4.88 |
| miR-597 | 5.01 | 5.61 | 4.02 | 3.86 | 3.78 | 7.85 | 4.98 | 2.23 | 3.36 | 3.21 | 7.45 | 5.18 |
| miR-600 | 4.58 | 3.13 | 2.85 | 3.44 | 2.59 | 4.66 | 2.29 | 2.63 | 2.65 | 4.48 | 5.12 | 4.31 |
| miR-602 | 2.04 | 2.33 | 2.75 | 2.83 | 2.84 | 3.90 | 2.75 | 2.34 | 2.16 | 1.84 | 2.11 | 2.21 |
| miR-611 | 3.20 | 4.84 | 6.23 | 2.87 | 3.28 | 3.04 | 3.95 | 3.18 | 3.09 | 2.51 | 1.77 | 1.32 |
| miR-617 | 3.01 | 2.43 | 3.19 | 1.89 | 1.97 | 3.10 | 1.42 | 1.74 | 1.09 | 2.27 | 2.69 | 2.13 |
| miR-623 | 2.79 | 2.53 | 2.37 | 4.56 | 2.88 | 6.76 | 2.39 | 2.98 | 2.81 | 3.37 | 3.12 | 2.19 |
| miR-629* | 2.94 | 3.78 | 3.97 | 2.93 | 3.25 | 6.77 | 2.96 | 1.86 | 1.58 | 2.77 | 4.91 | 4.82 |
| miR-634 | -4.54 | -9.26 | -37.22 | -2.34 | -3.30 | -2.55 | -2.98 | -2.70 | -3.99 | -3.20 | -2.50 | -2.92 |
| miR-637 | 3.03 | 3.37 | 4.44 | 3.59 | 3.59 | 3.98 | 2.97 | 3.22 | 2.64 | 2.37 | 2.05 | 1.85 |
| miR-638 | 5.28 | 3.59 | 4.41 | 4.59 | 5.17 | 5.90 | 5.07 | 4.12 | 3.33 | 4.40 | 3.83 | 4.88 |
| miR-652 | 1.78 | 1.83 | 2.30 | 2.00 | 1.89 | 1.85 | 2.47 | 1.87 | 2.15 | 1.38 | 1.45 | 1.23 |
| miR-659 | 2.95 | 3.42 | 2.31 | 4.45 | 5.82 | 3.56 | 2.77 | 2.42 | 2.23 | 2.56 | 3.25 | 3.00 |
| miR-665 | -1.87 | -1.44 | -1.47 | -1.29 | -1.03 | -1.29 | -1.22 | -1.23 | -1.74 | -1.70 | -1.71 | -2.24 |
| miR-668 | 2.64 | 1.54 | 2.43 | 3.28 | 3.62 | 5.94 | 1.86 | 2.72 | 2.27 | 3.69 | 3.01 | 3.89 |
| miR-671-5p | 3.87 | 3.16 | 2.14 | 5.00 | 5.08 | 6.24 | 6.33 | 3.72 | 3.55 | 6.18 | 5.53 | 6.36 |
| miR-675 | 5.48 | 4.98 | 3.06 | 7.15 | 9.13 | 8.10 | 5.94 | 3.91 | 3.49 | 5.47 | 6.34 | 7.67 |
| miR-765 | 1.26 | 1.46 | 1.53 | 1.51 | 1.79 | 1.51 | 1.27 | 1.23 | 1.08 | 1.66 | 1.26 | 1.31 |
| miR-874 | 1.64 | 1.08 | 1.55 | 2.69 | 2.62 | 3.86 | 2.41 | 2.36 | 1.90 | 1.78 | 2.83 | 2.65 |
| miR-887 | 4.99 | 4.21 | 4.01 | 3.37 | 3.71 | 5.57 | 4.51 | 2.62 | 2.32 | 4.48 | 4.69 | 4.63 |
| miR-888* | 1.41 | 1.68 | 1.87 | 1.23 | 1.34 | 1.72 | 1.55 | 1.13 | 1.17 | 1.53 | 1.47 | 1.32 |
| miR-890 | 2.81 | 2.42 | 1.57 | 1.90 | 1.47 | 1.96 | 2.87 | 1.41 | 2.12 | 1.75 | 2.91 | 1.10 |
| miR-891a | 2.38 | 2.21 | 2.67 | 2.21 | 2.30 | 3.20 | 2.45 | 2.19 | 1.94 | 2.72 | 2.84 | 3.16 |

| Hsa-miRNA | IS 24hr | IS 48hr | IS 168hr | LA 24hr | LA 48hr | LA 168hr | CE 24hr | CE 48hr | CE 168hr | SV 24hr | SV 48hr | SV 168hr |
|---|---|---|---|---|---|---|---|---|---|---|---|---|
| miR-923 | -5.93 | -4.23 | -2.95 | -4.49 | -3.73 | -4.63 | -4.03 | -3.96 | -5.27 | -4.86 | -7.63 | -8.18 |
| miR-933 | 3.04 | 3.22 | 4.30 | 2.22 | 2.32 | 3.15 | 2.45 | 1.73 | 1.56 | 3.22 | 2.64 | 2.72 |
| miR-934 | 2.95 | 1.64 | 1.62 | 2.01 | 2.08 | 3.04 | 1.63 | 2.54 | 1.73 | 2.74 | 3.12 | 2.34 |
| miR-937 | 2.19 | 2.09 | 1.41 | 1.75 | 1.48 | 3.26 | 2.41 | 1.14 | 2.08 | 3.49 | 3.47 | 2.13 |
| miR-943 | 2.13 | 1.10 | 1.28 | 3.90 | 3.76 | 3.37 | 3.16 | 2.91 | 2.14 | 3.62 | 2.29 | 2.93 |
| miR-1201 | 2.13 | 1.93 | 1.83 | 2.40 | 2.13 | 2.36 | 2.05 | 2.35 | 2.38 | 1.11 | 2.48 | 2.11 |
| miR-1255a | 1.24 | 1.33 | 1.58 | 1.41 | 1.48 | 1.55 | 1.40 | 1.50 | 1.26 | 1.37 | 1.25 | 1.29 |
| miR-1259 | 2.64 | 2.09 | 3.22 | 1.95 | 1.93 | 2.40 | 1.89 | 1.85 | 2.02 | 3.14 | 2.82 | 2.81 |
| miR-1260 | 1.71 | 1.37 | 1.17 | 1.73 | 1.17 | 2.73 | 1.39 | 1.16 | 1.09 | 1.17 | 2.40 | 1.79 |
| miR-1261 | 7.05 | 9.21 | 9.86 | 8.52 | 7.87 | 11.12 | 7.68 | 7.42 | 5.66 | 4.67 | 6.32 | 4.12 |
| miR-1264 | 1.79 | 2.01 | 3.31 | 1.50 | 1.71 | 2.26 | 1.68 | 1.74 | 1.55 | 2.09 | 1.91 | 2.10 |
| miR-1265 | -1.95 | -1.86 | -1.57 | -2.41 | -2.59 | -1.97 | -2.58 | -2.79 | -3.20 | -2.30 | -1.92 | -2.79 |
| miR-1274a | 4.32 | 4.30 | 4.97 | 5.34 | 5.17 | 12.29 | 5.11 | 2.90 | 2.99 | 4.18 | 7.63 | 7.84 |
| miR-1274b | 8.45 | 8.75 | 10.06 | 4.81 | 4.82 | 10.06 | 5.76 | 3.15 | 3.81 | 6.06 | 8.68 | 8.06 |
| miR-1280 | -1.93 | -1.89 | -1.51 | -1.51 | -1.96 | -1.01 | -1.78 | -2.54 | -2.54 | -2.58 | -1.25 | -1.52 |
| miR-1297 | 5.80 | 5.29 | 9.35 | 5.57 | 9.96 | 13.77 | 14.31 | 4.91 | 9.92 | 2.39 | 3.67 | 3.43 |
| miR-1299 | -1.70 | -1.64 | -1.23 | -1.49 | -1.32 | -1.18 | -1.59 | -1.17 | -1.62 | -2.02 | -1.42 | -1.77 |
| miR-1301 | 1.38 | 1.31 | 1.20 | 1.30 | 1.16 | 1.66 | 1.98 | 1.05 | 1.38 | 1.16 | 1.57 | 1.31 |
| miR-1307 | 2.53 | 2.30 | 3.30 | 2.40 | 2.48 | 3.67 | 3.48 | 1.60 | 2.75 | 1.12 | 2.13 | 1.62 |
| miR-1321 | 4.78 | 3.18 | 3.71 | 4.09 | 4.19 | 5.49 | 3.92 | 4.03 | 3.02 | 4.60 | 4.57 | 5.48 |

### 3.5 miRNAs specific for various stroke subtypes

From the previous results, the miRNA profiles demonstrated segregation of samples according to stroke subtypes. Hence, an in-depth analysis was performed to identify miRNAs specific for each of the stroke subtype. The results from the analysis yielded lists of miRNAs specific for each stroke subtype.

For large artery (LA) stroke, there were 10 miRNAs (miR-27a*, -129-5p, -382, -585, -602, -637, -659, -744, -1184 and -1261) showing unique expression pattern for large artery stroke and were able to distinguish large artery stroke samples from the other samples (demonstrated by hierarchical clustering of samples; Figure 3.3A; Table 3.4). All of these 10 miRNAs were found to have higher expression in large artery stroke samples as compared to other stroke subtypes (CE and SV; Figure 3.3A; Table 3.4).

As for cardioembolic stroke specific miRNAs, there were 14 miRNAs (miR-19a, -130b*, -181a-2*, -198, -200b, -208a, -412, -525-5p, -550, -617, -618, -630, -668 and -1321) detected (Figure 3.3B; Table 3.4). Among these 14 miRNAs, 2 miRNAs (hsa-miR-19a and -550) had higher expression in cardioembolic stroke samples as compared with large artery stroke and small vessel stroke samples, while the remaining 12 miRNAs (miR-130b*, -181a-2*, -198, -200b, -208a, -412, -525-5p, -617, -618, -630, -668 and -1321) showed lower expression in cardioembolic stroke samples in contrast with large artery stroke and small vessel stroke samples (Figure 3.3; Table 3.4).

In the case of small vessel stroke specific miRNAs, 141 miRNAs were detected as capable of distinguishing small vessel stroke samples from cardioembolic stroke samples and large artery stroke samples (Figure 3.3C;

Table 3.4). The expression of these 141 miRNAs was shown to be lower in small vessel stroke samples when compared against other stroke subtypes (CE and LA; Figure 3.3C; Table 3.4).

Among these stroke subtype specific miRNAs, there were 8 miRNAs (miR-19a, -129-5p, -198, -320b, -320d, -331-3p, -637 and -744) that were able to segregate the samples according to stroke subtype, shown in the hierarchical clustering of the samples (Figure 3.3D; Table 3.4). These 8 miRNAs (miR-19a, -129-5p, -198, -320b, -320d, -331-3p, -637 and -744) may serve as potential diagnostic markers for stroke subtype and further investigation, especially pathway analysis could yield more information on the pathogenesis for different stroke subtype.

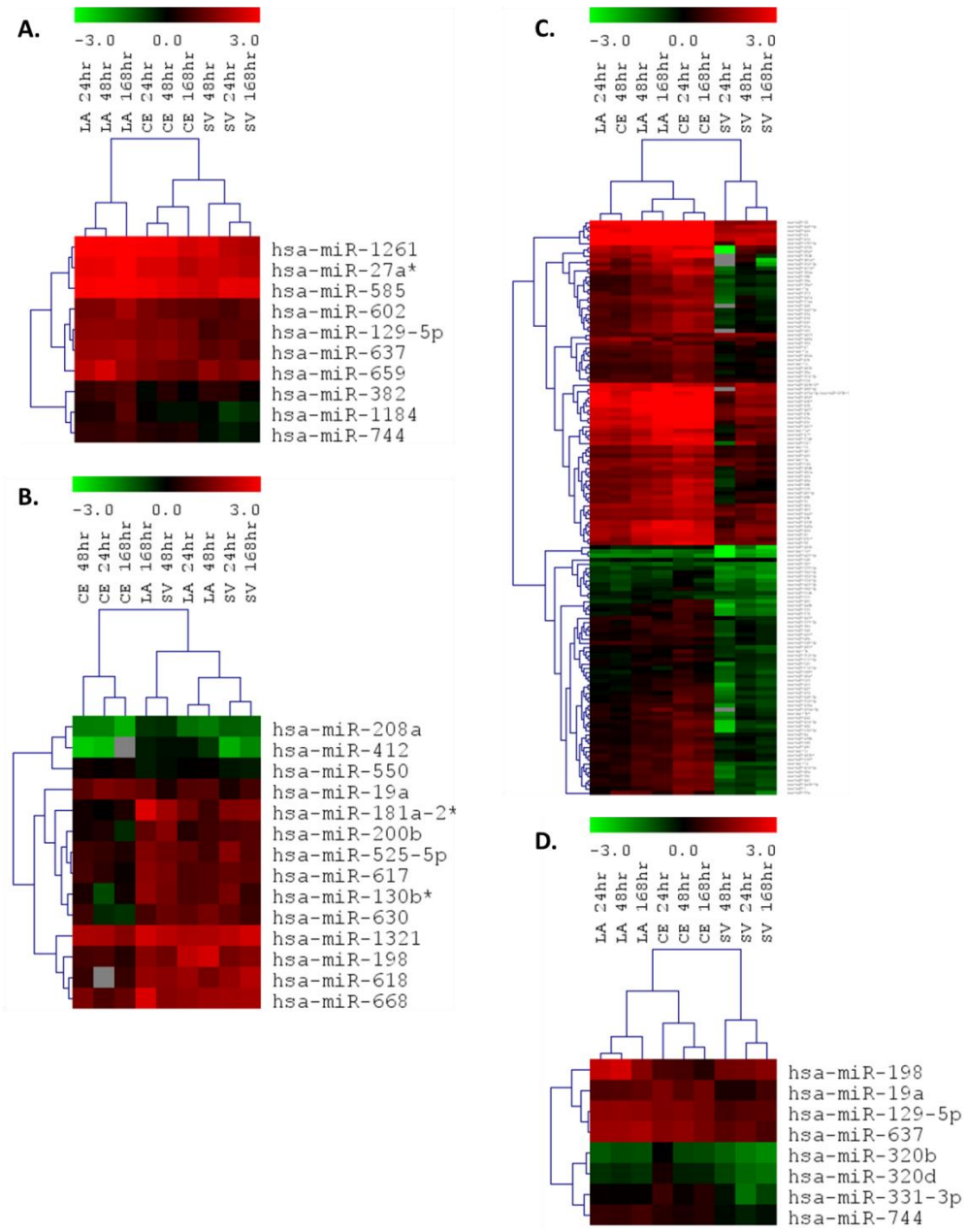


**Figure 3.3:** Hierarchical clustering of stroke subtype specific miRNAs. **A**. Large artery stroke specific miRNAs. **B**. Cardioembolic stroke subtype specific miRNAs. **C**. Small vessel stroke subtype specific miRNAs. **D**. MiRNAs that can segregate samples according to stroke subtype. The miRNA expression were expressed as signal log ratio (SLR) with respect to control samples Green represents down-regulation. Red represents up-regulation. Grey represents absence. LA: large artery stroke. CE: cardioembolic stroke. SV: small vessel stroke.

**Table 3.4:** List of stroke subtype specific miRNAs. miRNAs were expressed as fold change compared with healthy controls. ND represents not detected. LA: large artery stroke. CE: cardioembolic stroke. SV: small vessel stroke. miRNAs highlighted in bold are able to segregate samples according to stroke subtypes.

| Hsa-miRNA | LA 24hr | LA 48hr | LA 168hr | CE 24hr | CE 48hr | CE 168hr | SV 24hr | SV 48hr | SV 168hr |
|---|---|---|---|---|---|---|---|---|---|
| **LA specific miRNAs** | | | | | | | | | |
| miR-27a* | 6.69 | 6.86 | 10.87 | 6.06 | 6.03 | 4.55 | 5.05 | 5.34 | 4.35 |
| **miR-129-5p** | **3.20** | **3.29** | **3.18** | **2.75** | **2.90** | **2.53** | **2.00** | **1.76** | **2.05** |
| miR-382 | 1.47 | 1.70 | 1.88 | -1.06 | 1.36 | 1.03 | 1.38 | 1.43 | 1.07 |
| miR-585 | 7.70 | 8.16 | 10.01 | 7.48 | 6.67 | 5.91 | 6.77 | 5.40 | 6.37 |
| miR-602 | 2.83 | 2.84 | 3.90 | 2.75 | 2.34 | 2.16 | 1.84 | 2.11 | 2.21 |
| **miR-637** | **3.59** | **3.59** | **3.98** | **2.97** | **3.22** | **2.64** | **2.37** | **2.05** | **1.85** |
| miR-659 | 4.45 | 5.82 | 3.56 | 2.77 | 2.42 | 2.23 | 2.56 | 3.25 | 3.00 |
| **miR-744** | **1.52** | **1.48** | **1.72** | **1.36** | **1.25** | **1.35** | **-1.27** | **-1.08** | **-1.11** |
| miR-1184 | 1.25 | 1.29 | 2.05 | 1.05 | -1.13 | -1.13 | -1.59 | -1.04 | -1.35 |
| miR-1261 | 8.52 | 7.87 | 11.12 | 7.68 | 7.42 | 5.66 | 4.67 | 6.32 | 4.12 |
| **CE specific miRNAs** | | | | | | | | | |
| **miR-19a** | **1.93** | **2.00** | **2.02** | **2.77** | **2.03** | **2.52** | **1.26** | **1.25** | **1.75** |
| miR-130b* | 1.89 | 1.96 | 3.25 | -1.81 | 1.25 | 1.15 | 2.63 | 2.57 | 1.57 |
| miR-181a-2* | 2.47 | 1.65 | 6.07 | 1.02 | 1.17 | 1.29 | 2.85 | 3.75 | 3.02 |
| **miR-198** | **4.79** | **5.72** | **3.01** | **1.87** | **1.75** | **1.38** | **2.60** | **2.49** | **3.03** |
| miR-200b | 1.37 | 1.68 | 2.20 | 1.28 | 1.16 | -1.40 | 1.82 | 2.99 | 1.98 |
| miR-208a | -2.47 | -2.72 | -1.52 | -2.82 | -2.79 | -4.08 | -2.14 | -1.44 | -2.23 |
| miR-412 | -1.11 | -1.57 | -1.23 | -4.66 | -5.19 | ND | -4.16 | -1.12 | -3.01 |
| miR-525-5p | 2.17 | 1.71 | 2.87 | 1.53 | 1.67 | 1.30 | 2.98 | 2.43 | 2.00 |
| miR-550 | -1.00 | 1.03 | -1.23 | 1.05 | 1.16 | 1.16 | -1.18 | -1.10 | -1.25 |
| miR-617 | 1.89 | 1.97 | 3.10 | 1.42 | 1.74 | 1.09 | 2.27 | 2.69 | 2.13 |
| miR-618 | 3.52 | 2.62 | 3.37 | ND | 1.58 | 1.55 | 3.36 | 3.11 | 4.36 |
| miR-630 | 2.17 | 2.65 | 1.79 | -1.38 | 1.67 | -1.49 | 2.11 | 2.37 | 1.70 |
| miR-668 | 3.28 | 3.62 | 5.94 | 1.86 | 2.72 | 2.27 | 3.69 | 3.01 | 3.89 |

| Hsa-miRNA | LA 24hr | LA 48hr | LA 168hr | CE 24hr | CE 48hr | CE 168hr | SV 24hr | SV 48hr | SV 168hr |
|---|---|---|---|---|---|---|---|---|---|
| miR-1321 | 4.09 | 4.19 | 5.49 | 3.92 | 4.03 | 3.02 | 4.60 | 4.57 | 5.48 |
| **SV specific miRNAs** | | | | | | | | | |
| Let-7a | 1.70 | 1.86 | 1.99 | 2.58 | 1.80 | 2.34 | 1.05 | 1.08 | -1.09 |
| Let-7a* | 4.13 | 4.22 | 6.89 | 4.84 | 3.51 | 4.26 | -1.27 | 2.22 | 2.49 |
| Let-7b | 1.00 | 1.25 | 1.03 | 1.87 | -1.05 | 1.28 | -1.45 | -1.38 | -1.90 |
| **Hsa-miRNA** | **LA 24hr** | **LA 48hr** | **LA 168hr** | **CE 24hr** | **CE 48hr** | **CE 168hr** | **SV 24hr** | **SV 48hr** | **SV 168hr** |
| Let-7b* | 1.40 | 1.48 | 1.57 | 2.45 | 1.22 | 1.79 | -3.08 | -1.13 | -1.42 |
| Let-7c | 1.22 | 1.84 | 1.62 | 2.69 | 1.29 | 1.85 | -1.10 | -1.08 | -1.44 |
| Let-7d | 2.18 | 2.97 | 3.04 | 4.72 | 2.25 | 3.99 | 1.30 | 1.49 | 1.28 |
| Let-7d* | -2.20 | -2.26 | -2.94 | -2.35 | -2.69 | -2.16 | -13.00 | -3.86 | -4.65 |
| Let-7e | 2.72 | 3.83 | 4.08 | 5.41 | 2.60 | 3.91 | 1.99 | 2.08 | 1.67 |
| Let-7f | 1.54 | 1.60 | 1.77 | 2.21 | 1.62 | 2.01 | 1.01 | 1.00 | 1.31 |
| Let-7g | 1.52 | 2.30 | 2.08 | 3.38 | 1.72 | 3.22 | -1.89 | -1.55 | -1.63 |
| Let-7i | 1.16 | 1.98 | 1.60 | 3.11 | 1.28 | 2.69 | -2.09 | -1.84 | -1.96 |
| miR-7 | 1.08 | 1.42 | 1.70 | 2.83 | 1.14 | 2.55 | -1.75 | -1.57 | -1.68 |
| miR-15b* | 8.24 | 7.56 | 12.53 | 16.42 | 6.38 | 13.15 | 1.40 | 3.21 | 3.22 |
| miR-16-2* | 3.27 | 3.40 | 3.91 | 5.23 | 2.16 | 4.26 | -2.45 | -1.08 | -1.68 |
| miR-17 | 1.99 | 2.06 | 2.28 | 2.85 | 2.09 | 2.59 | 1.05 | 1.22 | 1.07 |
| miR-17* | 3.43 | 3.90 | 6.57 | 6.43 | 3.12 | 6.02 | -1.03 | 2.22 | 2.01 |
| miR-18a | 2.57 | 3.13 | 3.76 | 5.86 | 2.73 | 4.98 | -1.59 | 1.44 | 1.08 |
| miR-18a* | -1.03 | 1.15 | 1.14 | 1.35 | -1.10 | -1.14 | -2.13 | -1.21 | -1.61 |
| miR-18b | 2.15 | 2.72 | 3.45 | 5.01 | 2.25 | 4.02 | -1.61 | 1.19 | 1.00 |
| miR-19b | 2.72 | 2.82 | 3.12 | 3.91 | 2.87 | 3.54 | 1.57 | 1.77 | 2.69 |
| miR-20a | 1.29 | 1.89 | 1.70 | 2.66 | 1.36 | 2.31 | -2.43 | -1.59 | -1.83 |
| miR-20a* | 4.15 | 4.56 | 6.03 | 7.45 | 3.54 | 7.89 | -12.06 | 1.93 | 1.49 |
| miR-20b | 2.43 | 3.82 | 4.47 | 5.12 | 2.15 | 3.69 | -1.26 | 1.58 | 1.40 |
| miR-21 | 10.09 | 10.67 | 11.82 | 14.79 | 10.70 | 13.42 | 4.53 | 4.76 | 5.56 |
| miR-22* | 1.03 | 1.20 | 1.47 | 1.75 | -1.14 | 1.76 | -3.04 | -1.20 | -1.51 |
| miR-24 | 1.16 | 1.42 | 1.67 | 2.01 | 1.17 | 2.14 | -1.46 | -1.10 | -1.14 |
| miR-25 | 4.11 | 4.98 | 5.71 | 6.01 | 3.41 | 5.39 | 2.21 | 3.07 | 2.81 |

| Hsa-miRNA | LA 24hr | LA 48hr | LA 168hr | CE 24hr | CE 48hr | CE 168hr | SV 24hr | SV 48hr | SV 168hr |
|---|---|---|---|---|---|---|---|---|---|
| miR-26a | 2.02 | 2.75 | 3.01 | 3.80 | 1.85 | 3.04 | -1.27 | 1.06 | -1.03 |
| miR-26b | 1.84 | 1.90 | 2.11 | 2.64 | 1.94 | 2.39 | -1.27 | 1.19 | 1.38 |
| miR-28-5p | 2.23 | 3.35 | 3.16 | 5.81 | 2.64 | 4.69 | -1.03 | 1.46 | 1.57 |
| miR-29a | 5.14 | 5.59 | 8.00 | 12.14 | 4.38 | 9.52 | 2.16 | 2.63 | 2.21 |
| miR-29b | 5.81 | 6.99 | 10.71 | 12.16 | 5.62 | 10.81 | 2.41 | 3.65 | 3.82 |
| miR-29c | 5.94 | 6.08 | 8.74 | 14.80 | 5.69 | 12.56 | 1.35 | 2.74 | 2.29 |
| miR-29c* | 3.68 | 4.43 | 5.45 | 5.51 | 2.60 | 5.69 | 2.02 | 2.54 | 1.73 |
| miR-30a | 1.59 | 1.60 | 1.82 | 2.21 | 1.67 | 2.07 | -1.29 | 1.03 | 1.29 |
| miR-30b | 1.53 | 2.11 | 2.41 | 3.64 | 1.52 | 3.01 | -1.48 | -1.24 | -1.51 |
| miR-30c | 1.14 | 1.71 | 1.90 | 2.81 | 1.18 | 2.51 | -2.84 | -1.47 | -1.70 |
| miR-30d | 1.25 | 1.58 | 1.59 | 1.86 | 1.20 | 1.37 | -1.73 | -1.01 | -1.28 |
| miR-30e | 1.51 | 2.21 | 2.65 | 3.44 | 1.49 | 2.53 | -2.14 | -1.25 | -1.47 |
| miR-30e* | 1.47 | 2.20 | 2.63 | 3.43 | 1.57 | 2.74 | -1.75 | -1.10 | -1.27 |
| miR-32 | 9.18 | 8.92 | 15.90 | 20.00 | 8.16 | 14.20 | 3.00 | 2.82 | 3.58 |
| miR-32* | -1.99 | -1.91 | -2.27 | -1.62 | -1.72 | -1.95 | -2.43 | -2.59 | -3.01 |
| miR-96 | 2.26 | 3.46 | 3.71 | 4.93 | 2.47 | 4.09 | -1.37 | 1.24 | 1.28 |
| miR-98 | 2.57 | 3.99 | 5.81 | 7.10 | 2.76 | 6.19 | 2.44 | 2.38 | 2.37 |
| miR-99a | 1.12 | 2.10 | 1.32 | 2.33 | 2.34 | 1.36 | -1.88 | -1.49 | -2.93 |
| miR-101 | 3.57 | 3.54 | 4.09 | 5.12 | 3.75 | 4.64 | 1.59 | 2.32 | 3.02 |
| miR-101* | 7.76 | 10.59 | 11.79 | 13.72 | 6.18 | 11.12 | 1.52 | 3.22 | 2.84 |
| miR-103 | 2.92 | 3.03 | 3.35 | 4.19 | 3.08 | 3.81 | 2.13 | 1.90 | 2.34 |
| miR-106a | 2.34 | 2.42 | 2.68 | 3.36 | 2.46 | 3.05 | -1.41 | 1.50 | 1.34 |
| miR-106a* | 3.82 | 3.76 | 5.18 | 4.53 | 2.07 | 3.04 | ND | 1.62 | -5.12 |
| miR-106b | 1.49 | 1.54 | 1.71 | 2.11 | 1.57 | 1.94 | 1.18 | -1.03 | 1.17 |
| miR-106b* | 1.52 | 1.67 | 1.92 | 2.44 | 1.20 | 2.05 | -1.21 | 1.10 | -1.16 |
| miR-107 | 2.44 | 3.12 | 3.35 | 4.40 | 2.46 | 3.99 | 1.48 | 1.66 | 1.41 |
| miR-125b | -1.02 | -1.25 | -1.23 | -1.21 | -1.34 | -1.11 | -27.06 | -2.51 | -6.13 |
| miR-125b-2* | 6.58 | 5.48 | 7.20 | 5.01 | 6.17 | 4.69 | 2.44 | 4.62 | 3.34 |
| miR-126 | 1.42 | 1.78 | 1.96 | 2.27 | 1.18 | 2.29 | -1.86 | -1.58 | -1.89 |
| miR-126* | 5.29 | 6.27 | 7.27 | 8.10 | 4.38 | 7.61 | -1.19 | 1.57 | 1.93 |

| Hsa-miRNA | LA 24hr | LA 48hr | LA 168hr | CE 24hr | CE 48hr | CE 168hr | SV 24hr | SV 48hr | SV 168hr |
|---|---|---|---|---|---|---|---|---|---|
| miR-128 | 1.80 | 2.12 | 2.58 | 3.30 | 1.77 | 3.15 | ND | 1.26 | -1.14 |
| miR-130a | 1.31 | 1.65 | 1.63 | 1.67 | 1.16 | 1.48 | -3.35 | -1.30 | -1.77 |
| miR-130b | 1.13 | 1.44 | 1.47 | 2.00 | 1.08 | 1.59 | -1.11 | 1.00 | -1.38 |
| miR-135b | 3.87 | 4.88 | 7.02 | 6.78 | 3.62 | 4.58 | 1.58 | 2.21 | 2.07 |
| miR-140-3p | -1.01 | 1.39 | 1.31 | 2.10 | 1.13 | 1.74 | -2.31 | -1.24 | -1.52 |
| miR-140-5p | 6.50 | 9.30 | 14.93 | 15.41 | 7.08 | 13.24 | 3.44 | 4.52 | 4.63 |
| miR-142-5p | 1.98 | 2.06 | 2.29 | 2.86 | 1.74 | 2.60 | -1.54 | 1.05 | -1.18 |
| miR-144* | 3.03 | 3.14 | 3.47 | 4.35 | 3.19 | 3.95 | 2.76 | 1.97 | 2.59 |
| miR-146a | 2.19 | 2.94 | 2.97 | 3.04 | 2.23 | 3.39 | -2.24 | 1.23 | -1.42 |
| miR-146b-5p | 1.27 | 1.76 | 1.86 | 2.39 | 1.34 | 2.43 | -1.53 | -1.37 | -1.96 |
| miR-148a | 3.61 | 5.59 | 7.38 | 6.90 | 3.30 | 5.06 | 1.42 | 2.85 | 2.77 |
| miR-148b | -1.10 | 1.28 | 1.26 | 1.79 | -1.11 | 1.60 | -4.93 | -1.92 | -2.25 |
| miR-149* | 1.34 | 1.67 | 1.10 | 1.68 | 1.49 | 1.15 | 1.07 | -1.34 | -1.41 |
| miR-151-3p | 1.20 | 1.32 | 1.55 | 2.62 | 1.21 | 2.44 | -4.90 | -1.56 | -1.41 |
| miR-151-5p | 1.22 | 1.80 | 1.60 | 2.93 | 1.48 | 2.65 | -2.67 | -1.40 | -1.35 |
| miR-155 | 1.01 | 1.12 | 1.39 | 1.49 | -1.06 | 1.48 | -4.03 | -1.43 | -1.89 |
| miR-181a | 1.73 | 1.97 | 2.09 | 2.78 | 1.52 | 2.37 | -1.19 | 1.12 | -1.02 |
| miR-181b | 3.09 | 2.77 | 4.03 | 3.59 | 2.38 | 3.61 | -1.21 | 2.10 | 1.71 |
| miR-182 | 1.08 | 1.50 | 1.44 | 2.59 | 1.13 | 2.27 | -5.10 | -1.61 | -1.92 |
| miR-185 | -1.52 | -1.19 | 1.01 | 1.83 | -1.58 | 1.58 | -3.07 | -2.36 | -3.25 |
| miR-185* | 1.07 | 1.20 | 1.10 | 1.14 | 1.07 | -1.04 | -1.39 | -1.82 | -2.02 |
| miR-186 | 1.42 | 1.75 | 1.61 | 2.68 | 1.28 | 2.35 | -1.42 | -1.31 | -1.28 |
| miR-188-5p | 6.85 | 5.34 | 11.73 | 7.91 | 5.69 | 9.66 | ND | 3.69 | 3.82 |
| miR-190 | 7.27 | 8.35 | 12.52 | 15.48 | 7.11 | 13.34 | 2.06 | 2.71 | 2.47 |
| miR-191 | -1.07 | 1.18 | -1.00 | 1.90 | 1.08 | 1.82 | -2.60 | -1.57 | -1.83 |
| miR-192 | 1.81 | 2.30 | 2.83 | 3.88 | 1.69 | 3.11 | -1.48 | -1.09 | -1.39 |
| miR-193a-3p | 1.29 | 1.70 | 2.47 | 1.68 | -1.02 | 1.38 | ND | -1.14 | -1.54 |
| miR-194 | 2.11 | 2.25 | 2.98 | 4.04 | 1.60 | 3.88 | -1.34 | -1.04 | -1.15 |
| miR-196b | 4.86 | 4.70 | 6.70 | 5.31 | 3.52 | 6.00 | -14.05 | 2.34 | 1.94 |
| miR-199a-3p | 8.32 | 9.04 | 12.31 | 6.43 | 5.05 | 11.54 | 2.13 | 3.94 | 3.56 |

| Hsa-miRNA | LA 24hr | LA 48hr | LA 168hr | CE 24hr | CE 48hr | CE 168hr | SV 24hr | SV 48hr | SV 168hr |
|---|---|---|---|---|---|---|---|---|---|
| miR-215 | 1.86 | 2.46 | 3.07 | 4.01 | 1.82 | 3.15 | -1.71 | 1.00 | -1.12 |
| miR-221 | 3.95 | 6.20 | 6.28 | 6.77 | 3.62 | 5.51 | 1.99 | 3.24 | 3.14 |
| miR-222 | 1.30 | 1.68 | 1.84 | 2.01 | 1.03 | 1.90 | -2.58 | -1.03 | -1.20 |
| miR-301a | 2.05 | 2.64 | 3.42 | 6.03 | 2.46 | 5.40 | -2.15 | -1.12 | -1.07 |
| miR-301b | 3.16 | 2.93 | 5.32 | 8.13 | 3.10 | 8.75 | ND | 1.42 | -1.60 |
| **miR-320b** | **-2.05** | **-1.82** | **-1.89** | **-1.00** | **-1.74** | **-1.81** | **-2.71** | **-2.19** | **-3.08** |
| **miR-320d** | **-1.48** | **-1.36** | **-1.49** | **1.23** | **-1.28** | **-1.30** | **-2.31** | **-1.75** | **-2.52** |
| miR-324-5p | -1.45 | -1.51 | -1.83 | 1.05 | -1.54 | 1.01 | -2.72 | -2.67 | -2.99 |
| **miR-331-3p** | **1.06** | **1.04** | **1.03** | **1.59** | **1.08** | **1.36** | **-2.50** | **-1.14** | **-1.70** |
| miR-331-5p | -1.53 | -1.42 | -1.35 | -1.00 | -1.65 | -1.63 | -2.54 | -1.82 | -2.88 |
| miR-335 | 1.00 | 1.12 | 1.49 | 1.66 | -1.13 | 1.57 | -3.61 | -2.26 | -2.76 |
| miR-339-3p | 1.35 | 1.62 | 1.41 | 1.50 | -1.05 | 1.46 | -1.74 | -1.09 | -1.46 |
| miR-339-5p | -1.50 | -1.32 | -1.40 | -1.49 | -2.01 | -1.33 | -3.39 | -2.28 | -3.20 |
| miR-340 | 1.24 | 1.23 | 1.71 | 1.61 | 1.12 | 1.47 | -1.70 | 1.01 | -1.28 |
| miR-361-3p | 1.59 | 1.96 | 1.62 | 2.95 | 1.93 | 2.06 | 1.14 | 1.03 | -1.00 |
| miR-361-5p | -1.07 | 1.00 | 1.01 | 1.42 | -1.17 | 1.21 | -1.56 | -1.25 | -1.38 |
| miR-362-3p | 2.46 | 2.56 | 4.13 | 3.90 | 1.78 | 3.09 | ND | 1.00 | -3.88 |
| miR-362-5p | 1.01 | 1.40 | 1.37 | 2.35 | 1.10 | 1.83 | -1.96 | -1.55 | -1.76 |
| miR-363 | 2.11 | 2.30 | 2.26 | 2.76 | 1.57 | 3.02 | -1.99 | -1.37 | -1.56 |
| miR-374a | 2.21 | 2.76 | 3.43 | 4.25 | 2.04 | 3.71 | -2.52 | -1.07 | -1.22 |
| miR-374b | 3.93 | 5.08 | 6.87 | 7.94 | 3.25 | 6.87 | 1.27 | 2.39 | 2.13 |
| miR-378 | -1.24 | 1.08 | 1.01 | 1.66 | -1.18 | 1.30 | -3.62 | -2.20 | -2.52 |
| miR-381 | 2.47 | 1.91 | 2.86 | 1.98 | 2.62 | 1.86 | -1.10 | 1.84 | 1.13 |
| miR-421 | 2.25 | 2.50 | 2.81 | 4.15 | 2.13 | 3.35 | -1.29 | 1.52 | 1.50 |
| miR-423-3p | -1.23 | -1.25 | -1.28 | -1.01 | -1.63 | -1.25 | -2.00 | -1.78 | -2.37 |
| miR-423-5p | -3.05 | -2.96 | -2.72 | -2.18 | -2.98 | -3.16 | -9.16 | -3.24 | -4.24 |
| miR-424 | 8.46 | 9.98 | 13.43 | 17.95 | 6.57 | 13.59 | 3.59 | 3.66 | 3.83 |
| miR-425 | 1.94 | 2.54 | 2.56 | 3.44 | 1.92 | 2.71 | 1.38 | 1.72 | 1.32 |
| miR-425* | 1.10 | 1.32 | 1.47 | 1.71 | 1.04 | 1.64 | -2.07 | -1.18 | -1.29 |
| miR-454 | 8.77 | 10.33 | 16.37 | 20.18 | 8.58 | 17.87 | 4.63 | 5.88 | 4.80 |

| Hsa-miRNA | LA 24hr | LA 48hr | LA 168hr | CE 24hr | CE 48hr | CE 168hr | SV 24hr | SV 48hr | SV 168hr |
|---|---|---|---|---|---|---|---|---|---|
| miR-484 | 1.17 | 1.40 | 1.29 | 1.40 | 1.12 | 1.17 | -1.39 | 1.00 | -1.30 |
| miR-500 | 1.18 | 1.48 | 1.47 | 2.14 | 1.10 | 1.88 | -1.36 | -1.10 | -1.51 |
| miR-500* | -1.16 | 1.03 | 1.04 | 1.46 | -1.27 | 1.05 | -2.16 | -1.42 | -2.06 |
| miR-501-5p | -1.53 | -1.44 | -1.68 | 1.02 | -1.79 | -1.11 | -3.01 | -2.64 | -3.91 |
| miR-502-3p | -1.31 | -1.10 | -1.16 | 1.35 | -1.35 | -1.11 | -2.21 | -1.68 | -2.55 |
| miR-505 | 1.88 | 3.02 | 3.22 | 3.91 | 2.10 | 3.54 | ND | 1.21 | -1.02 |
| miR-532-5p | 1.29 | 1.50 | 1.61 | 2.06 | 1.11 | 1.90 | -5.23 | -1.37 | -1.44 |
| miR-550* | 1.46 | 1.67 | 1.61 | 2.24 | 1.27 | 1.96 | -1.23 | 1.04 | -1.29 |
| miR-551b | -1.14 | -1.15 | -1.29 | -1.38 | -1.23 | -1.42 | -1.42 | -1.63 | -1.62 |
| miR-574-5p | -1.07 | -1.01 | -1.26 | 1.17 | -1.02 | -1.02 | -1.96 | -1.40 | -1.67 |
| miR-576-5p | 1.12 | 1.07 | 1.27 | 1.72 | -1.11 | 1.38 | -1.14 | -1.27 | -1.41 |
| miR-590-5p | 10.18 | 14.47 | 21.69 | 25.69 | 11.58 | 19.80 | 1.65 | 5.47 | 4.88 |
| miR-611 | 2.87 | 3.28 | 3.04 | 3.95 | 3.18 | 3.09 | 2.51 | 1.77 | 1.32 |
| miR-620 | -1.32 | -1.19 | -1.06 | -1.61 | -1.09 | -1.34 | 1.04 | 1.13 | 1.02 |
| miR-625 | 1.10 | 1.35 | 1.17 | 1.15 | -1.11 | 1.02 | -3.05 | -1.37 | -1.55 |
| miR-627 | 4.52 | 5.34 | 6.48 | 6.35 | 4.02 | 6.77 | -2.33 | 3.72 | 1.80 |
| miR-628-3p | 1.56 | 1.52 | 1.34 | 1.48 | 1.67 | 1.30 | -1.50 | -1.10 | -1.27 |
| miR-629 | -1.13 | 1.17 | 1.35 | 1.61 | -1.03 | 1.12 | -2.29 | -1.42 | -1.82 |
| miR-652 | 2.00 | 1.89 | 1.85 | 2.47 | 1.87 | 2.15 | 1.38 | 1.45 | 1.23 |
| miR-660 | 2.51 | 3.12 | 3.73 | 5.02 | 2.32 | 4.61 | -1.21 | 1.04 | -1.04 |
| miR-665 | -1.29 | -1.03 | -1.29 | -1.22 | -1.23 | -1.74 | -1.70 | -1.71 | -2.24 |
| miR-1259 | 1.95 | 1.93 | 2.40 | 1.89 | 1.85 | 2.02 | 3.14 | 2.82 | 2.81 |
| miR-1284 | 2.95 | 3.18 | 1.74 | 2.76 | 3.77 | 2.54 | 2.10 | 1.64 | 2.18 |
| miR-1297 | 5.57 | 9.96 | 13.77 | 14.31 | 4.91 | 9.92 | 2.39 | 3.67 | 3.43 |

### 3.6 Pathway analysis of miRNAs with similar expression in acute ischemic stroke

Previously, there were 147 miRNAs highlighted to show similar expression in all the ischemic stroke samples (Table 3.3). These miRNAs were used for pathway analysis to identify the dysregulated pathways in ischemic stroke patients.

Pathway analysis was conducted in the following manner: The list of 147 miRNAs was used to predict for their gene targets through miRWalk database (http://www.umm.uni-heidelberg.de/apps/zmf/mirwalk/index.html) [170]. The list of target gene was used for further analysis in an online gene annotation software, GENECODIS (http://genecodis.cnb.csic.es/) [212-214]. The result of the analysis produced a number of pathways found to be significantly (p-value < 0.05) targeted by the 147 miRNAs. The pathways were annotated according to Kyoto Encyclopedia of Genes and Genomes (KEGG) pathway database [215-217]. The p-value of each pathway was converted to enrichment score by taking the negative natural logarithm of the p-value.


Enrichment score
0
20
40
60
80
100
120
140
MAPK signaling pathway
Pathways in cancer
Calcium signaling pathway
Neuroactive ligand-receptor interaction
Chemokine signaling pathway
Purine metabolism
Lysosome
Insulin signaling pathway
Regulation of actin cytoskeleton
Cytokine-cytokine receptor interaction
Focal adhesion
Cell adhesion molecules (CAMs)
Neurotrophin signaling pathway
Vascular smooth muscle contraction
Glutamatergic synapse
Axon guidance
Tuberculosis
Alzheimer's disease
Viral myocarditis
Tight junction
T cell receptor signaling pathway
Hepatitis C
Jak-STAT signaling pathway
Toxoplasmosis
Prostate cancer
Melanoma
GnRH signaling pathway
Amoebiasis
Huntington's disease
Endocytosis
Wnt signaling pathway
ErbB signaling pathway
Complement and coagulation cascades
Small cell lung cancer
Protein processing in endoplasmic reticulum
Progesterone-mediated oocyte maturation
Osteoclast differentiation
Bile secretion
Protein digestion and absorption
Glioma
B cell receptor signaling pathway
Oocyte meiosis
Measles
Long-term depression
Peroxisome
Salivary secretion
Arrhythmogenic right ventricular cardiomyopathy (ARVC)
Chronic myeloid leukemia
Apoptosis
Natural killer cell mediated cytotoxicity

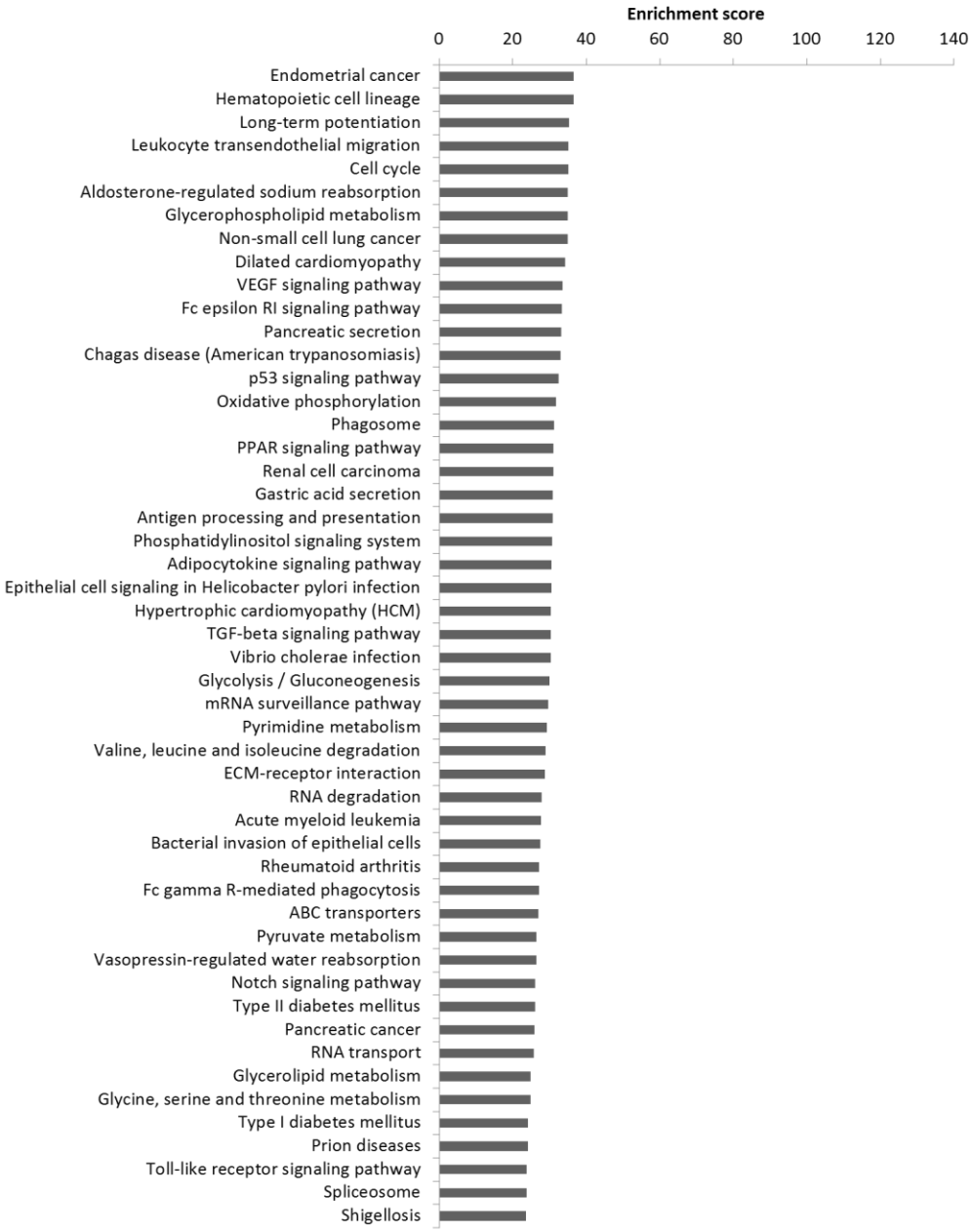


**Figure 3.4:** Top 100 biological pathways according to enrichment score, regulated by 147 miRNAs that showed similar expression in all the ischemic stroke samples.

From the pathway analysis, biological pathways associated with inflammation (Adipocytokine signaling pathway, B cell receptor signaling pathway, Chemokine signaling pathway, Complement and coagulation cascade, Cytokine-cytokine receptor interaction, Leukocyte transendothelial migration, T cell receptor signaling pathway and Toll-like receptor signaling pathway), cell death (Apoptosis, Natural killer cell mediated cytotoxicity and p53 signaling pathway), neurons (Axon guidance, Glutamatergic synapse, Long-term depression, Long-term potentiation, Neuroactive ligand-receptor interaction, Neurotrophin signaling pathway, Notch signaling pathway and Wnt signaling pathway), metabolic dysregulation (Glycerolipid metabolism, Glycerophospholipid metabolism, Glycine, serine and threonine metabolism, Glycolysis / Gluconeogenesis, Oxidative phosphorylation, Pyrimidine metabolism, Purine metabolism, Pyruvate metabolism and Valine, leucine and isoleucine degradation) and vascular permeability (Cell adhesion molecules (CAMs), ECM-receptor interaction, Focal adhesion, Tight junction and VEGF signaling pathway) were detected (Figure 3.4).

Within the top 10 pathways, inflammation related biological pathways, Chemokine signaling pathway and Cytokine-cytokine receptor interaction, were ranked $5^{th}$ and $10^{th}$, while other processes such as neuron related biological pathway (Neuroactive ligand-receptor interaction: ranked $4^{th}$) and metabolic dysregulation related biological pathway (Purine metabolism: ranked $7^{th}$) only had 1 biological pathway in the top 10 (Figure 3.4). This observation suggested that inflammation is a critical process during ischemic stroke.

### 3.7 Pathway analysis of stroke subtype specific miRNAs

In previous section (section 3.5), stroke subtype specific miRNAs were highlighted for each stroke subtype (large artery stroke, cardioembolic stroke and small vessel stroke). The list of miRNAs specific for each stroke subtype was used for pathway analysis to identify the pathways dysregulated in each stroke subtype and compared among the stroke subtypes.

From previous results in section 3.5, 10 large artery specific miRNAs (miR-27a*, -129-5p, -382, -585, -602, -637, -659, -744, -1184 and -1261), 14 cardioembolic stroke specific miRNAs (miR-19a, -130b*, -181a-2*, -198, -200b, -208a, -412, -525-5p, -550, -617, -618, -630, -668 and -1321) and 141 small vessel stroke specific miRNAs were described (Figure 3.3A-C; Table 3.4). These lists of miRNAs were therefore used for pathway analysis that was performed in the same manner as described in section 3.6.

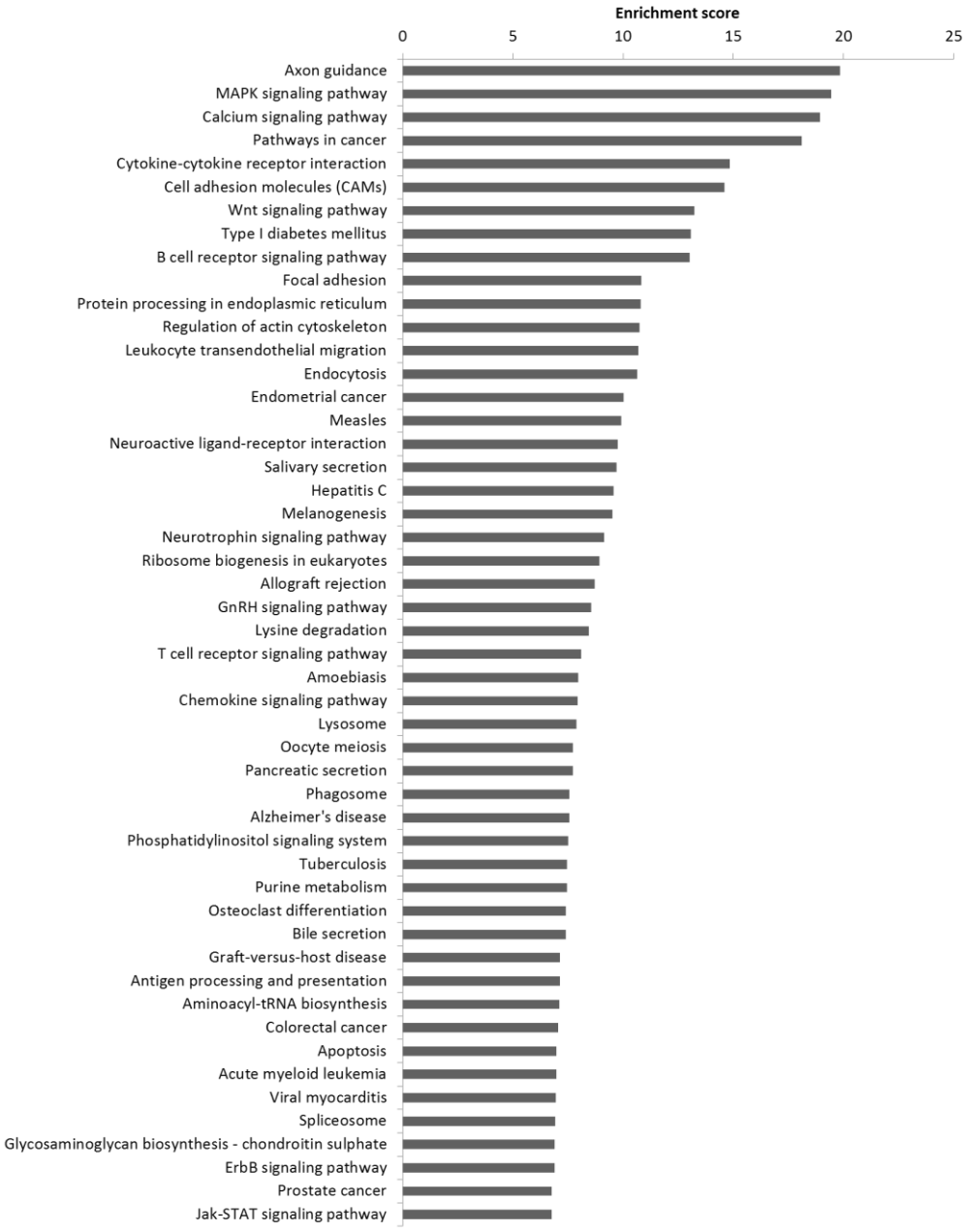
Enrichment score
0
5
10
15
20
25
Axon guidance
MAPK signaling pathway
Calcium signaling pathway
Pathways in cancer
Cytokine-cytokine receptor interaction
Cell adhesion molecules (CAMs)
Wnt signaling pathway
Type I diabetes mellitus
B cell receptor signaling pathway
Focal adhesion
Protein processing in endoplasmic reticulum
Regulation of actin cytoskeleton
Leukocyte transendothelial migration
Endocytosis
Endometrial cancer
Measles
Neuroactive ligand-receptor interaction
Salivary secretion
Hepatitis C
Melanogenesis
Neurotrophin signaling pathway
Ribosome biogenesis in eukaryotes
Allograft rejection
GnRH signaling pathway
Lysine degradation
T cell receptor signaling pathway
Amoebiasis
Chemokine signaling pathway
Lysosome
Oocyte meiosis
Pancreatic secretion
Phagosome
Alzheimer's disease
Phosphatidylinositol signaling system
Tuberculosis
Purine metabolism
Osteoclast differentiation
Bile secretion
Graft-versus-host disease
Antigen processing and presentation
Aminoacyl-tRNA biosynthesis
Colorectal cancer
Apoptosis
Acute myeloid leukemia
Viral myocarditis
Spliceosome
Glycosaminoglycan biosynthesis - chondroitin sulphate
ErbB signaling pathway
Prostate cancer
Jak-STAT signaling pathway

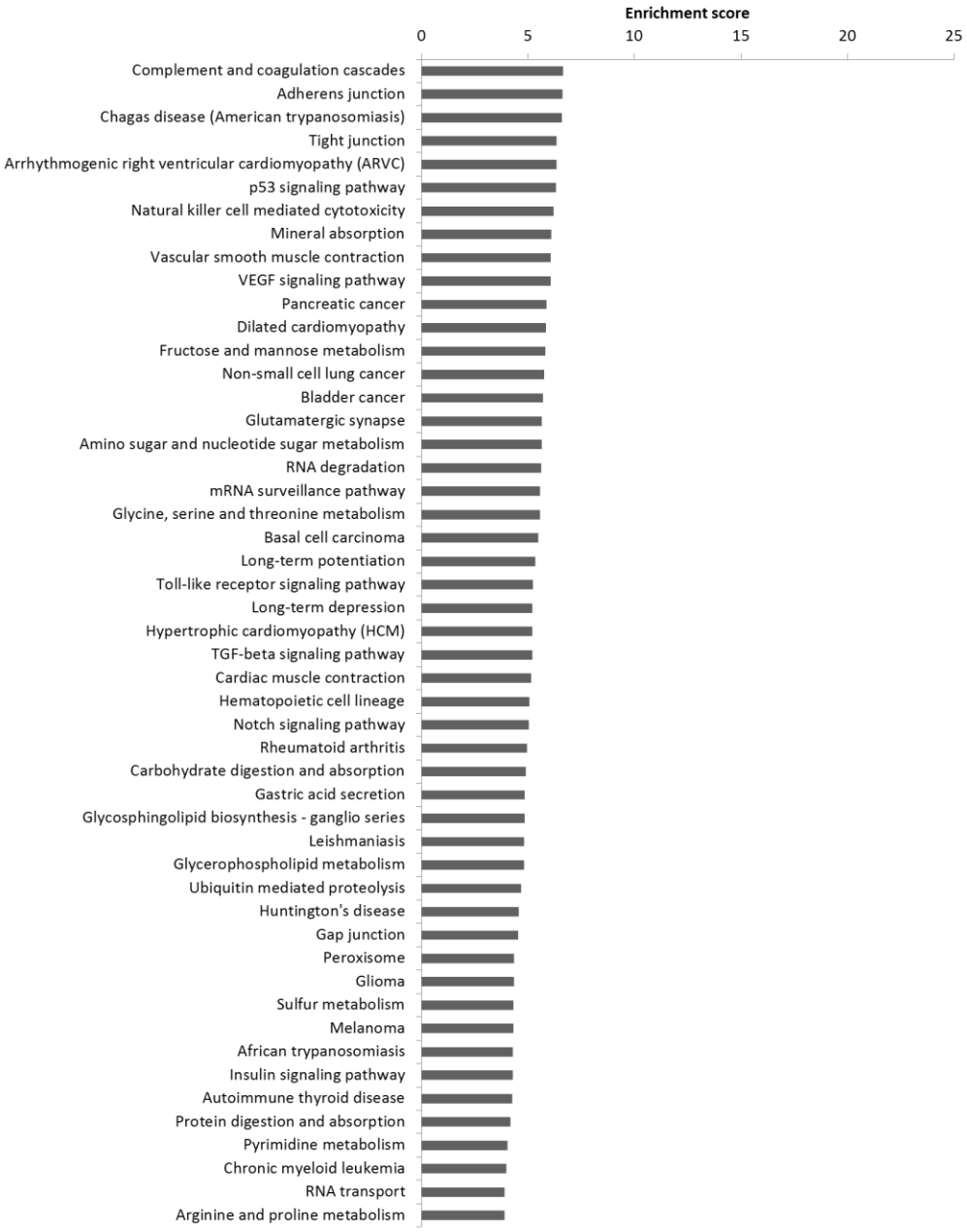


**Figure 3.5:** Top 100 biological pathways according to enrichment score, regulated by the 10 large artery stroke specific miRNAs (miR-27a*, -129-5p, -382, -585, -602, -637, -659, -744, -1184 and -1261)

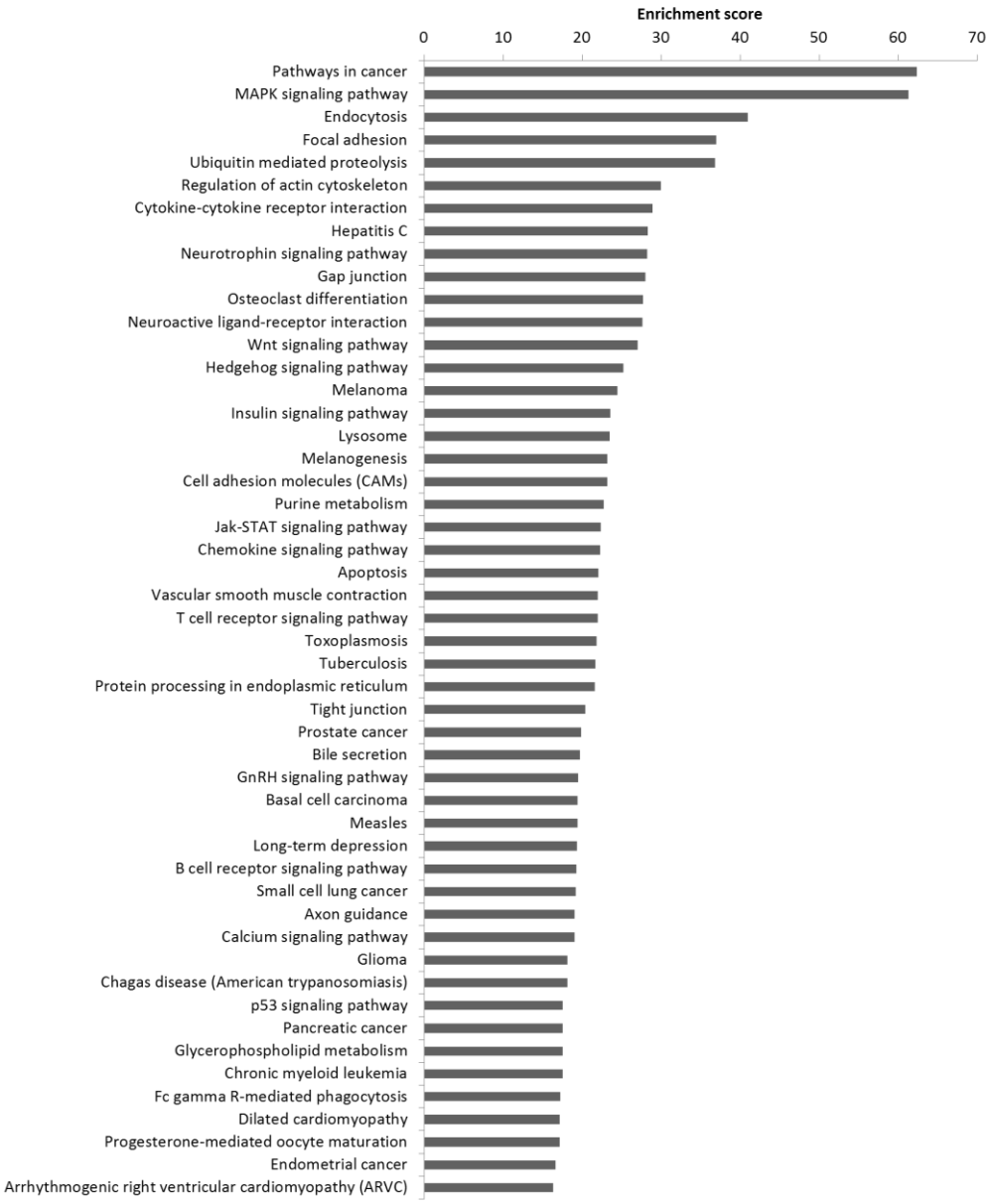
Enrichment score
0
10
20
30
40
50
60
70
Pathways in cancer
MAPK signaling pathway
Endocytosis
Focal adhesion
Ubiquitin mediated proteolysis
Regulation of actin cytoskeleton
Cytokine-cytokine receptor interaction
Hepatitis C
Neurotrophin signaling pathway
Gap junction
Osteoclast differentiation
Neuroactive ligand-receptor interaction
Wnt signaling pathway
Hedgehog signaling pathway
Melanoma
Insulin signaling pathway
Lysosome
Melanogenesis
Cell adhesion molecules (CAMs)
Purine metabolism
Jak-STAT signaling pathway
Chemokine signaling pathway
Apoptosis
Vascular smooth muscle contraction
T cell receptor signaling pathway
Toxoplasmosis
Tuberculosis
Protein processing in endoplasmic reticulum
Tight junction
Prostate cancer
Bile secretion
GnRH signaling pathway
Basal cell carcinoma
Measles
Long-term depression
B cell receptor signaling pathway
Small cell lung cancer
Axon guidance
Calcium signaling pathway
Glioma
Chagas disease (American trypanosomiasis)
p53 signaling pathway
Pancreatic cancer
Glycerophospholipid metabolism
Chronic myeloid leukemia
Fc gamma R-mediated phagocytosis
Dilated cardiomyopathy
Progesterone-mediated oocyte maturation
Endometrial cancer
Arrhythmogenic right ventricular cardiomyopathy (ARVC)

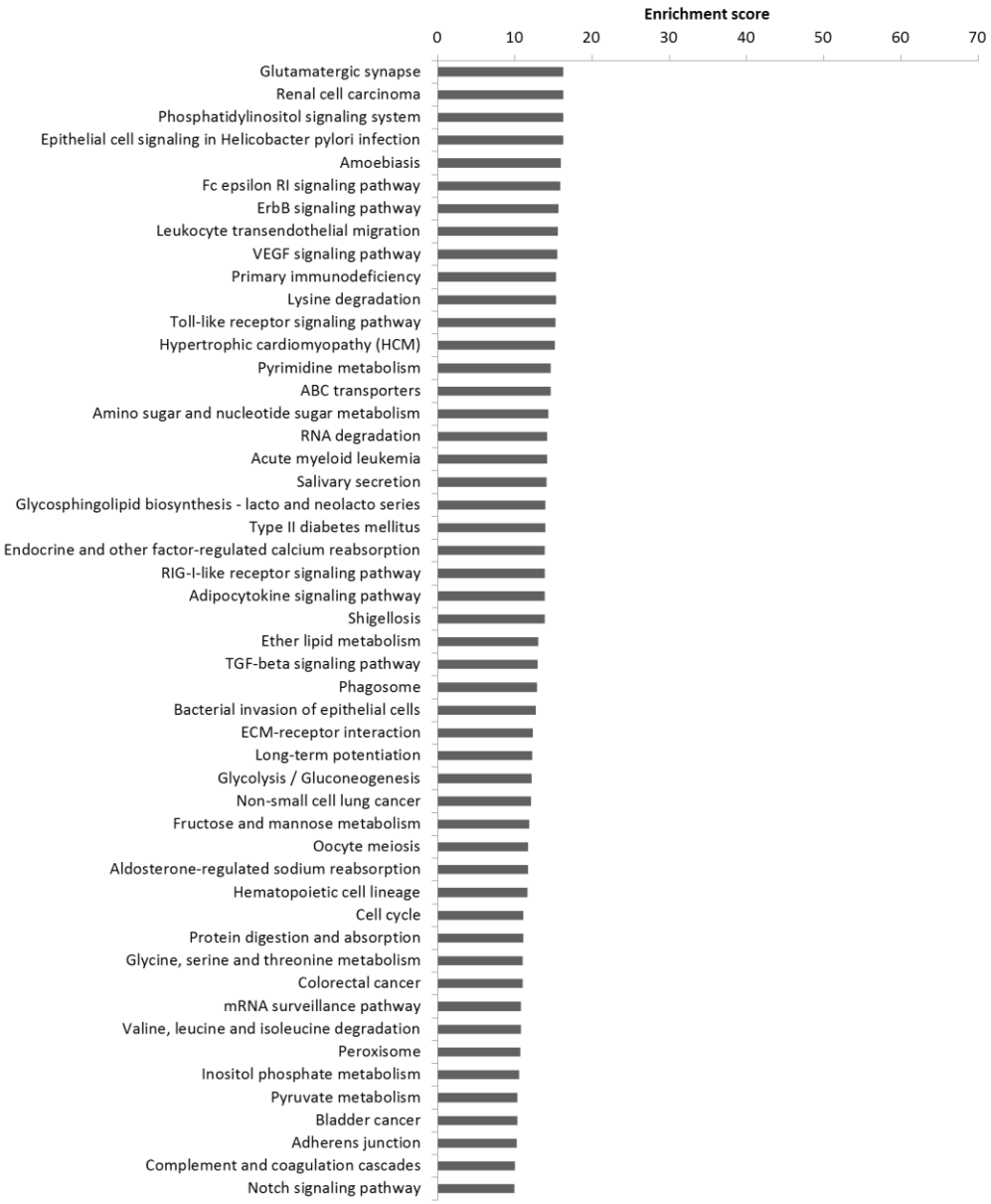


**Figure 3.6:** Top 100 biological pathways according to enrichment score, regulated by the 14 cardioembolic stroke specific miRNAs (miR-19a, -130b*, -181a-2*, -198, -200b, -208a, -412, -525-5p, -550, -617, -618, -630, -668 and -1321)


Enrichment score
0
20
40
60
80
100
120
140
160
180
Pathways in cancer
MAPK signaling pathway
Cytokine-cytokine receptor interaction
Focal adhesion
Chemokine signaling pathway
Regulation of actin cytoskeleton
Protein processing in endoplasmic reticulum
Neuroactive ligand-receptor interaction
Wnt signaling pathway
Endocytosis
Calcium signaling pathway
Insulin signaling pathway
Lysosome
Neurotrophin signaling pathway
Purine metabolism
Ubiquitin mediated proteolysis
Axon guidance
Tuberculosis
Hepatitis C
Cell adhesion molecules (CAMs)
Measles
Apoptosis
Prostate cancer
T cell receptor signaling pathway
Toxoplasmosis
Tight junction
Jak-STAT signaling pathway
Small cell lung cancer
Osteoclast differentiation
Phagosome
Leukocyte transendothelial migration
Melanoma
Glutamatergic synapse
Endometrial cancer
Cell cycle
Chagas disease (American trypanosomiasis)
Pancreatic cancer
Huntington's disease
ErbB signaling pathway
TGF-beta signaling pathway
Melanogenesis
Amoebiasis
Toll-like receptor signaling pathway
Arrhythmogenic right ventricular cardiomyopathy (ARVC)
Chronic myeloid leukemia
B cell receptor signaling pathway
Alzheimer's disease
Renal cell carcinoma
Pyrimidine metabolism
RNA transport

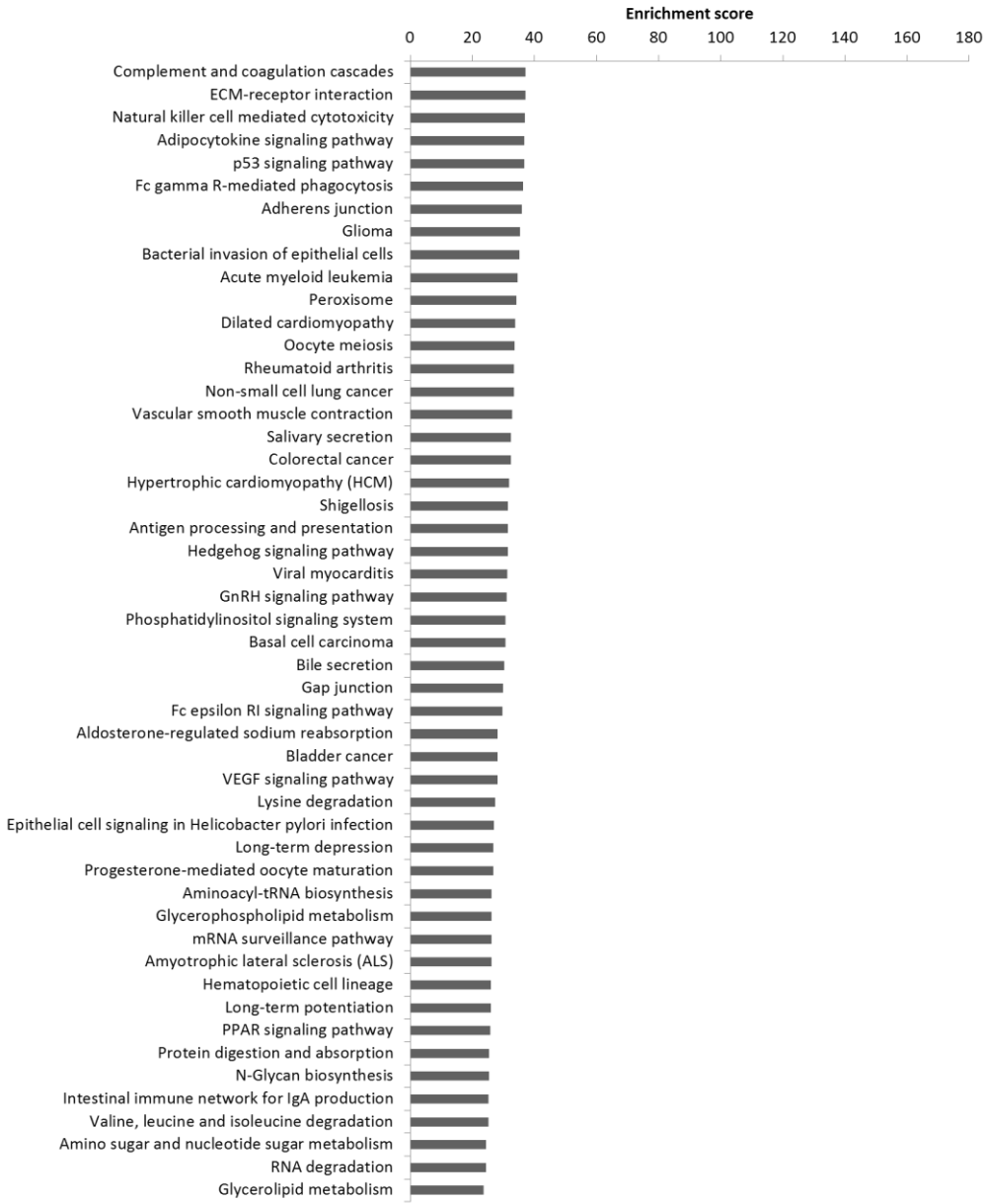


**Figure 3.7:** Top 100 biological pathways according to enrichment score, regulated by the 141 small vessel stroke specific miRNAs

The results of the pathway analysis showed that the biological pathways previously detected in 147 miRNAs showing similar expression in all ischemic stroke samples, were also detected, such as biological pathways associated with inflammation (Adipocytokine signaling pathway, B cell receptor signaling pathway, Chemokine signaling pathway, Complement and coagulation cascade, Cytokine-cytokine receptor interaction, Leukocyte transendothelial migration, T cell receptor signaling pathway and Toll-like receptor signaling pathway), cell death (Apoptosis, Natural killer cell mediated cytotoxicity and p53 signaling pathway), neurons (Axon guidance, Glutamatergic synapse, Long-term depression, Long-term potentiation, Neuroactive ligand-receptor interaction, Neurotrophin signaling pathway, Notch signaling pathway and Wnt signaling pathway), metabolism dysregulation (Glycerolipid metabolism, Glycerophospholipid metabolism, Glycine, serine and threonine metabolism, Glycolysis / Gluconeogenesis, Oxidative phosphorylation, Pyrimidine metabolism, Purine metabolism, Pyruvate metabolism and Valine, leucine and isoleucine degradation) and vascular permeability (Cell adhesion molecules (CAMs), ECM-receptor interaction, Focal adhesion, Tight junction and VEGF signaling pathway) (Figure 3.5, 3.6 and 3.7)

While comparing the biological pathways detected in each stroke subtype, there were biological pathways which were distinctly detected for a particular stroke subtype. The biological pathways, Arginine and proline metabolism and Glycosphingolipid biosynthesis - ganglio series, were only found among the biological pathways regulated by large artery stroke specific miRNAs (Figure 3.5). Also, biological pathways, ABC transporters, Glycosphingolipid

biosynthesis - lacto and neolacto series, Inositol phosphate metabolism and Pyruvate metabolism, were specifically found in the pathway analysis of miRNAs specific for cardioembolic stroke (Figure 3.6). As for small vessel stroke, there were 2 biological pathways (Glycerolipid metabolism and PPAR signaling pathway) that were exclusively present (Figure 3.7). Furthermore, there were biological pathways commonly detected in all stroke subtypes but showed major difference in the ranks between respective groups. B cell receptor signaling pathway and Cell adhesion molecules (CAMs) were highly ranked in large artery stroke as compared with cardioembolic stroke and small vessel stroke, while Tight junction was having lower rank in large artery stroke compared with other stroke subtype (Table 3.5). The biological pathways, Dilated cardiomyopathy, Gap junction and Glycerophospholipid metabolism, were having higher ranks in cardioembolic stroke, whilst Adherens junction and Complement and coagulation cascades were very lowly ranked in cardioembolic stroke (Table 3.5). As for small vessel stroke, Chemokine signaling pathway and TGF-beta signaling pathway were scored higher compared with other stroke subtypes (Table 3.5). On the other hand, the biological pathways, Amino sugar and nucleotide sugar metabolism and VEGF signaling pathway, were lowly scored in small vessel stroke (Table 3.5).

**Table 3.5:** List of biological pathways with distinct ranks for respective stroke subtypes. Ranks showed in bold have found to be specific for the respective stroke subtype.

| **Pathways** | **Rank** | | |
|---|---|---|---|
| | **LA** | **CE** | **SV** |
| Adherens junction | 52 | **98** | 57 |
| Amino sugar and nucleotide sugar metabolism | 67 | 66 | **98** |
| B cell receptor signaling pathway | **9** | 36 | 46 |
| Cell adhesion molecules (CAMs) | **6** | 19 | 20 |
| Chemokine signaling pathway | 28 | 22 | **5** |
| Complement and coagulation cascades | 51 | **99** | 51 |
| Dilated cardiomyopathy | 62 | **47** | 62 |
| Gap junction | 88 | **10** | 78 |
| Glycerophospholipid metabolism | 85 | **44** | 88 |
| TGF-beta signaling pathway | 76 | 77 | **40** |
| Tight junction | **54** | 29 | 26 |
| VEGF signaling pathway | 60 | 59 | **82** |

The 8 miRNAs (miR-19a, -129-5p, -198, -320b, -320d, -331-3p, -637 and -744) that have been selected, which segregated the samples according to stroke subtypes, were also subjected to pathway analysis (Figure 3.3D; Table 3.4). The results of the analysis highlighted biological pathways such as ABC transporters, Amino sugar and nucleotide sugar metabolism, B cell receptor signaling pathway, Cell adhesion molecules (CAMs), Chemokine signaling pathway, Complement and coagulation cascades, Dilated cardiomyopathy, Gap junction, Glycerophospholipid metabolism, Glycosphingolipid biosynthesis - lacto and neolacto series, TGF-beta signaling pathway, Tight junction and VEGF signaling pathway (Figure 3.8). Among these biological pathways, the inflammation related pathways, B cell receptor signaling pathway and Chemokine signaling pathway were ranked highly at $8^{th}$ and $15^{th}$ respectively. This signified that the dysregulation of inflammatory processes may differ between different stroke subtypes which may be potential markers for diagnosis of various stroke subtypes.

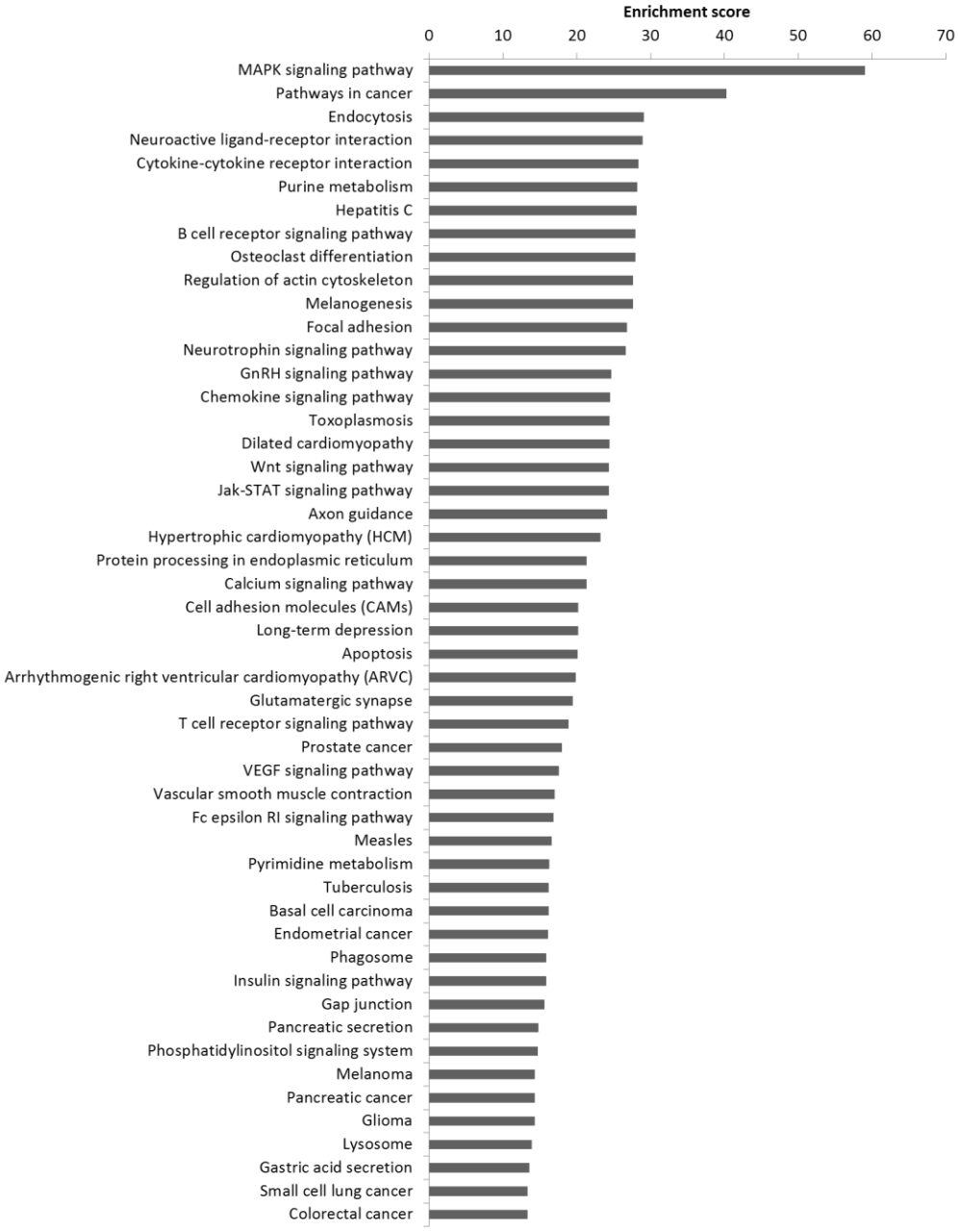
Enrichment score
0
10
20
30
40
50
60
70
MAPK signaling pathway
Pathways in cancer
Endocytosis
Neuroactive ligand-receptor interaction
Cytokine-cytokine receptor interaction
Purine metabolism
Hepatitis C
B cell receptor signaling pathway
Osteoclast differentiation
Regulation of actin cytoskeleton
Melanogenesis
Focal adhesion
Neurotrophin signaling pathway
GnRH signaling pathway
Chemokine signaling pathway
Toxoplasmosis
Dilated cardiomyopathy
Wnt signaling pathway
Jak-STAT signaling pathway
Axon guidance
Hypertrophic cardiomyopathy (HCM)
Protein processing in endoplasmic reticulum
Calcium signaling pathway
Cell adhesion molecules (CAMs)
Long-term depression
Apoptosis
Arrhythmogenic right ventricular cardiomyopathy (ARVC)
Glutamatergic synapse
T cell receptor signaling pathway
Prostate cancer
VEGF signaling pathway
Vascular smooth muscle contraction
Fc epsilon RI signaling pathway
Measles
Pyrimidine metabolism
Tuberculosis
Basal cell carcinoma
Endometrial cancer
Phagosome
Insulin signaling pathway
Gap junction
Pancreatic secretion
Phosphatidylinositol signaling system
Melanoma
Pancreatic cancer
Glioma
Lysosome
Gastric acid secretion
Small cell lung cancer
Colorectal cancer


**Figure 3.8:** Top 100 biological pathways according to enrichment score, regulated by the 8 miRNAs (miR-19a, -129-5p, -198, -320b, -320d, -331-3p, -637 and -744) that were able to segregate the samples according to stroke subtype.

# Chapter 4

# Minimal or no risk ischemic stroke patients - implication of dysregulated miRNAs in ischemic stroke pathophysiology

### 4.1 Risk factors of ischemic stroke

Ischemic stroke can be viewed as a possible end point for patients afflicted by metabolic syndrome. The pathogenesis of ischemic stroke in an individual is a process which intertwines with multiple pre-existing risk factors such as hypertension, dyslipidaemia and type 2 diabetes, to bring about a possible final disorder, cerebral ischemia. However, there are reports in current literature discussing the implication of miRNAs in the pathogenesis and pathophysiology of these risk factors.

Hypertension is the chronic increase of blood pressure above that of the normal blood pressure (Diastolic blood pressure: < 90 mmHg; Systolic blood pressure: < 140 mmHg; Table 4.1) [24]. Hypertension results in an increased sheer stress on the endothelial cells, leading to endothelial dysfunction and atherogenesis [26]. miRNA profiling had been performed in essential hypertension (most common form of hypertension) patients, demonstrating miRNA involvement in pathogenesis of essential hypertension [218]. Furthermore, miR-9 and -126 were reported to show lower level in blood of essential hypertension patients [219]. In addition, miR-21 and -26b were demonstrated to be involved in hypertension induced arterial remodelling [220]. Karolina *et al* [221] had also highlighted exosomal miR-130a and -195 as contributors to hypertension.

Dyslipidaemia is characterized by abnormal amount of lipids present in circulation. Clinically, it is defined as the following: having total cholesterol ≥ 5.2 mmol/L, triglyceride level ≥ 1.8 mmol/L, high density lipoprotein (HDL) ≤ 1.0 mmol/L and low density lipoprotein (LDL) ≥ 3.4 mmol/L (Table 4.1)

[33]. Dyslipidaemia often results in the deposition of excess lipid within the endothelium, leading to plaque formation. Similarly, miRNA profiling had been performed in humans as well as in animal models [221-224]. miRNA profile was obtained from baboon animal model for dyslipidaemia where the animals were fed high-cholestrol and high fat diet [222]. This study demonstrated miRNA dysregulation during dyslipidaemia. In addition, miRNA profile performed in human highlighted miRNAs associated with dylipidaemia. Circulating miR-21 was observed to be decreased in South Asian male with atherogenic dyslipidaemia and exosomal miR-23a, -197 and -509-5p were associated with dyslipidaemia [221, 223]. Liu *et al* [224] also reported miR-17-92 cluster was associated with dyslipidaemia in patients with coronary artery disease.

Type 2 diabetes is a disorder characterized by hyperglycemia due to insulin resistance or lack of insulin. This is diagnosed by measuring fasting glucose (> 6.1 mmol/L) and HbA1c (≥ 7%; Table 4.1) [40, 41]. The excessive glucose present in circulation can lead to endothelial dysfunction and promote formation of atherosclerotic plaque. miRNAs had also been shown to be involved in its pathophysiology and pathogenesis. miRNA profile of type 2 diabetes patients had been reported to demonstrate dysregulation of miRNA during onset of type 2 diabetes [225-227]. Moreover, miRNA expression in tissues affected by type 2 diabetes were also determined and showed miRNA dysregulation in these tissues as well [228, 229].

Given that risk factors of ischemic stroke also alters miRNA expression, it is imperative to look into the dysregulation of miRNA in no risk ischemic stroke patients so as to determine which miRNAs' expression become altered solely

due to ischemic stroke. Not to mention, the condition of no risk ischemic stroke patient is related most closely to the experimental setting for cellular and animal models of ischemic stroke, which could be compared with. Hence, this study was dedicated to identify miRNAs and the biological pathways that they regulate as a way of bridging clinical data with experimental data.

**Table 4.1**: Clinical measurements for risk factors of ischemic stroke [23].

| Risk factor | Clinical parameters |
|---|---|
| Hypertension | Blood pressure > 140/90 mmHg |
| Dyslipidaemia | Total cholesterol level ≥ 5.2 mmol/L, triglyceride level ≥ 1.8 mmol/L, high density lipoprotein (HDL) ≤ 1.0 mmol/L and low density lipoprotein (LDL) ≥ 3.4 mmol/L. |
| Type 2 diabetes | Fasting blood glucose > 6.1 mmol/L or HbA1c ≥ 7% |
| Smoking | Smoked > 10 cigarettes per day for more than one year |
| Alcohol consumption | Intake ≥ 30g of ethanol per day |

## 4.2 Patient recruitment and sample collection

Similar to chapter 3, patients were recruited from University Malaya Medical Centre (UMMC), Kuala Lumpur, Malaysia via the Neurology service and Accident and Emergency (A&E). Ischemic stroke was confirmed by magnetic resonance imaging (MRI) or computed tomography (CT) scan. Blood samples were collected after patient discharge during their follow-up at outpatient clinics (3 months onwards). The whole blood was stored in RNAlater™ (Ambion, Life Technology, Carlsbad, CA, USA) according to manufacturer's protocol and stored at -80°C until required.

For low or no risk ischemic stroke patients, stringent exclusion criteria were implemented. Exclusion criteria included hypertension, dyslipidaemia, diabetes, cardiac ailments, previous stroke, transient ischemic attack (TIA) cancer and other inflammatory diseases. Similar to acute ischemic stroke patients (Chapter 3), the patients classified into the different stroke subtypes according to TOAST classification and outcomes of patients represented by modified Rankin scale (mRS) [8, 211]. For research purposes, mRS was dichotomized into good and poor outcome. In general, mRS $< 2$ were denoted as good outcome, while mRS $\geq 2$ indicated poor outcome.

There were a total of 8 low or no risk ischemic stroke patients, of which, majority of the patients were large artery stroke (n=6), while there were only 1 cardioembolic stroke and 1 small vessel stroke (Table 4.2). As low or no risk patients are rather limited and difficult to recruit, further studies were carried out with these available patients.

For healthy control samples, healthy volunteers were recruited for this study. Exclusion criteria included hypertension, dyslipidaemia, diabetes, cardiac ailments, previous stroke, cancer and other inflammatory diseases.

**Table 4.2:** Patient demographics of ischemic stroke patients with low or no risk factors.

| | **Low or no risk ischemic stroke (n=8)** |
|---|---|
| Male, n (%) | 6 (75.0%) |
| Female, n (%) | 2 (25.0%) |
| Age, mean ± standard deviation | 36.7 ± 8.48 |
| **Stroke Subtype** | |
| Large-artery atherosclerosis, n (%) | 6 (75.0%) |
| Cardioembolic, n (%) | 1 (12.5%) |
| Small vessel occlusion, n (%) | 1 (12.5%) |
| **Functional outcome (mRS)** | |
| mRS <2, n (%) | 7 (87.5%) |
| mRS ≥2, n (%) | 1 (12.5%) |
| **Blood test results for risk factors** | |
| Cholesterol, mmol/L, mean | 5.20 |
| Triglyceride, mmol/L, mean | 1.57 |
| HDL, mmol/L, mean | 1.10 |
| LDL, mmol/L, mean | 3.51 |
| Fasting glucose, mmol/L, mean | 5.81 |
| HbA1c, %, mean | 5.72 |

### 4.3 miRNA profiles of low or no risk ischemic stroke patients

Ribopure™ Blood RNA purification kit (Ambion, Life Technology, Carlsbad, CA, USA) was used to isolate total RNA (including small RNAs). Similar to acute ischemic stroke samples, Nanodrop™ N2000C spectrophotometer (Thermo Scientific™, Rockford, IL, USA) and RNA gel electrophoresis (1% agarose) was used to measure RNA concentration and determine integrity. Small RNAs species (less than 200 nucleotides) was visualised using denaturing polyacrylamide gel electrophoresis (15% polyacrylamide).

RNA samples were used on the same miRNA microarray platform, miRCURY LNA™ miRNA array. Same selection criteria (raw signal intensities > 0 and FDR < 0.05) were also applied for this cohort of patient samples. The results were also visualized on TMEV [209].

Three hundred and fifty two (352) miRNAs were detected in this cohort of patients (Figure 4.1, 4.2; Supplementary table 2). The hierarchical clustering showed that the control samples segregated away from the ischemic stroke samples (Figure 4.1).

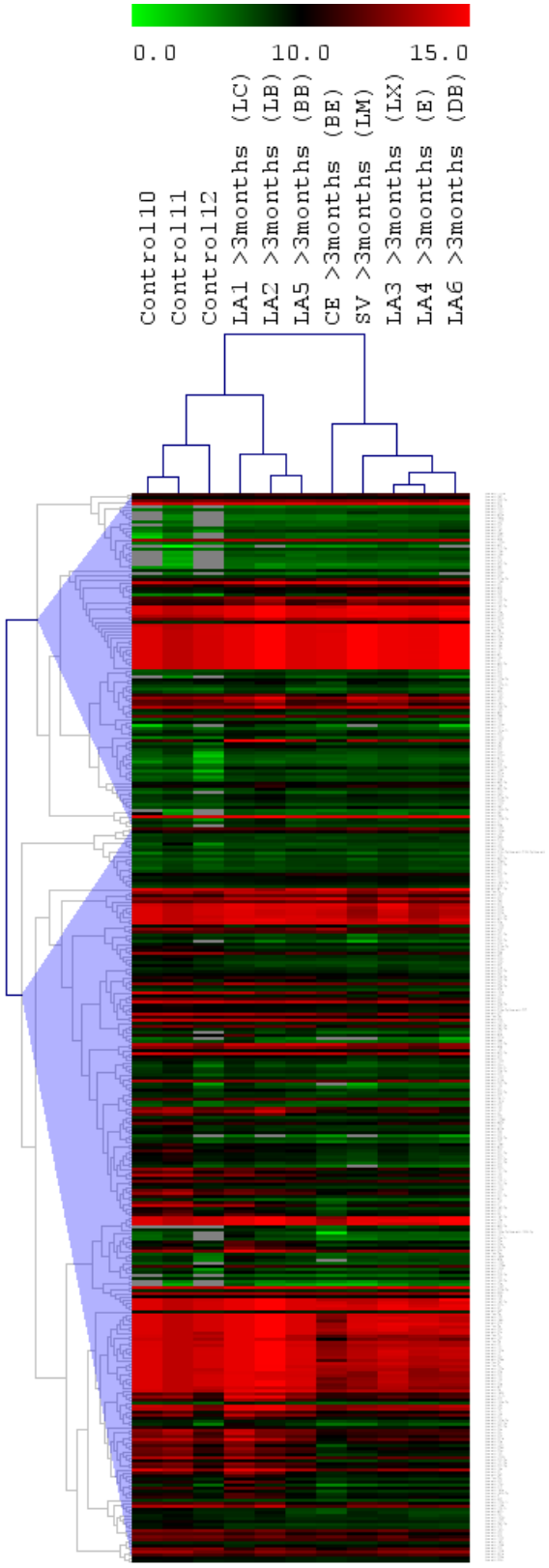


**Figure 4.1:** Hierarchical clustering analysis of 352 miRNAs in low or no risk ischemic stroke patients and healthy controls. The miRNA expression were expressed logarithm of raw intensity. Green represents low signal intensity. Red represents high signal intensity. Grey represents absence. LA: large artery; CE: cardioembolic; SV: small vessel

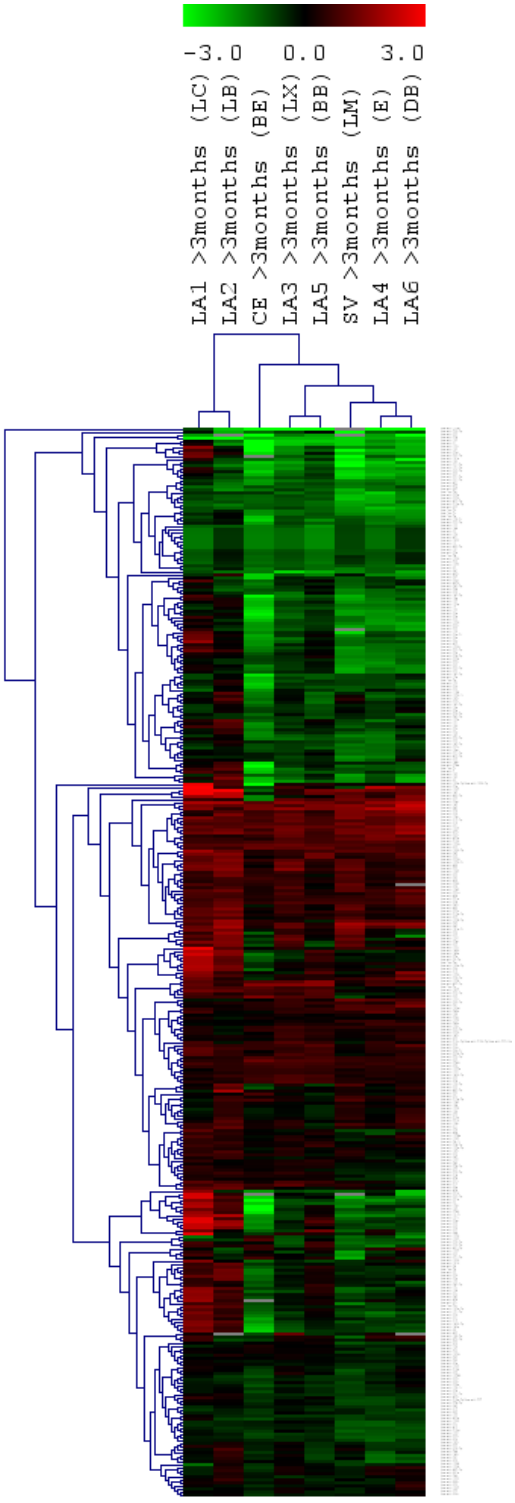


**Figure 4.2:** Heatmap of 352 miRNAs in low or no risk ischemic stroke patients. The miRNA expression were expressed as signal log ratio (SLR) with respect to control samples. Green represents down-regulation. Red represents up-regulation. Grey represents absence. LA: large artery; CE: cardioembolic; SV: small vessel

### 4.4 miRNAs with similar expression in all ischemic stroke samples

Among the 352 miRNAs, there were 111 miRNAs that showed similar expression in all the low or no risk ischemic stroke patients (Table 4.3). 54 miRNAs were down-regulated in all the low or no risk samples while 57 miRNAs were up-regulated in all the low or no risk samples (Table 4.3).

In comparison with the 147 miRNAs that showed similar expression in all the acute ischemic stroke samples, there were 38 miRNAs (let-7d*, -7f, miR-15a, -29b-2*, -32*, -92b, -103, -125b-2*, -138-1*, -142-3p, -146b-3p, -196a*, -200b*, -302c*, -320b, -320c, -331-5p, -374b*, -423-3p, -423-5p, -487b, -488, -494, -498, -508-5p, -576-3p, -585, -617, -659, -668, -887, -923, -934, -943, -1255a, -1299, -1301 and -1321) that were common between the 2 cohorts (Figure 4.3). Among these 38 miRNAs, 27 miRNAs (let-7d*, miR-29b-2*, -32*, -125b-2*, -146b-3p, -196a*, -200b*, -302c*, -320b, -320c, -331-5p, -374b*, -423-3p, -423-5p, -488, -494, -498, -576-3p, -585, -659, -668, -923, -934, -943, -1255a, -1299 and -1321) showed similar expression in both cohorts (Figure 4.3). These 27 miRNAs were considered to provide clues to the critical processes during ischemic stroke regardless of presence of risk factors.

**Table 4.3**: Expression of 111 miRNAs showing similar expression in low or no risk ischemic stroke sample. miRNAs were expressed as fold change with respect to healthy controls.

| Hsa-miRNA | LA1 >3months (LC) | LA2 >3months (LB) | LA3 >3months (LX) | LA4 >3months (E) | LA5 >3months (BB) | LA6 >3months (DB) | SV >3months (LM) | CE >3months (BE) |
|---|---|---|---|---|---|---|---|---|
| Let-7a | -1.75 | -1.01 | -1.78 | -2.55 | -2.06 | -3.09 | -2.04 | -5.00 |
| Let-7b | -1.81 | -1.23 | -2.43 | -3.72 | -2.17 | -3.31 | -3.30 | -3.11 |
| Let-7c | -1.36 | -1.02 | -2.39 | -3.34 | -1.91 | -3.22 | -2.88 | -3.22 |
| Let-7d* | -1.43 | -1.48 | -2.44 | -5.39 | -1.82 | -2.80 | -3.77 | -1.53 |
| Let-7f | -2.03 | -1.18 | -1.84 | -1.94 | -2.40 | -1.29 | -1.35 | -2.35 |
| miR-7 | 1.88 | 1.39 | -2.20 | -1.33 | -2.01 | -1.67 | -1.92 | -4.82 |
| miR-15a | -1.76 | -1.02 | -1.59 | -1.67 | -2.07 | -1.29 | -1.77 | -4.39 |
| miR-15b | -2.63 | -1.53 | -2.38 | -2.51 | -3.11 | -1.54 | -1.75 | -2.87 |
| miR-16 | -2.64 | -1.53 | -2.38 | -2.51 | -3.11 | -1.54 | -1.76 | -2.87 |
| miR-18a* | -1.04 | -1.13 | -1.64 | -2.32 | -1.21 | -1.39 | -2.60 | -1.78 |
| miR-22 | -2.60 | -1.51 | -2.35 | -2.48 | -3.07 | -1.52 | -1.73 | -2.83 |
| miR-26b* | 2.14 | 1.66 | 1.43 | 1.40 | 1.64 | 1.50 | 1.06 | 1.51 |
| miR-29a* | 4.12 | 3.88 | 3.09 | 3.39 | 2.52 | 4.22 | 1.98 | 2.04 |
| miR-29b-2* | 2.13 | 1.47 | 1.51 | 1.33 | 1.73 | 1.30 | 1.01 | 1.02 |
| miR-30a | -1.98 | -1.15 | -1.79 | -1.89 | -2.33 | -1.29 | -1.87 | -2.16 |
| miR-32* | -1.44 | -1.31 | -1.18 | -2.16 | -1.20 | -1.80 | -2.05 | -1.26 |
| miR-92b | -1.19 | -1.16 | -1.42 | -2.20 | -1.24 | -1.45 | -1.68 | -1.34 |
| miR-93 | -2.05 | -1.19 | -1.86 | -2.16 | -2.42 | -2.06 | -2.78 | -2.74 |
| miR-103 | -1.07 | -1.21 | -1.90 | -3.41 | -1.33 | -2.97 | -3.72 | -6.31 |
| miR-122 | -2.20 | -2.07 | -1.97 | -2.15 | -3.32 | -1.86 | -1.70 | -2.79 |
| miR-124* | 2.79 | 1.97 | 2.20 | 2.02 | 1.75 | 2.25 | 2.90 | 1.84 |

| Hsa-miRNA | LA1 >3months (LC) | LA2 >3months (LB) | LA3 >3months (LX) | LA4 >3months (E) | LA5 >3months (BB) | LA6 >3months (DB) | SV >3months (LM) | CE >3months (BE) |
|---|---|---|---|---|---|---|---|---|
| miR-125b-2* | 1.72 | 1.41 | 1.99 | 1.05 | 1.09 | -1.23 | 2.04 | 1.20 |
| miR-130b* | 1.96 | 2.00 | 2.40 | 1.67 | 2.01 | 1.63 | 1.93 | 2.24 |
| miR-138-1* | -1.16 | -1.03 | -1.10 | -1.33 | -1.37 | -1.14 | -1.65 | -1.50 |
| miR-138-2* | 2.75 | 2.85 | 1.90 | 1.34 | 1.27 | -1.02 | -1.85 | -5.57 |
| miR-142-3p | -1.76 | -1.02 | -2.05 | -1.68 | -2.07 | -1.19 | -1.79 | -6.45 |
| miR-144 | -2.56 | -1.49 | -2.31 | -2.44 | -3.02 | -1.49 | -1.70 | -2.79 |
| miR-145 | 2.70 | 2.19 | 1.80 | 2.52 | 2.77 | 5.20 | 3.17 | 2.58 |
| miR-145* | 1.12 | 1.18 | 1.67 | 1.19 | 1.33 | 1.53 | 1.07 | 1.12 |
| miR-146b-3p | 1.29 | 1.57 | 1.86 | 1.35 | 1.74 | 1.27 | 1.16 | 1.57 |
| miR-186 | -1.15 | -2.02 | -3.77 | -5.11 | -2.43 | -2.92 | -7.72 | -5.19 |
| miR-191 | -2.09 | -1.22 | -1.89 | -2.02 | -2.47 | -1.73 | -1.83 | -2.28 |
| miR-196a* | 1.48 | 1.13 | 1.39 | 1.90 | 1.50 | 1.45 | 1.94 | 1.29 |
| miR-199b-5p | 3.70 | 2.31 | 1.50 | 2.02 | 1.72 | 1.74 | 2.11 | 1.26 |
| miR-200b* | 1.40 | 1.52 | 1.51 | 1.05 | 1.12 | -1.36 | 2.00 | 1.52 |
| miR-299-3p | 1.14 | 1.28 | 1.59 | 1.28 | 1.54 | 2.20 | 1.58 | 1.37 |
| miR-302c* | 1.84 | 1.77 | 1.86 | 1.54 | 1.20 | 1.78 | 1.21 | 1.26 |
| miR-302e | 2.09 | 2.24 | 1.71 | 1.36 | 1.42 | 1.41 | 1.70 | 1.03 |
| miR-320a | -1.75 | -2.06 | -1.76 | -4.26 | -2.06 | -2.90 | -4.80 | -2.22 |
| miR-320b | -1.64 | -2.16 | -1.92 | -4.07 | -1.88 | -3.03 | -5.01 | -2.27 |
| miR-320c | -1.76 | -1.15 | -1.60 | -2.37 | -2.08 | -1.68 | -2.35 | -1.92 |
| miR-320d | -1.11 | -1.44 | -1.42 | -2.89 | -1.32 | -2.06 | -3.24 | -1.66 |
| miR-328 | 1.71 | 1.47 | 1.61 | 1.46 | 2.02 | 2.14 | 1.11 | 1.50 |
| miR-331-5p | -1.55 | -2.90 | -2.96 | -4.27 | -1.93 | -4.85 | -9.51 | -4.45 |
| miR-345 | 2.72 | 2.96 | 1.47 | 1.51 | 2.50 | 2.12 | 1.40 | 1.27 |
| miR-361-5p | 2.03 | 1.14 | 1.29 | 1.26 | 1.73 | -1.19 | -2.89 | -3.60 |

| Hsa-miRNA | LA1 >3months (LC) | LA2 >3months (LB) | LA3 >3months (LX) | LA4 >3months (E) | LA5 >3months (BB) | LA6 >3months (DB) | SV >3months (LM) | CE >3months (BE) |
|---|---|---|---|---|---|---|---|---|
| miR-363* | 1.37 | 1.23 | 2.24 | 2.74 | 1.64 | 2.03 | 1.91 | 1.52 |
| miR-365 | 2.10 | 2.54 | 1.31 | 1.46 | 2.51 | 1.90 | 1.21 | 1.03 |
| miR-374b* | 1.74 | 1.43 | 1.79 | 1.60 | 1.69 | 1.39 | 1.40 | 1.73 |
| miR-382 | 1.41 | 1.66 | 1.51 | 1.19 | 1.18 | 1.29 | 1.88 | 1.65 |
| miR-412 | -1.26 | -1.48 | -1.23 | -1.81 | -1.34 | -1.94 | -1.85 | -1.38 |
| miR-421 | -1.33 | -2.60 | -1.92 | -2.15 | -1.72 | -2.73 | -2.60 | -3.42 |
| miR-423-3p | -1.35 | -1.30 | -1.76 | -2.78 | -1.31 | -1.25 | -3.27 | -1.22 |
| miR-423-5p | -2.05 | -1.87 | -1.99 | -4.06 | -2.41 | -2.24 | -3.88 | -2.23 |
| miR-450a | 1.57 | 1.50 | 1.88 | 2.63 | 1.69 | 2.59 | 2.19 | 1.28 |
| miR-451 | -2.63 | -1.53 | -2.38 | -2.51 | -3.11 | -1.54 | -1.75 | -2.87 |
| miR-486-5p | -2.64 | -1.53 | -2.38 | -2.51 | -3.11 | -1.54 | -1.75 | -2.87 |
| miR-487b | -1.10 | -1.56 | -1.26 | -1.65 | -1.31 | -1.14 | -2.12 | -2.83 |
| miR-488 | 2.75 | 2.82 | 2.30 | 1.23 | 1.21 | 1.30 | 2.15 | 1.02 |
| miR-490-3p | 2.20 | 1.34 | 3.01 | 1.77 | 3.15 | 1.71 | 1.09 | 3.03 |
| miR-494 | 1.76 | 1.69 | 1.61 | 1.64 | 1.39 | 2.16 | 1.47 | 1.35 |
| miR-498 | 1.30 | 1.62 | 1.64 | 1.37 | 1.25 | 1.66 | 1.77 | 1.50 |
| miR-501-5p | -1.19 | -1.79 | -1.80 | -3.54 | -1.59 | -2.84 | -5.25 | -2.89 |
| miR-502-5p | -1.26 | -1.10 | -1.66 | -2.82 | -2.17 | -2.35 | -1.81 | -3.77 |
| miR-504 | -7.13 | -8.12 | -4.50 | -4.06 | -4.40 | -4.53 | -5.74 | -4.43 |
| miR-505* | -1.22 | -1.30 | -1.42 | -2.12 | -1.34 | -1.96 | -2.07 | -1.72 |
| miR-508-5p | -1.09 | -1.49 | -1.08 | -1.53 | -1.70 | -2.38 | -1.26 | -2.40 |
| miR-513a-3p | 2.19 | 2.71 | 1.39 | 1.13 | 1.17 | 1.34 | 1.51 | 1.18 |
| miR-516a-5p | -2.17 | -2.73 | -2.00 | -3.10 | -2.35 | -3.38 | -3.71 | -2.07 |
| miR-516b | 1.61 | 1.60 | 1.98 | 2.01 | 1.70 | 1.79 | 1.81 | 1.77 |
| miR-542-3p | -1.35 | -1.48 | -1.55 | -1.46 | -2.01 | -1.72 | -1.33 | -1.82 |

| Hsa-miRNA | LA1 >3months (LC) | LA2 >3months (LB) | LA3 >3months (LX) | LA4 >3months (E) | LA5 >3months (BB) | LA6 >3months (DB) | SV >3months (LM) | CE >3months (BE) |
|---|---|---|---|---|---|---|---|---|
| miR-550* | -1.03 | -1.45 | -1.54 | -3.39 | -1.10 | -2.20 | -3.20 | -1.77 |
| miR-551a | 1.58 | 2.02 | 1.52 | 1.48 | 1.57 | 2.05 | 1.57 | 1.24 |
| miR-553 | 2.56 | 3.11 | 3.09 | 1.42 | 1.45 | 1.39 | 2.42 | 1.39 |
| miR-576-3p | 1.21 | 1.32 | 1.59 | 1.43 | 1.77 | 1.55 | 1.50 | 1.89 |
| miR-578 | 1.34 | 1.94 | 1.86 | 2.34 | 1.33 | 3.57 | 2.81 | 1.60 |
| miR-581 | 1.07 | 1.08 | 1.55 | 1.84 | 1.20 | 2.72 | 1.92 | 1.35 |
| miR-585 | 1.76 | 3.34 | 2.19 | 2.85 | 1.26 | 3.23 | 3.88 | 1.35 |
| miR-601 | 2.26 | 1.97 | 2.46 | 2.70 | 2.21 | 3.48 | 2.10 | 2.26 |
| miR-615-3p | 2.14 | 2.04 | 2.36 | 2.01 | 1.78 | 2.38 | 1.90 | 1.66 |
| miR-617 | -1.56 | -1.24 | -1.12 | -1.57 | -1.46 | -1.89 | -1.21 | -1.53 |
| miR-618 | 1.78 | 1.84 | 1.92 | 1.99 | 1.77 | 2.68 | 2.63 | 1.95 |
| miR-620 | 1.42 | 1.38 | 1.93 | 1.46 | 1.91 | 1.51 | 1.57 | 2.42 |
| miR-625* | -1.29 | -1.48 | -1.30 | -1.38 | -1.50 | -1.10 | -1.51 | -1.52 |
| miR-629 | -1.02 | -1.46 | -2.57 | -2.36 | -1.02 | -2.05 | -2.84 | -2.15 |
| miR-630 | 1.11 | 1.31 | 1.88 | 1.15 | 1.62 | 1.24 | 1.29 | 1.69 |
| miR-642 | -1.41 | -1.08 | -1.15 | -1.56 | -1.33 | -1.23 | -1.46 | -1.23 |
| miR-659 | 1.46 | 1.41 | 1.70 | 1.38 | 1.55 | 1.55 | 1.53 | 1.55 |
| miR-664 | 1.73 | 2.28 | 1.90 | 1.64 | 1.69 | 2.08 | 1.71 | 1.44 |
| miR-668 | 1.19 | 2.77 | 2.38 | 2.55 | 1.51 | 2.77 | 2.76 | 1.68 |
| miR-720 | -2.26 | -1.31 | -2.04 | -2.15 | -2.66 | -1.32 | -1.52 | -2.46 |
| miR-769-5p | -1.13 | -4.27 | -1.69 | -2.19 | -1.05 | -1.81 | -16.31 | -2.36 |
| miR-877 | -2.27 | -2.79 | -2.11 | -2.43 | -1.93 | -1.69 | -2.77 | -1.85 |
| miR-877* | 2.40 | 2.77 | 2.41 | 2.56 | 1.59 | 3.79 | 2.62 | 2.03 |
| miR-887 | -1.72 | -3.23 | -1.61 | -2.49 | -2.20 | -2.25 | -4.29 | -2.57 |
| miR-920 | 1.77 | 1.58 | 2.15 | 1.94 | 2.29 | 1.68 | 1.75 | 2.34 |

| Hsa-miRNA | LA1 >3months (LC) | LA2 >3months (LB) | LA3 >3months (LX) | LA4 >3months (E) | LA5 >3months (BB) | LA6 >3months (DB) | SV >3months (LM) | CE >3months (BE) |
|---|---|---|---|---|---|---|---|---|
| miR-923 | -1.81 | -2.22 | -1.64 | -4.71 | -2.14 | -3.84 | -3.36 | -1.98 |
| miR-934 | 1.35 | 1.21 | 1.98 | 1.39 | 1.70 | 1.17 | 1.32 | 1.60 |
| miR-941 | -1.81 | -2.47 | -5.79 | -2.20 | -4.17 | -3.87 | -2.95 | -2.60 |
| miR-942 | 3.02 | 1.45 | 3.37 | 4.37 | 2.71 | 4.45 | 2.93 | 2.64 |
| miR-943 | 2.30 | 3.89 | 2.27 | 1.84 | 1.34 | 2.66 | 3.34 | 1.22 |
| miR-1227 | 1.98 | 2.41 | 2.57 | 2.37 | 1.78 | 3.12 | 2.53 | 1.59 |
| miR-1249 | 2.00 | 2.43 | 1.56 | 1.66 | 1.23 | 2.50 | 2.07 | 1.22 |
| miR-1255a | 1.03 | 1.43 | 1.52 | 1.38 | 1.50 | 1.37 | 1.16 | 1.50 |
| miR-1275 | -1.67 | -1.44 | -2.07 | -2.29 | -2.37 | -2.64 | -1.90 | -2.21 |
| miR-1285 | 1.44 | 2.44 | 1.61 | 1.34 | 1.23 | 1.84 | 1.72 | 1.34 |
| miR-1299 | -1.41 | -1.33 | -1.02 | -2.10 | -1.08 | -1.61 | -2.05 | -1.24 |
| miR-1301 | -1.07 | -1.21 | -1.56 | -1.97 | -1.40 | -1.94 | -1.86 | -1.82 |
| miR-1304 | 2.07 | 1.22 | 2.28 | 1.65 | 3.48 | -1.08 | 1.22 | 2.01 |
| miR-1321 | 1.18 | 1.29 | 1.51 | 1.32 | 1.42 | 1.24 | 1.28 | 1.48 |
| miR-1826 | -2.64 | -1.53 | -2.39 | -2.51 | -3.11 | -1.54 | -1.75 | -2.87 |

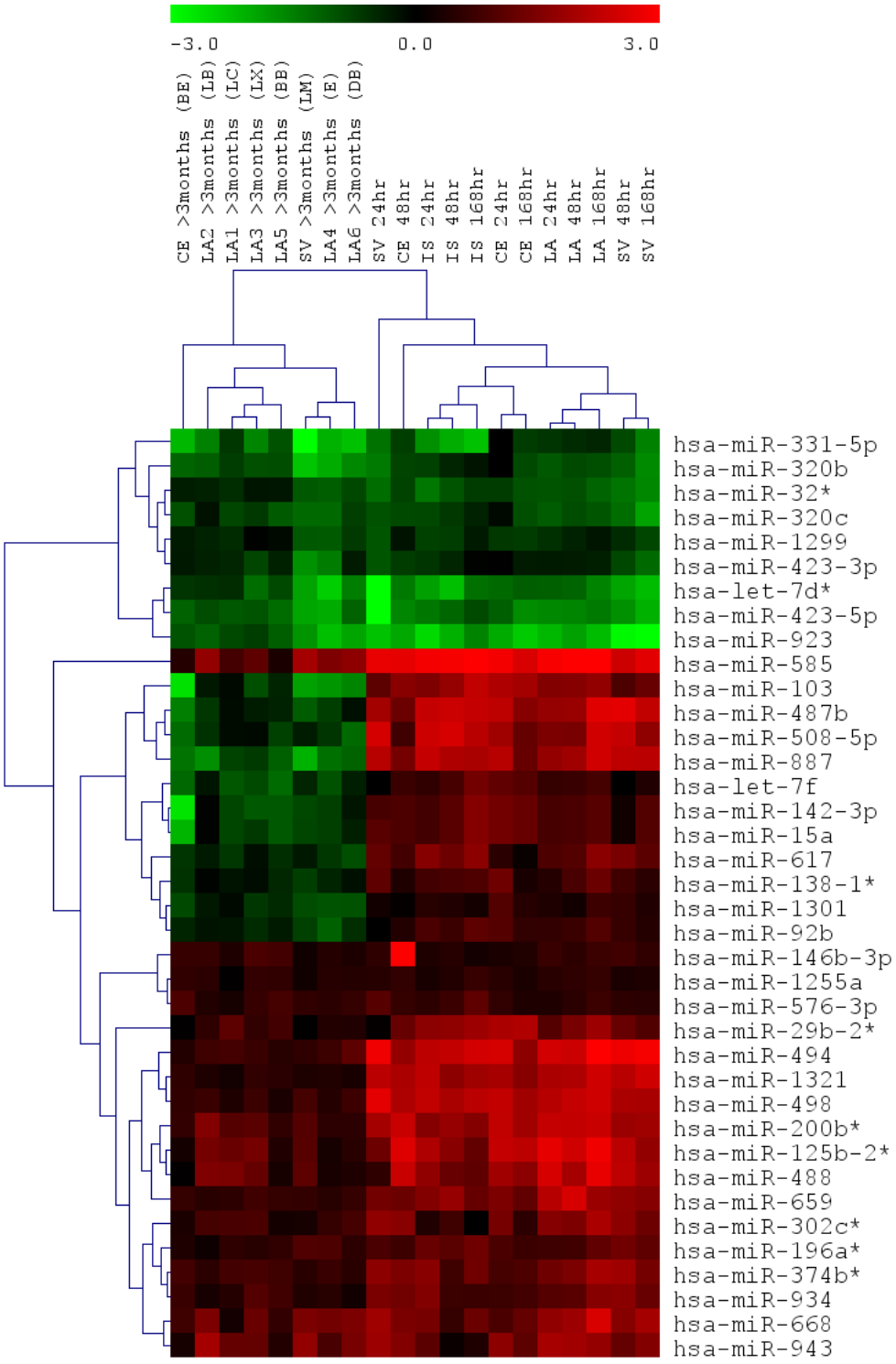


**Figure 4.3:** Hierarchical clustering (HCL) of 38 miRNAs commonly detected as ischemic stroke specific miRNAs. The miRNA expression were expressed as signal log ratio (SLR) with respect to control samples. Green represents down-regulation. Red represents up-regulation. Grey represents absence.

### 4.5 miRNA profile in low or no risk large artery stroke patients

In this cohort, the samples were derived from low or no risk ischemic stroke patients. Due to the exclusive nature of the samples, there were only 8 samples in this cohort. 6 of the 8 samples were classified as large artery (LA) stroke samples (according to TOAST classification; Table 4.2). In-depth analysis was carried out on these 6 samples to identify the underlying relationship between the miRNA expression and large artery stroke pathophysiology. Principal component analysis (PCA) was used for analysis. In brief, PCA transforms the miRNA expression profile of each sample into 3 principal components and these components form coordinates in a 3-dimensional plot (PCA plot). The spatial location of the sample represents the underlying relationship between the samples. PCA was performed and visualized on the TMEV [209].

In the PCA plot, the samples appeared to be distributed in a radial fashion according to the functional outcome of the patients (Figure 4.4). The patients with good functional outcome (LB, LX and BB; mRS=1) were clustered together in the center of the PCA plot, while patients with mRS=2 (LC and E) segregated along the periphery of the cluster of patients with mRS=1 (Figure 4.4). Sample DB with mRS=4 was located at the extreme periphery of the plot (Figure 4.4). Hence, the miRNA profiles of low or no risk large artery stroke patients were associated with the functional outcome of patients.

Upon closer inspection, there was group of 24 miRNAs (let-7e, miR-125b, -125b-2*, -138-2*, -150, -181a-2*, -195, -200b*, -206, -208a, -214, -221, -221*, -361-5p, -509-5p, -519e*, -574-3p, -635, -636, -874, -937, -1275, -1304 and -1827) which showed a differential expression between patients with mRS $\leq$ 2 (BB, E, LB, LC and LX) and patient with mRS > 2 (DB; Table 4.4).

Amongst these 24 miRNAs, 2 miRNAs (miR-208 and -636) were found to be up-regulated only in DB (mRS > 2) and down-regulated in other samples with mRS ≤ 2 (BB, E, LB, LC and LX; Table 4.4). Whilst the other 22 miRNAs (let-7e, miR-125b, -125b-2*, -138-2*, -150, -181a-2*, -195, -200b*, -206, -214, -221, -221*, -361-5p, -509-5p, -519e*, -574-3p, -635, -874, -937, -1275, -1304 and -1827) were up-regulated in large artery samples with mRS ≤ 2 and showing opposite expression in DB (mRS > 2; Table 4.4). However, due to the small sample size, further investigation in a larger cohort will be required to validate the findings.

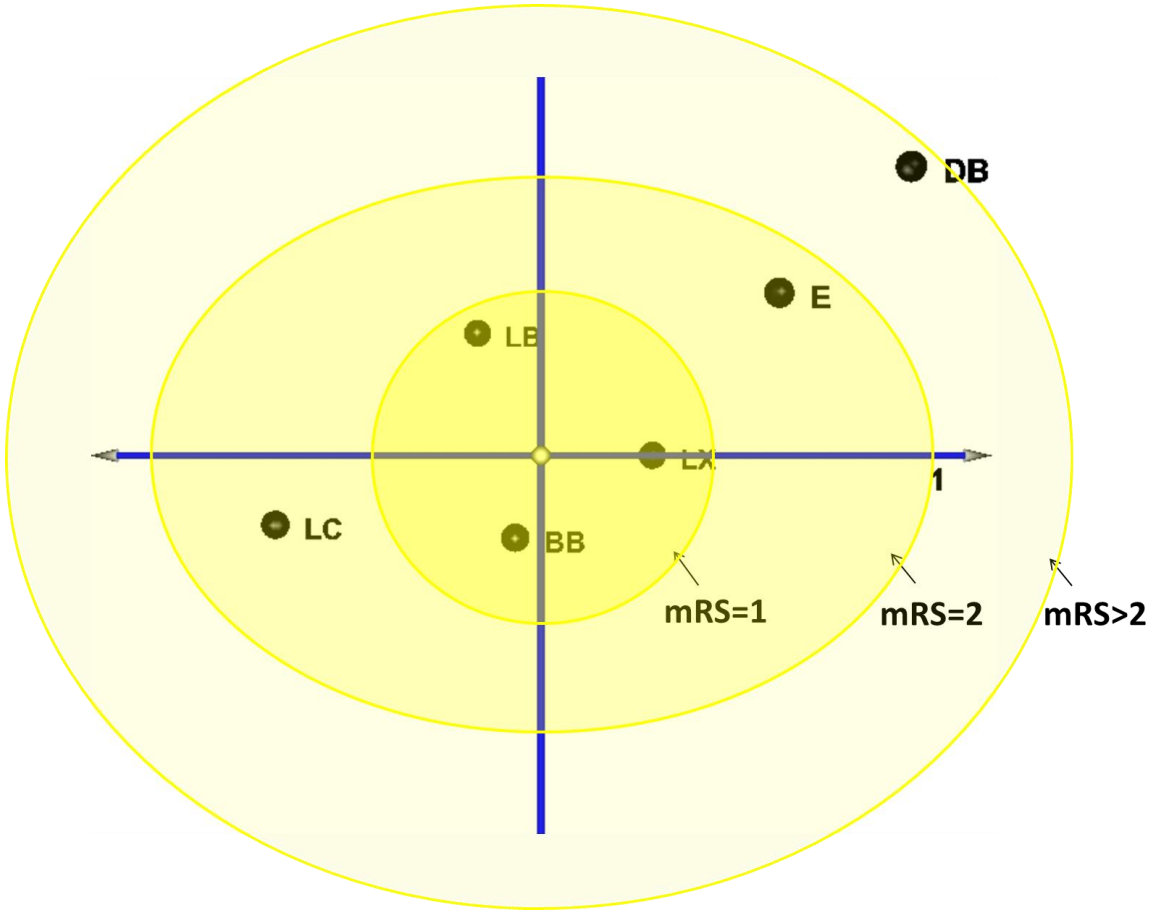


**Figure 4.4:** Principal component analysis of low or no risk large artery stroke patient samples. mRS: modified Rankin scale.

**Table 4.4:** 24 miRNAs that showed differential expression between patients with mRS ≤ 2 and patient with mRS > 2. Expression of miRNAs were presented as fold change with respect to healthy controls.

| **Hsa-miRNA** | **mRS=1** | | | **mRS=2** | | **mRS=4** |
|---|---|---|---|---|---|---|
| | LA2 >3months (LB) | LA3 >3months (LX) | LA5 >3months (BB) | LA1 >3months (LC) | LA4 >3months (E) | LA6 >3months (DB) |
| Let-7e | 1.83 | 1.57 | 1.71 | 2.04 | 1.00 | -1.12 |
| miR-125b | 2.03 | 1.43 | 2.35 | 1.10 | 1.82 | -1.39 |
| miR-125b-2* | 1.41 | 1.99 | 1.09 | 1.72 | 1.05 | -1.23 |
| miR-138-2* | 2.85 | 1.90 | 1.27 | 2.75 | 1.34 | -1.02 |
| miR-150 | 1.54 | 1.48 | 2.14 | 2.39 | 1.32 | -1.74 |
| miR-181a-2* | 1.86 | 1.50 | 1.42 | 2.94 | 1.10 | -1.75 |
| miR-195 | 1.84 | 1.04 | 2.04 | 3.44 | 1.13 | -2.02 |
| miR-200b* | 1.52 | 1.51 | 1.12 | 1.40 | 1.05 | -1.36 |
| miR-206 | 3.46 | 1.43 | 1.19 | 1.49 | 1.07 | -1.48 |
| miR-208a | -1.11 | -1.36 | -1.58 | -1.15 | -1.41 | 1.10 |
| miR-214 | 1.58 | 1.77 | 1.86 | 1.84 | 1.04 | -1.49 |
| miR-221 | 1.39 | 1.30 | 1.66 | 3.28 | 1.07 | -1.26 |
| miR-221* | 1.61 | 1.82 | 1.59 | 2.07 | 1.19 | -1.45 |
| miR-361-5p | 1.14 | 1.29 | 1.73 | 2.03 | 1.26 | -1.19 |
| miR-509-5p | 1.86 | 2.22 | 2.03 | 2.07 | 1.21 | -1.30 |
| miR-519e* | 1.15 | 2.27 | 1.91 | 1.89 | 1.11 | -1.09 |
| miR-574-3p | 1.20 | 1.62 | 1.73 | 1.68 | 1.01 | -1.06 |
| miR-635 | 2.75 | 2.06 | 1.05 | 2.02 | 1.09 | -3.06 |
| miR-636 | -1.37 | -1.16 | -1.01 | -1.02 | -1.15 | 1.27 |

| **Hsa-miRNA** | **mRS=1** | | | **mRS=2** | | **mRS=4** |
|---|---|---|---|---|---|---|
| | LA2 >3months (LB) | LA3 >3months (LX) | LA5 >3months (BB) | LA1 >3months (LC) | LA4 >3months (E) | LA6 >3months (DB) |
| miR-874 | 1.40 | 1.75 | 1.93 | 1.94 | 1.11 | -1.32 |
| miR-937 | 1.65 | 1.14 | 1.44 | 1.90 | 1.13 | -1.19 |
| miR-1275 | 1.25 | 1.19 | 1.10 | 1.24 | 1.04 | -1.55 |
| miR-1304 | 1.22 | 2.28 | 3.48 | 2.07 | 1.65 | -1.08 |
| miR-1827 | 2.21 | 1.71 | 2.00 | 2.53 | 1.05 | -1.01 |

## 4.6 Pathway analysis of miRNAs with similar expression in all ischemic stroke samples

In section 4.4, 27 miRNAs (let-7d*, miR-29b-2*, -32*, -125b-2*, -146b-3p, -196a*, -200b*, -302c*, -320b, -320c, -331-5p, -374b*, -423-3p, -423-5p, -488, -494, -498, -576-3p, -585, -659, -668, -923, -934, -943, -1255a, -1299 and -1321) were identified as ischemic stroke specific miRNAs. These 27 miRNAs were used for pathway analysis. Pathway analysis was performed in the same manner as described in section 3.6

Similar to results from section 3.6, biological pathways associated with inflammation (B cell receptor signaling pathway, Chemokine signaling pathway, Complement and coagulation cascade, Cytokine-cytokine receptor interaction, Leukocyte transendothelial migration and T cell receptor signaling pathway), cell death (Apoptosis, Natural killer cell mediated cytotoxicity and p53 signaling pathway), neurons (Axon guidance, Glutamatergic synapse, Hedgehog signaling pathway, Long-term depression, Long-term potentiation, Neuroactive ligand-receptor interaction, Neurotrophin signaling pathway and Wnt signaling pathway), metabolism dysregulation (Amino acid and nucleotide sugar metabolism, Fructose and mannose metabolism, Galactose metabolism, Glycosaminoglycan degradation, Glycerophospholipid metabolism, Glycolysis / Gluconeogenesis, Inositol phosphate metabolism, Lysine degradation, Pyrimidine metabolism, Purine metabolism and Valine, leucine and isoleucine degradation) and vascular permeability (Adherens junction, Cell adhesion molecules (CAMs), Focal adhesion, Gap junction, Tight junction and VEGF signaling pathway) were also detected (Figure 4.5).

Looking at the top 10 biological pathways, they mainly consisted of neuron-related biological pathways (Neuroactive ligand-receptor interaction: ranked 4$^{th}$, Neurotrophin signaling pathway: ranked 5$^{th}$ and Wnt signaling pathway: ranked 7$^{th}$), inflammation-related pathway (Chemokine signaling pathway: ranked 6$^{th}$) and pathways associated with vascular permeability (Focal adhesion: ranked 9$^{th}$; Figure 4.5). The results suggest that neuro-inflammation is an important process during ischemic stroke and worth further investigation.

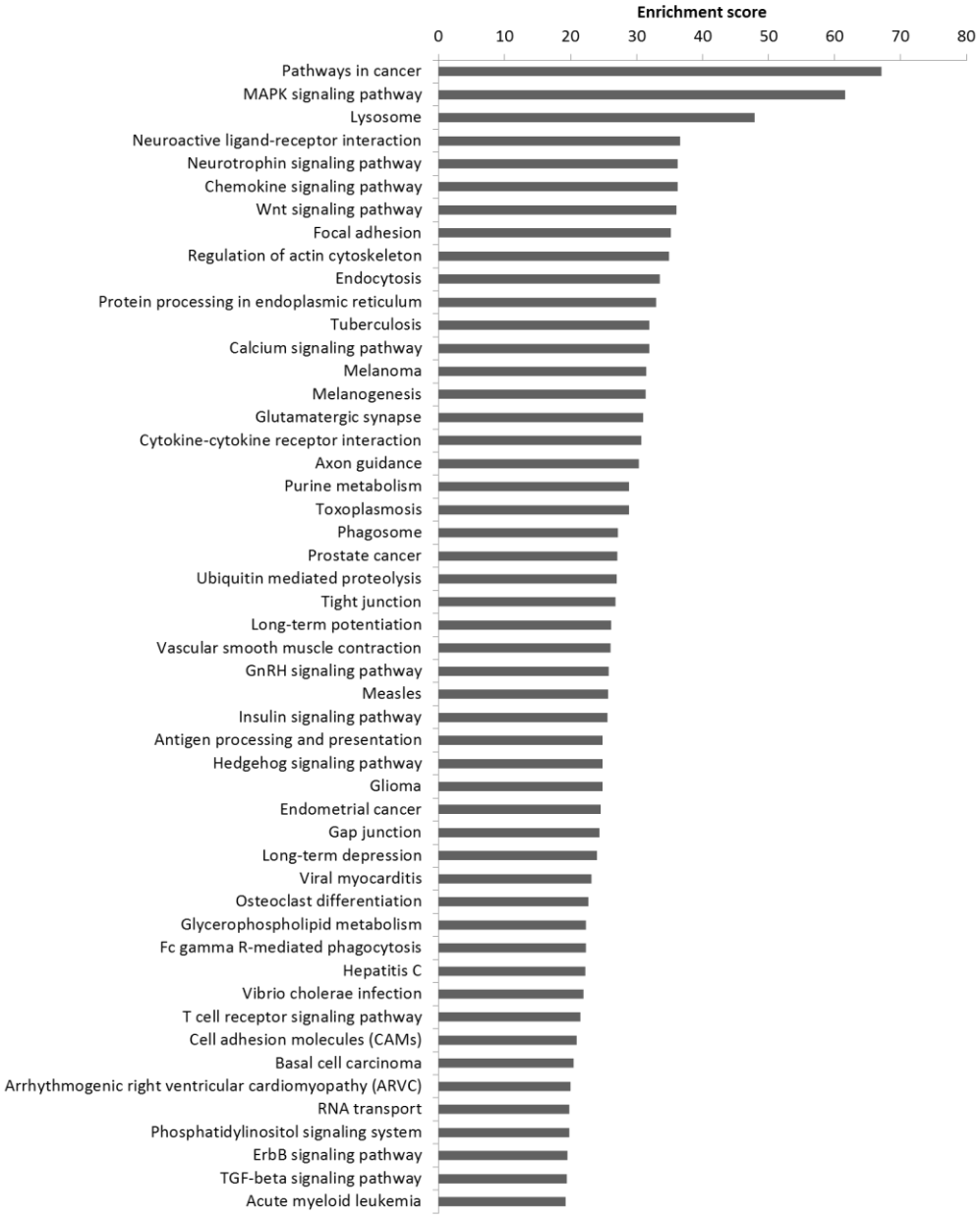
Enrichment score
0
10
20
30
40
50
60
70
80
Pathways in cancer
MAPK signaling pathway
Lysosome
Neuroactive ligand-receptor interaction
Neurotrophin signaling pathway
Chemokine signaling pathway
Wnt signaling pathway
Focal adhesion
Regulation of actin cytoskeleton
Endocytosis
Protein processing in endoplasmic reticulum
Tuberculosis
Calcium signaling pathway
Melanoma
Melanogenesis
Glutamatergic synapse
Cytokine-cytokine receptor interaction
Axon guidance
Purine metabolism
Toxoplasmosis
Phagosome
Prostate cancer
Ubiquitin mediated proteolysis
Tight junction
Long-term potentiation
Vascular smooth muscle contraction
GnRH signaling pathway
Measles
Insulin signaling pathway
Antigen processing and presentation
Hedgehog signaling pathway
Glioma
Endometrial cancer
Gap junction
Long-term depression
Viral myocarditis
Osteoclast differentiation
Glycerophospholipid metabolism
Fc gamma R-mediated phagocytosis
Hepatitis C
Vibrio cholerae infection
T cell receptor signaling pathway
Cell adhesion molecules (CAMs)
Basal cell carcinoma
Arrhythmogenic right ventricular cardiomyopathy (ARVC)
RNA transport
Phosphatidylinositol signaling system
ErbB signaling pathway
TGF-beta signaling pathway
Acute myeloid leukemia

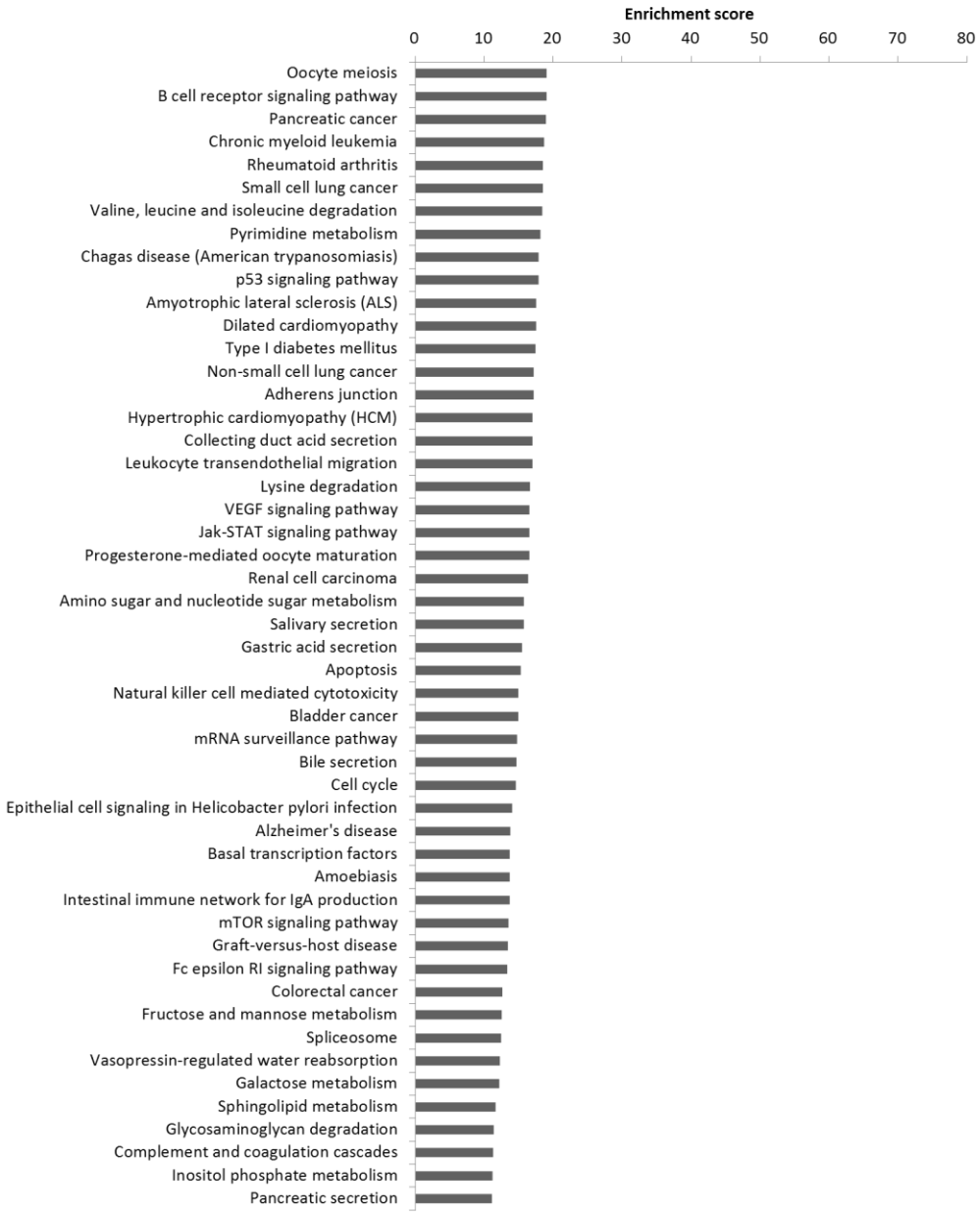


**Figure 4.5:** Top 100 biological pathways according to enrichment score, regulated by 27 miRNAs (let-7d*, miR-29b-2*, -32*, -125b-2*, -146b-3p, -196a*, -200b*, -302c*, -320b, -320c, -331-5p, -374b*, -423-3p, -423-5p, -488, -494, -498, -576-3p, -585, -659, -668, -923, -934, -943, -1255a, -1299 and -1321) that showed similar expression in all the ischemic stroke samples.

# Chapter 5

# miRNA profiles in rat middle cerebral artery occlusion (MCAo) model : correlation with human data

### 5.1 miRNAs in animal models of ischemic stroke

Dysregulation of miRNAs was first discovered in rat animal model, demonstrated in brain and blood [189]. Subsequently, other groups performed miRNA profiles on animal models for ischemic stroke and other forms of stroke. Dharp *et al* [191] profiled miRNA in ipsilateral cortex of rats subjected to MCAo while Liu *et al* [192] compared blood and brain profiles of rat animal models for ischemic stroke, haemorrhagic stroke and kainate-induced seizure. Lim *et al* [193] reported on the temporal miRNA profile in brains of rats subjected to MCAo and correlated with the corresponding protein expression as well as compared with profile of NMDA antagonist (MK801) treated animal. On the other hand, other groups looked at miRNA in different aspect ischemic stroke. Ziu *et al* [194] looked at the specific miRNA expression in astrocytes and neurons after ischemic injury, while Lee *et al* [195] looked into miRNA expression during ischemic preconditioning. More recently, Liu *et al* [196] profiled temporal miRNA changes in an embolic stroke model and demonstrated a spontaneous recovery in the animal up to 7 days with the corresponding changes in miRNA expression.

Translation between clinical data from ischemic stroke patients and experimental data had little success, probably due to factors not taken into account. One of which is the presence of risk factors present in human patients while these were not taken into account for experimental setup.

In the previous chapter 4, miRNA profiles from low or no risk ischemic stroke patients were obtained and the clinical setting was closest to that of experimental setup. In this chapter, miRNA profile in animal model of ischemic stroke obtained and biological pathways affected were highlighted.

These biological pathways were compared with those biological pathways from human ischemic stroke patients. In addition, to have a parallel for stroke subtype comparison in animal model, miRNA profiles for suture model was compared with the miRNA profiles of embolic model, where suture model resembles large artery and small vessel stroke while the embolic model resembles cardioembolic stroke.

Suture model involved the occlusion of the middle cerebral artery (MCA) by introducing a silicone-coated suture at the origin of MCA, while embolic model was achieved by using a blood clot instead of a suture. The models also differ in the nature of the occlusion, where embolic model results in permanent occlusion until the autolysis of blood clot while suture model results in a transient occlusion such that reperfusion is achieved upon removing suture.

### 5.2 Laser-doppler flowmetry

For this study, the well-established suture model was used to mimic ischemic stroke in rat animal model. In order to assess the successful occlusion of middle cerebral artery, laser-doppler flowmetry was utilised to measure the blood flow in the left middle cerebral artery. The laser-doppler probe was fixed on the temporal surface of the cranium, adjacent to the middle cerebral artery. The probe detected the blood flow in terms of blood perfusion units. The basal level of blood flow was measured and expressed as 100%. Upon occluding the left middle cerebral artery using the silicon coated suture, the blood perfusion in the vessel decreased to a level of 20% of the basal level or less, to signify a successful occlusion of the left middle cerebral artery (Figure

5.1). The blood flow in the vessel was monitored throughout the period of occlusion (1 hour). After an hour of occlusion, the suture was removed to allow for reperfusion which is denoted by the increase in blood perfusion in the left middle cerebral artery shown in the read out from the laser-doppler (Figure 5.1).

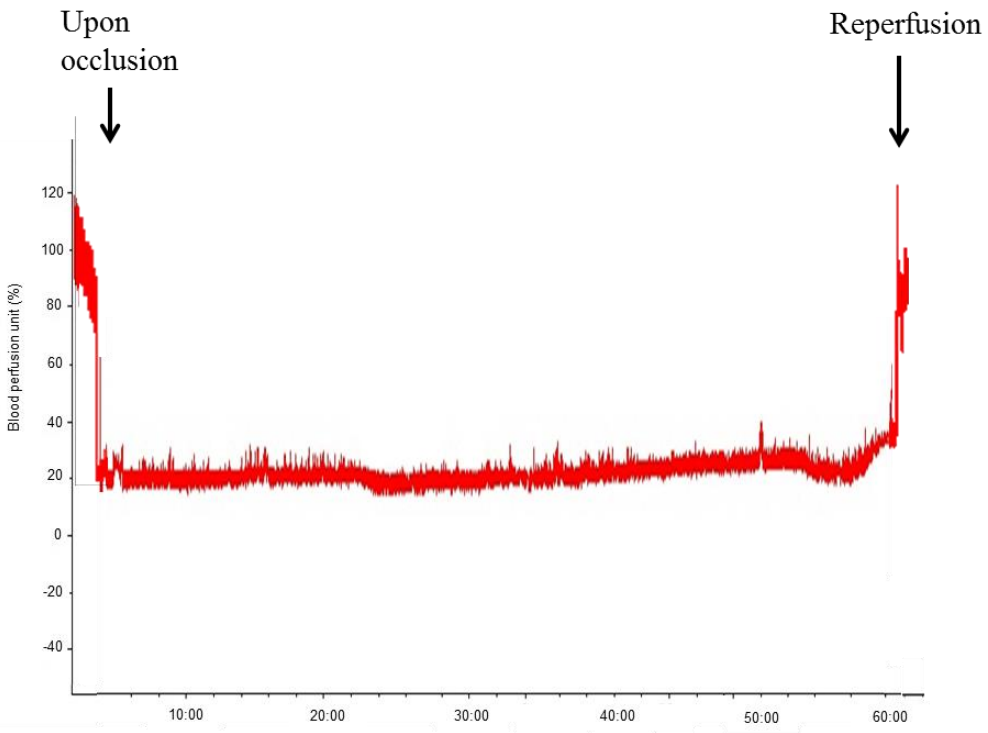


**Figure 5.1**: Laser-doppler flowmetery. Blood flow in the left middle cerebral artery was measured and expressed as a percentage to basal blood flow. Measurements were taken before occlusion, during occlusion and reperfusion.

### 5.3 Neurological outcome

The neurological deficit of the operated animal is accessed at 24 hours after surgery followed by every other day. The animals were observed and scored according to the Bederson score (range from 0 to 3; Table 5.1) [207]. Operated animals that were scored as normal (grade 0) or moderate (grade 1) at 24 hours after surgery were excluded from the study. The rat subjected to MCAo developed decreased right forelimb flexion and decreased resistance to lateral push towards the right. Rats having very severe neurological deficit exhibited the above mentioned physical presentations together with the manifestation of circling movement in a clockwise direction. The neurological scoring of the animals showed improvement as time progressed (Table 5.2).

Subsequently, the animals were sacrificed at various time points after reperfusion (12hr, 24hr, 48hr, 72hr, 120hr and 168hr) and the brains were harvested for further study. Three animals were sacrificed for each time point for this study (12hr, 24hr, 48hr, 72hr, 120hr and 168hr) and 6 control animals were used.

**Table 5.1**: Bederson score. Adapted from Bederson *et al* [207]

| **Severity** | **Grade** | **Observation** |
|---|---|---|
| Normal | 0 | No observable deficit |
| Moderate | 1 | Decrease forelimb flexion |
| Severe | 2 | Decrease forelimb flexion and resistance to lateral push |
| Very Severe | 3 | Same as grade 2 with circling |

## 5.4 Infarct volume

The brains harvested were sectioned into 2mm slices and stained with 2,3,5-triphenyltetrazolium chloride (TTC) for an hour. The viable cells in the tissue were stained red as the TTC become oxidized to red 1,3,5-triphenylformazan (TPF), while the dead cell remained unstained. The left hemisphere is denoted as the ipsilateral half where infarction had occurred, while the right hemisphere is designated as the contralateral half. The infarct volume was calculated using ImageJ software and plotted in the graph shown (Figure 5.2). The infarct volume was expressed as percentage based on the total infarct volume that was observed at 24 hours. The infarct volume was shown to increase from 12 hours to 24 hours and thereafter gradually decreased from 24 hours to 168 hours (Figure 5.2). The rats were also imaged at 24, 48, 72 and 168 hours using magnetic resonance imaging (MRI). The brain was visualized using T2 imaging which demonstrated decrease of the infarct lesion with time, similar to the results of TTC staining (Figure 5.3). The infarct lesion is denoted as the area of hyperintensity.

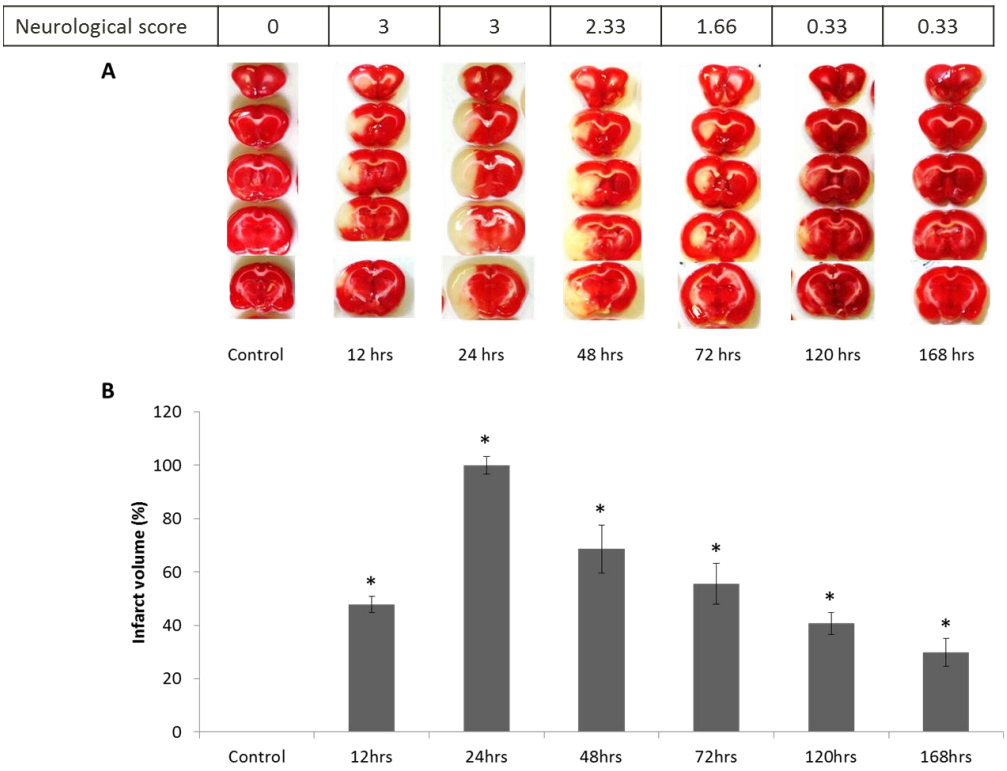


**Figure 5.2**: Infarct volume of rats subjected to MCAo. **A**. Brain slices of rats subjected MCAo and subsequently sacrificed at various time points after reperfusion (12, 24, 48, 72, 120 and 168 hours). Brain slices were stained with TTC, where red stain denotes viable cells and unstained region consists of dead cells. **B**. Graph showing infarct volume of rats sacrificed at various time points after reperfusion (12, 24, 48, 72, 120 and 168 hours). Infarct volume was expressed as mean percentage ± standard deviation, 12hr: 47.71% ± 3.00%; 24hr: 100% ± 3.30%; 48hr: 68.55% ± 8.92%; 72hr: 55.58% ± 7.64%; 120hr: 40.69% ± 4.15% and 168hr: 29.74% ± 5.23%. There were n=3 animals for each time-point. * denoted tested significantly different (p value < 0.05) as compared to control. The neurological score is the average score of n=3 based on the Bederson score [207].

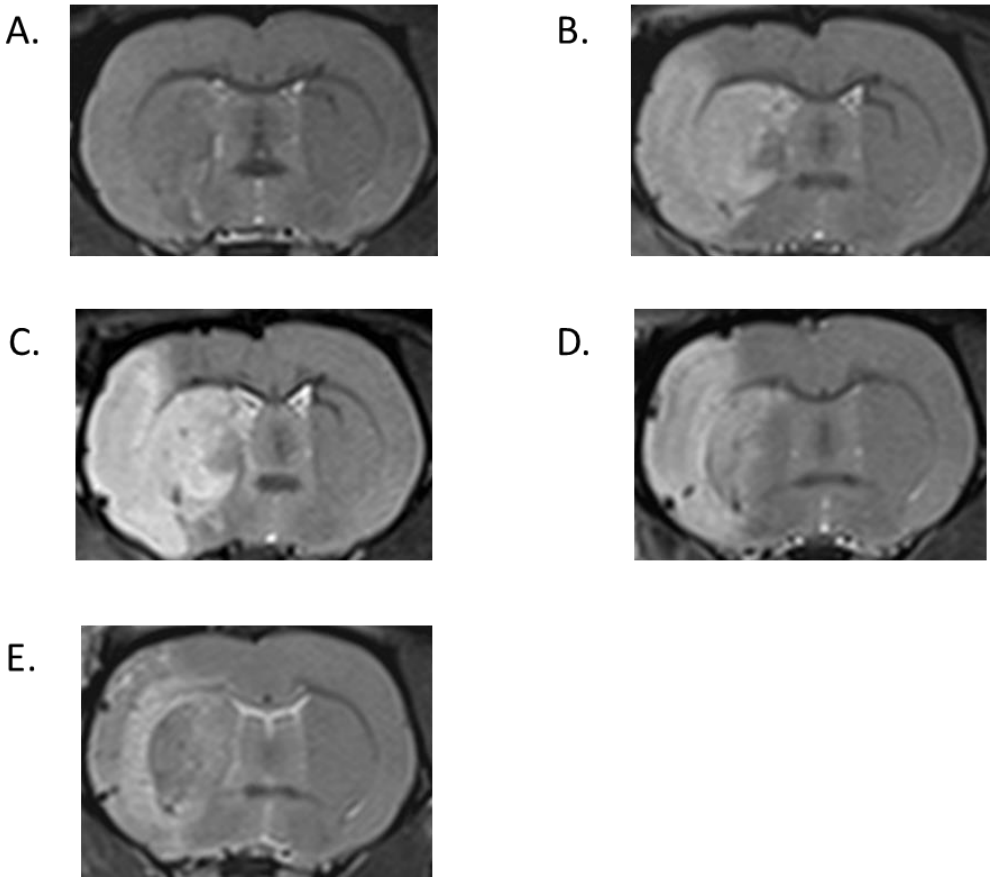


**Figure 5.3:** T2 images of rat brain. **A**. Control. **B**. 24 hours after reperfusion. **C**. 48 hours after reperfusion. **D**. 72 hours after reperfusion. **E**. 168 hours after reperfusion. The ischemic lesion was shown as the area of hyperintensity.

### 5.5 miRNA profiles of rats MCAo suture model

Total RNA was isolated from the brain slices using TRIzol (Invitrogen, Life Technology, Carlsbad, CA, USA) method. The concentration and integrity of the RNA was determined using Nanodrop™ N2000C spectrophotometer (Thermo Scientific™, Rockford, IL, USA) and RNA gel electrophoresis (1% agarose). The presence and integrity of small RNAs species (less than 200 nucleotides) was verified using denaturing polyacrylamide gel electrophoresis (15% polyacrylamide).

Total RNA from the brain was used to perform miRNA microarray on miRCURY LNA miRNA array (version 11.0) platform, based on miRBase version 12.0 annotations [165]. The data obtained were analysed using TIGR multiple experiment viewer (TMEV) [209]. All positive raw intensities were taken into account and statistical testing was performed at 5% significance level comparing control rats and rats subjected to MCAo. False discovery rate (FDR) was also calculated (at 5% significance level) to identify miRNAs that are significantly different across the time-points. 250 miRNAs were observed to be significantly different, of which 242 miRNAs were detectable at all 6 time points (Figure 5.4; Supplementary Table 3). There were 13 miRNAs that were up-regulated at all 6 time points while there were 195 miRNAs that were down-regulated at all 6 time points (Supplementary Table 3).

According to the miRNA profile, majority of the miRNAs were down-regulated in all the time points (12hr: 218 miRNAs; 24hr: 220 miRNAs; 48hr: 220 miRNAs; 72hr: 226 miRNAs; 120hr: 218 miRNAs; 168hr: 220 miRNAs; Table 5.3). Among all the time points, there were higher numbers of up-

regulated miRNAs within 24 hours of reperfusion (12hr: 31 miRNAs; 24hr: 29 miRNAs; Table 5.3) and at the time points after 72 hours (120hr: 31 miRNAs; 168hr: 27 miRNAs; Table 5.3).

**Table 5.3**: Number of miRNAs up-regulated and down-regulated at various time points.

| | **Number of miRNAs** | | | | | |
|---|---|---|---|---|---|---|
| | 12hr | 24hr | 48hr | 72hr | 120hr | 168hr |
| Down-regulated | 218 | 220 | 220 | 226 | 218 | 220 |
| Up-regulated | 31 | 29 | 24 | 23 | 31 | 27 |

Hiearchical clustering (HCL) was performed using TMEV software based on the raw signal intensity of the 250 miRNAs detected. In Figure 5.4, HCL showed segregation of control samples from MCAo sample, demonstrating that there was differential miRNA expression between rats subjected to MCAo and normal control rats. Subsequently, HCL was performed using expression value of the 250 miRNAs. HCL demonstrated the clustering of samples according to early time-points (12hr, 24hr and 48hr) and late time-points (72hr, 120hr and 168hr; Figure 5.5).

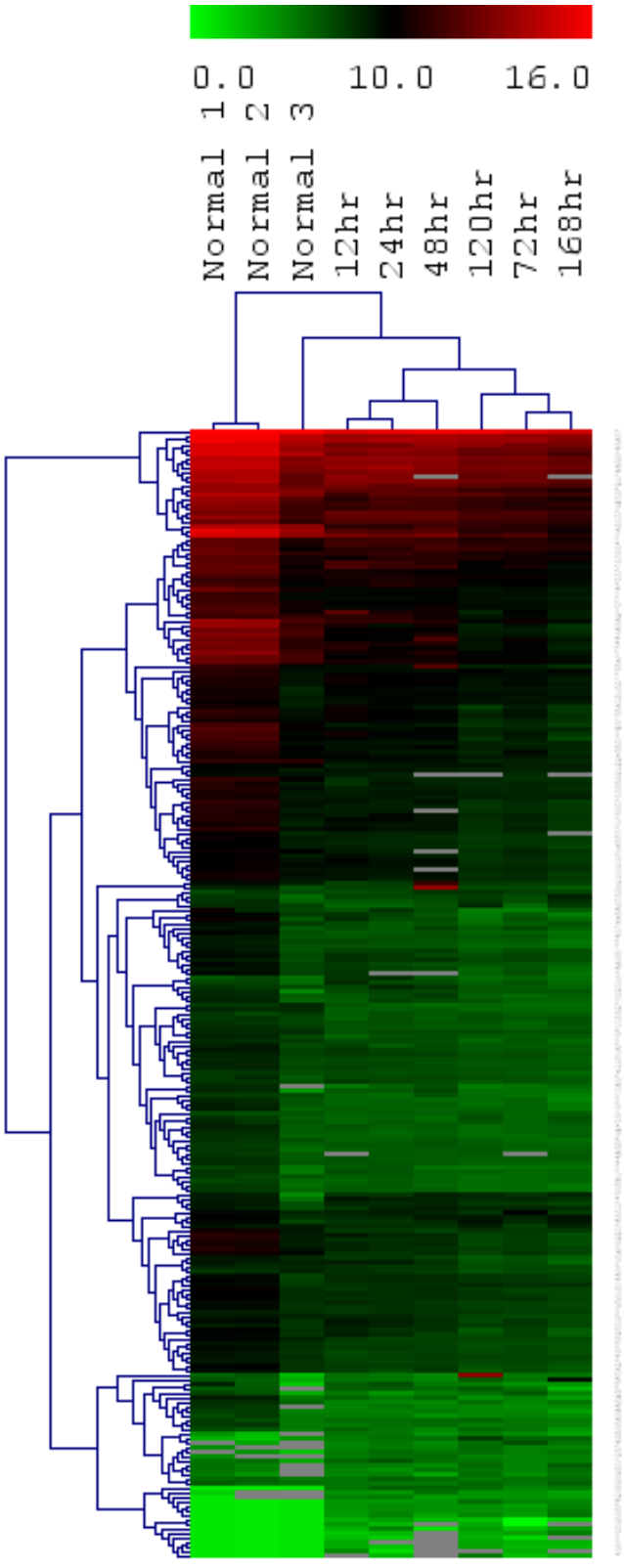


**Figure 5.4**: Hierarchical clustering analysis of 250 miRNAs in samples across 6 time-points (12hr, 24hr, 48hr, 72hr, 120hr and 168hr) and normal control samples. The miRNA expression were expressed logarithm of raw intensity Green represents low signal intensity. Red represents high signal intensity. Grey represents absence.

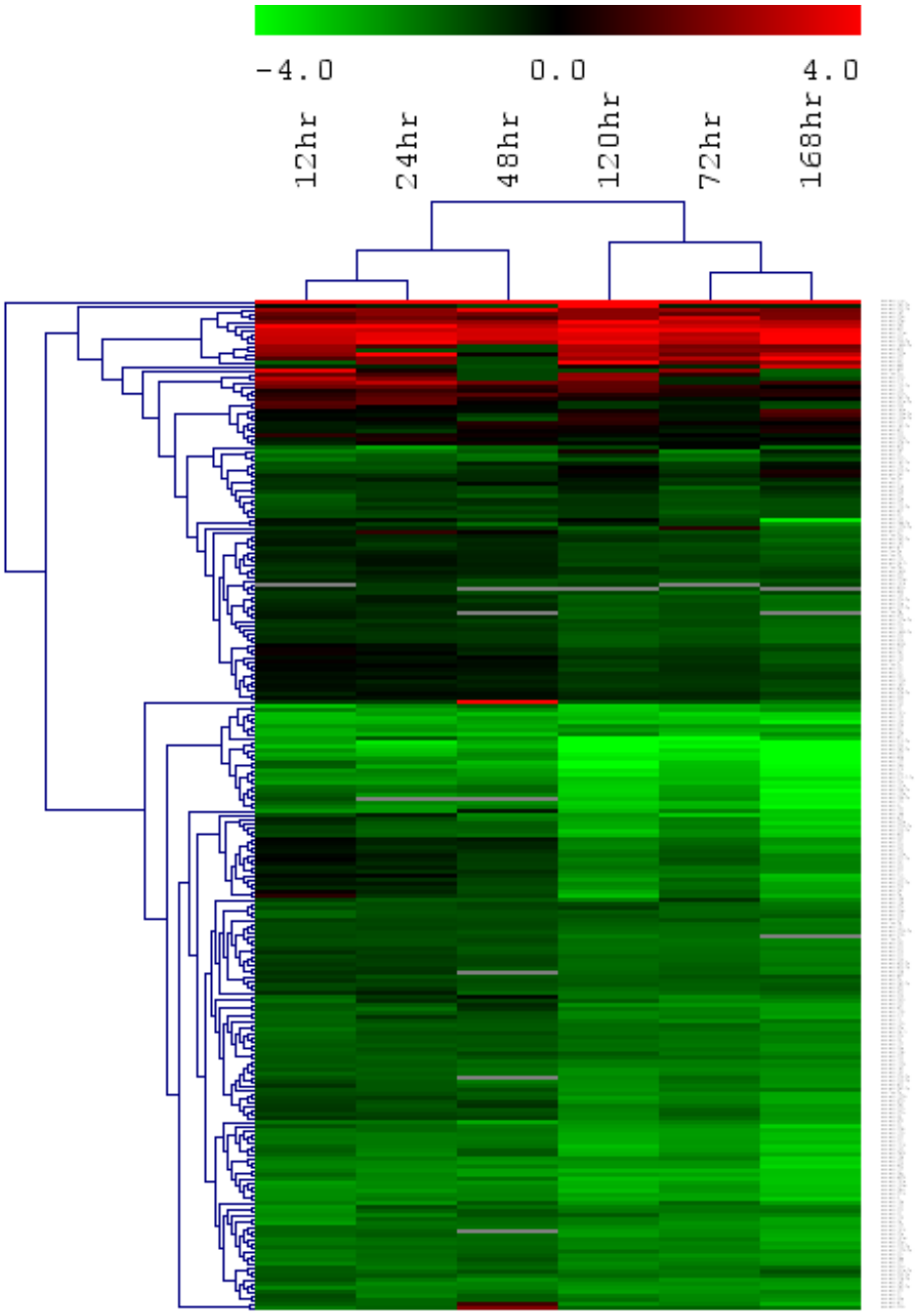


**Figure 5.5**: Heatmap of 250 miRNAs across the 6 time-points (12hr, 24hr, 48hr, 72hr, 120hr and 168hr). The miRNA expression were expressed as signal log ratio (SLR) with respect to control samples. Green represents down-regulation. Red represents up-regulation. Grey represents absence.

### 5.6 miRNAs correlating with infarct volume

Within the miRNA profiles, 28 miRNAs (let-7b, -7c, miR-9, -21*, -24-2*, -27a, -29a, -30a, -30b-5p, -30c, -125b*, -129, -135b, -181a, -186, -195, -204*, -206, -212, -218, -291a-5p, 300-5p, -322, -340-3p, -376c, -383, -409-3p and -674-5p) were found to positively correlate with infarct volume, where expression of these miRNAs increased and decreased with corresponding increase and decrease of infarct volume respectively (Figure 5.6). It is noteworthy to mention that amongst these 28 miRNAs, miR-206 has been determined to show the strongest correlation (Pearson's R for miR-206: 0.963) with infarct volume.

### 5.7 Temporal miRNA profile in rat MCAo suture model

Within the miRNA profiles, there were miRNAs that showed a progressive expression pattern across time. There were 35 miRNAs (let-7e, miR-7b, -26a, -29c, -32, -92b, -103, -107, -130a, -136, -136*, -137, -140*, -148b-3p, -298, -300-3p, -300-5p, -320, -323, -329, -330*, -337, -351, -361, -365, -376a, -376b-5p, -379, -381, -409-5p, -410, -433, -495, -539 and -541) that showed decreasing expression as time progresses (Figure 5.7A).

In addition, there were 26 miRNAs (let-7e*, miR-10b, -16, -25, -27a*, -29c*, -128, -139-5p, -144, -146b, -147, -151, -192, -199a-5p, -204, -217, -221, -222, -326, -328, -375, -382*, -540, -542-3p, 542-5p and -881) demonstrated to have biphasic expression across time (Figure 5.7B). Among these 26 miRNAs, miR-29c* and -542-3p were found to have a lower expression at 24 and 120 hours while the remaining 24 miRNAs showed higher expression at these 2 time-points.

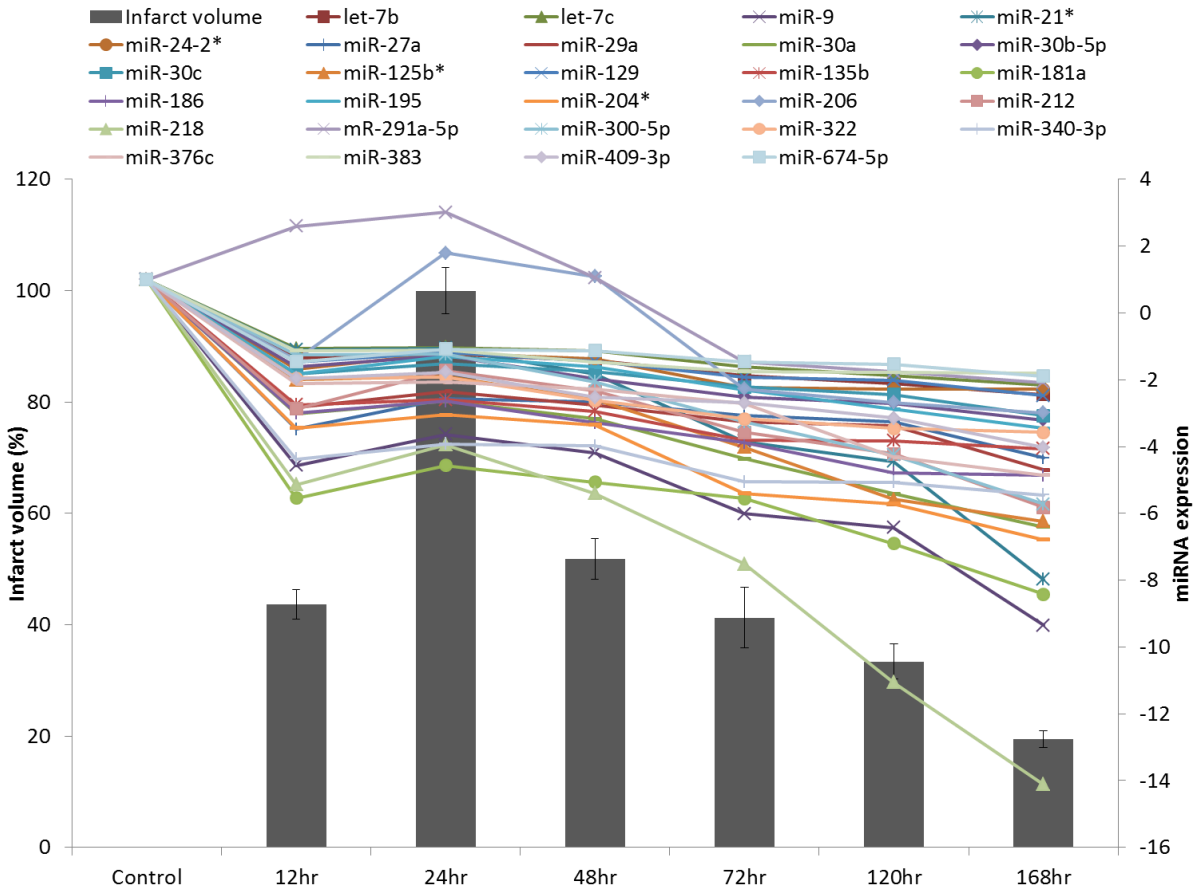


**Figure 5.6**: Expression of 28 miRNAs that positively correlate with infarct volume in suture model. The expression of the miRNAs were expressed as fold change compared to normal control.

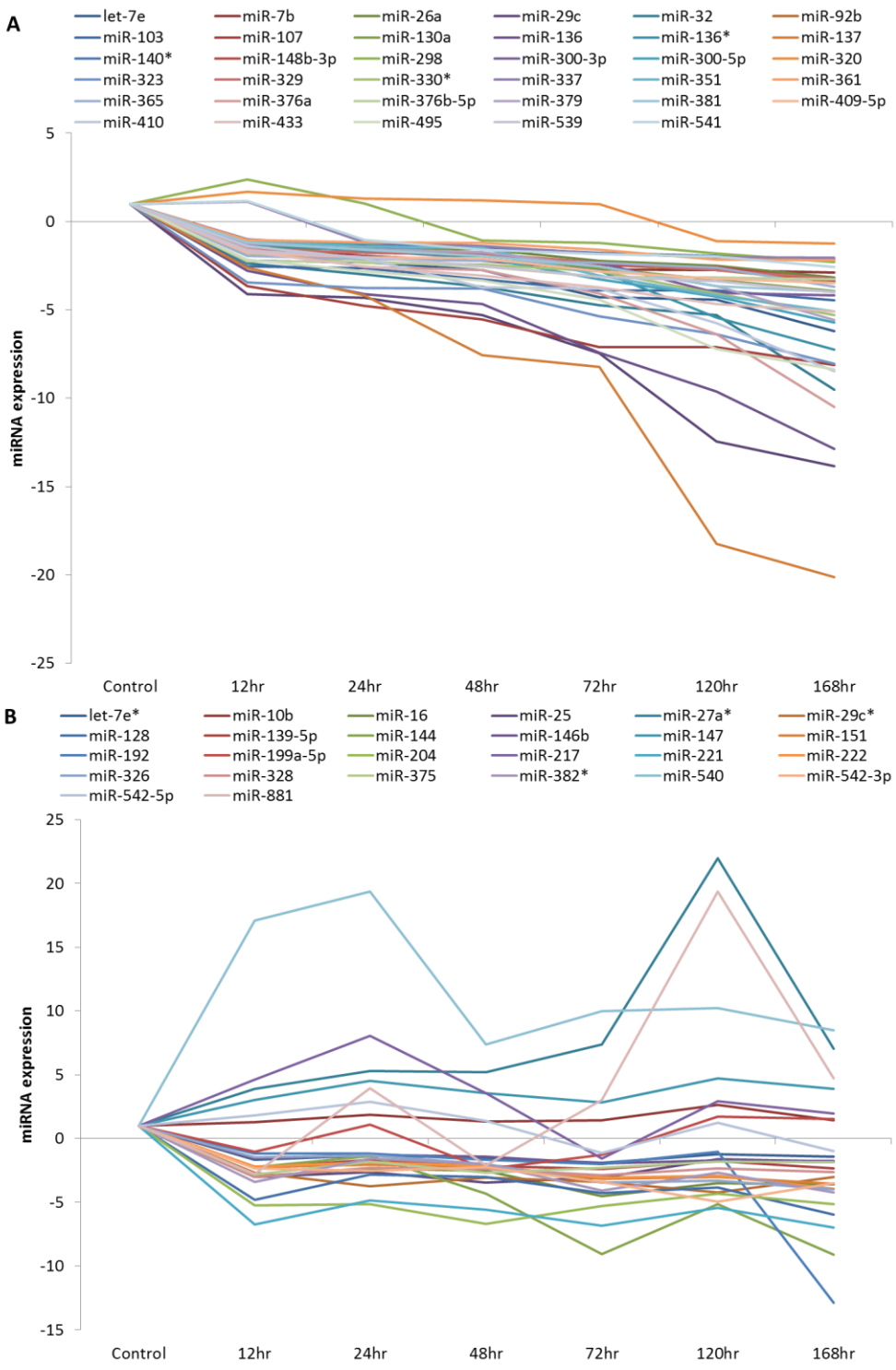


**Figure 5.7**: Expression of **A.** 35 miRNAs that showed decreasing expression across time. **B.** 26 miRNAs that showed biphasic expression. The expression of the miRNAs were expressed as fold change compared to normal control.

### 5.8 Comparison of miRNA expression between suture model and embolic model

Comparison of miRNA profiles between embolic model and suture model was conducted. Embolic model miRNA profile was obtained from Liu *et al* [196] which deposited in NCBI's gene expression omnibus (GEO) with accession number GSE46269. The infarct volume of embolic model was similar to that of suture model where it increased and reacted maximal infarction at 24 hours and decrease after that [196]. The miRNA profiles of suture model and embolic model were visualized on TMEV. HCL was performed on the miRNA profiles (Figure 5.8). The samples clustered according to the respective models which demonstrated difference in miRNA expression between the 2 animal models.

There were 28 miRNAs (let-7e, miR-10b, -21*, -24-2*, -136, -142-3p, -181c, -183, -200a, -208, -290, -300-3p, -300-5p, -326, -345-5p, -351, -376b-5p, -382, -382*, -409-5p, -423, -425, -466b, -494, -503, -542-3p, -872* and -877) that showed differential expression patterns between the 2 animal models (Figure 5.9). 2 of these miRNAs (miR-10b and -200a) were up-regulated in suture model and down-regulated in embolic model while the remaining 26 miRNAs (let-7e, miR-21*, -24-2*, -136, -142-3p, -181c, -183, -208, -290, -300-3p, -300-5p, -326, -345-5p, -351, -376b-5p, -382, -382*, -409-5p, -423, -425, -466b, -494, -503, -542-3p, -872* and -877) were down-regulated in suture model and up-regulated in embolic model(Figure 5.9).

Liu *et al* [196] previously identified 10 miRNAs (miR-21*,-30c-1*, -206, -290, -291a-5p, -300-5p, -503, -542-5p, -874 and -877) in embolic model that correlated well with infarct volume. Together with the suture model which

identified 28 miRNAs (let-7b, -7c, miR-9, -21*, -24-2*, -27a, -29a, -30a, -30b-5p, -30c, -125b*, -129, -135b, -181a, -186, -195, -204*, -206, -212, -218, -291a-5p, -300-5p, -322, -340-3p, -376c, -383, -409-3p and -674-5p) that positively correlated with infarct volume, there 4 miRNAs (miR-21*, -206, -291a-5p and -300-5p) that showed strong correlation with infarct volume (Figure 5.10). Among which, miR-206 had been determined to show the strongest correlation (Pearson's R for rno-miR-206: 0.963) with infarct volume.

Similarly, there were 26 miRNAs (let-7e*, miR-10b, -16, -25, -27a*, -29c*, -128, -139-5p, -144, -146b, -147, -151, -192, -199a-5p, -204, -217, -221, -222, -326, -328, -375, -382*, -540, -542-3p, 542-5p and -881) that showed biphasic expression. When compared with embolic model, 4 miRNAs (miR-10b, -217, -326 and -881) showed biphasic expression in both animal model (Figure 5.11A, B).

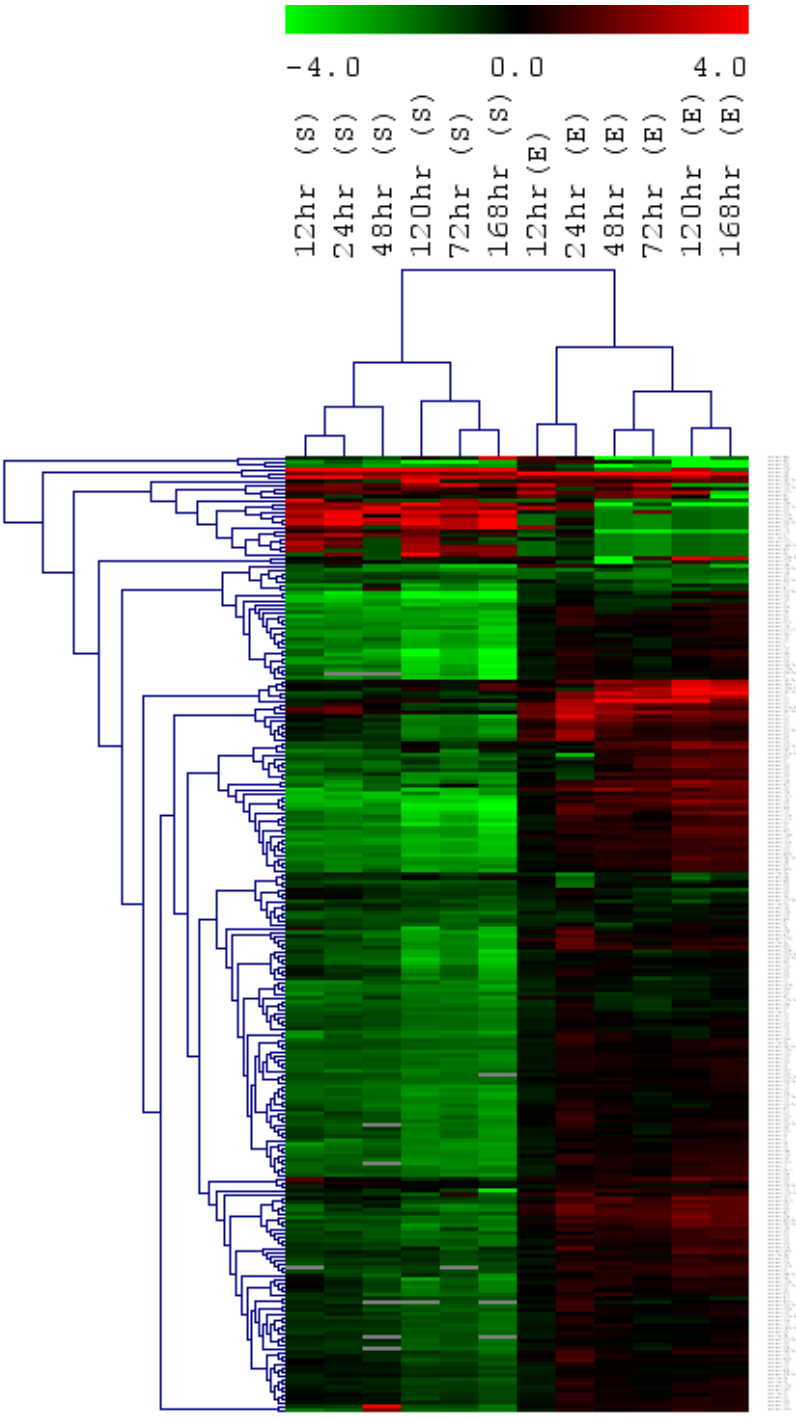


**Figure 5.8**: Hierarchical clustering (HCL) analysis of 250 miRNAs between suture model and embolic stroke. The miRNA expression were expressed as signal log ratio (SLR) with respect to control samples. Green represents down-regulation. Red represents up-regulation. Grey represents absence. Suture model samples were denoted with (S) and embolic model samples were denoted with (E).

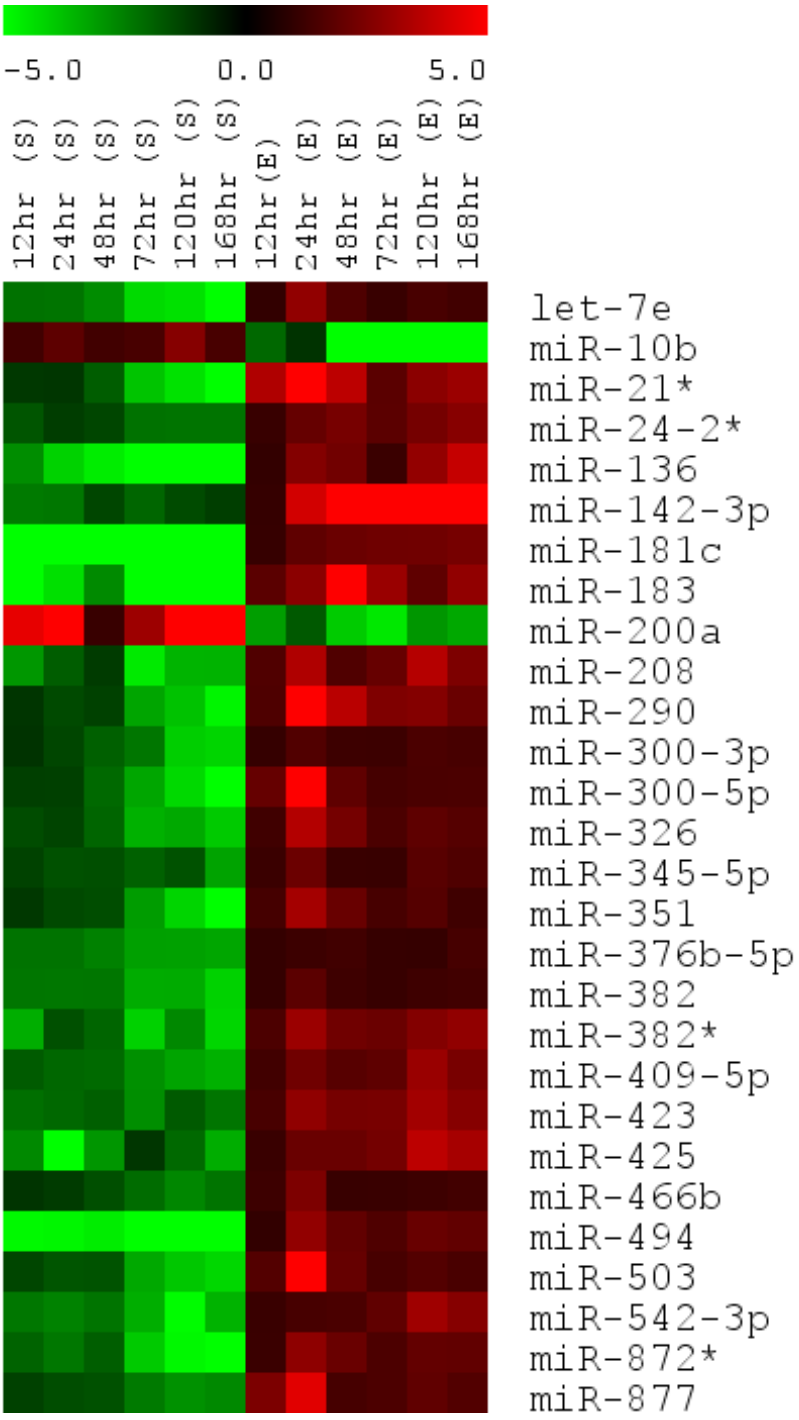


**Figure 5.9:** Heatmap of 28 miRNAs with differential expression patterns between embolic model and suture model. The miRNA expression was expressed as fold change with respect to control samples. Green represents down-regulation. Red represents up-regulation. Suture model samples were denoted with (S) and embolic model samples were denoted with (E).

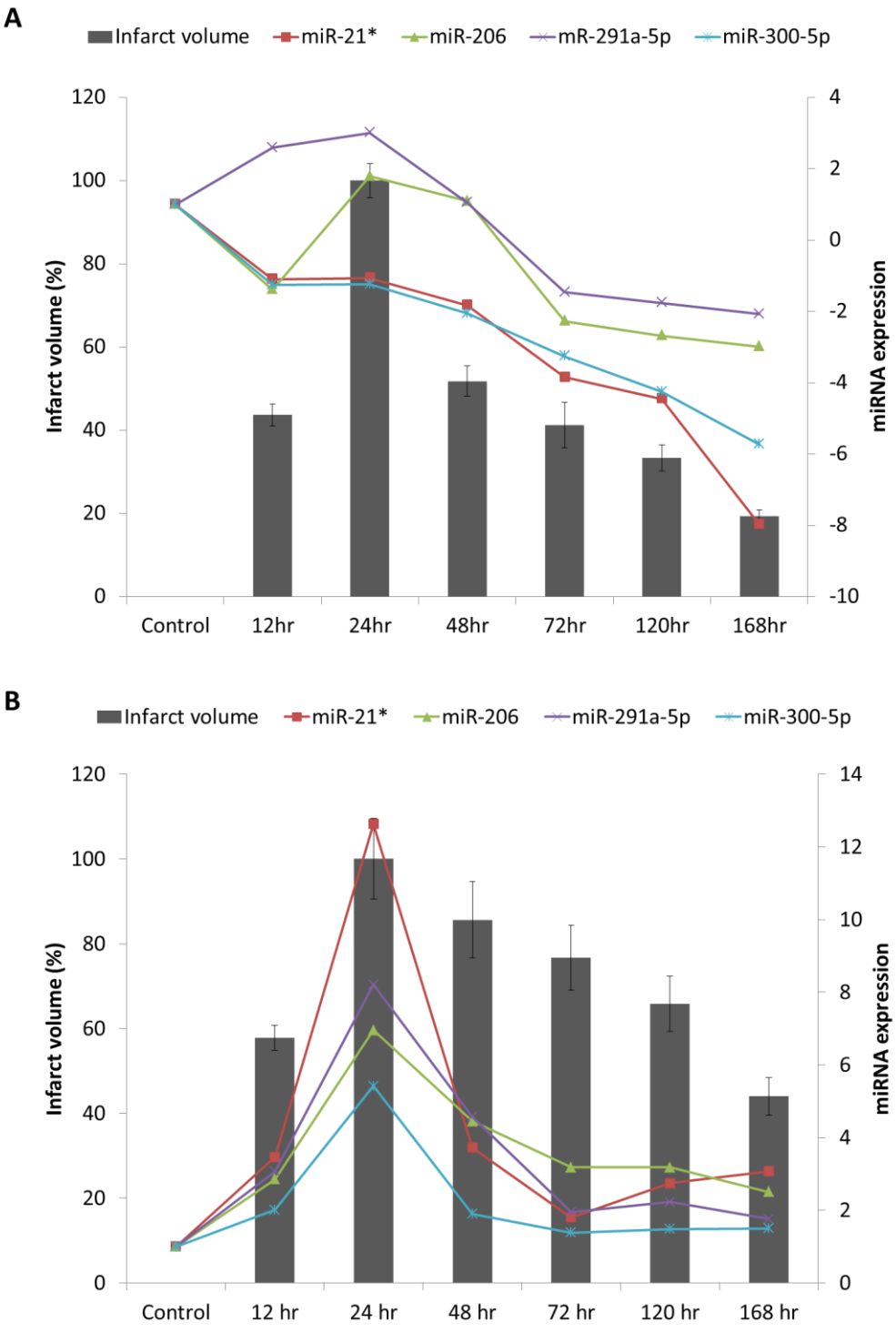


**Figure 5.10:** Expression of 4 miRNAs (miR-21*, -206, -291a-5p and -300-5p) that were positively correlate with infarct volume in **A**. suture model and **B**. embolic model. The miRNA expression were expressed as fold change with respect to control samples.

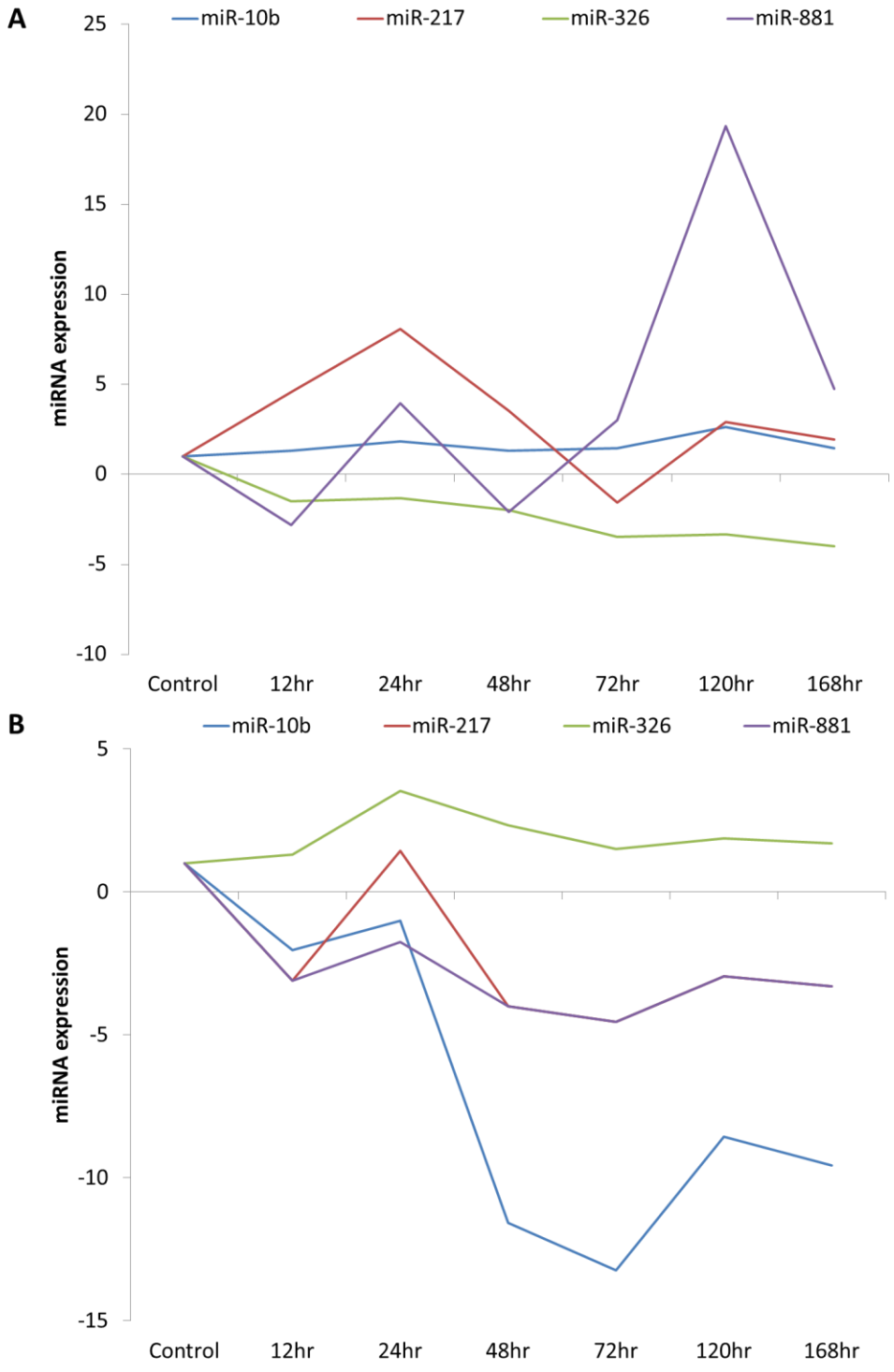


**Figure 5.11:** Expression of 4 miRNAs (miR-10b, -217, -326 and -881) that showed biphasic expression in **A**. suture model and **B**. embolic model. The miRNA expression were expressed as fold change with respect to control samples.

## 5.9 Pathway analysis of miRNAs with differential expression pattern between embolic and suture model

The 28 miRNAs (let-7e, miR-10b, -21*, -24-2*, -136, -142-3p, -181c, -183, -200a, -208, -290, -300-3p, -300-5p, -326, -345-5p, -351, -376b-5p, -382, -382*, -409-5p, -423, -425, -466b, -494, -503, -542-3p, -872* and -877) with differential expression pattern between embolic and suture model were used for pathway analysis. Pathway analysis was performed in the same manner as described in section 3.6.

The pathway analysis of the 28 miRNAs detected cardioembolic associated biological pathways from human patient analysis such as Complement and coagulation cascades, Dilated cardiomyopathy, Gap junction, Glycerophospholipid metabolism and Pyruvate metabolism. This signified that these biological pathways were significant in the pathogenesis of cardioembolic stroke in both human patients as well as in animal model. Thus, investigation into genes and miRNAs in these pathways may yield potential biomarkers for the diagnosis of cardioembolic stroke.

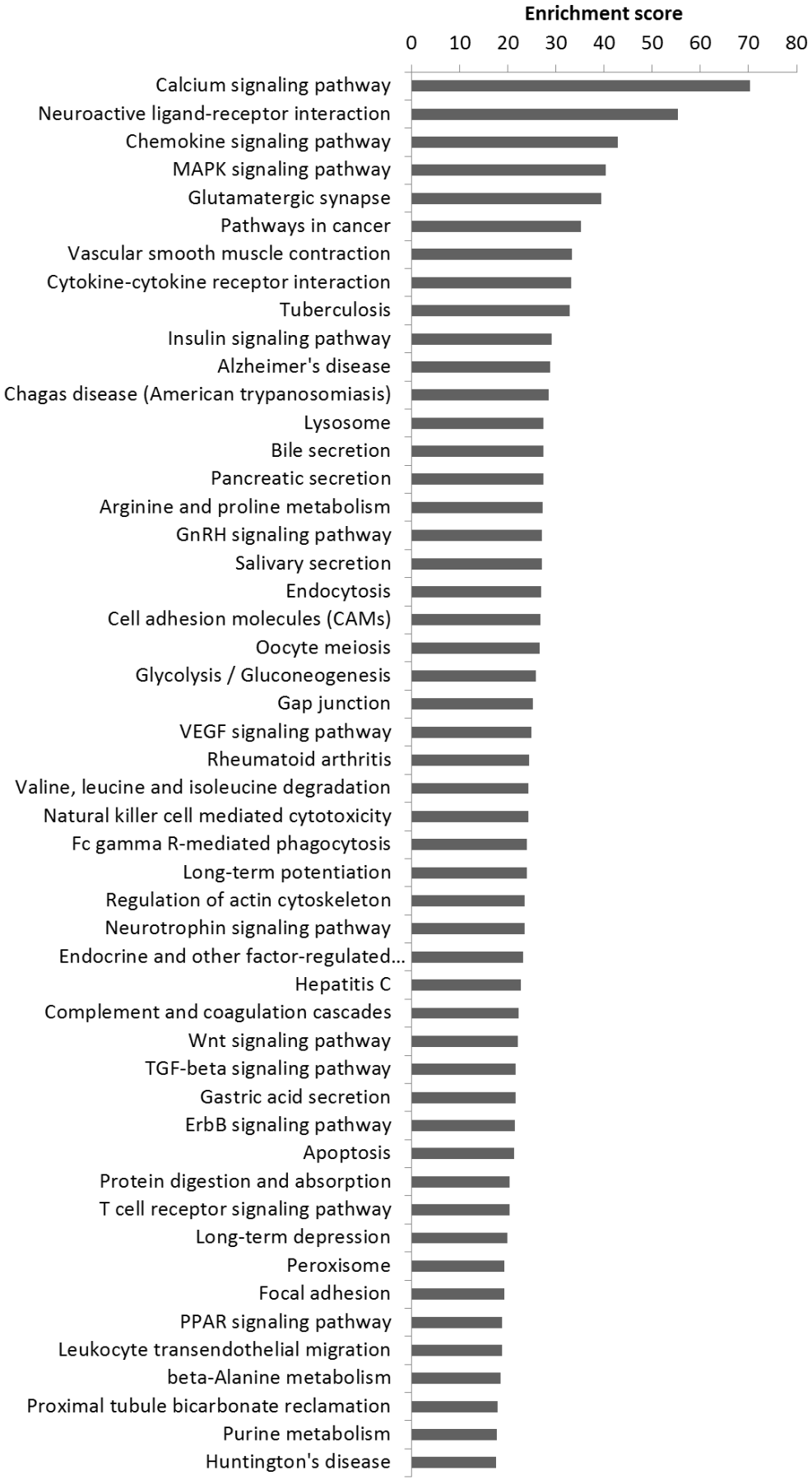
Enrichment score
0
10
20
30
40
50
60
70
80
Calcium signaling pathway
Neuroactive ligand-receptor interaction
Chemokine signaling pathway
MAPK signaling pathway
Glutamatergic synapse
Pathways in cancer
Vascular smooth muscle contraction
Cytokine-cytokine receptor interaction
Tuberculosis
Insulin signaling pathway
Alzheimer's disease
Chagas disease (American trypanosomiasis)
Lysosome
Bile secretion
Pancreatic secretion
Arginine and proline metabolism
GnRH signaling pathway
Salivary secretion
Endocytosis
Cell adhesion molecules (CAMs)
Oocyte meiosis
Glycolysis / Gluconeogenesis
Gap junction
VEGF signaling pathway
Rheumatoid arthritis
Valine, leucine and isoleucine degradation
Natural killer cell mediated cytotoxicity
Fc gamma R-mediated phagocytosis
Long-term potentiation
Regulation of actin cytoskeleton
Neurotrophin signaling pathway
Endocrine and other factor-regulated...
Hepatitis C
Complement and coagulation cascades
Wnt signaling pathway
TGF-beta signaling pathway
Gastric acid secretion
ErbB signaling pathway
Apoptosis
Protein digestion and absorption
T cell receptor signaling pathway
Long-term depression
Peroxisome
Focal adhesion
PPAR signaling pathway
Leukocyte transendothelial migration
beta-Alanine metabolism
Proximal tubule bicarbonate reclamation
Purine metabolism
Huntington's disease

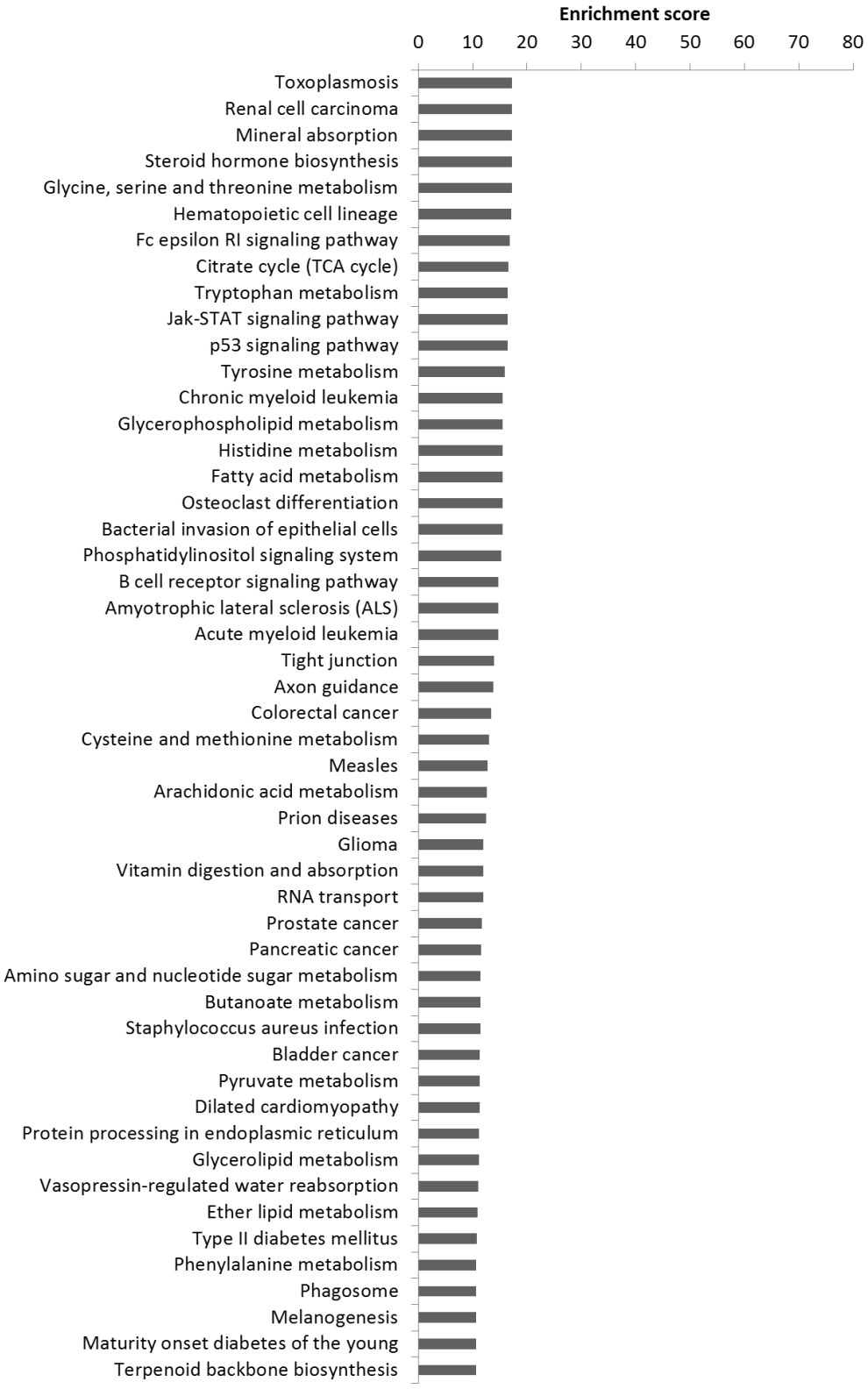


**Figure 5.12:** Top 100 biological pathways according to enrichment score, regulated by 28 miRNAs that showed differential expression patterns between embolic and suture model.

### 5.10 Pathway analysis of miRNAs that positively correlate with infarct volume

Similarly, the 5 miRNAs (miR-21*, -206, -291a-5p and -300-5p) that correlated well with infarct volume were used for pathway analysis. The result showed similar biological pathways detected in human patients. Same biological pathways associated with inflammation (B cell receptor signaling pathway, Chemokine signaling pathway, Complement and coagulation cascade, Cytokine-cytokine receptor interaction, Leukocyte transendothelial migration and T cell receptor signaling pathway), cell death (Natural killer cell mediated cytotoxicity and p53 signaling pathway), neurons (Glutamatergic synapse, Long-term depression, Long-term potentiation, Neuroactive ligand-receptor interaction, Neurotrophin signaling pathway and Wnt signaling pathway), metabolism dysregulation (Amino acid and nucleotide sugar metabolism, Glycerophospholipid metabolism, Glycolysis / Gluconeogenesis, Purine metabolism and Valine, leucine and isoleucine degradation) and vascular permeability (Adherens junction, Cell adhesion molecules (CAMs), Focal adhesion, Gap junction, Tight junction and VEGF signaling pathway). Similarly, in the top 10 biological pathways, neuron-related biological pathways (Neuroactive ligand-receptor interaction: ranked $2^{nd}$) and inflammation-related pathway (Chemokine signaling pathway: ranked $4^{th}$) were highly ranked. This suggested that neuroinflammation played a critical role in ischemic stroke pathophysiology in both clinical and experimental setting. Thus, further investigation into neuroinflammation during ischemic stroke was required for further understanding of the miRNA-regulated mechanism in ischemic stroke.

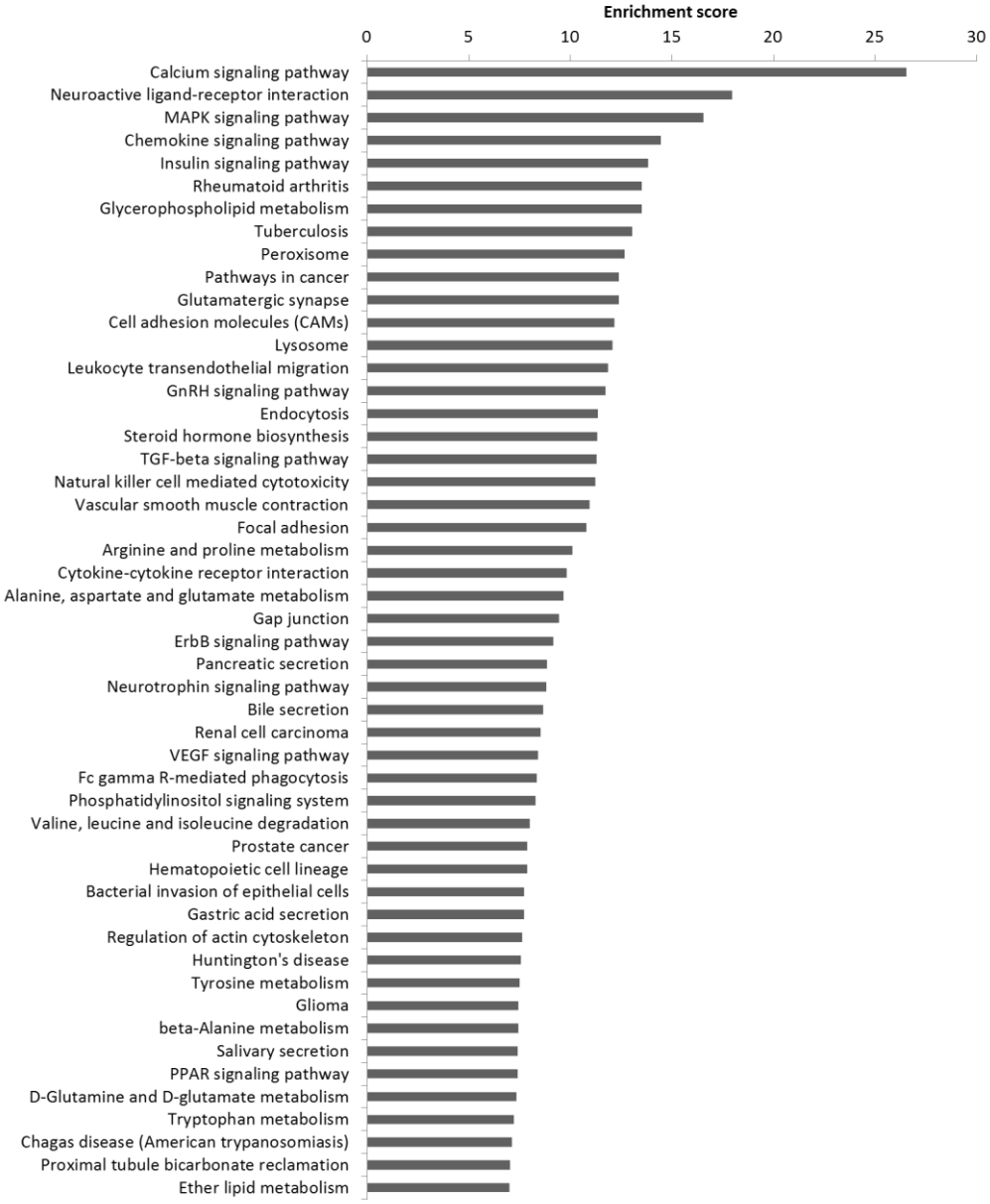
Enrichment score
0
5
10
15
20
25
30
Calcium signaling pathway
Neuroactive ligand-receptor interaction
MAPK signaling pathway
Chemokine signaling pathway
Insulin signaling pathway
Rheumatoid arthritis
Glycerophospholipid metabolism
Tuberculosis
Peroxisome
Pathways in cancer
Glutamatergic synapse
Cell adhesion molecules (CAMs)
Lysosome
Leukocyte transendothelial migration
GnRH signaling pathway
Endocytosis
Steroid hormone biosynthesis
TGF-beta signaling pathway
Natural killer cell mediated cytotoxicity
Vascular smooth muscle contraction
Focal adhesion
Arginine and proline metabolism
Cytokine-cytokine receptor interaction
Alanine, aspartate and glutamate metabolism
Gap junction
ErbB signaling pathway
Pancreatic secretion
Neurotrophin signaling pathway
Bile secretion
Renal cell carcinoma
VEGF signaling pathway
Fc gamma R-mediated phagocytosis
Phosphatidylinositol signaling system
Valine, leucine and isoleucine degradation
Prostate cancer
Hematopoietic cell lineage
Bacterial invasion of epithelial cells
Gastric acid secretion
Regulation of actin cytoskeleton
Huntington's disease
Tyrosine metabolism
Glioma
beta-Alanine metabolism
Salivary secretion
PPAR signaling pathway
D-Glutamine and D-glutamate metabolism
Tryptophan metabolism
Chagas disease (American trypanosomiasis)
Proximal tubule bicarbonate reclamation
Ether lipid metabolism

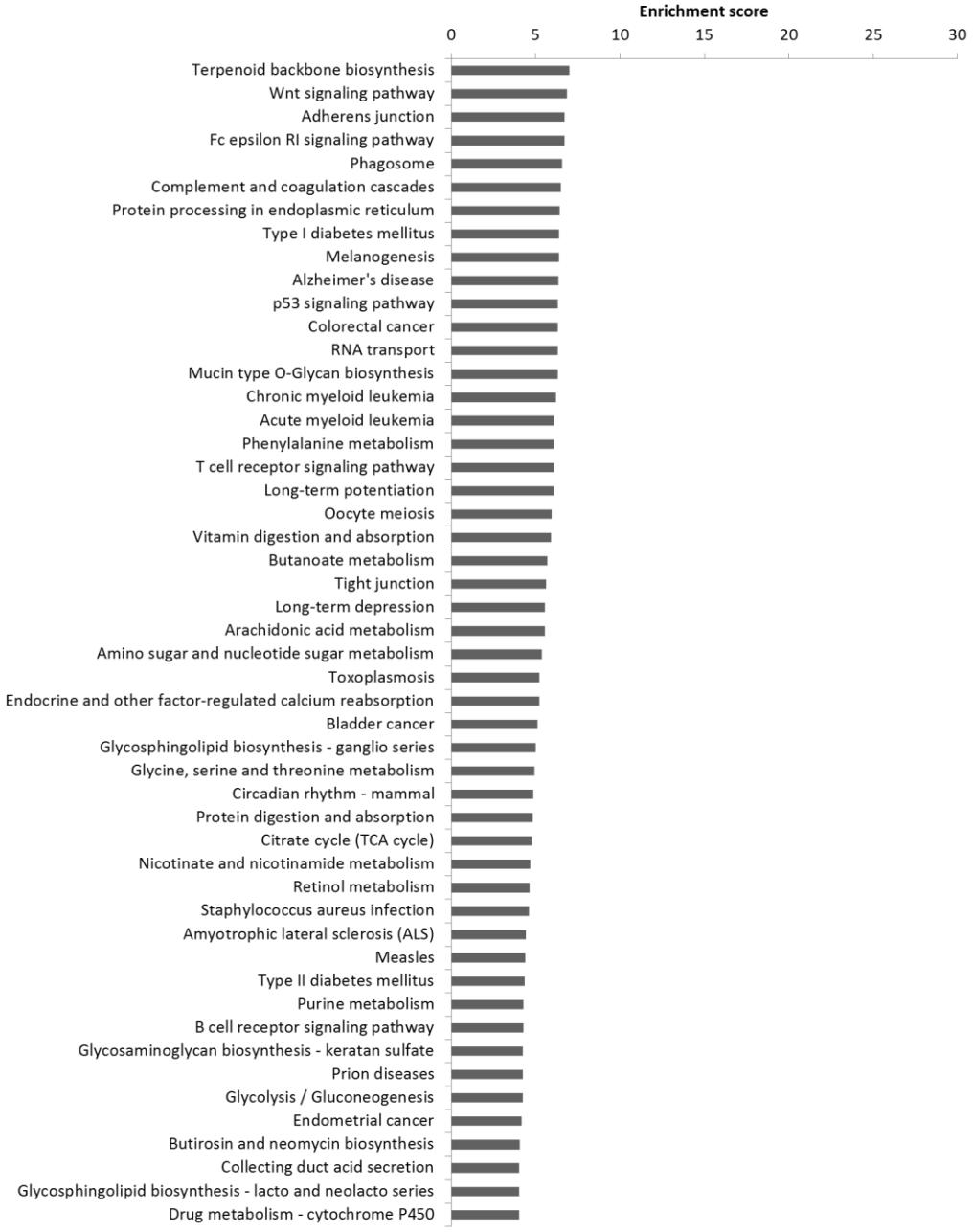


**Figure 5.13:** Top 100 biological pathways according to enrichment score, regulated by 4 miRNAs (miR-21*, -206, -291a-5p and -300-5p) that correlated well with infarct volume.

# Chapter 6

# miRNAs in neuroinflammation – potential biomarkers and therapeutic targets

## 6.1 Neuroinflammation and ischemic stroke

The results from the previous chapters suggested that neuroinflammation is a critical process in the pathophysiology of ischemic stroke [230]. Inflammation in the central nervous system is a complex process involving leukocytes and other blood-derived protein components or modulators [231].

Complement and coagulation cascade (biological pathway associated with inflammation) was found to be differentially regulated stroke subtypes: large artery and small vessel stroke versus cardioembolic stroke. Complement is a component of innate immunity, which responds to pathogen during infection, and in pathological state, complement can cause inflammation in self-tissue [128]. Among the components of complement, Cluster of differentiation 46 (*CD46*) was previously reported by Jickling *et al* [232] to be among a list of 40 genes that can distinguish between cardioembolic stroke and large artery stroke. *CD46* functions as a negative regulator of complement activation such that it binds to C3b and C4b complement protein fragments, and recruits serum factor I to degrade the protein fragments [233]. CD46 exists as 4 protein isoforms (BC1, BC2, C1 and C2) and has 8 transcript varients (a, b, c, d, e, f, l and n) of which transcript a is most abundant [234, 235]. Being an important regulator of complement activation, *CD46* may be used as potential diagnostic marker for cardioembolic stroke and hence the study of miRNAs regulating *CD46* is also beneficial.

Pathway analysis described in chapters 3 to 5, highlighted Chemokine signaling pathway as a crucial pathway as it was consistently found to be in the top 10 biological pathways. Chemokines are protein molecules involved in

recruitment of leukocytes to site of injury [236]. There had been many reports about the involvement of chemokines in ischemic stroke [237]. Among which, monocyte chemoattractant protein-1(*MCP-1*) or chemokine C-C motif ligand 2 (*CCL2*) demonstrated to be involved in the pathophysiology of ischemic stroke. In animal models, *Ccl2* has been demonstrated to be involved in blood brain barrier disruption [124]. Furthermore, animals with CCL2 or its receptor CCR2 knockout have smaller infarct following middle cerebral artery occlusion (MCAo) as compared with wild-type [125, 126]. In addition, CCL2 in serum of patients had been demonstrated to correlate with outcome of patients [238]. However, there were also other reports stating the possible beneficial effect of *CCL2* during ischemic stroke [239, 240]. *Ccl2* had been demonstrated to be involved in ischemic preconditioning [239] and *Ccl2* was reported to mediate neuroblast migration after cerebral ischemia [240]. In addition, *CCL2* was reported to promote angiogenesis in ischemia affected brain tissue [241]. Thus, the role of *CCL2/Ccl2* in ischemic stroke is worth investigating as well as the miRNAs targeting *CCL2/Ccl2*, as *CCL2* may prove to be a useful therapeutic target in ischemic stroke.

### 6.2 *CD46* mRNA level in different ischemic stroke subtype

*CD46* mRNA level was quantified using real-time qPCR. The measurements showed that *CD46* mRNA level was significantly higher (p-value=0.002) in large artery stroke and small vessel stroke (median relative expression=2.00) as compared with cardioembolic stroke (median relative expression=1.32; Figure 6.1). Hence, the identification of miRNAs targeting *CD46* was

considered a useful line of investigation in understanding the regulation of expression of *CD46* as it may become a possible marker in diagnosis of stroke especially cardioembolic stroke from large artery and small vessel stroke.

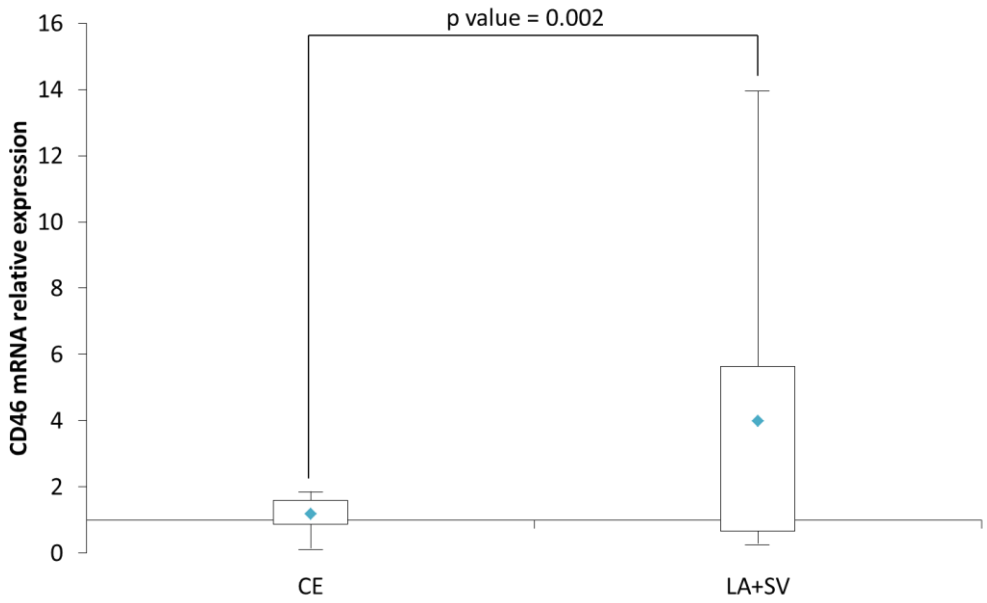


**Figure 6.1:** *CD46* mRNA relative expression in individual ischemic stroke patients according to various ischemic stroke subtypes. The relative expression of *CD46* mRNA was expressed as relative expression as compared with healthy controls (n=8). CE: cardioembolic stroke (n=13); LA: large artery stroke (n=13); SV: small vessel stroke (n=13). The box represents the interquartile range. The line denotes the range of readings. ♦ represents the median reading. The data was tested to be significantly different (p value = 0.002)

### 6.3 miRNAs predicted to target *CD46*

Bioinformatics prediction was carried out to select miRNAs that could target *CD46*. The search was conducted on 9 databases: Targetscan version 6.2 (www.targetscan.org) [156-159], miRanda August 2010 release (www.microRNA.org) [160-163], microcosm version 5 (www.ebi.ac.uk/enright-srv/microcosm/htdocs/targets/v5/) [163-165], DIANA microT version 3 (http://diana.cslab.ece.ntua.gr/microT/) [166, 167], miRDB version 4 (mirdb.org/) [29, 30], miRWalk March 2011 update (www.umm.uni-heidelberg.de/apps/zmf/mirwalk/) [170], PITA 2007 release (genie.weizmann.ac.il/pubs/mir07/mir07_prediction.html) [171], RepTar version 1.2 (reptar.ekmd.huji.ac.il/) [172] and StarBase version 2 (starbase.sysu.edu.cn/) [173, 174].

A total of 857 miRNAs (at least in one of the database) found to target CD46 3'UTR (Supplementary Table 4). Of which, 157 miRNAs (at least in one of the database) were detected in the microarray. Among these 157 miRNAs, 12 miRNAs (miR-17, -18a, -19a, -19b, -20a, -20b, -106a, -181a, -181b, -185, -374b and -421) were selected for further screening as these 12 miRNAs (miR-17, -18a, -19a, -19b, -20a, -20b, -106a, -181a, -181b, -185, -374b and -421) had been predicted by a large number of databases (more than 5). Interestingly, these miRNAs have also been found to belong to miRNA clusters [miR-17-92a cluster (miR-17, -18a, -19a, -19b and -20a), miR-106a-363 cluster (miR-19b, -20b and -106a), miR-181a cluster (miR-181a and -181b) and miR-374b-421 (miR-374b and -421) cluster.

### 6.4 miRNA expression in ischemic stroke subtype

The expression of the 12 miRNAs (miR-17, -18a, -19a, -19b, -20a, -20b, -106a, -181a, -181b, -185, -374b and -421) were measured in the pooled samples for each stroke subtype (cardioembolic, large artery and small vessel), using stemloop PCR (Figure 6.2). The results showed that 4 miRNAs (miR-19a, -20a, -185 and -374b) demonstrated corresponding inverse expression as compared with *CD46* mRNA expression, where the expression of the miRNAs were higher in cardioembolic stroke samples as compared to large artery stroke and small vessel stroke samples (Figure 6.2).

The expression pattern of 4 miRNAs (miR-19a, -20a, -185 and -374b) were further measured in individual stroke samples. It was found that the expression of miR-19a, miR-185 and miR-374b were significantly different (miR-19a: p-value=0.009, miR-185: p-value=0.024 and miR-374b: p-value=0.027) between cardioembolic stroke (miR-19a: median=0.90, miR-20a: median=0.69, miR-185: median=0.55 and miR-374b: median=0.59) and large artery and small vessel stroke (miR-19a: median=0.32, miR-20a: median=0.33, miR-185: median=0.23 and miR-374b: median=0.22; Figure 6.3). In order to validate the interaction between the miRNAs and *CD46* mRNA, the 3'untranslated region (3'UTR) of *CD46* was cloned into luciferase reporter vector to assess the interaction.

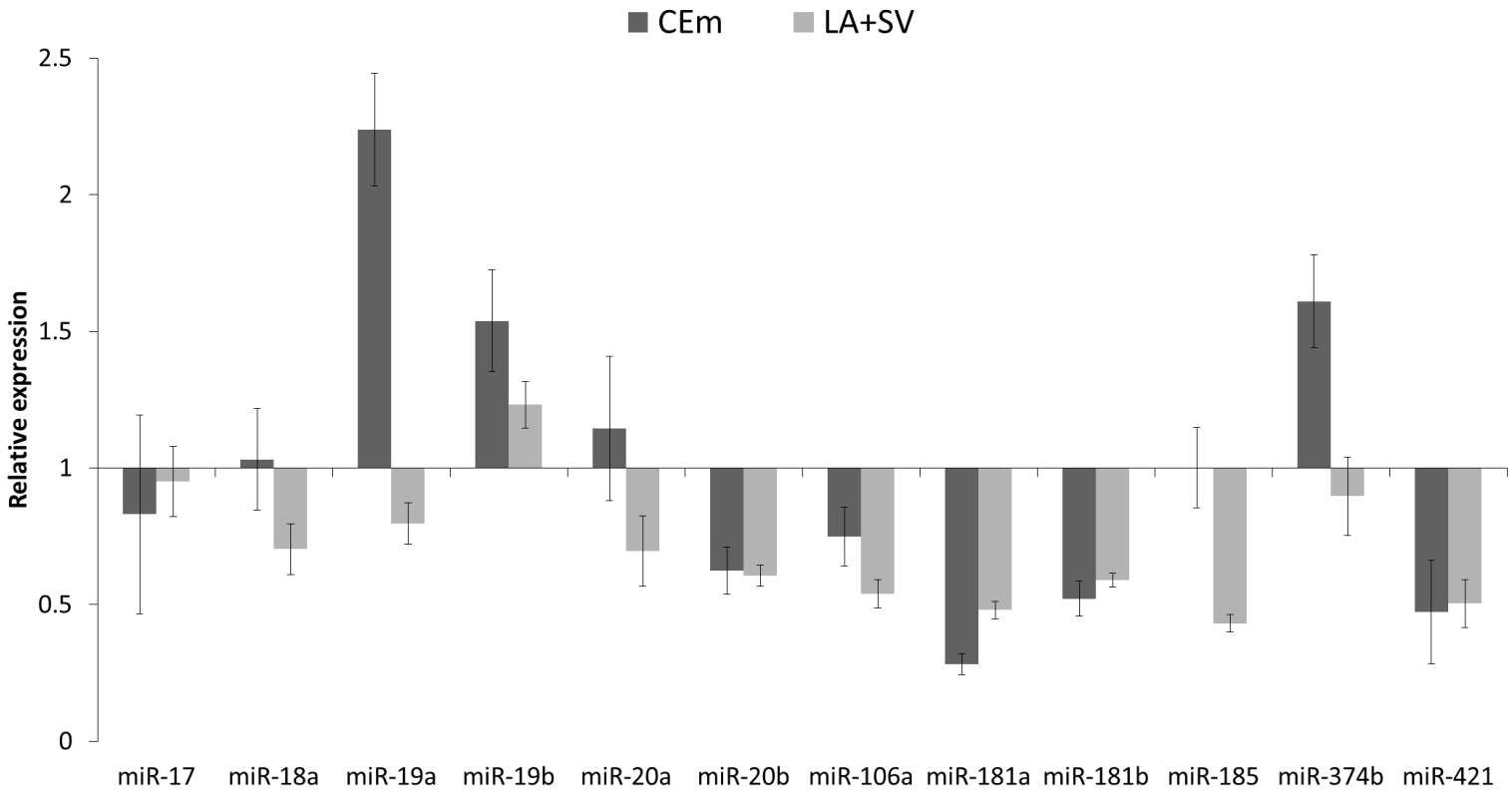


**Figure 6.2:** Relative expression of 12 miRNAs predicted to target 3'UTR of *CD46* in pooled samples. The expression of the 12 miRNAs were expressed relative to pooled healthy control samples. CE: cardioembolic stroke; LA: large artery stroke; SV: small vessel stroke.

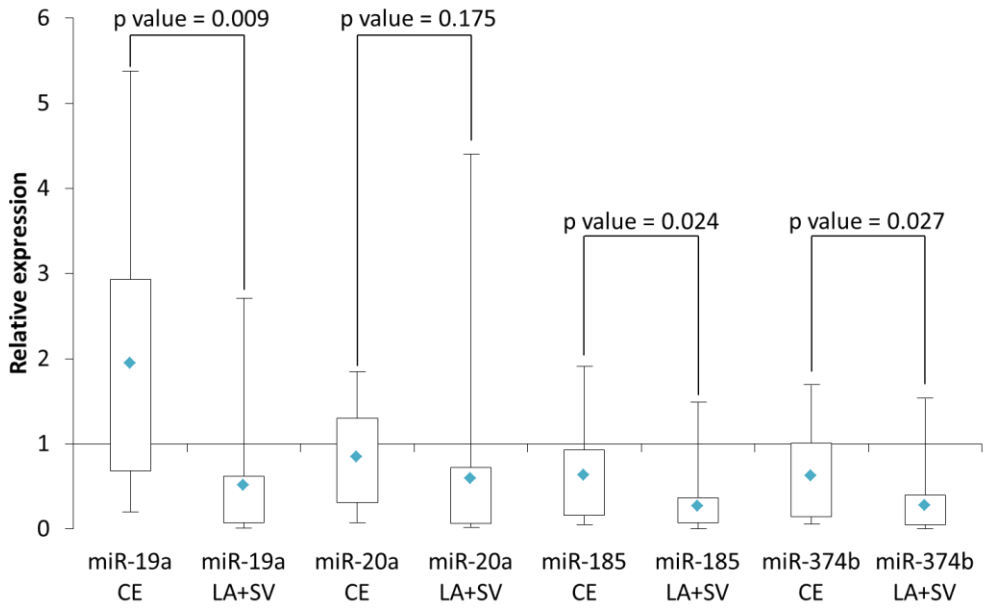


**Figure 6.3:** Relative expression of 4 miRNAs (miR-19a, -20a, -185 and -374b) in individual ischemic stroke patients according to their various stroke subtype. The expression of the 4 miRNAs were expressed relative to healthy control samples. CE: cardioembolic stroke (n=13); LA: large artery stroke (n=13); SV: small vessel stroke (n=13). The box represents the interquartile range. The line denotes the range of readings. ♦ represents the median reading. Levels of miR-19a, -185 and -374b were found to be significantly different (miR-19a: p-value=0.009, miR-185: p-value=0.024 and miR-374b: p-value=0.027) between CE and LA+SV.

## 6.5 Cloning of CD46 3'UTR

For validation of microRNA-mRNA interaction, the 3'UTR of *CD46* mRNA was cloned for downstream luciferase reporter assay. Since there were 8 mRNA transcripts, a mRNA sequence alignment was performed and found that the 3'UTR region of all the transcripts were mostly conserved including the region containing the seed regions for miR-19a, -20a, -185 and -374b (Supplementary Figure 1; Table 6.1). The following primer pairs were used cloning the selected region of *CD46* 3'UTR (Table 6.2). The selected region of *CD46* 3'UTR was cloned as a single fragment of size 1028 base pair. The fragment was amplified using polymerase chain reaction (PCR) and visualized using DNA gel electrophoresis (Figure 6.4). The fragment was sub-cloned into pCR®4-TOPO vector and subsequently sequenced using pCR®4-TOPO vector specific primers (M13F and M13R) to verify the correct sequence for the cloned fragment (Figure 6.5A).

The verified fragment was later sub-cloned the pMIR-REPORT™ Luciferase vector (Figure 6.5B). Restriction sites (*SpeI* and *HindIII*) were introduced into the fragment using the following primer pair (Table 5.1). The fragment in pCR®4-TOPO vector was amplified using the primer set with RE sites and sub-cloned into pCR®4-TOPO vector. The clones were sequenced to verify for correct sequence of fragment and presence of RE sites.

The correct fragment and pMIR-REPORT™ luciferase vector were excised using the appropriate restriction enzymes (*SpeI* and *HindIII*) via sequential digestion. The resultant fragments were ligated together using T4 DNA ligase. The ligated vector containing *CD46* 3'UTR was sequenced using primers

specific for pMIR-REPORT™ luciferase vector to verify the presence of correct fragment in the vector.

**Table 6.1:** Seed regions of miR-19a, -20a, -185 and -374b on *CD46* mRNA transcript variant a (NM_002389.4)

| Nucleotide number on *CD46* mRNA transcript variant a (NM_002389.4) | Respective miRNA and miRNA seed region |
|---|---|
| 2311 – 2332 | miR-185 AGUCCUUGACGGAAAGAGAGGU<br>gttacatgtgtttt**tctctcc**c |
| 2584 – 2606 | miR-20a GAUGGACGUGAUAUUCGUGAAAU<br>aatatagctcaggta**gcacttt**a |
| 2731 – 2753 | miR-19a AGUCAAAACGUAUCUAAACGUGU<br>gaaattttatgtttag**ttgcac**a |
| 3063 – 3084 | miR-374b GUGAAUCGUCCAACAUAAUAUA<br>atgtataaaataaa**tattata**c |

**Table 6.2:** Primers used in cloning of *CD46* 3'UTR. The table above shows the sequences of primers using in cloning of *CD46* 3'UTR. Sub-cloning of fragment into pMIR report vector was performed with primers containing specific restriction sites at the 5' ends of the primers.

| Primer | Primer Sequence (5' to 3') |
|---|---|
| CD46 Forward | GACAGCCATAACAGGAGTGC |
| CD46 Reverse | ACTTCCAGAGAAAACTGGTC |
| CD46 Forward with *Spe I* site | GACACTAGTAACAGGAGTGC |
| CD46 Reverse with *Hind III* site | ACTAAGCTTGAAAACTGGTC |

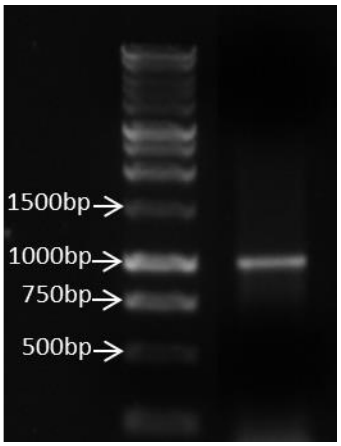


**Figure 6.4:** Amplification of selected region of *CD46* 3'UTR. The region of *CD46* 3'UTR containing the seed regions of the selected miRNAs (miR-19a, -20a, -185 and -374b) was amplified using sequence specific primers. The size of the region amplified was 1028 base pairs.

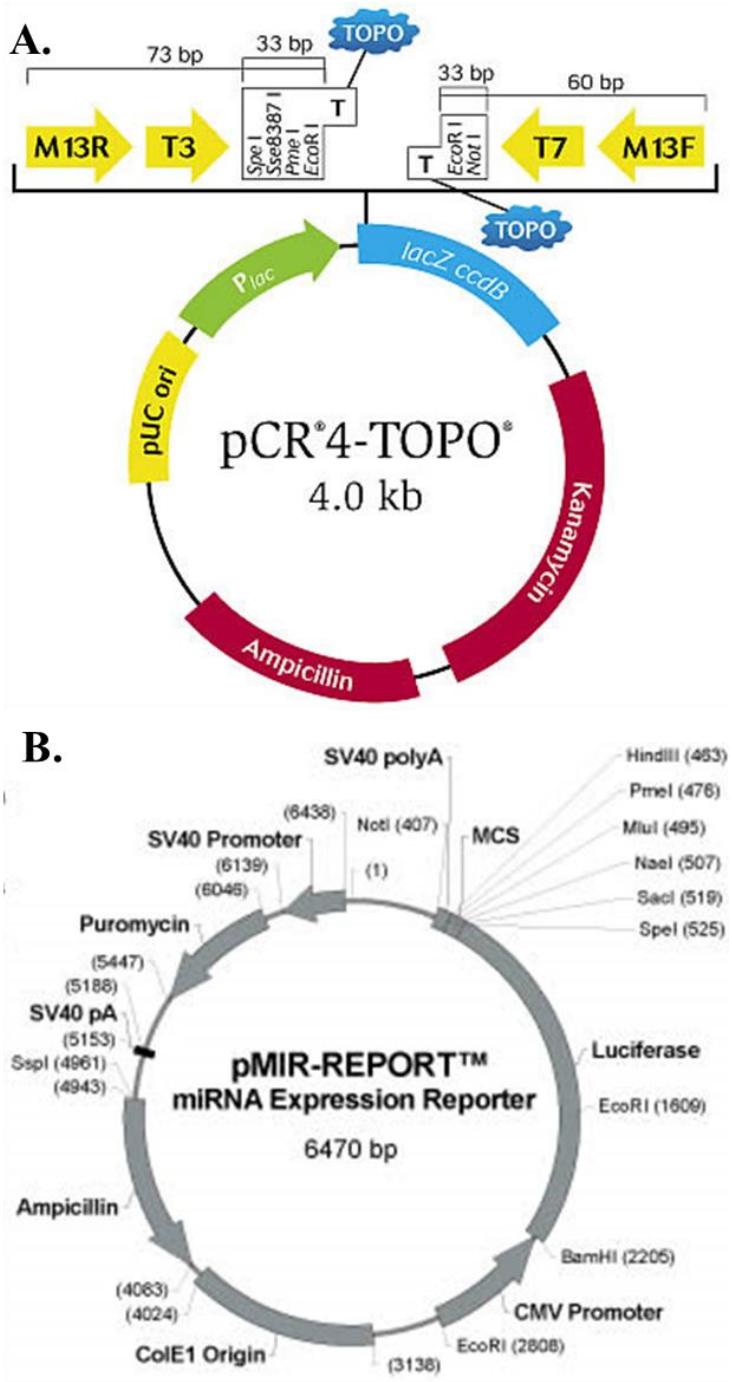


**Figure 6.5:** Vector maps of pCR®4-TOPO vector and pMIR-REPORT™ Luciferase vector. **A**. pCR®4-TOPO vector was used in the TA-cloning of amplified PCR product. **B**. The fragment of interest was ligated into pMIR-REPORT™ Luciferase vector using restriction enzymes (*Spe I* and *Hind III*).

## 6.6 Luciferase reporter assays for *CD46* 3'UTR

In order to show the interaction between the miRNA and *CD46* 3'UTR, luciferase assay was performed. The assay was typically performed in HELA cells as the cell line can be easily transfected. The cells were first transfected with the respective anti-miRNAs or miRNA mimics (miR-19a, -20a, -185 and -374b) along with their corresponding negative controls. Subsequently, the cells were transfected with the pMIR-Report™ Luciferase vector containing *CD46* 3'UTR construct. Luciferase activity was measured 48 hours after transfection.

In order to validate that the transfection of anti-miRNA and miRNA mimic had repressed or elevated the miRNA levels in the cells, total RNA isolated from the cells were used to measure miRNA level using stem-loop qPCR. The measurement showed a significant change (p-value < 0.05) in miRNA level after transfection (Table 6.3).

It was observed that cells transfected with anti-miRNAs demonstrated an increase in luciferase activity (anti-miR-19a: 140.63%; anti-miR-20a: 124.08%; anti-miR-185: 141.47% and anti-miR-374b: 141.52%), while cells transfected with miRNA mimics showed lower luciferase activity (miR-19a mimic: 78.17%; miR-20a mimic: 82.86%; miR-185 mimic: 62.51% and miR-374b mimic: 64.02%; Figure 6.6), when compared to control. The differences in luminescence between respective anti-miRNA/miRNA mimic and control were tested and found to be statistically significant (p-value < 0.05; Figure 6.6). Among the 4 miRNAs (miR-19a, -20a, -185 and -374b), miR-19a, -185 and -374b showed stronger interaction with *CD46* 3'UTR as demonstrated by

greater increase luciferase activity when transfected with anti-miRNAs and more reduction in luciferase activity when transfected with miRNA mimics (Figure 6.6).

In order to investigate the differentiate expression of *CD46* and the 4 miRNAs (miR-19a, -20a, -185 and 374b) targeting *CD46* in cardioembolic stroke patients, transfection study was performed on human umbilical vein endothelial cells (HUVECs; ATCC® CRL-1730™), as the endothelial cells are in constant contact with circulation and there is a possible difference in the endothelial cell gene expression in cardioembolic stroke patients as compared to large artery and small vessel stroke patients.

**Table 6.3:** Relative expression of respective miRNAs (miR-19a, -20a, -185 and -374b) in anti-miRNA and miRNA mimic transfected HELA cells. The levels of miRNAs were expressed relative to controls. The expression of miRNAs were found to be statistically significant (p-value < 0.05) as compared with control.

| **Anti-miRNA/miRNA mimic transfected** | **Relative expression ± SEM** |
|---|---|
| | **miR-19a** |
| Anti-miR-19a | 0.30 ± 0.13 |
| miR-19a mimic | 277.33 ± 33.07 |
| | **miR-20a** |
| Anti-miR-20a | 0.54 ± 0.04 |
| miR-20a mimic | 189.93 ± 38.07 |
| | **miR-185** |
| Anti-miR-185 | 0.07 ± 0.00 |
| miR-185 mimic | 3280.01 ± 868.17 |
| | **miR-374** |
| Anti-miR-374b | 0.07 ± 0.01 |
| miR-374b mimic | 14864.70 ± 4095.53 |

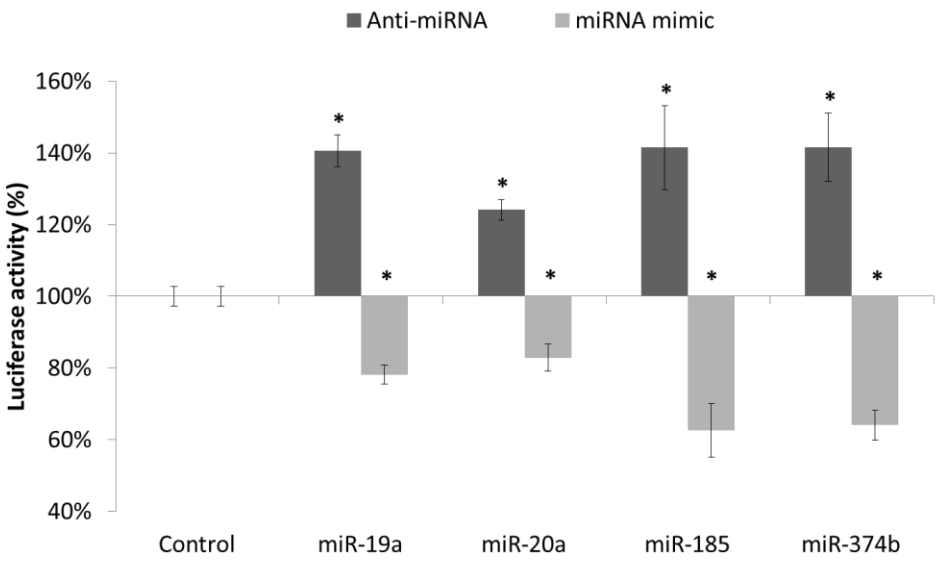


**Figure 6.6:** Dual Luciferase assay for miRNAs (miR-19a, -20a, -185 and -374b) predicted to target *CD46*. The plasmid construct was co-transfected with either anti-miRNA or miRNA mimic. Relative luminescence was obtained by normalizing the values against control plasmids, pMIR-REPORT™ Luciferase vector without any 3'UTR insert. * denoted tested significantly different (p value < 0.05) as compared to control. Data were shown as mean ± SD, n=3.

### 6.7 Anti-miRNA and miRNA mimic transfection in HUVEC

To investigate the possible regulation of CD46 by miRNAs in the endothelium, anti-miRNA and miRNA mimic were transfected into HUVECs which is an *in vitro* mimic for endothelial cells. HUVECs were seed at density of 3 X $10^4$ cells per well in 24 well plate. The cells were transfected with anti-miRNA and miRNA mimic for 48 hours after which the cells were collected in TRIzol™ reagent (Invitrogen, Life Technology, Carlsbad, CA, USA). Total RNA (including miRNAs) were isolated from the cells according to manufacturer's protocol. The concentration and integrity was determined using Nanodrop™ N2000C spectrophotometer (Thermo Scientific™, Rockford, IL, USA) and RNA gel electrophoresis (1% agarose). Presence of small RNAs was verified using denaturing polyacrylamide gel electrophoresis (15% polyacrylamide). RNA samples were used for qPCR and stem-loop qPCR to quantitate level of mRNA and miRNAs respectively.

The results of stem-loop qPCR demonstrated successful transfection of anti-miRNA and miRNA mimics. Upon transfection of respective anti-miRNAs (miR-19a, -20a, -185 and -374b), the level of respective miRNAs decreased significantly ($p$ value $< 0.05$), while transfection of respective miRNA mimics resulted in increase of the respective miRNAs level (Table 6.4).

Following which, the *CD46* mRNA level was quantified and the results showed that these 4 miRNAs (miR-19a, -20a, -185 and -374b) target *CD46*. HUVECs transfected with respective anti-miRNAs showed increased level of *CD46* mRNA while cells transfected with miRNA mimics showed reduced *CD46* mRNA.

The results suggested that miR-19a, -20a, -185 and 374b can regulate CD46 expression in endothelial cells which may be a possible source of differential expression of *CD46* and miRNAs targeting *CD46*, in cardioembolic stroke as compared with large artery and small vessel stroke. This put forth a possible cause for the observation seen in the clinical samples and also a possible mechanism. Hence, miR-19a, -185 and 374b could possibly act as a marker for cardioembolic stroke.

**Table 6.4:** Relative expression of respective miRNAs (miR-19a, -20a, -185 and -374b) in anti-miRNA and miRNA mimic transfected HUVECs. The levels of miRNAs were expressed relative to control. The expression of miRNAs were found to be statistically significant (p-value < 0.05) as compared with control.

| **Anti-miRNA/miRNA mimic transfected** | **Relative expression ± SEM** |
|---|---|
| | **miR-19a** |
| Anti-miR-19a | 0.55 ± 0.14 |
| miR-19a mimic | 23.09 ± 4.17 |
| | **miR-20a** |
| Anti-miR-20a | 0.54 ± 0.07 |
| miR-20a mimic | 24.52 ± 11.03 |
| | **miR-185** |
| Anti-miR-185 | 0.13 ± 0.06 |
| miR-185 mimic | 180.77 ± 52.08 |
| | **miR-374** |
| Anti-miR-374b | 0.33 ± 0.15 |
| miR-374b mimic | 213.57 ± 50.50 |

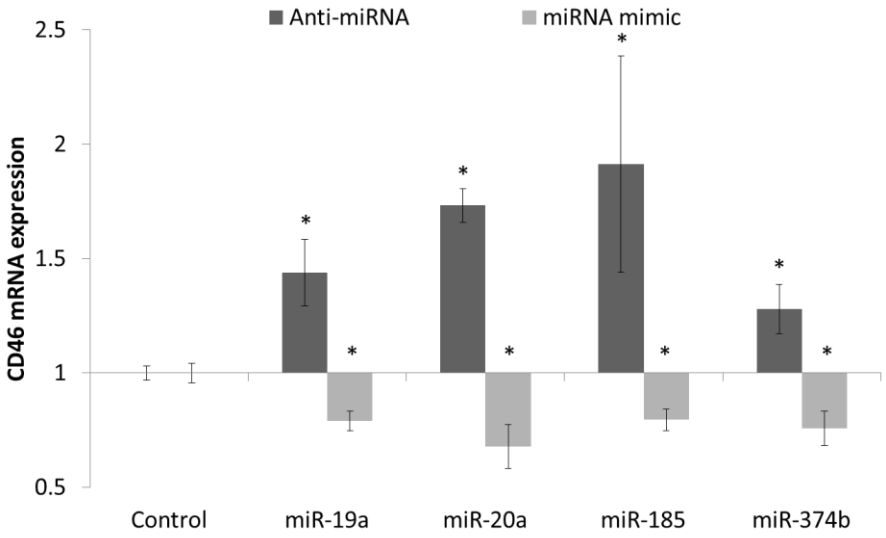


**Figure 6.7:** *CD46* mRNA expression in anti-miRNA and miRNA mimic transfected HUVECs. All values were expressed relative to control. * denoted tested significantly different (p value < 0.05) as compared to control. Data were shown as mean ± SD, n=3.

## 6.8 Screening for chemokines in rat MCAo model

Results from previous chapters demonstrated that biological pathway, Chemokine signaling pathway, was critical to pathophysiology of ischemic stroke. Thus, chemokine screening was performed on serum collected from rat animal models using MILLIPLEX® MAP rat cytokine/chemokine kit assay (Millipore Corporation, Billerica, MA, US). For screening, the following time points, 12, 24 and 48 hours were used, as 24 hours was when the maximum infarct volume occurred while 12 and 48 hours were time-points before and after that.

In brief, whole blood samples collected from rats subjected to middle cerebral artery occlusion (MCAo) were left to clot at 4°C for at least 2 hours and centrifuged at 1000 X g for 10 minutes. Serum was collected and stored in -80°C until required. Serum samples were diluted five folds using sample diluent provided. Assay was performed based on manufacturer's protocol. Detection and analysis was conducted on Luminex 100™ system (Luminex Corporation, Austin, TX, US).

The assay detected 3 chemokines, chemokine CXC motif ligand 1 (CXCL1), chemokine CC motif ligand 2 (CCL2) and chemokine CC motif ligand 5 (CCL5; Figure 6.8). CCL2 and CCL5 showed similar expression in suture and embolic model while CXCL1 did not (Figure 6.8A, B and C). CCL2 showed upregulation from 12 hours, reached maximum expression at 24 hours and decreased after 24 hours (Figure 6.8B). CCL5 expression was maximal at 12 hours and decreased after 12 hours (Figure 6.8C).

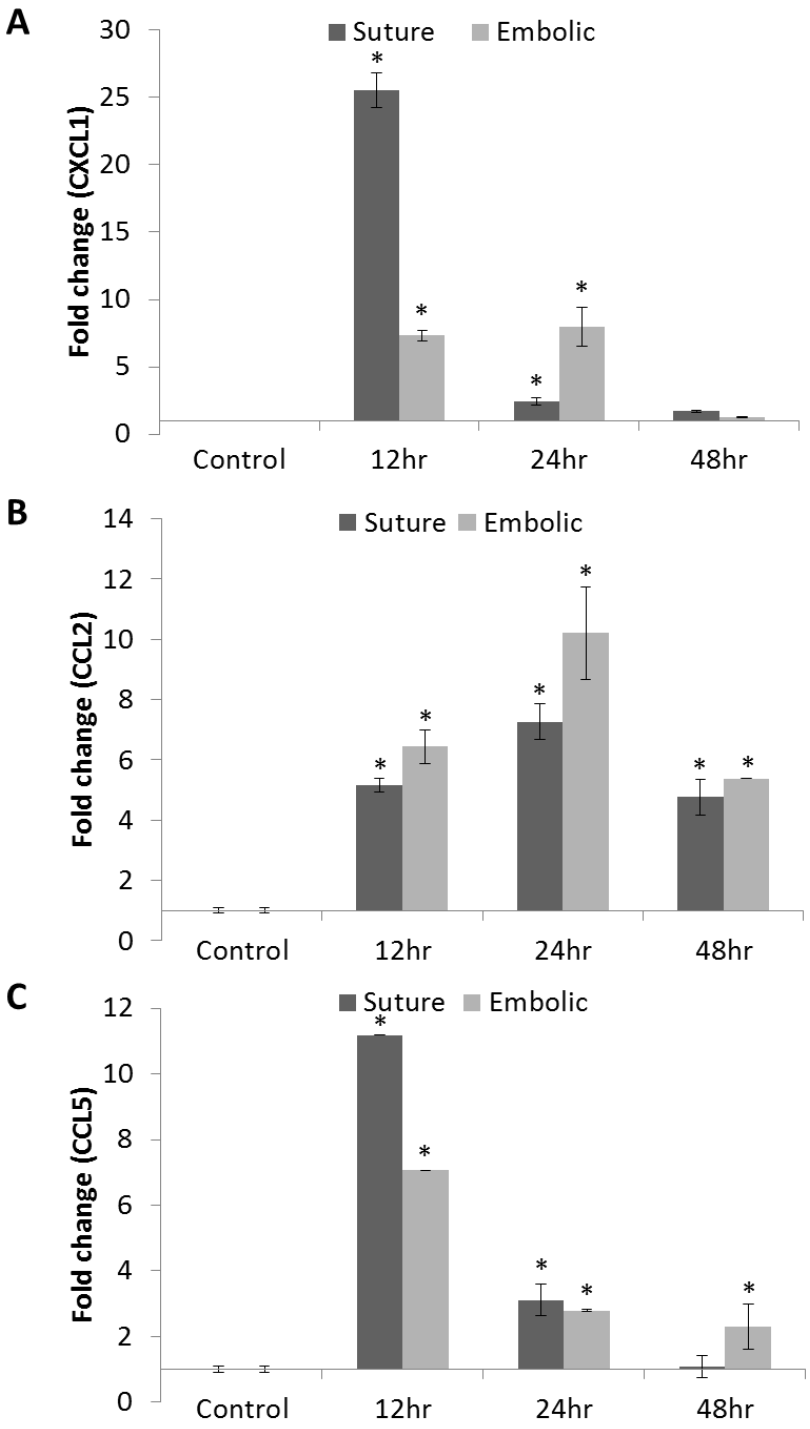


**Figure 6.8:** Chemokine levels in suture and embolic models at 12, 24 and 48 hours. **A.** CXCL1. **B.** CCL2. **C.** CCL5. Levels of chemokine were expressed as fold change with respect to control. For each time-point, there were n=3 for rats used in stroke models and there were n=6 for control rats. * denoted tested significantly different (p value < 0.05) as compared to control. Data were shown as mean ± SD.

### 6.9 *Ccl2* and *Ccl5* mRNA level in embolic and suture model

After screening chemokine level in serum of embolic and suture model, CCL2 and CCL5 were found to have similar expression in embolic and suture models. Hence, *Ccl2* and *Ccl5* mRNA level was measured in embolic and suture model by qRT PCR.

The results showed that the *Ccl2* and *Ccl5* mRNA expression pattern were similar between suture and embolic model. *Ccl2* mRNA was upregulated at 12 hours, reached maximum level at 24 hours and decreased progressively after 24 hours (Figure 6.9A). While *Ccl5* mRNA level reached maximal expression at 12 hours, followed by a decrease from 12 hours to 72 hours, then the expression increased again at 120 hours and decreased after 120 hours (Figure 6.9B). Between *Ccl2* and *Ccl5*, *Ccl2* mRNA and protein level correlated better compared with *Ccl5*. In addition, *Ccl2* mRNA expression pattern correlated with infarct volume (Figure 6.10). Thus, it would be useful to identify miRNAs that target *Ccl2* to regulate its expression.

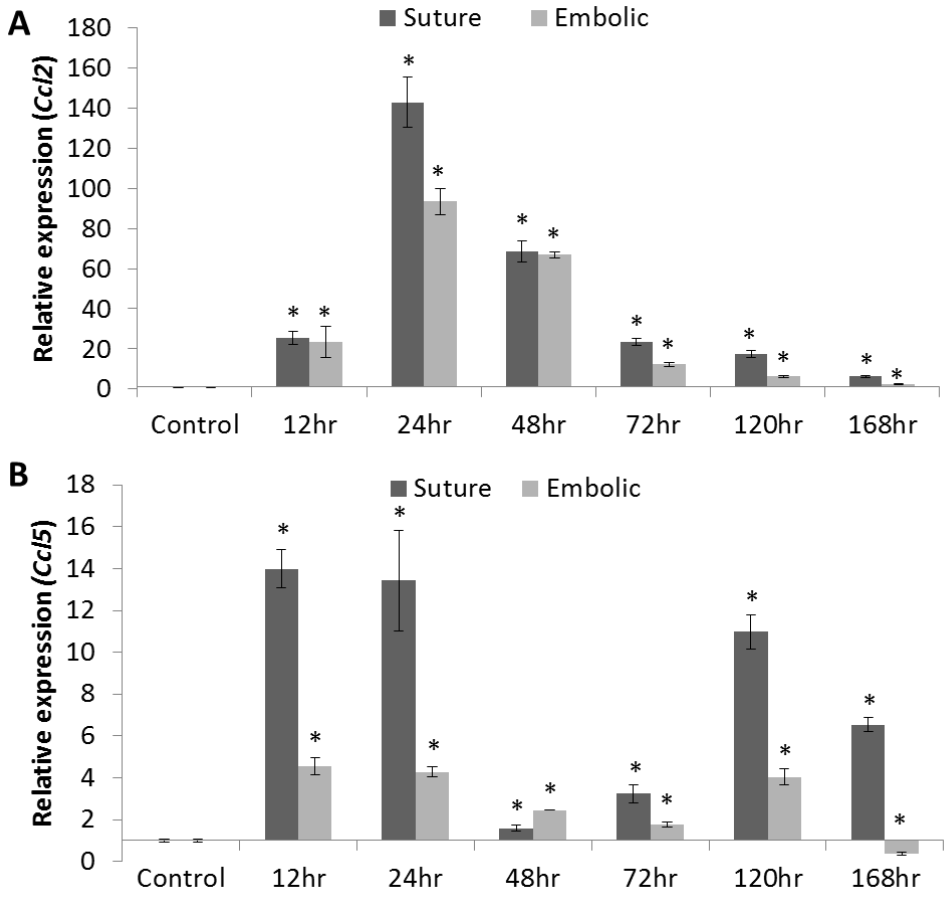


**Figure 6.9:** Expression of **A.** Ccl2 and **B.** Ccl5 in suture and embolic model. All values were expressed relative to control. * denoted tested significantly different (p value < 0.05) as compared to control. Data were shown as mean ± SD, n=3.

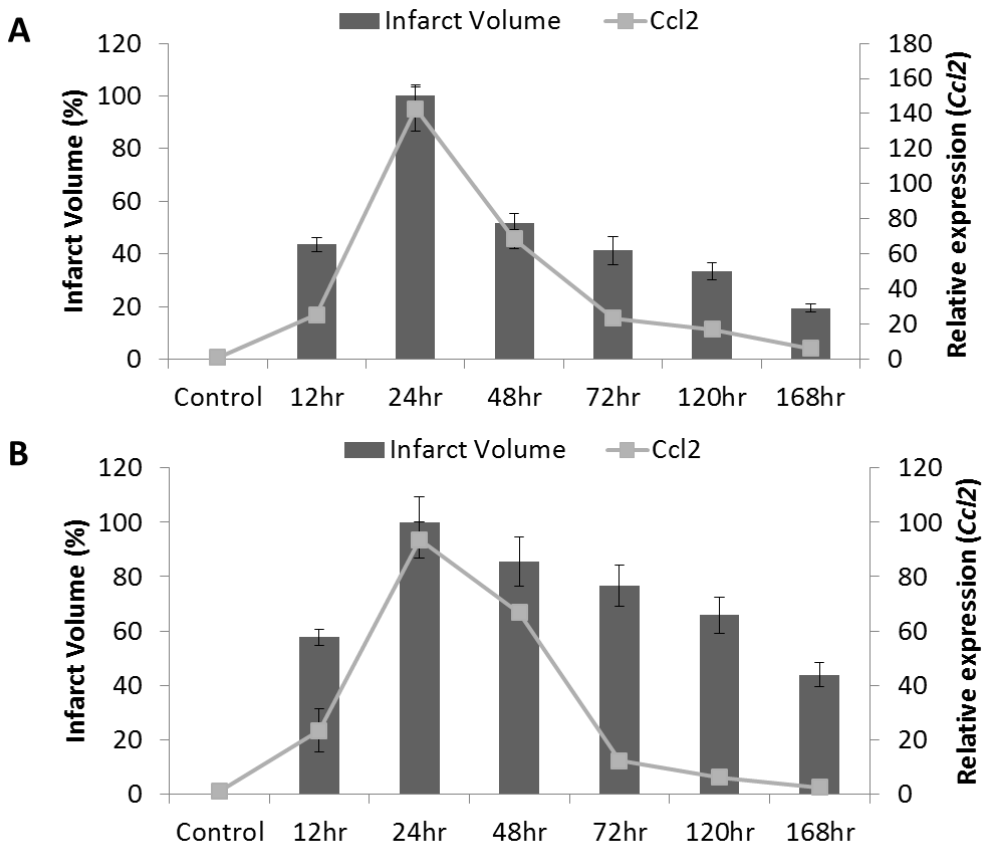


**Figure 6.10:** Expression of *Ccl2* and infarct volume in **A.** suture model and **B.** embolic model. All values were expressed relative to control. For each time-point, there were n=3 animals and there were n=6 for controls. Data were shown as mean ± SD.

### 6.10 CCL2 level in serum of ischemic stroke patients

*Ccl2* was shown to be associated with infarct volume in animal models of ischemic stroke, it was necessary to determine the similar role in human ischemic stroke patients. Hence, measurement of CCL2 levels in patient serum samples were performed using CCL2 ELISA kit (R&D systems, MN, US) according to manufacturer's protocol. Samples were obtained in BD Vacutainer ® (Becton, Dickinson and Company, New Jersey, US) at Day 1, 2 and 7 upon admission. They were left for at least 30 minutes to allow clotting and subsequently, spun down and aliquot for storage at -80°C until required.

The results showed that CCL2 levels in patient serum were higher than that of healthy control at all time-points (Day 1, 2 and 7; Figure 6.11A). When compared with between samples with good outcome (mRS < 2) and samples with poor outcome (mRS ≥ 2), CCL2 levels were higher in samples with good outcome across all the time-points (Figure 6.11B). This unexpected finding suggested that CCL2 up-regulation in ischemic stroke patients may be beneficial. In order to further investigate, identification of miRNAs targeting *CCL2* is necessary as these miRNAs can be used to regulate *CCL2* in *in vitro* experiment mimicking ischemic stroke, to elucidate possible function of *CCL2* in the patients.

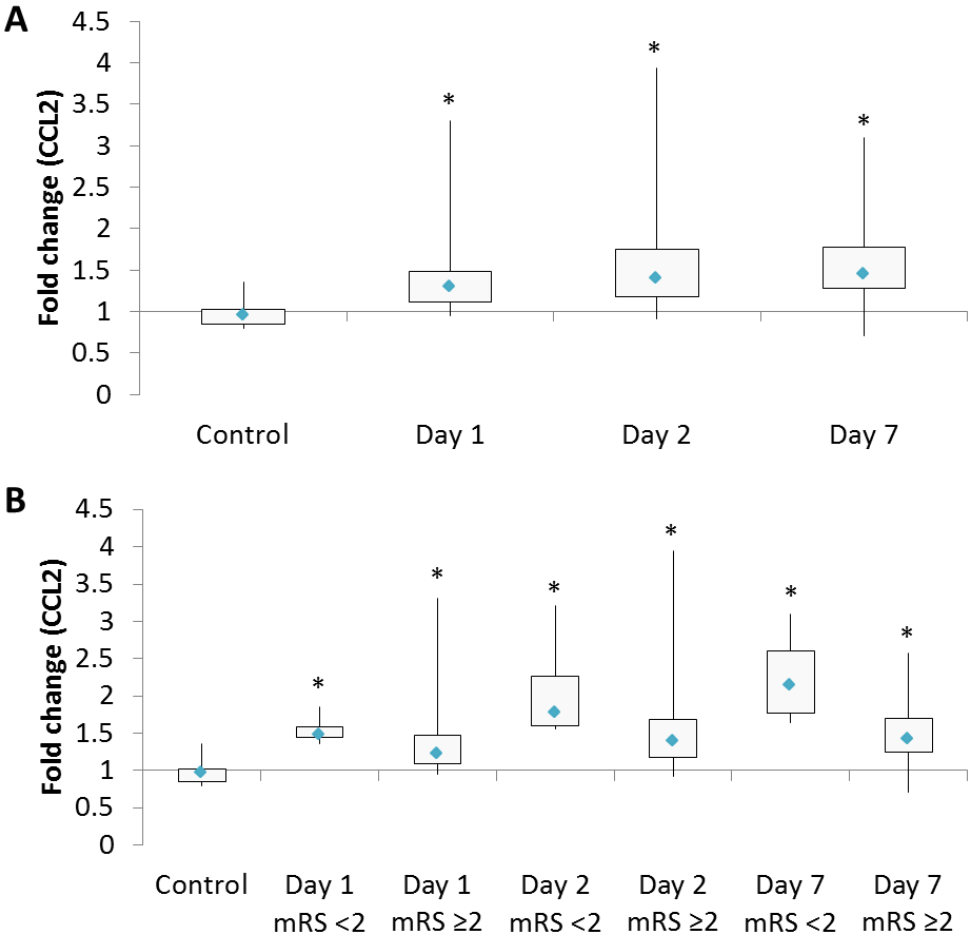


**Figure 6.11**: Level of CCL2 in serum of ischemic stroke patients. **A**. Level of CCL2 in ischemic stroke patients at Day 1, 2 and 7. **B**. Level of CCL2 in patients with good outcome (mRS < 2) and patients with poor outcome (mRS ≥ 2) at Day 1, 2 and 7. The box represents the interquartile range. The line denotes the range of readings. ♦ represents the median reading. All values were expressed relative to control. * denoted tested significantly different (p value < 0.05) as compared to control. Data obtained from 39 ischemic stroke patients and 8 healthy controls. Day 1, 2 and 7 mRS < 2: n = 9. Day 1, 2 and 7 mRS ≥ 2: n = 30.

### 6.11 miRNAs predicted to target *Ccl2* and *CCL2*

In the search for miRNAs targeting *Ccl2* and *CCL2*, miRNA prediction databases were used for the shortlisting of miRNAs. The bioinformatics prediction utilized 5 databases for predicting miRNAs targeting *Ccl2*: Targetscan version 6.2 (www.targetscan.org) [156-159], miRanda August 2010 release (www.microRNA.org) [160-163], microcosm version 5 (www.ebi.ac.uk/enright-srv/microcosm/htdocs/targets/v5/) [163-165], miRDB version 4 (mirdb.org/) [168, 169] and miRWalk March 2011 update (www.umm.uni-heidelberg.de/apps/zmf/mirwalk/) [170]. While for prediction of miRNAs targeting *CCL2*, 8 databases were used: Targetscan version 6.2 (www.targetscan.org) [156-159], miRanda August 2010 release (www.microRNA.org) [160-163], microcosm version 5 (www.ebi.ac.uk/enright-srv/microcosm/htdocs/targets/v5/) [163-165], DIANA microT version 3 (http://diana.cslab.ece.ntua.gr/microT/) [166, 167], miRDB version 4 (mirdb.org/) [168, 169], miRWalk March 2011 update (www.umm.uni-heidelberg.de/apps/zmf/mirwalk/) [170], PITA 2007 release (genie.weizmann.ac.il/pubs/mir07/mir07_prediction.html) [171] and StarBase version 2 (starbase.sysu.edu.cn/) [173, 174].

The results from the prediction showed 66 miRNAs predicted to target *Ccl2* 3'UTR (Supplementary Table 5). Among these 66 miRNAs, there were 47 miRNAs that were detected in the microarray. Of these 47 miRNAs, 12 miRNAs (miR-23a, -23b, -27a, -27b, -33, -124, -137, -290, -323, -369-3p, -434 and -664) were selected for screening as these miRNAs were predicted by more than 1 database. As for *CCL2*, there were 419 miRNAs predicted to target it (Supplementary Table 6). There were 134 miRNAs detectable from

the microarray analysis. Amongst the 134 miRNAs, 10 miRNAs (miR-23a, -23b, -33a, -122, -206, -374a, -374b, -421, -518a-5p and -664) were selected for screening as these miRNAs were predicted by more than 4 databases.

By comparing the *Ccl2* mRNA measurements and the expression of 12 miRNAs (miR-23a, -23b, -27a, -27b, -33, -124, -137, -290, -323, -369-3p, -434 and -664) predicted to target *Ccl2* mRNA from miRNA profiles, miRNA-27b seems to show inverse correlation with the expression of *Ccl2* mRNA (Figure 6.12). The expression of these miRNAs still need to be quantified using stem-loop qPCR. The expression of *CCL2* mRNA and the 10 miRNAs (miR-23a, -23b, -33a, -122, -206, -374a, -374b, -421, -518a-5p and -664) predicted to target *CCL2* in ischemic stroke patients also need to be quantitated using qPCR based on their functional outcome (mRS > 2; mRS ≤ 2).

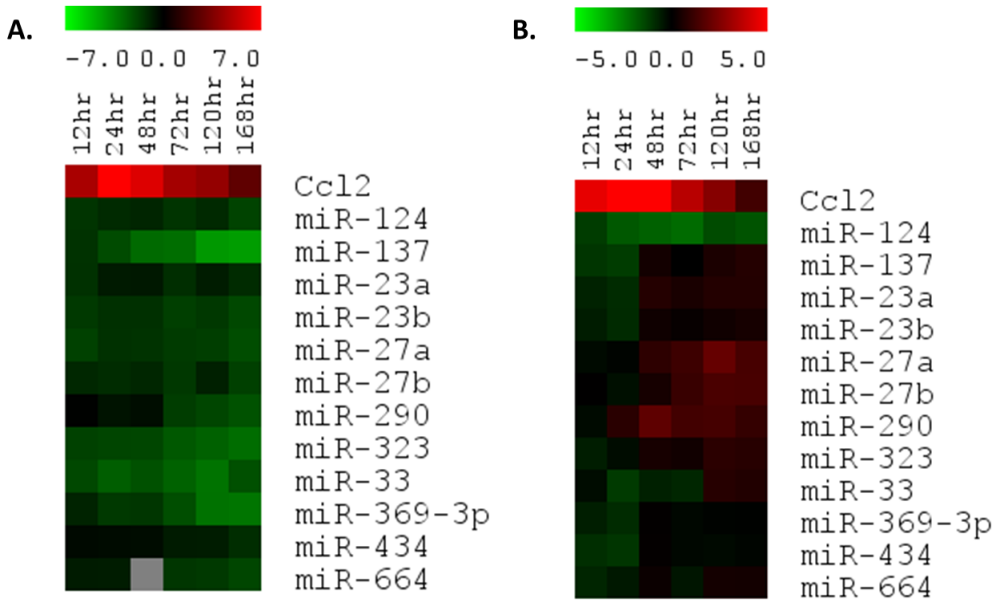


**Figure 6.12:** Expression of *Ccl2* and 12 miRNAs predicted to target *Ccl2* in **A.** suture model and **B.** embolic model. All values were expressed relative to control. Green represents down-regulation. Red represents up-regulation. Grey represents absence. For each time-point, there were n=3 animals and there were n=6 for controls.

# Chapter 7

# Discussion

## 7.1 Circulating miRNAs detected during systemic response to ischemic stroke

In this study, blood miRNAs were profiled in ischemic stroke patients. Though it was observed that blood miRNAs were dysregulated in patients as compared to healthy controls, the question remained to be answered that is: what does the dysregulated miRNAs reflect?

From the miRNA profile of the human ischemic stroke patients, there is a general correlation between miRNA expression with time, where the expression of miRNAs tend to increase with time. This observation seems to suggest that the up-regulation of miRNA can be part of the mechanism involving in progression of ischemic stroke towards either recovery or worsening. There is a need to profile patients according to their functional outcome as to identify the specific biological pathway involved in recovery so that this can form the basis for therapeutic intervention to promote recovery.

Jickling *et al* [198] recently published miRNA expression in ischemic stroke patients indicating that miRNAs detected were predominantly from circulating leukocytes. They identified 8 miRNAs (let-7i, miR-19a, -122, -148a, -320d, -363, -487b and -4429) as ischemic stroke specific miRNAs. Of these 8 miRNAs, 7 miRNAs (let-7i, miR-19a, -122, -148a, -320d, -363, -487b and -4429) were detectable in the array results from this study. From this observation, it could suggest that circulating miRNA profile could be reflective of the leukocyte response to stroke onset.

miRNAs can also be compartmentalized into secretory vesicles such as exosomes and apoptotic bodies [242, 243]. In addition, miRNAs can also be

found to complex with proteins such as Argonaute2 (Ago2) and high density lipoprotein (HDL) [244, 245]. These miRNA complexes and vesicles could be reflective of the condition of the source tissue. Apoptotic bodies are small membrane vesicles (0.5 μm – 200 μm) released from cells undergoing apoptosis [246]. Exosomes are small (diameter < 100nm) microvesicles secreted by various cells for cell to cell communication [247, 248]. Exosomal miRNAs had been shown to be stable and protected from RNaseA treatment [249]. Furthermore, some miRNAs enriched in exosomes (miR-26, -126 and -191) have been associated with neuronal function [249]. Interestingly, these miRNAs were also detected as dysregulated miRNAs in this study, suggesting that the miRNA profile was also reflective of conditions in the brain after stroke onset.

Therefore, blood miRNA profiling provides information about the local response in the brain and also a systemic response of the leukocytes, a possible inflammatory related response. Hence, blood miRNA profiling can provide much insight into the mechanisms underlying ischemic stroke pathophysiology.

### 7.2 Patient cohorts used for this study

The patient number recruited for this study was small in comparison with the numbers in published work [190, 197-205], which ranged from 24 to about 100 patient samples. There was a higher proportion of patients suffering for cardioembolic stroke. This was in agreement with literature as it was

previously reported that Asians have a higher incidence of cardioembolic stroke as compared with Caucasians [250].

From the statistical testing of the variables between the stroke subtypes (large artery, cardioembolic and small vessel stroke), there were no significant differences between age and gender. This ensures that the patient cohorts used for this study were not confounded by these 2 important variables.

There were slight differences in the comorbidities and outcome between stroke subtypes, where there were greater portion of cardioembolic stroke patients with atrial fibrillation as compared with large artery and small vessel stroke patients, and there were more small vessel stroke patients having good outcome as compared with cardioembolic and large artery stroke patients. These differences were well within expectations. Atrial fibrillation is a major cause of cardioembolic stroke and higher number of cardioembolic stroke patients with atrial fibrillation as compared with other stroke subtype was to be expected [16]. The demographics of the patients used were in agreement with the literature. Small vessel stroke was shown to have better outcome as compared with large artery stroke and cardioembolic stroke, similar with previous reports [251, 252]. Thus, these observations demonstrated that the patient cohorts used for this study are somewhat representative of the patient population needed for this study.

Despite the small sample size of the low or no risk ischemic stroke patients cohort, the findings were comparable with the findings in the animal model which is a close parallel in experimental setting. This evidence suggested that low or no risk ischemic stroke patients may be the bridge between

experimental and clinical setting. It will be beneficial to validate the findings observed in a larger cohort of low or no risk ischemic stroke patients.

### 7.3 Stroke subtype specific miRNAs

Among the 10 large artery specific miRNAs (miR-27a*, -129-5p, -382, -585, -602, -637, -659, -744, -1184 and -1261; Table 7.1), 4 miRNAs (miR-382, -637, -659 and -744) have been found to have validated targets specific to the etiology of large artery stroke [253-259]. These 4 miRNAs had higher expression in large artery stroke as compared with other stroke subtypes (cardioembolic and small vessel stroke). Large artery stroke is usually caused by the rupture of atherosclerotic plaque [258]. These 4 miRNAs were associated with atherosclerosis. miR-382-5p targets nuclear factor IA (NFIA) which inhibits atherogenesis by increasing high density lipoprotein and decreasing low density lipoprotein [253]. The up-regulated miR-382-5p in large artery stroke enhanced atherogenesis in the patients. V-akt murine thymoma viral oncogene homolog 1 (AKT1) is a gene protecting endothelial cells through the AKT1/eNOS pathway and is targeted by miR-637 [254]. The higher expression of miR-637 in large artery stroke patients contributes to the progression of atherosclerosis. While the up-regulated miR-659 targets the anti-inflammatory progranulin, resulting in atherosclerosis-promoting inflammation, enhancing atherosclerosis in large artery stroke [255, 256]. miR-744 had been shown to target Transforming Growth Factor Beta-1 (TGFβ-1) which inhibits atherogenesis [257, 259]. In large artery stroke patients, the up-regulated miR-744 exacerbated the progression of

atherosclerosis. Hence, these observations showed that the 10 large artery specific miRNAs are relevant to the pathogenesis of large artery stroke and hence are worthy of further investigation.

Similarly, 14 cardioembolic stroke specific miRNAs (miR-19a, -130b*, -181a-2*, -198, -200b, -208a, -412, -525-5p, -550, -617, -618, -630, -668 and -1321; Table 7.1) has validated targets specific to the etiology. miR-19a has been known to target atrogin-1 and MuRF-1 (muscle RING-finger protein-1) which are anti-hypertrophy genes [260]. Cardiac hypertrophy can be seen as a pre-existing condition leading to atrial fibrillation which is the underlying cause of most cardioembolic stroke [261]. Hence, the up-regulated miR-19a promotes a hypertrophic condition. Similarly, miR-200b which was found to have lower expression in cardioembolic stroke patients, targets GATA-4 that is pro-hypertrophy [262, 263]. This signified that lower expression of miR-200b in cardioembolic stroke patients could possibly correlate to cardiac hypertrophy. From the above-mentioned evidence, the miRNAs in this cluster could possibly be specific for cardioembolic stroke and account for the underlying etiology. Thus, these miRNAs should be considered for further study on their possible mechanism of actions.

Interestingly, among the 8 miRNAs (miR-19a, -129-5p, -198, -320b, -320d, -331-3p, -637 and -744; Table 7.1) that could segregate samples into various stroke subtypes (large artery, cardioembolic and small vessel stroke), 3 of them (miR-320b, -320d and -331-5p) have been reported by Sepramaniam *et al* [197] as miRNAs that could distinguish samples according to various stroke subtypes. Literature search was performed to identify reported biological pathways regulated by these 8 miRNAs. Among the 8 miRNAs, miR-19a had

been reported to be associated with inflammation [198], miR-129-5p regulates hippo signalling pathway and Wnt signalling pathway [264, 265], miR-198 was reported to regulate immune response, cell proliferation, apoptosis, cell metabolism and cell migration [266], miR-320 was found to be involved in angiogenesis, metabolic process regulation and hypoxia regulation [190], miR-331-3p was reported to regulate androgen receptor signalling [267] and miR-744 was found to regulate MAPK/ERK pathway [268]. Hence, these 3 miRNAs are most likely to be miRNAs that regulate processes that are explicitly different between individual stroke subtypes and should be investigated in detail.

**Table 7.1:** List of stroke subtype specific miRNAs.

| Groups of miRNAs | miRNAs |
|---|---|
| Large artery stroke specific miRNAs | miR-27a*, -129-5p, -382, -585, -602, -637, -659, -744, -1184 and -1261 |
| Cardioembolic stroke specific miRNAs | miR-19a, -130b*, -181a-2*, -198, -200b, -208a, -412, -525-5p, -550, -617, -618, -630, -668 and -1321 |
| miRNAs that could segregate samples into various stroke subtypes | miR-19a, -129-5p, -198, -320b, -320d, -331-3p, -637 and -744 |

### 7.4 Biological pathways specific for stroke subtype

The biological pathways were ranked from 1 to 100 in this study. The difference in ranking the biological pathways signified the difference in the degree of dysregulation among the ischemic stroke subtypes. Those biological pathways ranked higher implied that more components in the pathway are modulated by the dysregulated miRNAs. For complement and coagulation cascades, it was ranked 51st for LA and SV, while it was ranked 99th for CE. This suggests that complement and coagulation cascade could be more dysregulated in LA and SV as compared with CE.

In the pathway analysis for large artery stroke, the following biological pathways have been associated with large artery stroke: Arginine and proline metabolism, B-cell receptor signaling pathway, Cell adhesion molecules (CAM), Glycosphingolipid biosynthesis-ganglio series and Tight junction. Some of these pathways are associated with the etiology of large artery stroke. The cause of large artery stroke is often due to the formation and rupture of atherosclerotic plaque. Hypertension, hyperglycemia and dyslipidaemia are the pre-conditions to trigger atherogenesis which often involve endothelial dysfunction. One of the hallmarks of endothelial dysfunction is the loss of vascular tone due to decrease in nitric oxide (NO) production by the endothelium [269]. This usually implicates the de-regulation of arginine metabolism as arginine is a pre-cursor for NO production [269]. Furthermore, atherosclerosis progression is driven by inflammation, involving leukocytes and lymphocytes to infiltrate the endothelium, which include B-cells [270]. The infiltration of these immune cells involved the disruption of tight junction. Thus explaining the dysregulation of Cell adhesion molecules and Tight

junction [271]. It is known that gangliosides, the products of glycosphingolipid biosynthesis accumulate within atherosclerotic vessels [272]. Hence, the 10 miRNAs (miR-27a*, -129-5p, -382, -585, -602, -637, -659, -744, -1184 and -1261; Table 7.1) specific for large artery stroke are likely to be involved in these etiological processes, demonstrating the potential of these miRNAs for diagnosis of large artery stroke.

As for cardioembolic stroke, there were 9 biological pathways (ABC transporters, adherens junction, complement and coagulation cascades, dilated cardiomyopathy, gap junction, glycerophospholipid metabolism, glycosphingolipid biosynthesis – lacto and neolacto series, inositol phosphate metabolism and pyruvate metabolism) associated with it. Some of these pathways are also intricately related with the underlying pathogenesis of cardioembolic stroke. The generation of blood clot in cardioembolic stroke is generally by coagulation of stagnant pool of blood which is often due to cardiac ailment, explaining the dysregulation in complement and coagulation cascades and dilated cardiomyopathy [16, 273]. Atrial fibrillation is one of the important cause of cardioembolic stroke [16]. The structure of the heart undergoes remodelling during atrial fibrillation and these involve changes adherens junction and gap junction [274]. Thus, these 14 cardioembolic specific miRNAs (miR-19a, -130b*, -181a-2*, -198, -200b, -208a, -412, -525-5p, -550, -617, -618, -630, -668 and -1321; Table 7.1) could possibly reflect the underlying mechanism for cardioembolic stroke pathogenesis.

As for small vessel stroke, the pathogenesis is similar to that of large artery stroke. However, the small vessel stroke associated biological pathways (amino sugar and nucleotide sugar metabolism, chemokine signaling pathway,

glycerolipid metabolism, PPAR signaling pathway, TGF-beta signaling pathway and VEGF signaling pathway) showed novel dysregulated processes in small vessel stroke pathogenesis. The implications of these novel processes need to be elucidated to further the understanding in small vessel stroke pathogenesis.

### 7.5 Ischemic stroke specific miRNAs

In this study, the miRNA profiles of ischemic stroke patients with and without risk factors and 27 miRNAs (let-7d*, miR-29b-2*, -32*, -125b-2*, -146b-3p, -196a*, -200b*, -302c*, -320b, -320c, -331-5p, -374b*, -423-3p, -423-5p, -488, -494, -498, -576-3p, -585, -659, -668, -923, -934, -943, -1255a, -1299 and -1321) were identified as ischemic stroke specific miRNAs that showed similar expression pattern in ischemic stroke patients with and without risk factors. Among these 27 miRNAs, miR-494 has validated targets which are relevant to the pathology of ischemic stroke. miR-494 targets anti-apoptosis genes leukemia inhibitory factor (LIF) and fibroblast growth factor receptor 2 (FGFR2) [275]. miR-494 was detected to be up-regulated in all ischemic stroke samples, which signifies increased apoptosis in the patients due to the down-regulation of LIF and FGFR2. In addition, 7 of the 27 miRNAs (let-7d*, miR-125b-2*, -320b, -423-3p, -488, -1299 and -1321) were previously reported by Sepramaniam *et al* [197] as ischemic stroke specific miRNAs. From these observation, the above 27 miRNAs could be markers for ischemic stroke.

From previous reports, only Tan et al [190] and Jickling et al [198] have reported on pathways associated with ischemic stroke. Comparing the 27 ischemic stroke specific miRNAs with data from Tan et al [190] and Jickling et al [198], miR-320 was found to be involved in angiogenesis, metabolic process regulation and hypoxia regulation [190]. While searching through literature, the following miRNAs were found to be associated with known pathways: miR-488 was found to be associated with Corticotropin Releasing Hormone (CRH) Signaling [276], miR-494 is associated with PI3K/Akt pathway [277]; miR-659 is associated with focal adhesion pathway [278]; miR -1255a is associated with aging [279]. These pathways are related with ischemic stroke pathophysiology, demonstrating the relevance of these 27 ischemic stroke specific miRNAs.

### 7.6 miRNA profiles of rats subjected to MCAo by suture method

The miRNAs reported in several of the previously published reports were found to have similar expression patterns to those identified in this study.

In the rat MCAo model, miR-320 has been found to be up-regulated in early time-points (12, 24 and 48 hours) which coincided with high infarct volume. This is consistent with report that treatment with anti-miR-320 can reduce infarct volume [280]. miR-223 has been shown to target glutamate receptor subunits GluR2 and NR2B and proven to be neuroprotective [281]. In line with this report, miR-223 has been found to be down-regulated at 12 and 24 hours with a corresponding increase in infarct volume. Another miRNA, miR-181c which was down-regulated in all time-points, has been demonstrated to

target tumor necrosis factor α (TNF-α) that regulates microglial-mediated cell death [282]. This is in agreement with previous reported findings that TNF-α is increased upon ischemia. Furthermore, the down-regulated miR-21 seen in our miRNA profile also suggested an increased in microglial-mediated cell death, as miR-21 targets Fas ligand (FasL) which is part of death receptor induced cell death [283]. Interestingly, neuroprotective miR-124 was found to be down-regulated throughout our miRNA profile, as reported by several workers [284-287]. The miR-29 isoforms (miR-29a, -29b and 29c) that were previously reported [288-290] to be down-regulated during cerebral ischemia, were also found to be down-regulated in this study. In the case of miR-139-5p that was found to be down-regulated in this study, it was reported that miR-139-5p down-regulation during hypoxia-ischemia up-regulates human growth transformation dependent protein (HGTD-P), promoting neuronal apoptosis [291]. miR-376b-5p was demonstrated to be down-regulated after ischemia and is also in line with current literature [292]. Similarly for miR-375 which was down-regulated in the miRNA profile, had also been reported to be down-regulated during ischemia/reperfusion [293].

From the above data, it is evident that the miRNA profile in this study is consistent with the previously reported findings from various laboratories. Furthermore, this study also identified other miRNAs that were not reported in literature which may be of use in advancing the knowledge about ischemic stroke.

### 7.7 miRNAs correlating with infarct volume

Four miRNAs (miR-21*, -206, -291a-5p and -300-5p) were demonstrated to positively correlate with infarct volume. Among which, miR-206 showed the strongest correlation. However, miR-206 expression was found to be down-regulated during 12 hours time-point in suture model while it was up-regulated in the embolic model. This could be due to the difference in the extent of ischemia, where suture model is a transient ischemic model with reperfusion after 1 hour of occlusion while embolic is a permanent ischemic model without reperfusion. The time of ischemic insult differed between the models. Hence, the initial down-regulation of miR-206 at 12 hours in suture model could be due to a potential rescue mechanism which was more evident in the transient ischemic stroke model.

Some of the known targets of miR-206 may explain the possible mechanism of miR-206 correlating with infarct volume. miR-206 had been proven to target anti-apoptotic gene, *Notch3* and insulin-like growth factor 2 (*Igf1*) [294, 295]. Thus, the up-regulation of miR-206 corresponded with a decrease in *Notch3* and *Igf1* which resulted in increased cell death corresponding to infarct volume. In addition, miR-206 also targets brain-derived neurotrophic factor (*Bdnf*) which had been proven to reduce infarct volume [296-298]. Therefore, up-regulation of miR-206 repressed the neuroprotective *Bdnf* which led to increase cell death and greater infarct volume. These evidence showed that miR-206 could potentially be a predictor for severity of ischemic stroke while the other 3 miRNAs (miR-21*, -291a-5p and -300-5p) may be useful as predictors for severity.

### 7.8 miRNAs with biphasic expression pattern

Four miRNAs (miR-10b, -217, -326 and -881) were highlighted to have biphasic expression during cerebral ischemia, where their expression peaked at 24 hours and decreased till 72 hours and then increased at 120 hours followed by decreased expression. It was reported that inflammation played a biphasic role during ischemic stroke [299]. It was without surprise that 2 miRNAs (miR-10b and -326) have known targets associated with inflammation. Transfection of anti-miR-10b has been reported to reduction in matrix metalloproteinase 2 and 9 (*MMP2* and *MMP9*) expression [300]. miR-326 had been reported to promote differentiation of interleukin 17 producing T helper cells (TH-17 cells), hence it was found to be increased during ischemic stroke [301, 302]. Thus, miR-10b and -326 up-regulation corresponded to an increase in *MMP2*, *MMP9* and TH-17 cells at 24 and 120 hours, denoting a biphasic inflammatory response, agreeing with current reports.

This biphasic inflammation has been speculated to play dual role in the pathophysiology of ischemic stroke, where the initial inflammatory response could be viewed as detrimental, while inflammation in the late phase was seen as beneficial for recovery [299]. In this case, anti-miRNAs can be administered during the acute phase of ischemic stroke to ameliorate the detrimental effects of inflammation while miRNA mimics can be applied during the late recovery phase to enhance inflammation to promote recovery.

### 7.9 Biological pathways in ischemic stroke

Five key processes namely: inflammation, cell death, neuron signaling and development, metabolism and vascular maintenance, have been previously described in ischemic stroke pathophysiology [303-307]. Biological pathways related to these processes were identified in the pathway analysis in patients and animal model. Among these processes, inflammation, cell death and vascular maintenance were the only processes that were detected in ischemic stroke patients as well as animal models (Table 7.2). To a certain extent, majority of the biological pathways associated with neuron signaling and development were also common between patients and animal models. It can be inferred from this observation that these 4 processes (inflammation, cell death, vascular maintenance and neuron signaling and development) are likely to respond to ischemic stroke in a similar manner in both patients and animal model. While in the case of metabolism, there were only three biological pathways (Amino sugar and nucleotide sugar metabolism, glycerophospholipid metabolism and Purine metabolism) associated with metabolism that were commonly detected in patients and animal model. Among all the biological pathways, Chemokine signaling pathway was highly ranked in both patients (ranked $6^{th}$) and animal model (ranked $4^{th}$). This was within expectation as chemokines are crucial modulators of inflammation. Some of the chemokines hav been reported to be potential markers for ischemic stroke [233, 234]. Therefore, by studying the mechanism of actions of chemokines in ischemic stroke, there can be better understanding of the underlying mechanism in ischemic stroke pathophysiology.

**Table 7.2:** Biological pathways associated with known processes (inflammation, cell death, neuron signaling and development, metabolism and vascular maintenance) involved in ischemic stroke

| **Biological Pathway** | **Human** | **Rat** |
|---|---|---|
| **Inflammation** | | |
| B cell receptor signaling pathway | ✓ | ✓ |
| Chemokine signaling pathway | ✓ | ✓ |
| Complement and coagulation cascades | ✓ | ✓ |
| Cytokine-cytokine receptor interaction | ✓ | ✓ |
| Leukocyte transendothelial migration | ✓ | ✓ |
| T cell receptor signaling pathway | ✓ | ✓ |
| **Cell Death** | | |
| Natural killer cell mediated cytotoxicity | ✓ | ✓ |
| p53 signaling pathway | ✓ | ✓ |
| **Neuron signaling and development** | | |
| Axon guidance | ✓ | |
| Glutamatergic synapse | ✓ | ✓ |
| Long-term depression | ✓ | ✓ |
| Long-term potentiation | ✓ | ✓ |
| Neuroactive ligand-receptor interaction | ✓ | ✓ |
| Neurotrophin signaling pathway | ✓ | ✓ |
| **Vascular maintenance** | | |
| Adherens junction | ✓ | ✓ |
| Cell adhesion molecules (CAMs) | ✓ | ✓ |
| Focal adhesion | ✓ | ✓ |
| Gap junction | ✓ | ✓ |
| Tight junction | ✓ | ✓ |
| VEGF signaling pathway | ✓ | ✓ |
| **Metabolism** | | |
| Alanine, aspartate and glutamate metabolism | | ✓ |
| Amino sugar and nucleotide sugar metabolism | ✓ | ✓ |
| D-Glutamine and D-glutamate metabolism | | ✓ |
| Ether lipid metabolism | | ✓ |
| Fructose and mannose metabolism | ✓ | |
| Galactose metabolism | ✓ | |
| Glycerophospholipid metabolism | ✓ | ✓ |
| Glycine, serine and threonine metabolism | | ✓ |
| Glycolysis / Gluconeogenesis | | ✓ |
| Inositol phosphate metabolism | ✓ | |
| Nicotinate and nicotinamide metabolism | | ✓ |
| Phenylalanine metabolism | | ✓ |
| Purine metabolism | ✓ | ✓ |
| Pyrimidine metabolism | ✓ | |
| Sphingolipid metabolism | ✓ | |
| Tryptophan metabolism | | ✓ |
| Tyrosine metabolism | | ✓ |

Knowing the pathways involved in ischemic stroke, it would be useful to compare the difference between ischemic stroke and haemorrhagic stroke. In order to compare the mechanism is ischemic stroke with haemorrhagic stroke, data-mining was performed for the haemorrhagic stroke specific miRNAs in rat models reported by Liu *et al* [192]. 25 miRNAs were identified specific for haemorrhagic stroke and used for pathway analysis. The biological pathways in ischemic stroke rat animal models were compared with haemorrhagic stroke rat animal models. There were 9 biological pathways (Alanine, aspartate and glutamate metabolism, Arachidonic acid metabolism, Arginine and proline metabolism, beta-Alanine metabolism, D-Glutamine and D-glutamate metabolism, Glycolysis / Gluconeogenesis, Nicotinate and nicotinamide metabolism, Phenylalanine metabolism and Tryptophan metabolism) detected only in ischemic rat and 13 biological pathways (Adipocytokine signaling pathway, Arrhythmogenic right ventricular cardiomyopathy (ARVC), Axon guidance, Dilated cardiomyopathy, ECM-receptor interaction, Hedgehog signaling pathway, Hypertrophic cardiomyopathy (HCM), Inositol phosphate metabolism, Notch signaling pathway, Pyrimidine metabolism, Toll-like receptor signaling pathway, Ubiquitin mediated proteolysis and Vasopressin-regulated water reabsorption) detected in haemorrhagic rat (Table 7.3). There were 7 biological pathways (B cell receptor signaling pathway, Cell adhesion molecules (CAMs), Complement and coagulation cascades, ErbB signaling pathway, Ether lipid metabolism, Purine metabolism and T cell receptor signaling pathway) that showed different ranking between ischemic and haemorrhagic stroke models (Table 7.3). Among these, 3 biological pathways (B cell receptor signaling pathway, Purine metabolism and T cell receptor

signaling pathway) showed higher ranking in haemorrhagic stroke model while the remaining 4 (Cell adhesion molecules (CAMs), Complement and coagulation cascades, ErbB signaling pathway and Ether lipid metabolism) showed higher ranking in ischemic stroke model (Table 7.3). These dysregulated molecular pathways are currently uncharacterized in ischemic and haemorrhagic strokes. They are crucial for understanding the molecular mechanisms and need to be further investigated.

**Table 7.3:** Biological pathways distinct for ischemic stroke and hemorrhagic stroke.

| Biological pathway | Rank | |
|---|---|---|
| | Ischemic stroke | Haemorrhagic stroke |
| Adipocytokine signaling pathway | - | 65 |
| Alanine, aspartate and glutamate metabolism | 24 | - |
| Arachidonic acid metabolism | 75 | - |
| Arginine and proline metabolism | 22 | - |
| Arrhythmogenic right ventricular cardiomyopathy (ARVC) | - | 31 |
| Axon guidance | - | 5 |
| B cell receptor signaling pathway | 92 | 43 |
| beta-Alanine metabolism | 43 | - |
| Cell adhesion molecules (CAMs) | 12 | 87 |
| Complement and coagulation cascades | 56 | 96 |
| D-Glutamine and D-glutamate metabolism | 46 | - |
| Dilated cardiomyopathy | - | 27 |
| ECM-receptor interaction | - | 72 |
| ErbB signaling pathway | 26 | 99 |
| Ether lipid metabolism | 50 | 98 |
| Glycolysis / Gluconeogenesis | 95 | - |
| Hedgehog signaling pathway | - | 76 |
| Hypertrophic cardiomyopathy (HCM) | - | 37 |
| Inositol phosphate metabolism | - | 74 |
| Nicotinate and nicotinamide metabolism | 85 | - |
| Notch signaling pathway | - | 47 |
| Phenylalanine metabolism | 67 | - |
| Purine metabolism | 91 | 38 |
| Pyrimidine metabolism | - | 64 |
| T cell receptor signaling pathway | 68 | 19 |
| Toll-like receptor signaling pathway | - | 48 |
| Tryptophan metabolism | 47 | - |
| Ubiquitin mediated proteolysis | - | 6 |
| Vasopressin-regulated water reabsorption | - | 54 |

### 7.10 Implication of *CD46* in stroke subtype

*CD46* mRNA expression was found to be higher expression in large artery and small vessel stroke as compared with cardioembolic stroke. This observation was due to difference in the etiology between the stroke subtypes as large artery and small vessel strokes are caused by the rupture of atherosclerotic plaque while cardioembolic stroke is caused by the formation of blood clot in the ailing heart. Complement has been known to participate in atherogenesis. Furthermore, complement inhibitors have been reported to be present in atherosclerotic lesions and CD46 protein was shown to be increased in *in vitro* model of endothelial cells undergoing atherogenesis [308, 309]. Thus, it was observed that *CD46* mRNA level was higher in large artery and small vessel stroke.

In this study, 4 miRNAs (miR-19a, -20a, -185 and -374b) were demonstrated to target *CD46*. miR-19a was also among the cluster of 14 miRNAs that were specific for cardioembolic stroke and able to distinguish between individual stroke subtypes. These 4 miRNAs could potentially be diagnostic markers for cardioembolic stroke. To further investigate how these 4 miRNAs relate with the underlying pathogenesis of cardioembolic stroke, *in silico* prediction was performed to identify other gene targets (Table 7.4) in the biological pathway, Complement and coagulation cascades. The prediction was performed in a similar manner as described in previous chapters. The prediction showed interesting results. These 4 miRNAs targeted multiple regulators within the biological pathway, complement and coagulation cascades. This signifies that these 4 miRNAs could potentially act on the pathway to bring about a net effect seen only in cardioembolic stroke which requires further investigation.

**Table 7.4:** Predicted targets of miR-19a, -20a, -185 and -374b in biological pathway, Complement and coagulation cascades. *AT3*: Anti-thrombin III. *CD46*: Cluster of differentiation 46. *CD55*: Cluster of differentiation 55. *F5*: Factor V. *F7*: Factor VII. *F8*: Factor VIII. *F11*: Factor XI. *F13*: Factor XIII. *PAI-1*: Plasminogen activator inhibitor-1. *PAI-2*: Plasminogen activator inhibitor-2. *PLAT*: tissue plasminogen activator. *PLAU*: urokinase-type plasminogen activator. *TF*: Tissue factor. *TFPI*: Tissue factor pathway inhibitor.

| Hsa-miRNA | Predicted targets |
|---|---|
| miR-19a | *AT3*, *CD46*, *CD55*, *F5*, *F13*, *PAI-1*, *TF*, *TFPI* and *PLAU* |
| miR-20a | *CD46* and *PAI-1* |
| miR-185 | *CD46*, *F7*, *F8*, *F11*, *F13* and *PLAT* |
| miR-374b | *CD46*, *CD55*, *F5*, *PAI-2* and *TFPI* |

### 7.11 Role of *CCL2* in ischemic stroke

In this study, CCL2 protein level in serum was examined in human ischemic stroke patients as well as in rats subjected to MCAo. The results showed that in rats CCL2 protein level as well as *Ccl2* mRNA level was highest at 24 hours corresponding to maximum infarct volume, while in ischemic stroke patients, CCL2 protein level was found to be at higher level in patients with good outcome (mRS < 2) as compared with patients with poor outcome (mRS ≥ 2). This could possibly suggest that *Ccl2* level was high at infarct volume in response to ischemic injury and to rescue the cells in the infarct region. This in turn was able to correlate with the observation that CCL2 level being higher in patients with good outcome.

Furthermore, some had reported CCL2 to be beneficial during ischemic stroke [235-237], Stowe *et al* [235] demonstrated that hypoxic pre-conditioning only protected wildtype mice while CCL2-null mice were not conferred the same protection, which suggests that CCL2 expression during ischemic stroke could be beneficial. In addition, Yan *et al* [236] showed that CCL2 was crucial in neuroblast migration from the subventricular zone to the penumbra after cerebral ischemia and CCL2 was also found to be on blood vessels undergoing angiogenesis after cerebral ischemia, suggesting CCL2 to have pro-angiogenic properties [237]. Thus, CCL2 could possibly be beneficial during ischemic stroke and anti-miRNAs can be used to up-regulate CCL2 in patients in order to bring about a good outcome.

### 7.12 Limitation of study

This study is limited by the number of ischemic stroke samples obtained. The findings from this study needs to be validated in a larger cohort of patients. Furthermore, there was limited study into the selected pathways. There is a need for an in-depth study on how the dysregulated miRNAs affect the biological pathways, including its inner workings in an in vivo model. There was also a lack of a functional study to determine how regulating deregulating miRNAs using miRNA inhibitors and mimics has any therapeutic effect.

In addition, there was a lack of investigation into the relation between miRNA and outcome of patients. This is aspect of study can provide information about the mechanism of ischemic stroke progression and identify potential marker to prognosticating outcome of patients

### 7.13 Potential application of miRNAs in clinical setting

The results from this study demonstrated 4 miRNAs (miR-19a, -20a, -185 and -374b) were differentially expressed in cardioembolic stroke as compared with other stroke subtypes. These 4 miRNAs could be potential diagnostic biomarkers for cardioembolic stroke. It would be beneficial to have a diagnostic biomarker for cardioembolic stroke as it is the stroke subtype which has the highest portion of mortality and morbidity, and the early treatment of these patients can promote good outcome [16, 17].

Blood miRNAs are stable markers in circulation and can be assayed readily. These biomarkers could be used in diagnosing cardioembolic stroke patients by measuring the levels of these miRNAs using point of care or bedside

testing PCR which are mainly based on fluidic chip platforms. These miRNAs can be used in combination with various other potential markers of cardioembolic stroke such as brain natriuretic peptide (BNP) or *CD46* mRNA to enhance the accuracy of diagnosis, which needs further fine-tuning. Furthermore, the time taken to assay for miRNA expression is merely a few hours as compared with traditional blood biochemical test which takes a day to perform. There has been some success in a point of care PCR being used for influenza A diagnosis, which is a microfluidic chip-based real-time PCR [310]. A similar fluidic chip may be developed with a specific panel of miRNAs for cardioembolic stroke diagnosis.

In addition to being markers for disease, miRNAs can also be potential therapeutic targets. Anti-miRNAs or miRNA mimics may be delivered to the patients to regulate the expression of the miRNA to bring about good outcome in the patients. Chemical modifications have been made to increase stability of the oligonucleotides, among which locked nucleic acid (LNA™) has been widely cited [311]. The delivery system for miRNA therapy has been thoroughly investigated. There have been many different types of delivery systems of which liposomes have been used widely in pre-clinical and clinical trials [312]. Currently, there are 2 clinical trials involving miRNAs that are ongoing. Miravirsen developed by Santaris Pharma to treat Hepatitis C by inhibiting miR-122, and mRX34 developed miRNA Therapeutics as a miRNA replacement therapy for liver cancer [313-316]. Hence, in the case of CCL2, anti-miRNAs could be utilized to target miRNAs targeting CCL2 to increase CCL2 expression to bring about good outcome in patients.

### 7.14 Future work

In this study, the crucial molecular processes in ischemic stroke that are common between experimental and clinical samples were identified. Neuroinflammation was the process selected for further study. Complement cascade and chemokine signaling were studied in detail as they were shown to be the most relevant in cardioembolic stroke pathogenesis and ischemic stroke pathophysiology. Other inflammatory processes highlighted such as cell-mediated inflammation mediated by B-cells and T-cells, and also cytokine signaling, should also be investigated. Inflammation also has a much greater impact on ischemic stroke as it is also involved in the pathogenesis of various stroke subtypes. This is worth researching on as it may identify potential diagnostic biomarkers for stroke subtypes.

This study also highlighted clusters of miRNAs which were associated with the respective stroke subtypes. These clusters of miRNAs should be validated on another cohort of ischemic stroke patients to verify the validity. These miRNAs have been shown through pathway analysis to be involved in processes critical to the etiology of each subtype. The mechanisms of these miRNA should be researched upon as this could add new knowledge onto the current understanding of the etiology of stroke subtype.

Coagulation and complement cascade was identified as a biological pathway associated with cardioembolic stroke etiology and 4 miRNAs (miR-19a, -20a, -185 and -374b) have been demonstrated to target *CD46*, a regulator of complement activation. Further *in silico* prediction showed that these 4 miRNAs could potentially target other genes within this biological pathway. The regulation of these other genes (*AT3*, *CD46*, *CD55*, *F5*, *F7*, *F8*, *F11*, *F13*, *PAI-1*, *PAI-2*, *TF*, *TFPI*, *PLAT* and *PLAU*; Table 7.3) by these 4 miRNAs

should be inquired upon, to better understand how the regulation of coagulation and complement cascade differ between cardioembolic stroke and non cardioembolic stroke.

In this study, chemokine signaling pathway was determined to be a crucial biological pathway in ischemic stroke pathophysiology by pathway analysis and literature search. *CCL2* was selected as an important gene in ischemic stroke which was determined by measuring its protein and mRNA level in animal model and ischemic stroke patients. Though *CCL2* seems to have a contradictory role in ischemic stroke, which was also shown in the results, there is still a need to be resolved the possible detrimental or beneficial role that *CCL2* is playing. With the 3'UTR of *CCL2* and *Ccl2* subcloned in pMIR-REPORT™ luciferase vector, all that is needed is to identify miRNAs that target *CCL2* and *Ccl2* and demonstrate the targeting using luciferase assay. These miRNAs can be used to regulate *CCL2* and *Ccl2* by anti-miRNA and miRNA mimic transfection in experiments such as oxygen-glucose deprivation in SY5Y cells for human *in vitro* study and rat subjected to MCAo for animal *in vivo* study. By experimentally testing the function of *CCL2*, the therapeutic use of *CCL2* and miRNAs targeting *CCL2* can be determined.

There have been miRNAs associated with infarct volumes. The next step will be to conduct an in-depth analysis into the expression of miRNAs with can correlate with infarct volume at different time-points. However, this will require generation of more animal models at different time-points. This can provide more clarity on the processes critical for determining infarct volume.

There is a need to identify miRNAs correlating with outcome. Profiling of miRNAs according to functional outcome is needed. Once these miRNAs are identified, they can be compared with the stroke subtype specific miRNAs to investigate any miRNAs are specific for small vessel stroke and associated with good outcome as these miRNAs can possibly explain the higher proportion of good outcome in small vessel stroke.

### 7.15 Conclusion

In this study, miRNA profiles from ischemic stroke patients with and without risk factors were compared. 27 miRNAs (let-7d*, miR-29b-2*, -32*, -125b-2*, -146b-3p, -196a*, -200b*, -302c*, -320b, -320c, -331-5p, -374b*, -423-3p, -423-5p, -488, -494, -498, -576-3p, -585, -659, -668, -923, -934, -943, -1255a, -1299 and -1321) have been found to be specific for ischemic stroke. Among these miRNAs, there are 7 miRNAs (let-7d*, miR-125b-2*, -320b, -423-3p, -488, -1299 and -1321) that have been previously reported as ischemic stroke specific miRNAs [197]. This denotes that this cluster of miRNAs could potentially be markers for ischemic stroke and are worth further investigation.

In addition, stroke subtype specific miRNAs were also highlighted where there were 10 large artery stroke specific miRNAs (miR-27a*, -129-5p, -382, -585, -602, -637, -659, -744, -1184 and -1261), 14 cardioembolic stroke specific miRNAs (miR-19a, -130b*, -181a-2*, -198, -200b, -208a, -412, -525-5p, -550, -617, -618, -630, -668 and -1321) and 141 small vessel stroke specific miRNAs. Pathway analysis of these miRNAs revealed that the biological pathways regulated by each group of miRNAs were relevant to the etiology of the stroke subtype. Furthermore, some of the miRNAs have

validated targets associated with the pathogenesis of the stroke subtype as well, suggesting that these 3 groups of miRNAs were specific for each stroke subtype and could be utilized for further studies to better understand the mechanism for the pathogenesis of each stroke subtype. Furthermore, among these miRNAs, there were 8 miRNAs (miR-19a, -129-5p, -198, -320b, -320d, -331-3p, -637 and -744) that could segregate samples into various stroke subtypes, and 3 of them (miR-320b, -320d and -331-5p) had been reported previously [197]. This panel of 8 miRNAs could be exploited for the diagnosis of stroke subtypes in patients.

In comparison with the animal study, common biological pathways between patients and animal models were identified. Based on the pathway analysis, neuroinflammation was determined to be a critical process in the pathophysiology of ischemic stroke and it was also differentially regulated in different stroke subtype. 4 miRNAs (miR-19a, -20a, -185 and -374b) were demonstrated to target *CD46*, a potential biomarker for cardioembolic stroke. Thus, these 4 miRNAs can potentially form a panel of diagnostic biomarker for diagnosis of cardioembolic stroke. This requires further evaluations before being recommended as a panel to be used in differentiating clinical samples.

*Ccl2* was shown to be correlated with infarct volume in animal experiments while in human patients, serum CCL2 level seems to correlate positively with outcome of patients. The ambiguous role of *CCL2* in ischemic stroke needs to be clarified and possibly through the use of miRNAs. Regardless of the role *CCL2* being detrimental or beneficial, *CCL2* and miRNAs targeting *CCL2* still serve as an attractive therapeutic target for ischemic stroke.

## References


1. Truelsen T, Begg S, Mathers, C. The global burden of cerebrovascular disease. Global Burden of Diseases 2006 update. *World Health Organization.* 2006.
2. World Health Organization. The Global Burden of Diseases, 2004 update. 2008
3. Strong K, Mathers C, Bonita R. Preventing stroke: saving lives around the world. *Lancet Neurol*. 2007, **6**(2):182-187.
4. Go AS, Mozaffarian D, Roger VL, Benjamin EJ, Berry JD, Blaha MJ, Dai S, Ford ES, Fox CS, Franco S, Fullerton HJ, Gillespie C, Hailpern SM, Heit JA, Howard VJ, Huffman MD, Judd SE, Kissela BM, Kittner SJ, Lackland DT, Lichtman JH, Lisabeth LD, Mackey RH, Magid DJ, Marcus GM, Marelli A, Matchar DB, McGuire DK, Mohler ER 3rd, Moy CS, Mussolino ME, Neumar RW, Nichol G, Pandey DK, Paynter NP, Reeves MJ, Sorlie PD, Stein J, Towfighi A, Turan TN, Virani SS, Wong ND, Woo D, Turner MB; American Heart Association Statistics Committee and Stroke Statistics Subcommittee. Heart disease and stroke statistics--2014 update: a report from the american heart association. *Circulation*. 2014, **129**(3):e28-e292. doi: 10.1161/01.cir.0000441139.02102.80.
5. Hatano S. Experience from a multicentre stroke register: a preliminary report. *Bull World Health Organ*. 1976, **54**(5): 541–553.
6. Burke TA, Venketasubramanian RN. The epidemiology of stroke in the East Asian region: a literature-based review. *Int J Stroke*. 2006, **1**:208-215.
7. Sudlow CL, Warlow CP. Comparable studies of the incidence of stroke and its pathological types: results from an international collaboration. International Stroke Incidence Collaboration. *Stroke*. 1997, **28**:491-499.
8. Adams HP Jr, Bendixen BH, Kappelle LJ, Biller J, Love BB, Gordon DL, Marsh EE 3rd. Classification of subtype of acute ischemic stroke. Definitions for use in a multicenter clinical trial. TOAST. Trial of Org 10172 in Acute Stroke Treatment. *Stroke*. 1993, **24**(1):35-41.
9. Caplan LR. (2009) Caplan's Stroke: A Clinical Approach (Fourth Edition) ISBN: 978-1-4160-4721-6
10. Amarenco P, Bogousslavsky J, Caplan LR, Donnan GA, Hennerici MG. Classification of stroke subtypes. *Cerebrovasc Dis*. 2009, **27**(5):493-501. doi: 10.1159/000210432.
11. Ogata J, Yamanishi H, Ishibashi-Ueda H. Review: role of cerebral vessels in ischaemic injury of the brain. *Neuropathol Appl Neurobiol*. 2011, **37**(1):40-55. doi: 10.1111/j.1365-2990.2010.01141.x.
12. Weissberg PL. Atherogenesis: current understanding of the causes of atheroma. *Heart*. 2000, **83**(2):247-252.
13. Steinberg D. Atherogenesis in perspective: hypercholesterolemia and inflammation as partners in crime. *Nat Med*. 2002, **8**(11):1211-1217.
14. Hansson GK, Robertson AK, Söderberg-Nauclér C. Inflammation and atherosclerosis. *Annu Rev Pathol*. 2006, **1**:297-329.

15. Mohammad Y, Qattan M, Prabhakaran S. Epidemiology and pathophysiology of intracranial large artery stenosis. *The Open Atherosclerosis & Thrombosis Journal*. 2010, **3**: 3-7.
16. Arboix A, Alió J. Cardioembolic stroke: clinical features, specific cardiac disorders and prognosis. *Curr Cardiol Rev*. 2010, **6**(3):150-161. doi: 10.2174/157340310791658730.
17. Ferro JM. Cardioembolic stroke: an update. *Lancet Neurol*. 2003, **2**(3):177-188.
18. Munger TM, Wu LQ, Shen WK. Atrial fibrillation. *J Biomed Res*. 2014, **28**(1):1-17. doi: 10.7555/JBR.28.20130191.
19. Weir NU. An update on cardioembolic stroke. *Postgrad Med J* 2008, **84**: 133-142.
20. Valensi P, Lorgis L, Cottin Y. Prevalence, incidence, predictive factors and prognosis of silent myocardial infarction: a review of the literature. *Arch Cardiovasc Dis*. 2011, **104**(3):178-188. doi: 10.1016/j.acvd.2010.11.013.
21. Martino TA, Liu P, Sole MJ. Viral infection and the pathogenesis of dilated cardiomyopathy. *Circ Res*. 1994, **74**(2):182-188.
22. Carabello BA. Modern management of mitral stenosis. *Circulation*. 2005, **112**(3):432-437.
23. Tan KS, Tan CT, Churilov L, MacKay MT, Donnan GA. Ischaemic stroke in young adults: A comparative study between Malaysia and Australia. *Neurol. Asia* 2010, **15:**1–9.
24. Carretero OA, Oparil S. Essential hypertension. Part I: definition and etiology. *Circulation*. 2000, **101**: 329-335.
25. Park JB, Schiffrin EL. Effects of antihypertensive therapy on hypertensive vascular disease. *Curr Hypertens Rep*. 2000, **2**(3):280-288.
26. Schlaich MP, Parnell MM, Ahlers BA, Finch S, Marshall T, Zhang WZ, Kaye DM. Impaired L-arginine transport and endothelial function in hypertensive and genetically predisposed normotensive subjects. *Circulation*. 2004, **110**: 3680–3686.
27. DeSouza CA, Dengel DR, Macko RF, Cox K, Seals DR. Elevated levels of circulating cell adhesion molecules in uncomplicated essential hypertension. *Am J Hypertens*. 1997, **10**(12 Pt 1):1335-1341.
28. Psaty BM, Manolio TA, Kuller LH, Kronmal RA, Cushman M, Fried LP, White R, Furberg CD, Rautaharju PM. Incidence of and risk factors for atrial fibrillation in older adults. *Circulation*. 1997, **96**(7):2455-2461.
29. Kannel WB, Wolf PA, Benjamin EJ, Levy D. Prevalence, incidence, prognosis, and predisposing conditions for atrial fibrillation: population-based estimates. *Am J Cardiol*. 1998, **82**(8A):2N-9N.
30. Gerdts E, Oikarinen L, Palmieri V, Otterstad JE, Wachtell K, Boman K, Dahlöf B, Devereux RB; Losartan Intervention For Endpoint Reduction in Hypertension (LIFE) Study. Correlates of left atrial size in hypertensive patients with left ventricular hypertrophy: the Losartan Intervention For Endpoint Reduction in Hypertension (LIFE) Study. *Hypertension*. 2002, **39**(3):739-743.

31. Barbier P, Alioto G, Guazzi MD. Left atrial function and ventricular filling in hypertensive patients with paroxysmal atrial fibrillation. *J Am Coll Cardiol*. 1994, **24**(1):165-170.
32. Madu EC, Baugh DS, Gbadebo TD, Dhala A, Cardoso S; Phi-Res Multi-Study Group. Effect of ethnicity and hypertension on atrial conduction: evaluation with high-resolution P-wave signal averaging. *Clin Cardiol*. 2001, **24**(9):597-602.
33. Expert Panel on Detection, Evaluation, and Treatment of High Blood Cholesterol in Adults. Executive Summary of The Third Report of The National Cholesterol Education Program (NCEP) Expert Panel on Detection, Evaluation, And Treatment of High Blood Cholesterol In Adults (Adult Treatment Panel III). *JAMA*. 2001, **285**(19):2486-2497.
34. Camejo G, Hurt-Camejo E, Wiklund O, Bondjers G. Association of apo B lipoproteins with arterial proteoglycans: pathological significance and molecular basis. *Atherosclerosis*. 1998, **139**(2):205-222.
35. Skålén K, Gustafsson M, Rydberg EK, Hultén LM, Wiklund O, Innerarity TL, Borén J. Subendothelial retention of atherogenic lipoproteins in early atherosclerosis. *Nature*. 2002, **417**(6890):750-754.
36. Berliner J. Introduction. Lipid oxidation products and atherosclerosis. *Vascul Pharmacol*. 2002, **38**(4):187-191.
37. Leitinger N. Oxidized phospholipids as modulators of inflammation in atherosclerosis. *Curr Opin Lipidol*. 2003, **14**(5):421-430.
38. Subbanagounder G, Wong JW, Lee H, Faull KF, Miller E, Witztum JL, Berliner JA. Epoxyisoprostane and epoxycyclopentenone phospholipids regulate monocyte chemotactic protein-1 and interleukin-8 synthesis. Formation of these oxidized phospholipids in response to interleukin-1beta. *J Biol Chem*. 2002, **277**(9):7271-7281.
39. Liu W, Yin Y, Zhou Z, He M, Dai Y. OxLDL-induced IL-1 beta secretion promoting foam cells formation was mainly via CD36 mediated ROS production leading to NLRP3 inflammasome activation. *Inflamm Res*. 2014, **63**(1):33-43.
40. Alberti KG, Zimmet PZ. Definition, diagnosis and classification of diabetes mellitus and its complications. Part 1: diagnosis and classification of diabetes mellitus provisional report of a WHO consultation. *Diabet Med*. 1998, **15**: 539-553.
41. Patel P, Macerollo A. Diabetes mellitus: diagnosis and screening. *Am Fam Physician* 2010, **81**: 863-870.
42. Schmidt AM, Hori O, Brett J, Yan SD, Wautier JL, Stern D. Cellular receptors for advanced glycation end products. Implications for induction of oxidant stress and cellular dysfunction in the pathogenesis of vascular lesions. *Arterioscler Thromb*. 1994, **14**(10):1521-1528.
43. Singh R, Barden A, Mori T, Beilin L. Advanced glycation end-products: a review. *Diabetologia*. 2001, **44**(2):129-146.
44. Tanaka S, Avigad G, Brodsky B, Eikenberry EF. Glycation induces expansion of the molecular packing of collagen. *J Mol Biol*. 1988, **203**(2):495-505.
45. Haitoglou CS, Tsilibary EC, Brownlee M, Charonis AS. Altered cellular interactions between endothelial cells and nonenzymatically

glucosylated laminin/type IV collagen. *J Biol Chem*. 1992, **267**(18):12404-12407.
46. Schmidt AM, Vianna M, Gerlach M, Brett J, Ryan J, Kao J, Esposito C, Hegarty H, Hurley W, Clauss M. Isolation and characterization of two binding proteins for advanced glycosylation end products from bovine lung which are present on the endothelial cell surface. *J Biol Chem*. 1992, **267**(21):14987-14997.
47. Neeper M, Schmidt AM, Brett J, Yan SD, Wang F, Pan YC, Elliston K, Stern D, Shaw A. Cloning and expression of a cell surface receptor for advanced glycosylation end products of proteins. *J Biol Chem*. 1992, **267**(21):14998-15004.
48. Yan SD, Schmidt AM, Anderson GM, Zhang J, Brett J, Zou YS, Pinsky D, Stern D. Enhanced cellular oxidant stress by the interaction of advanced glycation end products with their receptors/binding proteins. *J Biol Chem*. 1994, **269**(13):9889-9897.
49. Schiekofer S, Andrassy M, Chen J, Rudofsky G, Schneider J, Wendt T, Stefan N, Humpert P, Fritsche A, Stumvoll M, Schleicher E, Häring HU, Nawroth PP, Bierhaus A. Acute hyperglycemia causes intracellular formation of CML and activation of ras, p42/44 MAPK, and nuclear factor kappaB in PBMCs. *Diabetes*. 2003, **52**(3):621-633.
50. Huttunen HJ, Fages C, Rauvala H. Receptor for advanced glycation end products (RAGE)-mediated neurite outgrowth and activation of NF-kappaB require the cytoplasmic domain of the receptor but different downstream signaling pathways. *J Biol Chem*. 1999, **274**(28):19919-19924.
51. Neumann A, Schinzel R, Palm D, Riederer P, Münch G. High molecular weight hyaluronic acid inhibits advanced glycation endproduct-induced NF-kappaB activation and cytokine expression. *FEBS Lett*. 1999, **453**(3):283-287.
52. Basta G, Schmidt AM, De Caterina R. Advanced glycation end products and vascular inflammation: implications for accelerated atherosclerosis in diabetes. *Cardiovasc Res*. 2004, **63**(4):582-592.
53. Bucala R, Tracey KJ, Cerami A. Advanced glycosylation products quench nitric oxide and mediate defective endothelium-dependent vasodilatation in experimental diabetes. *J Clin Invest*. 1991, **87**(2):432-438.
54. Asahi K, Ichimori K, Nakazawa H, Izuhara Y, Inagi R, Watanabe T, Miyata T, Kurokawa K. Nitric oxide inhibits the formation of advanced glycation end products. *Kidney Int*. 2000, **58**(4):1780-1787.
55. Bierhaus A, Illmer T, Kasper M, Luther T, Quehenberger P, Tritschler H, Wahl P, Ziegler R, Müller M, Nawroth PP. Advanced glycation end product (AGE)-mediated induction of tissue factor in cultured endothelial cells is dependent on RAGE. *Circulation*. 1997, **96**(7):2262-2271.
56. Gawlowski T, Stratmann B, Ruetter R, Buenting CE, Menart B, Weiss J, Vlassara H, Koschinsky T, Tschoepe D. Advanced glycation end products strongly activate platelets. *Eur J Nutr*. 2009, **48**(8):475-481. doi: 10.1007/s00394-009-0038-6.

57. Pop-Busui R. Cardiac autonomic neuropathy in diabetes: a clinical perspective. *Diabetes Care*. 2010, **33**(2):434-441. doi: 10.2337/dc09-1294.
58. Otake H, Suzuki H, Honda T, Maruyama Y. Influences of autonomic nervous system on atrial arrhythmogenic substrates and the incidence of atrial fibrillation in diabetic heart. *Int Heart J*. 2009, **50**(5):627-641.
59. Kato T, Yamashita T, Sekiguchi A, Sagara K, Takamura M, Takata S, Kaneko S, Aizawa T, Fu LT. What are arrhythmogenic substrates in diabetic rat atria? *J Cardiovasc Electrophysiol*. 2006, **17**(8):890-894.
60. Karabag T, Aydin M, Dogan SM, Cetiner MA, Sayin MR, Gudul NE, Kucuk E. Prolonged P wave dispersion in pre-diabetic patients. *Kardiol Pol*. 2011, **69**(6):566-571.
61. Anderson EJ, Kypson AP, Rodriguez E, Anderson CA, Lehr EJ, Neufer PD. Substrate-specific derangements in mitochondrial metabolism and redox balance in the atrium of the type 2 diabetic human heart. *J Am Coll Cardiol*. 2009, **54**(20):1891-1898. doi: 10.1016/j.jacc.2009.07.031.
62. Mitasíková M, Lin H, Soukup T, Imanaga I, Tribulová N. Diabetes and thyroid hormones affect connexin-43 and PKC-epsilon expression in rat heart atria. *Physiol Res*. 2009, **58**(2):211-217.
63. Boudina S, Abel ED. Diabetic cardiomyopathy, causes and effects. *Rev Endocr Metab Disord*. 2010, **11**(1):31-39. doi: 10.1007/s11154-010-9131-7.
64. Astrup J, Siesjö BK, Symon L. Thresholds in cerebral ischemia - The ischemic penumbra. *Stroke*. 1981, **12**: 723-725.
65. Kaufmann AM, Firlik AD, Fukui MB, Wechsler LR, Jungries CA, Yonas H. Ischemic core and penumbra in human stroke. *Stroke*. 1999, **30**(1):93-99.
66. Astrup J, Symon L, Branston NM, Lassen NA. Cortical evoked potential and extracellular K+ and H+ at critical levels of brain ischemia. *Stroke*. 1977, **8**(1):51-57.
67. Ly JV, Zavala JA, Donnan GA. Neuroprotection and thrombolysis: combination therapy in acute ischaemic stroke. *Expert Opin Pharmacother*. 2006, **7**(12):1571-1581.
68. Ginsberg MD. Adventures in the pathophysiology of brain ischemia: penumbra, gene expression, neuroprotection: the 2002 Thomas Willis Lecture. *Stroke*. 2003, **34**(1):214-223.
69. Sheldon AL, Robinson MB. The role of glutamate transporters in neurodegenerative diseases and potential opportunities for intervention. *Neurochem Int*. 2007, **51**(6-7):333-355.
70. Sims NR, Muyderman H. Mitochondria, oxidative metabolism and cell death in stroke. *Biochim Biophys Acta*. 2010, **1802**(1):80-91. doi: 10.1016/j.bbadis.2009.09.003.
71. Susin SA, Zamzami N, Kroemer G. Mitochondria as regulators of apoptosis: doubt no more. *Biochim Biophys Acta*. 1998, **1366**(1-2):151-165.
72. Nicholls DG, Budd SL. Mitochondria and neuronal survival. *Physiol Rev*. 2000, **80**(1):315-360.
73. Cheng YL, Park JS, Manzanero S, Choi Y, Baik SH, Okun E, Gelderblom M, Fann DY, Magnus T, Launikonis BS, Mattson MP,

Sobey CG, Jo DG, Arumugam TV. Evidence that collaboration between HIF-1α and Notch-1 promotes neuronal cell death in ischemic stroke. *Neurobiol Dis*. 2014, **62**:286-295. doi: 10.1016/j.nbd.2013.10.009.

74. Perrotta I, Moraca FM, Sciangula A, Aquila S, Mazzulla S. HIF-1α and VEGF: Immunohistochemical Profile and Possible Function in Human Aortic Valve Stenosis. *Ultrastruct Pathol*. 2015, **8**:1-9.
75. Whyte MK, Walmsley SR. The regulation of pulmonary inflammation by the hypoxia-inducible factor-hydroxylase oxygen-sensing pathway. *Ann Am Thorac Soc*. 2014, **11 Suppl 5**:S271-S276. doi: 10.1513/AnnalsATS.201403-108AW.
76. Patel AR, Ritzel R, McCullough LD, Liu F. Microglia and ischemic stroke: a double-edged sword. *Int J Physiol Pathophysiol Pharmacol*. 2013, **5**(2):73-90.
77. Huang L, Wu ZB, Zhuge Q, Zheng W, Shao B, Wang B, Sun F, Jin K. Glial scar formation occurs in the human brain after ischemic stroke. *Int J Med Sci*. 2014, **11**(4):344-348. doi: 10.7150/ijms.8140.
78. Budd SL. Mechanisms of neuronal damage in brain hypoxia/ischemia: focus on the role of mitochondrial calcium accumulation. *Pharmacol Ther*. 1998, **80**:203-229.
79. Meldrum BS. Glutamate as a neurotransmitter in the brain: review of physiology and pathology. *J Nutr*. 2000, **130**(4S Suppl):1007S-1015S.
80. Ferguson AL, Stone TW. Glutamate-induced depression of EPSP-spike coupling in rat hippocampal CA1 neurons and modulation by adenosine receptors. *Eur J Neurosci*. 2010, **31**(7):1208-1218. doi: 10.1111/j.1460-9568.2010.07157.x.
81. Pizzi M, Fallacara C, Arrighi V, Memo M, Spano P. Attenuation of excitatory amino acid toxicity by metabotropic glutamate receptor agonists and aniracetam in primary cultures of cerebellar granule cells. *J. Neurochem*. 1993, **61**: 683–689.
82. Moriyoshi K, Masu M, Ishii T, Shigemoto R, Mizuno N, Nakanishi S. Molecular cloning and characterization of the rat NMDA receptor. *Nature* 1991, **354**:31–37.
83. Mosbacher J, Schoepfer R, Monyer H, Burnashev N, Seeburg PH, Ruppersberg JP. A molecular determinant for submillisecond desensitization in glutamate receptors. *Science* 1994, **266**:1059–1062.
84. Masu M, Tanabe Y, Tsuchida K, Shigemoto R, Nakanishi S. Sequence and expression of a metabotropic glutamate receptor. *Nature* 1991, **349**:760–765.
85. Bazán NG Jr. Effects of ischemia and electroconvulsive shock on free fatty acid pool in the brain. *Biochim Biophys Acta*. 1970, **218**(1):1-10.
86. Bazán NG. Free arachidonic acid and other lipids in the nervous system during early ischemia and after electroshock. *Adv Exp Med Biol*. 1976, **72**:317-335.
87. Choi DW. Glutamate neurotoxicity and diseases of the nervous system. *Neuron*. 1988, **1**(8):623-634.
88. Seubert P, Larson J, Oliver M, Jung MW, Baudry M, Lynch G. Stimulation of NMDA receptors induces proteolysis of spectrin in hippocampus. *Brain Res*. 1988, **460**(1):189-194.

89. Siman R, Noszek JC. Excitatory amino acids activate calpain I and induce structural protein breakdown in vivo. *Neuron*. 1988, **1**(4):279-287.
90. Bano D, Young KW, Guerin CJ, Lefeuvre R, Rothwell NJ, Naldini L, Rizzuto R, Carafoli E, Nicotera P. Cleavage of the plasma membrane Na+/Ca2+ exchanger in excitotoxicity. *Cell*. 2005, **120**(2):275-285.
91. Nicholls DG. Mitochondria and calcium signaling. *Cell Calcium*. 2005, **38**(3-4):311-317.
92. Schinder AF, Olson EC, Spitzer NC, Montal M. Mitochondrial dysfunction is a primary event in glutamate neurotoxicity. *J Neurosci*. 1996, **16**(19):6125-6133.
93. Beckman JS, Beckman TW, Chen J, Marshall PA, Freeman BA. Apparent hydroxyl radical production by peroxynitrite: implications for endothelial injury from nitric oxide and superoxide. *Proc. Natl. Acad. Sci. U. S. A.* 1990, **87**:1620–1624.
94. Che Y, Wang JF, Shao L, Young T. Oxidative damage to RNA but not DNA in the hippocampus of patients with major mental illness. *J Psychiatry Neurosci*. 2010, **35**(5):296-302. doi: 10.1503/jpn.090083.
95. Nita DA, Nita V, Spulber S, Moldovan M, Popa DP, Zagrean AM, Zagrean L. Oxidative damage following cerebral ischemia depends on reperfusion—A biochemical study in rat. *J. Cell. Mol. Med*. 2001, **5**:163–170.
96. Bretón RR, Rodríguez JCG (2012). Excitotoxicity and Oxidative Stress in Acute Ischemic Stroke, Acute Ischemic Stroke, Prof. Julio Cesar Garcia Rodriguez (Ed.), ISBN: 978-953-307-983-7, InTech, DOI: 10.5772/28300.
97. Okun E, Arumugam TV, Tang SC, Gleichmann M, Albeck M, Sredni B, Mattson MP. The organotellurium compound ammonium trichloro(dioxoethylene-0,0') tellurate enhances neuronal survival and improves functional outcome in an ischemic stroke model in mice. *J Neurochem*. 2007, **102**(4):1232-1241.
98. Nagotani S, Hayashi T, Sato K, Zhang W, Deguchi K, Nagano I, Shoji M, Abe K. Reduction of cerebral infarction in stroke-prone spontaneously hypertensive rats by statins associated with amelioration of oxidative stress. *Stroke*. 2005, **36**(3):670-672.
99. Abramov AY, Scorziello A, Duchen MR. Three distinct mechanisms generate oxygen free radicals in neurons and contribute to cell death during anoxia and reoxygenation. *J Neurosci*. 2007, **27**(5):1129-1138.
100. Kushnareva Y, Murphy AN, Andreyev A. Complex I-mediated reactive oxygen species generation: modulation by cytochrome c and NAD(P)+ oxidation-reduction state. *Biochem J*. 2002, **368**(Pt 2):545-553.
101. Loukogeorgakis SP, van den Berg MJ, Sofat R, Nitsch D, Charakida M, Haiyee B, de Groot E, MacAllister RJ, Kuijpers TW, Deanfield JE. Role of NADPH oxidase in endothelial ischemia/reperfusion injury in humans. *Circulation*. 2010, **121**(21):2310-2316. doi: 10.1161/CIRCULATIONAHA.108.814731.
102. Lazarewicz JW, Wroblewski JT, Costa E. N-methyl-d-aspartate-sensitive glutamate receptors induced calcium-mediated arachidonic

acid release in primary cultures of cerebellar granule cells. *J. Neurochem*. 1990, **55**: 1875–1881.
103. Endo H, Kamada H, Nito C, Nishi T, Chan PH. Mitochondrial translocation of p53 mediates release of cytochrome c and hippocampal CA1 neuronal death after transient global cerebral ischemia in rats. *J Neurosci*. 2006, **26**(30):7974-7983.
104. MacManus JP, Linnik MD. Gene expression induced by cerebral ischemia: an apoptotic perspective. *J. Cereb. Blood Flow Metab*. 1997, **17**:815–832.
105. Broughton BR, Reutens DC, Sobey CG. Apoptotic mechanisms after cerebral ischemia. *Stroke*. 2009, **40**:e331-339.
106. Chan PH. Reactive oxygen radicals in signaling and damage in the ischemic brain. *J. Cereb. Blood Flow Metab*. 2001, **21**:2–14.
107. Nicholson DW, Thornberry NA. Apoptosis. Life and death decisions. *Science* 2003, **299**:214–215.
108. Taylor JM, Crack PJ. Impact of oxidative stress on neuronal survival. *Clin Exp Pharmacol Physiol*. 2004, **31**(7):397-406.
109. Miyashita T, Reed JC. Tumor suppressor p53 is a direct transcriptional activator of the human bax gene. *Cell*. 1995, **80**(2):293-299.
110. Culmsee C, Zhu C, Landshamer S, Becattini B, Wagner E, Pellecchia M, Blomgren K, Plesnila N. Apoptosis-inducing factor triggered by poly(ADP-ribose) polymerase and Bid mediates neuronal cell death after oxygen-glucose deprivation and focal cerebral ischemia. *J Neurosci*. 2005, **25**(44):10262-10272.
111. Love S. Apoptosis and brain ischaemia. *Prog Neuropsychopharmacol Biol Psychiatry*. 2003, **27**(2):267-282.
112. Sugawara T, Fujimura M, Noshita N, Kim GW, Saito A, Hayashi T, Narasimhan P, Maier CM, Chan PH. Neuronal death/survival signaling pathways in cerebral ischemia. *NeuroRx*. 2004, **1**(1):17-25.
113. Namura S, Zhu J, Fink K, Endres M, Srinivasan A, Tomaselli KJ, Yuan J, Moskowitz MA. Activation and cleavage of caspase-3 in apoptosis induced by experimental cerebral ischemia. *J Neurosci*. 1998, **18**(10):3659-3668.
114. Endres M, Wang ZQ, Namura S, Waeber C, Moskowitz MA. Ischemic brain injury is mediated by the activation of poly(ADP-ribose)polymerase. *J Cereb Blood Flow Metab.* 1997, **17**(11):1143-1151.
115. Jin K, Graham SH, Mao X, Nagayama T, Simon RP, Greenberg DA. Fas (CD95) may mediate delayed cell death in hippocampal CA1 sector after global cerebral ischemia. *J. Cereb. Blood Flow Metab*. 2001, **21**:1411–1421.
116. Markiewski MM, Lambris JD. The role of complement in inflammatory diseases from behind the scenes into the spotlight. *Am J Pathol*. 2007, **171**(3):715-727.
117. Martin P, Leibovich SJ. Inflammatory cells during wound repair: the good, the bad and the ugly. *Trends Cell Biol*. 2005, **15**(11):599-607.
118. Zhang JM, An J. Cytokines, inflammation, and pain. *Int Anesthesiol Clin*. 2007, **45**(2):27-37.

119. Le Y, Zhou Y, Iribarren P, Wang J. Chemokines and chemokine receptors: their manifold roles in homeostasis and disease. *Cell Mol Immunol*. 2004, **1**(2):95-104.
120. Wang Q, Tang XN, Yenari MA. The inflammatory response in stroke. *J Neuroimmunol*. 2007, **184**(1-2):53-68.
121. Barone FC, Feuerstein GZ. Inflammatory mediators and stroke: new opportunities for novel therapeutics. *J Cereb Blood Flow Metab*. 1999, **19**(8):819-834.
122. Becker KJ. Targeting the central nervous system inflammatory response in ischemic stroke. *Curr. Opin. Neurol*. 2001, **14**:349–353.
123. Lindsberg PJ, Carpén O, Paetau A, Karjalainen-Lindsberg ML, Kaste M. Endothelial ICAM-1 expression associated with inflammatory cell response in human ischemic stroke. *Circulation*. 1996, **94**(5):939-945.
124. Dimitrijevic OB, Stamatovic SM, Keep RF, Andjelkovic AV. Effects of the chemokine CCL2 on blood-brain barrier permeability during ischemia-reperfusion injury. *J Cereb Blood Flow Metab*. 2006, **26**(6):797-810.
125. Strecker JK, Minnerup J, Gess B, Ringelstein EB, Schäbitz WR, Schilling M. Monocyte chemoattractant protein-1-deficiency impairs the expression of IL-6, IL-1β and G-CSF after transient focal ischemia in mice. *PLoS One*. 2011, **6**(10):e25863. doi: 10.1371/journal.pone.0025863
126. Dimitrijevic OB, Stamatovic SM, Keep RF, Andjelkovic AV. Absence of the chemokine receptor CCR2 protects against cerebral ischemia/reperfusion injury in mice. *Stroke*. 2007, **38**(4):1345-1353.
127. Jovanovic, M., Stefanoska, I., Radojcic, L., Vicovac, L. (2010) Interleukin-8 (CXCL8) stimulates trophoblast cell migration and invasion by increasing levels of MMP-2 and MMP-9 and integrins {alpha}5 and {beta}1. Reproduction. 139:789-798.
128. Sarma JV, Ward PA. The complement system. *Cell Tissue Res*. 2011, **343**(1):227-235. doi: 10.1007/s00441-010-1034-0.
129. Song FY, Wu MH, Zhu LH, Zhang ZQ, Qi QD, Lou CL. Elevated Serum Mannose-Binding Lectin Levels Are Associated with Poor Outcome After Acute Ischemic Stroke in Patients with Type 2 Diabetes. *Mol Neurobiol*. 2014 [Epub ahead of print]
130. Zhang ZG, Wang C, Wang J, Zhang Z, Yang YL, Gao L, Zhang XY, Chang T, Gao GD, Li LH. Prognostic Value of Mannose-Binding Lectin: 90-Day Outcome in Patients with Acute Ischemic Stroke. *Mol Neurobiol*. 2014. [Epub ahead of print]
131. Wang ZY, Sun ZR, Zhang LM. The relationship between serum mannose-binding lectin levels and acute ischemic stroke risk. *Neurochem Res*. 2014, **39**(2):248-253. doi: 10.1007/s11064-013-1214-x.
132. Zhang B, Yang N, Gao C. Is plasma C3 and C4 levels useful in young cerebral ischemic stroke patients? Associations with prognosis at 3 months. *J Thromb Thrombolysis*. 2014. [Epub ahead of print]

133. Széplaki G, Szegedi R, Hirschberg K, Gombos T, Varga L, Karádi I, Entz L, Széplaki Z, Garred P, Prohászka Z, Füst G. Strong complement activation after acute ischemic stroke is associated with unfavorable outcomes. *Atherosclerosis*. 2009, **204**(1):315-320. doi: 10.1016/j.atherosclerosis.2008.07.044.
134. Liu Q, He S, Groysman L, Shaked D, Russin J, Scotton TC, Cen S, Mack WJ. White matter injury due to experimental chronic cerebral hypoperfusion is associated with C5 deposition. *PLoS One*. 2013, **8**(12):e84802. doi: 10.1371/journal.pone.0084802.
135. Pavlovski D, Thundyil J, Monk PN, Wetsel RA, Taylor SM, Woodruff TM. Generation of complement component C5a by ischemic neurons promotes neuronal apoptosis. *FASEB J*. 2012, **26**(9):3680-3690. doi: 10.1096/fj.11-202382.
136. de la Rosa X, Cervera A, Kristoffersen AK, Valdés CP, Varma HM, Justicia C, Durduran T, Chamorro Á, Planas AM. Mannose-binding lectin promotes local microvascular thrombosis after transient brain ischemia in mice. *Stroke*. 2014, **45**(5):1453-1459. doi: 10.1161/STROKEAHA.113.004111.
137. Lee RC, Feinbaum RL, Ambros V. The C. elegans heterochronic gene lin-4 encodes small RNAs with antisense complementarity to lin-14. *Cell*. 1993, **75**:843-854.
138. Reinhart BJ, Slack FJ, Basson M, Pasquinelli AE, Bettinger JC, Rougvie AE, Horvitz HR, Ruvkun G. The 21-nucleotide let-7 RNA regulates developmental timing in Caenorhabditis elegans. *Nature*. 2000, **403**(6772):901-906.
139. Bartel DP. MicroRNAs: genomics, biogenesis, mechanism, and function. Cell. 2004, **116**:281-297.
140. Rodriguez A, Griffiths-Jones S, Ashurst JL, Bradley A. Identification of mammalian microRNA host genes and transcription units. *Genome Res*. 2004, **14**: 1902 -1910.
141. Lee Y, Kim M, Han J, Yeom KH, Lee S, Baek SH, Kim VN. MicroRNA genes are transcribed by RNA polymerase II. *EMBO J*. 2004, **23**: 4051–4060
142. Cai X, Hagedorn CH, Cullen BR. Human microRNAs are processed from capped, polyadenylated transcripts that can also function as mRNAs. *RNA* 2004, **10**: 1957–1966.
143. Hamilton AJ, Baulcombe DC. A novel species of small antisense RNA in posttranscriptional gene silencing. *Science* 1999, **286**:950–952.
144. Yi R, Qin Y, Macara IG, Cullen BR. Exportin-5 mediates the nuclear export of pre-microRNAs and short hairpin RNAs. *Genes Dev*. 2003, **17**:3011-3016.
145. Shivdasani RA. MicroRNAs: regulators of gene expression and cell differentiation. *Blood*. 2006, **108**(12):3646-3653.
146. Khvorova A, Reynolds A, Jayasena SD. Functional siRNAs and miRNAs exhibit strand bias. *Cell* 2003, **115**: 209-216.
147. Alvarez-Garcia I, Miska EA. MicroRNA functions in animal development and human disease. *Development* 2005, **132**: 4653-4662.

148. Fire A, Xu S, Montgomery MK, Kostas SA, Driver SE, Mello CC. Potent and specific genetic interference by double-stranded RNA in Caenorhabditis elegans. *Nature*. 1998, **391**:806-811.
149. Krek A, Grun D, Poy MN, Wolf R, Rosenberg L, Epstein EJ, MacMenamin P, da Piedade I, Gunsalus KC, Stoffel M, Rajewsky N. Combinatorial microRNA target predictions. *Nat. Genet*. 2005, **37**: 495-500
150. Li LC, Okino ST, Zhao H, Pookot D, Place RF, Urakami S, Enokida H, Dahiya R. Small dsRNAs induce transcriptional activation in human cells. *Proc Natl Acad Sci U S A.* 2006, **103**:17337-17342.
151. Place RF, Li LC, Pookot D, Noonan EJ, Dahiya R. MicroRNA-373 induces expression of genes with complementary promoter sequences. *Proc. Natl. Acad. Sci. U.S.A.* 2008, **105**: 1608-1613.
152. Janowski BA, Younger ST, Hardy DB, Ram R, Huffman KE, Corey DR. Activating gene expression in mammalian cells with promoter-targeted duplex RNAs. *Nat. Chem. Biol*. 2007, **3**: 166-173.
153. Chandrasekaran K, Karolina DS, Sepramaniam S, Armugam A, Wintour EM, Bertram JF, Jeyaseelan K. Role of microRNAs in kidney homeostasis and disease. *Kidney Int*. 2012, **81**(7):617-627. doi: 10.1038/ki.2011.448.
154. Ambros V. The functions of animal microRNAs. *Nature*. 2004, **431**: 350-355.
155. Brennecke J, Stark A, Russell RB, Cohen SM. Principles of microRNA-target recognition. *PLoS Biol*. 2005, **3**: e85.
156. Lewis BP, Burge CB, Bartel DP. Conserved seed pairing, often flanked by adenosines, indicates that thousands of human genes are microRNA targets. *Cell*. 2005, **120**(1):15-20.
157. Friedman RC, Farh KK, Burge CB, Bartel DP. Most mammalian mRNAs are conserved targets of microRNAs. *Genome Res*. 2009, **19**(1):92-105. doi: 10.1101/gr.082701.108.
158. Grimson A, Farh KK, Johnston WK, Garrett-Engele P, Lim LP, Bartel DP. MicroRNA targeting specificity in mammals: determinants beyond seed pairing. *Mol Cell*. 2007, **27**(1):91-105.
159. Garcia DM, Baek D, Shin C, Bell GW, Grimson A, Bartel DP. Weak seed-pairing stability and high target-site abundance decrease the proficiency of lsy-6 and other microRNAs. *Nat Struct Mol Biol*. 2011, **18**(10):1139-46. doi: 10.1038/nsmb.2115.
160. Betel D, Wilson M, Gabow A, Marks DS, Sander C. The microRNA.org resource: targets and expression. *Nucleic Acids Res*. 2008, **36**(Database issue):D149-153.
161. Betel D, Koppal A, Agius P, Sander C, Leslie C. Comprehensive modeling of microRNA targets predicts functional non-conserved and non-canonical sites. *Genome Biol*. 2010, **11**(8):R90. doi: 10.1186/gb-2010-11-8-r90.
162. John B, Enright AJ, Aravin A, Tuschl T, Sander C, Marks DS. Human MicroRNA targets. *PLoS Biol*. 2004, **2**(11):e363. Epub 2004 Oct 5.

163. Enright AJ, John B, Gaul U, Tuschl T, Sander C, Marks DS. MicroRNA targets in Drosophila. *Genome Biol*. 2003, **5**(1):R1.
164. Griffiths-Jones S, Grocock RJ, van Dongen S, Bateman A, Enright AJ. miRBase: microRNA sequences, targets and gene nomenclature. *Nucleic Acids Res*. 2006, **34**(Database issue):D140-144.
165. Griffiths-Jones S, Saini HK, van Dongen S, Enright AJ. miRBase: tools for microRNA genomics. *Nucleic Acids Res*. 2008, **36**(Database issue):D154-158.
166. Maragkakis M, Alexiou P, Papadopoulos GL, Reczko M, Dalamagas T, Giannopoulos G, Goumas G, Koukis E, Kourtis K, Simossis VA, Sethupathy P, Vergoulis T, Koziris N, Sellis T, Tsanakas P, Hatzigeorgiou AG. Accurate microRNA target prediction correlates with protein repression levels. *BMC Bioinformatics*. 2009, **10**:295. doi: 10.1186/1471-2105-10-295.
167. Maragkakis M, Reczko M, Simossis VA, Alexiou P, Papadopoulos GL, Dalamagas T, Giannopoulos G, Goumas G, Koukis E, Kourtis K, Vergoulis T, Koziris N, Sellis T, Tsanakas P, Hatzigeorgiou AG. DIANA-microT web server: elucidating microRNA functions through target prediction. *Nucleic Acids Res*. 2009, **37**(Web Server issue):W273-6. doi: 10.1093/nar/gkp292.
168. Wang X, El Naqa IM. Prediction of both conserved and nonconserved microRNA targets in animals. *Bioinformatics*. 2008, **24**(3):325-332.
169. Wang X. miRDB: a microRNA target prediction and functional annotation database with a wiki interface. *RNA*. 2008, **14**(6):1012-1017. doi: 10.1261/rna.965408.
170. Dweep H, Sticht C, Pandey P, Gretz N. miRWalk--database: prediction of possible miRNA binding sites by "walking" the genes of three genomes. *J Biomed Inform*. 2011, **44**(5):839-847. doi: 10.1016/j.jbi.2011.05.002.
171. Kertesz M, Iovino N, Unnerstall U, Gaul U, Segal E. The role of site accessibility in microRNA target recognition. *Nat Genet*. 2007, **39**(10):1278-1284.
172. Elefant N, Berger A, Shein H, Hofree M, Margalit H, Altuvia Y. RepTar: a database of predicted cellular targets of host and viral miRNAs. *Nucleic Acids Res*. 2011, **39**(Database issue):D188-194. doi: 10.1093/nar/gkq1233.
173. Yang JH, Li JH, Shao P, Zhou H, Chen YQ, Qu LH. starBase: a database for exploring microRNA-mRNA interaction maps from Argonaute CLIP-Seq and Degradome-Seq data. *Nucleic Acids Res*. 2011, **39**(Database issue):D202-209. doi: 10.1093/nar/gkq1056.
174. Li JH, Liu S, Zhou H, Qu LH, Yang JH. starBase v2.0: decoding miRNA-ceRNA, miRNA-ncRNA and protein-RNA interaction networks from large-scale CLIP-Seq data. *Nucleic Acids Res*. 2014, **42**(Database issue):D92-97. doi: 10.1093/nar/gkt1248.

175. Nielsen CB, Shomron N, Sandberg R, Hornstein E, Kitzman J, Burge CB. Determinants of targeting by endogenous and exogenous microRNAs and siRNAs. *RNA*. 2007, **13**(11):1894-1910.
176. Wuchty S, Fontana W, Hofacker IL, Schuster P. Complete suboptimal folding of RNA and the stability of secondary structures. *Biopolymers*. 1999, **49**(2):145-165.
177. Benson DA, Karsch-Mizrachi I, Lipman DJ, Ostell J, Wheeler DL. GenBank. *Nucleic Acids Res*. 2007, **35**(Database issue):D21-5.
178. Maglott D, Ostell J, Pruitt KD, Tatusova T. Entrez Gene: gene-centered information at NCBI. *Nucleic Acids Res*. 2007, **35**(Database issue):D26-31.
179. Rehmsmeier M, Steffen P, Hochsmann M, Giegerich R. Fast and effective prediction of microRNA/target duplexes. *RNA*. 2004, **10**(10):1507-1517.
180. Hofacker IL. Vienna RNA secondary structure server. *Nucleic Acids Res*. 2003, **31**(13):3429-3431.
181. Chi SW, Zang JB, Mele A, Darnell RB. Argonaute HITS-CLIP decodes microRNA-mRNA interaction maps. *Nature*. 2009, **460**:479-486.
182. Zisoulis DG, Lovci MT, Wilbert ML, Hutt KR, Liang TY, Pasquinelli AE, Yeo GW. Comprehensive discovery of endogenous Argonaute binding sites in Caenorhabditis elegans. *Nat. Struct. Mol. Biol*. 2010, **17**:173–179.
183. Hafner M, Landthaler M, Burger L, Khorshid M, Hausser J, Berninger P, Rothballer A, Ascano M, Jr, Jungkamp AC, Munschauer M. Transcriptome-wide identification of RNA-binding protein and microRNA target sites by PAR-CLIP. *Cell*. 2010, **141**:129–141.
184. German MA, Pillay M, Jeong DH, Hetawal A, Luo S, Janardhanan P, Kannan V, Rymarquis LA, Nobuta K, German R. Global identification of microRNA-target RNA pairs by parallel analysis of RNA ends. *Nat. Biotechnol*. 2008, **26**:941–946.
185. Addo-Quaye C, Eshoo TW, Bartel DP, Axtell MJ. Endogenous siRNA and miRNA targets identified by sequencing of the Arabidopsis degradome. *Curr Biol*. 2008, **18**:758–762.
186. Wu L, Zhang Q, Zhou H, Ni F, Wu X, Qi Y. Rice MicroRNA effector complexes and targets. *Plant Cell*. 2009, **21**:3421–3435.
187. Pantaleo V, Szittya G, Moxon S, Miozzi L, Moulton V, Dalmay T, Burgyan J. Identification of grapevine microRNAs and their targets using high throughput sequencing and degradome analysis. *Plant J*. 2010, **62**:960–976.
188. Zhou M, Gu L, Li P, Song X, Wei L, Chen Z, Cao X. Degradome sequencing reveals endogenous small RNA targets in rice (Oryza sativa L. ssp. indica) *Front. Biol*. 2010, **5**:67-90.
189. Jeyaseelan K, Lim KY, Armugam A. MicroRNA expression in the blood and brain of rats subjected to transient focal ischemia by middle cerebral artery occlusion. *Stroke*. 2008, **39**(3):959-966. doi: 10.1161/STROKEAHA.107.500736.
190. Tan KS, Armugam A, Sepramaniam S, Lim KY, Setyowati KD, Wang CW, Jeyaseelan K. Expression profile of MicroRNAs in young stroke

patients. *PLoS One*. 2009, **4**(11):e7689. doi: 10.1371/journal.pone.0007689.

191. Dharap A, Bowen K, Place R, Li LC, Vemuganti R. Transient focal ischemia induces extensive temporal changes in rat cerebral microRNAome. *J Cereb Blood Flow Metab*. 2009, **29**(4):675-687. doi: 10.1038/jcbfm.2008.157.
192. Liu DZ, Tian Y, Ander BP, Xu H, Stamova BS, Zhan X, Turner RJ, Jickling G, Sharp FR. Brain and blood microRNA expression profiling of ischemic stroke, intracerebral hemorrhage, and kainate seizures. *J Cereb Blood Flow Metab*. 2010, **30**(1):92-101. doi: 10.1038/jcbfm.2009.186.
193. Lim KY, Chua JH, Tan JR, Swaminathan P, Sepramaniam S, Armugam A, Wong PT, Jeyaseelan K. MicroRNAs in Cerebral Ischemia. *Transl Stroke Res*. 2010, **1**(4):287-303. doi: 10.1007/s12975-010-0035-3.
194. Ziu M, Fletcher L, Rana S, Jimenez DF, Digicaylioglu M. Temporal differences in microRNA expression patterns in astrocytes and neurons after ischemic injury. *PLoS One*. 2011, **6**(2):e14724. doi: 10.1371/journal.pone.0014724.
195. Lee ST, Chu K, Jung KH, Yoon HJ, Jeon D, Kang KM, Park KH, Bae EK, Kim M, Lee SK, Roh JK. MicroRNAs induced during ischemic preconditioning. *Stroke*. 2010, **41**(8):1646-1451. doi: 10.1161/STROKEAHA.110.579649.
196. Liu FJ, Lim KY, Kaur P, Sepramaniam S, Armugam A, Wong PT, Jeyaseelan K. microRNAs Involved in Regulating Spontaneous Recovery in Embolic Stroke Model. *PLoS One*. 2013, **8**(6):e66393.
197. Sepramaniam S, Tan JR, Tan KS, DeSilva DA, Tavintharan S, Woon FP, Wang CW, Yong FL, Karolina DS, Kaur P, Liu FJ, Lim KY, Armugam A, Jeyaseelan K. Circulating microRNAs as biomarkers of acute stroke. *Int J Mol Sci*. 2014, **15**(1):1418-1432. doi: 10.3390/ijms15011418.
198. Jickling GC, Ander BP, Zhan X, Noblett D, Stamova B, Liu D. microRNA expression in peripheral blood cells following acute ischemic stroke and their predicted gene targets. *PLoS One*. 2014, **9**(6):e99283. doi: 10.1371/journal.pone.0099283.
199. Zeng L, Liu J, Wang Y, Wang L, Weng S, Tang Y, Zheng C, Cheng Q, Chen S, Yang GY. MicroRNA-210 as a novel blood biomarker in acute cerebral ischemia. *Front Biosci (Elite Ed)*. 2011, **3**:1265-72.
200. Zeng L, Liu J, Wang Y, Wang L, Weng S, Chen S, Yang GY. Cocktail blood biomarkers: prediction of clinical outcomes in patients with acute ischemic stroke. *Eur Neurol*. 2013, **69**(2):68-75. doi: 10.1159/000342896.
201. Tsai PC, Liao YC, Wang YS, Lin HF, Lin RT, Juo SH. Serum microRNA-21 and microRNA-221 as potential biomarkers for

cerebrovascular disease. *J Vasc Res*. 2013, **50**(4):346-354. doi: 10.1159/000351767.

202. Gan CS, Wang CW, Tan KS. Circulatory microRNA-145 expression is increased in cerebral ischemia. *Genet Mol Res*. 2012, **11**(1):147-52. doi: 10.4238/2012.January.27.1.
203. Long G, Wang F, Li H, Yin Z, Sandip C, Lou Y, Wang Y, Chen C, Wang DW. Circulating miR-30a, miR-126 and let-7b as biomarker for ischemic stroke in humans. *BMC Neurol*. 2013, **13**:178. doi: 10.1186/1471-2377-13-178.
204. Wang Y, Zhang Y, Huang J, Chen X, Gu X, Wang Y, Zeng L, Yang GY. Increase of circulating miR-223 and insulin-like growth factor-1 is associated with the pathogenesis of acute ischemic stroke in patients. *BMC Neurol*. 2014, **14**:77. doi: 10.1186/1471-2377-14-77.
205. Leung LY, Chan CP, Leung YK, Jiang HL, Abrigo JM, Wang de F, Chung JS, Rainer TH, Graham CA. Comparison of miR-124-3p and miR-16 for early diagnosis of hemorrhagic and ischemic stroke. *Clin Chim Acta*. 2014, **433**:139-44. doi: 10.1016/j.cca.2014.03.007.
206. Longa EZ, Weinstein PR, Carlson S, Cummins R. Reversible middle cerebral artery occlusion without craniectomy in rats. *Stroke*. 1989, **20**(1):84-91.
207. Bederson JB, Pitts LH, Tsuji M, Nishimura MC, Davis RL, Bartkowski H: Rat middle cerebral artery occlusion: evaluation of the model and development of a neurologic examination. *Stroke*. 1986, **17**(3):472-476.
208. Swanson RA, Morton MT, Tsao-Wu G, Savalos RA, Davidson C, Sharp FR: A semiautomated method for measuring brain infarct volume. *J Cereb Blood Flow Metab* 1990, **10**(2):290-293.
209. Saeed AI, Sharov V, White J, Li J, Liang W, Bhagabati N, Braisted J, Klapa M, Currier T, Thiagarajan M, Sturn A, Snuffin M, Rezantsev A, Popov D, Ryltsov A, Kostukovich E, Borisovsky I, Liu Z, Vinsavich A, Trush V, Quackenbush J: TM4: a free, open-source system for microarray data management and analysis. *Biotechniques*. 2003, **34**(2):374-378.
210. Jeon YJ, Kim OJ, Kim SY, Oh SH, Oh D, Kim OJ, Shin BS, Kim NK. Association of the miR-146a, miR-149, miR-196a2, and miR-499 polymorphisms with ischemic stroke and silent brain infarction risk. *Arterioscler Thromb Vasc Biol*. 2013, **33**(2):420-430. doi: 10.1161/ATVBAHA.112.300251.
211. Farrell B, Godwin J, Richards S, Warlow C. The United Kingdom transient ischaemic attack (UK-TIA) aspirin trial: final results. *J Neurol Neurosurg Psychiatry*. 1991, **54**(12):1044-1054.
212. Carmona-Saez P, Chagoyen M, Tirado F, Carazo JM, Pascual-Montano A: GENECODIS: a web-based tool for finding significant concurrent annotations in gene lists. *Genome Biol*. 2007, **8**(1):R3.

213. Nogales-Cadenas R, Carmona-Saez P, Vazquez M, Vicente C, Yang X, Tirado F, Carazo JM, Pascual-Montano A: GeneCodis: interpreting gene lists through enrichment analysis and integration of diverse biological information. *Nucleic Acids Res*. 2009, **37**(Web Server issue):W317-322. doi: 10.1093/nar/gkp416.
214. Tabas-Madrid D, Nogales-Cadenas R, Pascual-Montano A: GeneCodis3: a non-redundant and modular enrichment analysis tool for functional genomics. *Nucleic Acids Res*. 2012, **40**(Web Server issue):W478-483. doi: 10.1093/nar/gks402.
215. Ogata H, Goto S, Sato K, Fujibuchi W, Bono H, Kanehisa M: KEGG: Kyoto Encyclopedia of Genes and Genomes. *Nucleic Acids Res*. 1999, **27**(1):29-34.
216. Kanehisa M, Goto S, Kawashima S, Nakaya A: The KEGG databases at GenomeNet. *Nucleic Acids Res*. 2002, **30**(1):42-46.
217. Kanehisa M, Goto S, Sato Y, Kawashima M, Furumichi M, Tanabe M: Data, information, knowledge and principle: back to metabolism in KEGG. *Nucleic Acids Res*. 2014, **42**(Database issue):D199-205. doi: 10.1093/nar/gkt1076.
218. Li S, Zhu J, Zhang W, Chen Y, Zhang K, Popescu LM, Ma X, Lau WB, Rong R, Yu X, Wang B, Li Y, Xiao C, Zhang M, Wang S, Yu L, Chen AF, Yang X, Cai J. Signature microRNA expression profile of essential hypertension and its novel link to human cytomegalovirus infection. *Circulation*. 2011, **124**(2):175-184. doi: 10.1161/CIRCULATIONAHA.110.012237.
219. Kontaraki JE, Marketou ME, Zacharis EA, Parthenakis FI, Vardas PE. MicroRNA-9 and microRNA-126 expression levels in patients with essential hypertension: potential markers of target-organ damage. *J Am Soc Hypertens*. 2014, **8**(6):368-375. doi: 10.1016/j.jash.2014.03.324.
220. Ling S, Nanhwan M, Qian J, Kodakandla M, Castillo AC, Thomas B, Liu H, Ye Y. Modulation of microRNAs in hypertension-induced arterial remodeling through the β1 and β3-adrenoreceptor pathways. *J Mol Cell Cardiol*. 2013, **65**:127-136. doi: 10.1016/j.yjmcc.2013.10.003.
221. Karolina DS, Tavintharan S, Armugam A, Sepramaniam S, Pek SL, Wong MT, Lim SC, Sum CF, Jeyaseelan K. Circulating miRNA profiles in patients with metabolic syndrome. *J Clin Endocrinol Metab*. 2012, **97**(12):E2271-2276. doi: 10.1210/jc.2012-1996
222. Karere GM, Glenn JP, VandeBerg JL, Cox LA. Differential microRNA response to a high-cholesterol, high-fat diet in livers of low and high LDL-C baboons. *BMC Genomics*. 2012, **13**:320. doi: 10.1186/1471-2164-13-320.
223. Flowers E, Singh K, Molina C, Mathur A, Aouizerat BE. MicroRNA associated with atherogenic dyslipidemia in South Asian men. *Int J Cardiol*. 2013, **168**(5):4884-4885. doi: 10.1016/j.ijcard.2013.07.029.

224. Liu F, Li R, Zhang Y, Qiu J, Ling W. Association of plasma MiR-17-92 with dyslipidemia in patients with coronary artery disease. *Medicine (Baltimore)*. 2014, **93**(23):e98. doi: 10.1097/MD.0000000000000098.
225. Karolina DS, Armugam A, Tavintharan S, Wong MT, Lim SC, Sum CF, Jeyaseelan K. MicroRNA 144 impairs insulin signaling by inhibiting the expression of insulin receptor substrate 1 in type 2 diabetes mellitus. *PLoS One*. 2011, **6**(8):e22839. doi: 10.1371/journal.pone.0022839.
226. Pescador N, Pérez-Barba M, Ibarra JM, Corbatón A, Martínez-Larrad MT, Serrano-Ríos M. Serum circulating microRNA profiling for identification of potential type 2 diabetes and obesity biomarkers. *PLoS One*. 2013, **8**(10):e77251. doi: 10.1371/journal.pone.0077251.
227. Ortega FJ, Mercader JM, Moreno-Navarrete JM, Rovira O, Guerra E, Esteve E, Xifra G, Martínez C, Ricart W, Rieusset J, Rome S, Karczewska-Kupczewska M, Straczkowski M, Fernández-Real JM. Profiling of circulating microRNAs reveals common microRNAs linked to type 2 diabetes that change with insulin sensitization. *Diabetes Care*. 2014, **37**(5):1375-1383. doi: 10.2337/dc13-1847.
228. van de Bunt M, Gaulton KJ, Parts L, Moran I, Johnson PR, Lindgren CM, Ferrer J, Gloyn AL, McCarthy MI. The miRNA profile of human pancreatic islets and beta-cells and relationship to type 2 diabetes pathogenesis. *PLoS One*. 2013, **8**(1):e55272. doi: 10.1371/journal.pone.0055272.
229. Gallagher IJ, Scheele C, Keller P, Nielsen AR, Remenyi J, Fischer CP, Roder K, Babraj J, Wahlestedt C, Hutvagner G, Pedersen BK, Timmons JA. Integration of microRNA changes in vivo identifies novel molecular features of muscle insulin resistance in type 2 diabetes. *Genome Med.* 2010, **2**(2):9. doi: 10.1186/gm130.
230. O'Callaghan JP, Sriram K, Miller DB. Defining "neuroinflammation". *Ann N Y Acad Sci*. 2008, **1139**:318-330. doi: 10.1196/annals.1432.032.
231. Jin R, Liu L, Zhang S, Nanda A, Li G. Role of inflammation and its mediators in acute ischemic stroke. *J Cardiovasc Transl Res*. 2013, **6**(5):834-851. doi: 10.1007/s12265-013-9508-6.
232. Jickling GC, Xu H, Stamova B, Ander BP, Zhan X, Tian Y, Liu D, Turner RJ, Mesias M, Verro P, Khoury J, Jauch EC, Pancioli A, Broderick JP, Sharp FR. Signatures of cardioembolic and large-vessel ischemic stroke. *Ann Neurol*. 2010, **68**(5):681-92. doi: 10.1002/ana.22187.
233. Liszewski MK, Farries TC, Lublin DM, Rooney IA, Atkinson JP. Control of the complement system. *Adv Immunol*. 1996, **61**:201-283.
234. Riley RC, Kemper C, Leung M, Atkinson JP. Characterization of human membrane cofactor protein (MCP; CD46) on spermatozoa. *Mol Reprod Dev*. 2002, **62**(4):534-546.

235. Kemper C, Leung M, Stephensen CB, Pinkert CA, Liszewski MK, Cattaneo R, Atkinson JP. Membrane cofactor protein (MCP; CD46) expression in transgenic mice. *Clin Exp Immunol*. 2001, **124**(2):180-189.
236. Mélik-Parsadaniantz S, Rostène W. Chemokines and neuromodulation. *J Neuroimmunol*. 2008, **198**(1-2):62-68. doi: 10.1016/j.jneuroim.2008.04.022.
237. Mirabelli-Badenier M, Braunersreuther V, Viviani GL, Dallegri F, Quercioli A, Veneselli E, Mach F, Montecucco F. CC and CXC chemokines are pivotal mediators of cerebral injury in ischaemic stroke. *Thromb Haemost*. 2011, **105**(3):409-420. doi: 10.1160/TH10-10-0662.
238. Worthmann H, Tryc AB, Goldbecker A, Ma YT, Tountopoulou A, Hahn A, Dengler R, Lichtinghagen R, Weissenborn K. The temporal profile of inflammatory markers and mediators in blood after acute ischemic stroke differs depending on stroke outcome. *Cerebrovasc Dis*. 2010, **30**(1):85-92. doi: 10.1159/000314624.
239. Stowe AM, Wacker BK, Cravens PD, Perfater JL, Li MK, Hu R, Freie AB, Stüve O, Gidday JM. CCL2 upregulation triggers hypoxic preconditioning-induced protection from stroke. *J Neuroinflammation*. 2012, **9**:33. doi: 10.1186/1742-2094-9-33.
240. Yan YP, Sailor KA, Lang BT, Park SW, Vemuganti R, Dempsey RJ. Monocyte chemoattractant protein-1 plays a critical role in neuroblast migration after focal cerebral ischemia. *J Cereb Blood Flow Metab*. 2007, **27**(6):1213-1224.
241. Slevin M, Krupinski J, Rovira N, Turu M, Luque A, Baldellou M, Sanfeliu C, de Vera N, Badimon L. Identification of pro-angiogenic markers in blood vessels from stroked-affected brain tissue using laser-capture microdissection. *BMC Genomics*. 2009, **10**:113. doi: 10.1186/1471-2164-10-113.
242. Kosaka N, Iguchi H, Yoshioka Y, Takeshita F, Matsuki Y, Ochiya T. Secretory mechanisms and intercellular transfer of microRNAs in living cells. *J Biol Chem*. 2010, **285**(23):17442-17452. doi: 10.1074/jbc.M110.107821.
243. Zernecke A, Bidzhekov K, Noels H, Shagdarsuren E, Gan L, Denecke B, Hristov M, Köppel T, Jahantigh MN, Lutgens E, Wang S, Olson EN, Schober A, Weber C. Delivery of microRNA-126 by apoptotic bodies induces CXCL12-dependent vascular protection. *Sci Signal*. 2009, **2**(100):ra81. doi: 10.1126/scisignal.2000610.
244. Arroyo JD, Chevillet JR, Kroh EM, Ruf IK, Pritchard CC, Gibson DF, Mitchell PS, Bennett CF, Pogosova-Agadjanyan EL, Stirewalt DL, Tait JF, Tewari M. Argonaute2 complexes carry a population of circulating microRNAs independent of vesicles in human plasma. *Proc Natl Acad Sci U S A*. 2011, **108**(12):5003-5008. doi: 10.1073/pnas.1019055108.

245. Vickers KC, Palmisano BT, Shoucri BM, Shamburek RD, Remaley AT. MicroRNAs are transported in plasma and delivered to recipient cells by high-density lipoproteins. *Nat Cell Biol*. 2011, **13**(4):423-433. doi: 10.1038/ncb2210.
246. Holmgren L, Szeles A, Rajnavölgyi E, Folkman J, Klein G, Ernberg I, Falk KI. Horizontal transfer of DNA by the uptake of apoptotic bodies. *Blood*. 1999, **93**(11):3956-3963.
247. Keller S, Sanderson MP, Stoeck A, Altevogt P. Exosomes: from biogenesis and secretion to biological function. *Immunol Lett*. 2006, **107**(2):102-108.
248. Février B, Raposo G. Exosomes: endosomal-derived vesicles shipping extracellular messages. *Curr Opin Cell Biol*. 2004, **16**(4):415-421.
249. Cheng L, Sharples RA, Scicluna BJ, Hill AF. Exosomes provide a protective and enriched source of miRNA for biomarker profiling compared to intracellular and cell-free blood. *J Extracell Vesicles*. 2014, 3. doi: 10.3402/jev.v3.23743.
250. Sudlow, C. L. and C. P. Warlow. Comparable studies of the incidence of stroke and its pathological types: results from an international collaboration. International Stroke Incidence Collaboration. *Stroke* 1997, **28**(3): 491-499.
251. Grau AJ, Weimar C, Buggle F, Heinrich A, Goertler M, Neumaier S, Glahn J, Brandt T, Hacke W, Diener HC. Risk factors, outcome, and treatment in subtypes of ischemic stroke: the German stroke data bank. *Stroke*. 2001, **32**(11):2559-2566.
252. Clavier I, Hommel M, Besson G, Noèlle B, Perret JE. Long-term prognosis of symptomatic lacunar infarcts. A hospital-based study. *Stroke*. 1994, **25**(10):2005-2009
253. Hu YW, Zhao JY, Li SF, Huang JL, Qiu YR, Ma X, Wu SG, Chen ZP, Hu YR, Yang JY, Wang YC, Gao JJ, Sha YH, Zheng L, Wang Q. RP5-833A20.1/miR-382-5p/NFIA-dependent signal transduction pathway contributes to the regulation of cholesterol homeostasis and inflammatory reaction. *Arterioscler Thromb Vasc Biol*. 2015, **35**(1):87-101. doi: 10.1161/ATVBAHA.114.304296.
254. Que T, Song Y, Liu Z, Zheng S, Long H, Li Z, Liu Y, Wang G, Liu Y, Zhou J, Zhang X, Fang W, Qi S. Decreased miRNA-637 is an unfavorable prognosis marker and promotes glioma cell growth, migration and invasion via direct targeting Akt1. *Oncogene*. 2015, 0. doi: 10.1038/onc.2014.419.
255. Hwang HJ, Jung TW, Hong HC, Choi HY, Seo JA, Kim SG, Kim NH, Choi KM, Choi DS, Baik SH, Yoo HJ. Progranulin protects vascular endothelium against atherosclerotic inflammatory reaction via Akt/eNOS and nuclear factor-κB pathways. *PLoS One*. 2013, **8**(9):e76679. doi: 10.1371/journal.pone.0076679.
256. Rademakers R, Eriksen JL, Baker M, Robinson T, Ahmed Z, Lincoln SJ, Finch N, Rutherford NJ, Crook RJ, Josephs KA, Boeve BF, Knopman DS, Petersen RC, Parisi JE, Caselli RJ, Wszolek ZK, Uitti RJ, Feldman H, Hutton ML, Mackenzie IR, Graff-Radford NR, Dickson DW. Common variation in the miR-659 binding-site of GRN is a major risk factor for TDP43-positive frontotemporal dementia. *Hum Mol Genet*. 2008, **17**(23):3631-3642. doi: 10.1093/hmg/ddn257.

257. Grainger DJ. TGF-beta and atherosclerosis in man. *Cardiovasc Res*. 2007, **74**(2):213-222.
258. Mohammad Y, Qattan M, Prabhakaran S. Epidemiology and pathophysiology of intracranial large artery stenosis. *The Open Atherosclerosis & Thrombosis Journal*. 2010, **3**: 3-7
259. Martin J, Jenkins RH, Bennagi R, Krupa A, Phillips AO, Bowen T, Fraser DJ. Post-transcriptional regulation of Transforming Growth Factor Beta-1 by microRNA-744. *PLoS One*. 2011, **6**(10):e25044. doi: 10.1371/journal.pone.0025044.
260. Song DW, Ryu JY, Kim JO, Kwon EJ, Kim do H. The miR-19a/b family positively regulates cardiomyocyte hypertrophy by targeting atrogin-1 and MuRF-1. *Biochem J*. 2014, **457**(1):151-162. doi: 10.1042/BJ20130833.
261. Kirchhof P, Schotten U. Hypertension begets hypertrophy begets atrial fibrillation? Insights from yet another sheep model. *Eur Heart J*. 2006, **27**(24):2919-2920.
262. Yao CX, Wei QX, Zhang YY, Wang WP, Xue LX, Yang F, Zhang SF, Xiong CJ, Li WY, Wei ZR, Zou Y, Zang MX. miR-200b targets GATA-4 during cell growth and differentiation. *RNA Biol*. 2013, **10**(4):465-480. doi: 10.4161/rna.24370.
263. Liang Q, De Windt LJ, Witt SA, Kimball TR, Markham BE, Molkentin JD. The transcription factors GATA4 and GATA6 regulate cardiomyocyte hypertrophy in vitro and in vivo. *J Biol Chem*. 2001, **276**(32):30245-30253.
264. Tan, G., Cao, X., Dai, Q., Zhang, B., Huang, J., Xiong, S., Zhang, Y., Chen, W., Li, H., & Li, H. A novel role for microRNA-129-5p in inhibiting ovarian cancer cell proliferation and survival via direct suppression of transcriptional co-activators YAP and TAZ. *Oncotarget*. 2015, **6**(11), 8676-8686.
265. Li M, Tian L, Wang L, Yao H, Zhang J, Lu J, Sun Y, Gao X, Xiao H, Liu M. Down-regulation of miR-129-5p inhibits growth and induces apoptosis in laryngeal squamous cell carcinoma by targeting APC. *PLoS One*. 2013, **8**(10):e77829. doi: 10.1371/journal.pone.0077829.
266. Elfimova N, Sievers E, Eischeid H, Kwiecinski M, Noetel A, Hunt H, Becker D, Frommolt P, Quasdorff M, Steffen HM, Nürnberg P, Büttner R, Teufel A, Dienes HP, Drebber U, Odenthal M. Control of mitogenic and motogenic pathways by miR-198, diminishing hepatoma cell growth and migration. *Biochim Biophys Acta*. 2013, **1833**(5):1190-1198. doi: 10.1016/j.bbamcr.2013.01.023.
267. Epis MR, Giles KM, Barker A, Kendrick TS, Leedman PJ. miR-331-3p regulates ERBB-2 expression and androgen receptor signaling in prostate cancer. *J Biol Chem*. 2009, *284*(37):24696-24704. doi: 10.1074/jbc.M109.030098.
268. Lin F, Ding R, Zheng S, Xing D, Hong W, Zhou Z, Shen J. Decrease expression of microRNA-744 promotes cell proliferation by targeting c-Myc in human hepatocellular carcinoma. *Cancer Cell Int*. 2014, **14**:58. doi: 10.1186/1475-2867-14-58.
269. Tousoulis D, Böger RH, Antoniades C, Siasos G, Stefanadi E, Stefanadis C. Mechanisms of disease: L-arginine in coronary

atherosclerosis--a clinical perspective. *Nat Clin Pract Cardiovasc Med*. 2007, **4**(5):274-283.
270. Perry HM, Bender TP, McNamara CA. B cell subsets in atherosclerosis. *Front Immunol*. 2012, **3**:373. doi: 10.3389/fimmu.2012.00373.
271. Weber C, Fraemohs L, Dejana E. The role of junctional adhesion molecules in vascular inflammation. *Nat Rev Immunol*. 2007, **7**(6):467-477.
272. Wen FQ, Jabbar AA, Patel DA, Kazarian T, Valentino LA. Atherosclerotic aortic gangliosides enhance integrin-mediated platelet adhesion to collagen. *Arterioscler Thromb Vasc Biol*. 1999, **19**(3):519-524.
273. Takano K, Yamaguchi T, Kato H, Omae T. Activation of coagulation in acute cardioembolic stroke. *Stroke*. 1991, **22**(1):12-16.
274. Kostin S, Klein G, Szalay Z, Hein S, Bauer EP, Schaper J. Structural correlate of atrial fibrillation in human patients. *Cardiovasc Res*. 2002, **54**(2):361-379.
275. Wang X, Zhang X, Ren XP, Chen J, Liu H, Yang J, Medvedovic M, Hu Z, Fan GC. MicroRNA-494 targeting both proapoptotic and antiapoptotic proteins protects against ischemia/reperfusion-induced cardiac injury. *Circulation*. 2010, **122**(13):1308-1318. doi: 10.1161/CIRCULATIONAHA.
276. Muiños-Gimeno M, Espinosa-Parrilla Y, Guidi M, Kagerbauer B, Sipilä T, Maron E, Pettai K, Kananen L, Navinés R, Martín-Santos R, Gratacòs M, Metspalu A, Hovatta I, Estivill X. Human microRNAs miR-22, miR-138-2, miR-148a, and miR-488 are associated with panic disorder and regulate several anxiety candidate genes and related pathways. *Biol Psychiatry*. 2011, **69**(6):526-533. doi: 10.1016/j.biopsych.2010.10.010
277. Sun G, Zhou Y, Li H, Guo Y, Shan J, Xia M, Li Y, Li S, Long D, Feng L. Over-expression of microRNA-494 up-regulates hypoxia-inducible factor-1 alpha expression via PI3K/Akt pathway and protects against hypoxia-induced apoptosis. *J Biomed Sci*. 2013, *20*:100. doi: 10.1186/1423-0127-20-100.
278. Stigliani, S., Scaruffi, P., Lagazio, C., Persico, L., Carlini, B., Varesio, L., Morandi, F., Morini, M., Gigliotti, A., Esposito, M., Viscardi, E., Cecinati, V., Conte, M., & Corrias, M.. Deregulation of focal adhesion pathway mediated by miR-659-3p is implicated in bone marrow infiltration of stage M neuroblastoma patients. *Oncotarget*, 2015, **5** Ahead of print
279. Li W, Chen L1, Li W, Qu X, He W, He Y, Feng C, Jia X, Zhou Y, Lv J, Liang B, Chen B, Jiang J. Unraveling the characteristics of microRNA regulation in the developmental and aging process of the human brain. *BMC Med Genomics*. 2013, **6**:55. doi: 10.1186/1755-8794-6-55.
280. Sepramaniam S, Armugam A, Lim KY, Karolina DS, Swaminathan P, Tan JR, Jeyaseelan K. MicroRNA 320a functions as a novel endogenous modulator of aquaporins 1 and 4 as well as a potential therapeutic target in cerebral ischemia. *J Biol Chem.* 2010, **285**(38):29223-29230. doi: 10.1074/jbc.M110.144576.

281. Harraz MM, Eacker SM, Wang X, Dawson TM, Dawson VL. MicroRNA-223 is neuroprotective by targeting glutamate receptors. *Proc Natl Acad Sci U S A*. 2012, **109**(46):18962-18967. doi: 10.1073/pnas.1121288109.
282. Zhang L, Dong LY, Li YJ, Hong Z, Wei WS. The microRNA miR-181c controls microglia-mediated neuronal apoptosis by suppressing tumor necrosis factor. *J Neuroinflammation*. 2012, **9**:211. doi: 10.1186/1742-2094-9-211.
283. Zhang L, Dong LY, Li YJ, Hong Z, Wei WS. miR-21 represses FasL in microglia and protects against microglia-mediated neuronal cell death following hypoxia/ischemia. *Glia*. 2012, **60**(12):1888-18895. doi: 10.1002/glia.22404.
284. Sun Y, Gui H, Li Q, Luo ZM, Zheng MJ, Duan JL, Liu X. MicroRNA-124 protects neurons against apoptosis in cerebral ischemic stroke. *CNS Neurosci Ther*. 2013, **19**(10):813-819. doi: 10.1111/cns.12142.
285. Doeppner TR, Doehring M, Bretschneider E, Zechariah A, Kaltwasser B, Müller B, Koch JC, Bähr M, Hermann DM, Michel U. MicroRNA-124 protects against focal cerebral ischemia via mechanisms involving Usp14-dependent REST degradation. *Acta Neuropathol*. 2013, **126**(2):251-865. doi: 10.1007/s00401-013-1142-5.
286. Liu XS, Chopp M, Zhang RL, Tao T, Wang XL, Kassis H, Hozeska-Solgot A, Zhang L, Chen C, Zhang ZG. MicroRNA profiling in subventricular zone after stroke: MiR-124a regulates proliferation of neural progenitor cells through Notch signaling pathway. *PLoS One*. 2011, **6**(8):e23461. doi: 10.1371/journal.pone.0023461.
287. Zhu F, Liu JL, Li JP, Xiao F, Zhang ZX, Zhang L. MicroRNA-124 (miR-124) regulates Ku70 expression and is correlated with neuronal death induced by ischemia/reperfusion. *J Mol Neurosci*. 2014, **52**(1):148-155. doi: 10.1007/s12031-013-0155-9.
288. Ouyang YB, Xu L, Lu Y, Sun X, Yue S, Xiong XX, Giffard RG. Astrocyte-enriched miR-29a targets PUMA and reduces neuronal vulnerability to forebrain ischemia. *Glia*. 2013, **61**(11):1784-1794. doi: 10.1002/glia.22556.
289. Khanna S, Rink C, Ghoorkhanian R, Gnyawali S, Heigel M, Wijesinghe DS, Chalfant CE, Chan YC, Banerjee J, Huang Y, Roy S, Sen CK. Loss of miR-29b following acute ischemic stroke contributes to neural cell death and infarct size. *J Cereb Blood Flow Metab*. 2013, **33**(8):1197-1206. doi: 10.1038/jcbfm.2013.68.
290. Pandi G, Nakka VP, Dharap A, Roopra A, Vemuganti R. MicroRNA miR-29c down-regulation leading to de-repression of its target DNA methyltransferase 3a promotes ischemic brain damage. *PLoS One*. 2013, **8**(3):e58039. doi: 10.1371/journal.pone.0058039.
291. Qu Y, Wu J, Chen D, Zhao F, Liu J, Yang C, Wei D, Ferriero DM, Mu D. MiR-139-5p inhibits HGTD-P and regulates neuronal apoptosis induced by hypoxia-ischemia in neonatal rats. *Neurobiol Dis*. 2014, **63**:184-193. doi: 10.1016/j.nbd.2013.11.023.
292. Li LJ, Huang Q, Zhang N, Wang GB, Liu YH. miR-376b-5p regulates angiogenesis in cerebral ischemia. *Mol Med Rep*. 2014, **10**(1):527-535. doi: 10.3892/mmr.2014.2172.

293. Wang Y, Dong X, Li Z, Wang W, Tian J, Chen J. Downregulated RASD1 and upregulated miR-375 are involved in protective effects of calycosin on cerebral ischemia/reperfusion rats. *J Neurol Sci*. 2014, **339**(1-2):144-148. doi: 10.1016/j.jns.2014.02.002.
294. Song G, Zhang Y, Wang L. MicroRNA-206 targets notch3, activates apoptosis, and inhibits tumor cell migration and focus formation. *J Biol Chem*. 2009, **284**(46):31921-31927. doi: 10.1074/jbc.M109.046862.
295. Shan ZX, Lin QX, Fu YH, Deng CY, Zhou ZL, Zhu JN, Liu XY, Zhang YY, Li Y, Lin SG, Yu XY. Upregulated expression of miR-1/miR-206 in a rat model of myocardial infarction. *Biochem Biophys Res Commun*. 2009, **381**(4):597-601. doi: 10.1016/j.bbrc.2009.02.097
296. Lee ST, Chu K, Jung KH, Kim JH, Huh JY, Yoon H, Park DK, Lim JY, Kim JM, Jeon D, Ryu H, Lee SK, Kim M, Roh JK. miR-206 regulates brain-derived neurotrophic factor in Alzheimer disease model. *Ann Neurol*. 2012, **72**(2):269-277. doi: 10.1002/ana.23588.
297. Yamashita K, Wiessner C, Lindholm D, Thoenen H, Hossmann KA. Post-occlusion treatment with BDNF reduces infarct size in a model of permanent occlusion of the middle cerebral artery in rat. *Metab Brain Dis*. 1997, **12**(4):271-280.
298. Schäbitz WR, Schwab S, Spranger M, Hacke W. Intraventricular brain-derived neurotrophic factor reduces infarct size after focal cerebral ischemia in rats. *J Cereb Blood Flow Metab*. 1997, **17**(5):500-506.
299. Hayakawa K, Qiu J, Lo EH. Biphasic actions of HMGB1 signaling in inflammation and recovery after stroke. *Ann N Y Acad Sci*. 2010, **1207**:50-57. doi: 10.1111/j.1749-6632.2010.05728.x.
300. Liao CG, Kong LM, Zhou P, Yang XL, Huang JG, Zhang HL, Lu N. miR-10b is overexpressed in hepatocellular carcinoma and promotes cell proliferation, migration and invasion through RhoC, uPAR and MMPs. *J Transl Med*. 2014, **12**(1):234.
301. Du C, Liu C, Kang J, Zhao G, Ye Z, Huang S, Li Z, Wu Z, Pei G. MicroRNA miR-326 regulates TH-17 differentiation and is associated with the pathogenesis of multiple sclerosis. *Nat Immunol*. 2009, **10**(12):1252-1259. doi: 10.1038/ni.1798.
302. Hu Y, Zheng Y, Wu Y, Ni B, Shi S. Imbalance between IL-17A-producing cells and regulatory T cells during ischemic stroke. *Mediators Inflamm*. 2014, **2014**:813045. doi: 10.1155/2014/813045.
303. Lakhan SE, Kirchgessner A, Hofer M. Inflammatory mechanisms in ischemic stroke: therapeutic approaches. *J Transl Med*. 2009, **7**:97. doi: 10.1186/1479-5876-7-97.
304. Lipton P. Ischemic cell death in brain neurons. *Physiol Rev*. 1999, **79**(4):1431-1568.
305. Chao N, Li ST. Synaptic and extrasynaptic glutamate signaling in ischemic stroke. *Curr Med Chem*. 2014, **21**(18):2043-2064.
306. Zöllner JP, Hattingen E, Singer OC, Pilatus U. Changes of pH and Energy State in Subacute Human Ischemia Assessed by Multinuclear Magnetic Resonance Spectroscopy. *Stroke*. 2015, **46**(2):441-446. doi: 10.1161/STROKEAHA.114.007896.
307. Liu J, Wang Y, Akamatsu Y, Lee CC, Stetler RA, Lawton MT, Yang GY. Vascular remodeling after ischemic stroke: mechanisms and

therapeutic potentials. *Prog Neurobiol*. 2014, **115**:138-156. doi: 10.1016/j.pneurobio.2013.11.004.
308. Seifert PS, Hansson GK. Complement receptors and regulatory proteins in human atherosclerotic lesions. *Arteriosclerosis*. 1989, **9**(6):802-811.
309. Li SH, Szmitko PE, Weisel RD, Wang CH, Fedak PW, Li RK, Mickle DA, Verma S. C-reactive protein upregulates complement-inhibitory factors in endothelial cells. *Circulation*. 2004, **109**(7):833-836.
310. Song HO, Kim JH, Ryu HS, Lee DH, Kim SJ, Kim DJ, Suh IB, Choi du Y, In KH, Kim SW, Park H. Polymeric LabChip real-time PCR as a point-of-care-potential diagnostic tool for rapid detection of influenza A/H1N1 virus in human clinical specimens. *PLoS One*. 2012, **7**(12):e53325. doi: 10.1371/journal.pone.0053325.
311. Wahlestedt C, Salmi P, Good L, Kela J, Johnsson T, Hökfelt T, Broberger C, Porreca F, Lai J, Ren K, Ossipov M, Koshkin A, Jakobsen N, Skouv J, Oerum H, Jacobsen MH, Wengel J. Potent and nontoxic antisense oligonucleotides containing locked nucleic acids. *Proc Natl Acad Sci U S A*. 2000, **97**(10):5633-5638.
312. Lv H, Zhang S, Wang B, Cui S, Yan J. Toxicity of cationic lipids and cationic polymers in gene delivery. *J Control Release*. 2006, **114**(1):100-109.
313. Lanford RE, Hildebrandt-Eriksen ES, Petri A, Persson R, Lindow M, Munk ME, Kauppinen S, Ørum H. Therapeutic silencing of microRNA-122 in primates with chronic hepatitis C virus infection. *Science*. 2010, **327**(5962):198-201. doi: 10.1126/science.1178178.
314. Liu C, Kelnar K, Liu B, Chen X, Calhoun-Davis T, Li H, Patrawala L, Yan H, Jeter C, Honorio S, Wiggins JF, Bader AG, Fagin R, Brown D, Tang DG. The microRNA miR-34a inhibits prostate cancer stem cells and metastasis by directly repressing CD44. *Nat Med*. 2011, **17**(2):211-215. doi: 10.1038/nm.2284.
315. Trang P, Wiggins JF, Daige CL, Cho C, Omotola M, Brown D, Weidhaas JB, Bader AG, Slack FJ. Systemic delivery of tumor suppressor microRNA mimics using a neutral lipid emulsion inhibits lung tumors in mice. *Mol Ther*. 2011 Jun;**19**(6):1116-1122. doi: 10.1038/mt.2011.48.
316. Hydbring P and Badalian-Very G. Clinical applications of microRNAs *F1000Research* 2013, **2**:136 doi: 10.12688/f1000research.2-136.v1.

# Supplementary Data

**Supplementary Table 1**: Expression of 352 miRNAs detected in acute ischemic stroke patients. MiRNAs were expressed as fold change compared with normal control. All miRNAs selected have positive raw intensity values and FDR < 0.05. ND represents not detected. LA: large artery stroke. CE: cardioembolic stroke. SV: small vessel stroke.

| Hsa-miRNA | IS 24hr | IS 48hr | IS 168hr | LA 24hr | LA 48hr | LA 168hr | CE 24hr | CE 48hr | CE 168hr | SV 24hr | SV 48hr | SV 168hr |
|---|---|---|---|---|---|---|---|---|---|---|---|---|
| Let-7a | 1.64 | 2.09 | 3.00 | 1.70 | 1.86 | 1.99 | 2.58 | 1.80 | 2.34 | 1.05 | 1.08 | -1.09 |
| Let-7a* | 3.54 | 2.83 | 5.69 | 4.13 | 4.22 | 6.89 | 4.84 | 3.51 | 4.26 | -1.27 | 2.22 | 2.49 |
| Let-7b | 1.00 | 1.56 | 1.97 | 1.00 | 1.25 | 1.03 | 1.87 | -1.05 | 1.28 | -1.45 | -1.38 | -1.90 |
| Let-7b* | 1.26 | 1.29 | 1.61 | 1.40 | 1.48 | 1.57 | 2.45 | 1.22 | 1.79 | -3.08 | -1.13 | -1.42 |
| Let-7c | 1.25 | 1.85 | 2.23 | 1.22 | 1.84 | 1.62 | 2.69 | 1.29 | 1.85 | -1.10 | -1.08 | -1.44 |
| Let-7d | 2.43 | 3.21 | 4.66 | 2.18 | 2.97 | 3.04 | 4.72 | 2.25 | 3.99 | 1.30 | 1.49 | 1.28 |
| Let-7d* | -3.70 | -4.75 | -2.51 | -2.20 | -2.26 | -2.94 | -2.35 | -2.69 | -2.16 | -13.00 | -3.86 | -4.65 |
| Let-7e | 3.19 | 4.00 | 5.81 | 2.72 | 3.83 | 4.08 | 5.41 | 2.60 | 3.91 | 1.99 | 2.08 | 1.67 |
| Let-7f | 1.49 | 1.79 | 2.57 | 1.54 | 1.60 | 1.77 | 2.21 | 1.62 | 2.01 | 1.01 | 1.00 | 1.31 |
| Let-7g | 1.50 | 2.32 | 3.62 | 1.52 | 2.30 | 2.08 | 3.38 | 1.72 | 3.22 | -1.89 | -1.55 | -1.63 |
| Let-7i | 1.30 | 2.00 | 3.13 | 1.16 | 1.98 | 1.60 | 3.11 | 1.28 | 2.69 | -2.09 | -1.84 | -1.96 |
| miR-7 | 1.35 | 1.64 | 2.80 | 1.08 | 1.42 | 1.70 | 2.83 | 1.14 | 2.55 | -1.75 | -1.57 | -1.68 |
| miR-15a | 1.73 | 2.08 | 2.97 | 1.79 | 1.85 | 2.05 | 2.57 | 1.88 | 2.33 | 2.06 | 1.16 | 1.98 |
| miR-15b | 1.15 | 1.38 | 1.98 | 1.19 | 1.23 | 1.37 | 1.71 | 1.25 | 1.55 | 1.21 | -1.28 | 1.32 |
| miR-15b* | 7.81 | 6.55 | 13.07 | 8.24 | 7.56 | 12.53 | 16.42 | 6.38 | 13.15 | 1.40 | 3.21 | 3.22 |
| miR-16 | 1.15 | 1.38 | 1.99 | 1.19 | 1.23 | 1.36 | 1.71 | 1.25 | 1.55 | 1.56 | -1.28 | 1.32 |
| miR-16-2* | 2.60 | 2.80 | 5.03 | 3.27 | 3.40 | 3.91 | 5.23 | 2.16 | 4.26 | -2.45 | -1.08 | -1.68 |
| miR-17 | 1.92 | 2.31 | 3.31 | 1.99 | 2.06 | 2.28 | 2.85 | 2.09 | 2.59 | 1.05 | 1.22 | 1.07 |
| miR-17* | 3.67 | 3.58 | 7.12 | 3.43 | 3.90 | 6.57 | 6.43 | 3.12 | 6.02 | -1.03 | 2.22 | 2.01 |
| miR-18a | 2.67 | 2.91 | 5.06 | 2.57 | 3.13 | 3.76 | 5.86 | 2.73 | 4.98 | -1.59 | 1.44 | 1.08 |
| miR-18a* | -1.02 | -1.06 | 1.14 | -1.03 | 1.15 | 1.14 | 1.35 | -1.10 | 1.14 | -2.13 | -1.21 | -1.61 |

| Hsa-miRNA | IS 24hr | IS 48hr | IS 168hr | LA 24hr | LA 48hr | LA 168hr | CE 24hr | CE 48hr | CE 168hr | SV 24hr | SV 48hr | SV 168hr |
|---|---|---|---|---|---|---|---|---|---|---|---|---|
| miR-18b | 2.11 | 2.41 | 4.15 | 2.15 | 2.72 | 3.45 | 5.01 | 2.25 | 4.02 | -1.61 | 1.19 | 1.00 |
| miR-19a | 1.87 | 2.25 | 3.22 | 1.93 | 2.00 | 2.02 | 2.77 | 2.03 | 2.52 | 1.26 | 1.25 | 1.75 |
| miR-19b | 2.63 | 3.16 | 4.53 | 2.72 | 2.82 | 3.12 | 3.91 | 2.87 | 3.54 | 1.57 | 1.77 | 2.69 |
| miR-20a | 1.02 | 1.43 | 2.42 | 1.29 | 1.89 | 1.70 | 2.66 | 1.36 | 2.31 | -2.43 | -1.59 | -1.83 |
| miR-20a* | 3.63 | 4.02 | 7.49 | 4.15 | 4.56 | 6.03 | 7.45 | 3.54 | 7.89 | -12.06 | 1.93 | 1.49 |
| miR-20b | 2.70 | 2.71 | 3.85 | 2.43 | 3.82 | 4.47 | 5.12 | 2.15 | 3.69 | -1.26 | 1.58 | 1.40 |
| miR-20b* | 2.35 | 2.50 | 5.94 | 2.34 | 2.08 | 2.66 | 2.40 | 1.99 | 2.16 | 1.18 | 2.68 | 3.14 |
| miR-21 | 9.73 | 11.03 | 17.18 | 10.09 | 10.67 | 11.82 | 14.79 | 10.70 | 13.42 | 4.53 | 4.76 | 5.56 |
| miR-22 | 1.17 | 1.40 | 2.01 | 1.21 | 1.25 | 1.38 | 1.73 | 1.27 | 1.57 | 1.08 | -1.27 | 1.21 |
| miR-22* | -1.07 | 1.05 | 1.36 | 1.03 | 1.20 | 1.47 | 1.75 | -1.14 | 1.76 | -3.04 | -1.20 | -1.51 |
| miR-23a | 1.19 | 1.69 | 2.50 | 1.17 | 1.48 | 1.68 | 1.67 | 1.06 | 1.71 | 1.16 | 1.24 | 1.09 |
| miR-23b | 1.61 | 2.06 | 2.85 | 1.41 | 2.12 | 2.39 | 2.33 | 1.39 | 2.07 | 1.24 | 1.53 | 1.23 |
| miR-24 | 1.31 | 1.75 | 2.83 | 1.16 | 1.42 | 1.67 | 2.01 | 1.17 | 2.14 | -1.46 | -1.10 | -1.14 |
| miR-24-1* | 1.88 | 1.64 | 1.73 | 1.32 | 1.45 | 1.84 | 2.10 | 1.14 | 1.45 | 2.09 | 1.55 | -1.02 |
| miR-25 | 4.21 | 4.10 | 6.48 | 4.11 | 4.98 | 5.71 | 6.01 | 3.41 | 5.39 | 2.21 | 3.07 | 2.81 |
| miR-25* | 2.45 | 3.33 | 3.82 | 2.40 | 2.53 | 2.96 | 2.70 | 2.50 | 2.12 | 2.48 | 1.93 | 2.00 |
| miR-26a | 2.00 | 2.84 | 4.29 | 2.02 | 2.75 | 3.01 | 3.80 | 1.85 | 3.04 | -1.27 | 1.06 | -1.03 |
| miR-26a-2* | -3.15 | -1.79 | 1.74 | 1.34 | -1.12 | 2.03 | -1.06 | -1.19 | 1.29 | ND | 1.26 | -1.34 |
| miR-26b | 1.78 | 2.14 | 3.06 | 1.84 | 1.90 | 2.11 | 2.64 | 1.94 | 2.39 | -1.27 | 1.19 | 1.38 |
| miR-26b* | 1.28 | 1.04 | 2.42 | 2.39 | 2.29 | 3.59 | 2.18 | 2.11 | 1.83 | -1.40 | 2.85 | 1.85 |
| miR-27a | 3.57 | 4.71 | 6.53 | 3.34 | 4.63 | 6.61 | 5.13 | 2.84 | 5.06 | 2.69 | 3.80 | 3.59 |
| miR-27a* | 5.55 | 9.92 | 10.23 | 6.69 | 6.86 | 10.87 | 6.06 | 6.03 | 4.55 | 5.05 | 5.34 | 4.35 |
| miR-28-5p | 2.81 | 2.92 | 4.64 | 2.23 | 3.35 | 3.16 | 5.81 | 2.64 | 4.69 | -1.03 | 1.46 | 1.57 |
| miR-29a | 5.14 | 5.53 | 10.72 | 5.14 | 5.59 | 8.00 | 12.14 | 4.38 | 9.52 | 2.16 | 2.63 | 2.21 |
| miR-29a* | 2.12 | ND | ND | 5.45 | 6.47 | 7.23 | 6.66 | 4.71 | 3.32 | 1.61 | 5.41 | 4.25 |
| miR-29b | 6.35 | 6.27 | 10.99 | 5.81 | 6.99 | 10.71 | 12.16 | 5.62 | 10.81 | 2.41 | 3.65 | 3.82 |

| Hsa-miRNA | IS 24hr | IS 48hr | IS 168hr | LA 24hr | LA 48hr | LA 168hr | CE 24hr | CE 48hr | CE 168hr | SV 24hr | SV 48hr | SV 168hr |
|---|---|---|---|---|---|---|---|---|---|---|---|---|
| miR-29b-2* | 3.14 | 3.24 | 3.64 | 2.01 | 2.67 | 3.65 | 4.08 | 2.35 | 4.25 | 1.04 | 2.34 | 1.95 |
| miR-29c | 6.39 | 6.61 | 13.48 | 5.94 | 6.08 | 8.74 | 14.80 | 5.69 | 12.56 | 1.35 | 2.74 | 2.29 |
| miR-29c* | 2.91 | 3.21 | 4.85 | 3.68 | 4.43 | 5.45 | 5.51 | 2.60 | 5.69 | 2.02 | 2.54 | 1.73 |
| miR-30a | 1.53 | 1.84 | 2.64 | 1.59 | 1.60 | 1.82 | 2.21 | 1.67 | 2.07 | -1.29 | 1.03 | 1.29 |
| miR-30b | 1.64 | 2.13 | 3.29 | 1.53 | 2.11 | 2.41 | 3.64 | 1.52 | 3.01 | -1.48 | -1.24 | -1.51 |
| miR-30c | 1.21 | 1.52 | 2.62 | 1.14 | 1.71 | 1.90 | 2.81 | 1.18 | 2.51 | -2.84 | -1.47 | -1.70 |
| miR-30d | 1.22 | 1.30 | 1.62 | 1.25 | 1.58 | 1.59 | 1.86 | 1.20 | 1.37 | -1.73 | -1.01 | -1.28 |
| miR-30e | 1.48 | 2.08 | 3.67 | 1.51 | 2.21 | 2.65 | 3.44 | 1.49 | 2.53 | -2.14 | -1.25 | -1.47 |
| miR-30e* | 1.61 | 1.97 | 3.24 | 1.47 | 2.20 | 2.63 | 3.43 | 1.57 | 2.74 | -1.75 | -1.10 | -1.27 |
| miR-32 | 8.39 | 8.49 | 17.49 | 9.18 | 8.92 | 15.90 | 20.00 | 8.16 | 14.20 | 3.00 | 2.82 | 3.58 |
| miR-32* | -2.64 | -1.98 | -1.63 | -1.99 | -1.92 | -2.27 | -1.62 | -1.72 | -1.95 | -2.43 | -2.59 | -3.01 |
| miR-33a | 38.94 | 37.02 | 100.04 | 50.54 | 44.51 | 121.51 | 68.33 | 43.26 | 80.84 | 8.92 | 23.92 | 43.69 |
| miR-34b | 2.82 | 3.46 | 4.94 | 2.12 | 2.34 | 3.36 | 2.92 | 1.89 | 1.77 | 3.09 | 1.93 | 2.36 |
| miR-92a | 1.18 | 1.06 | 1.53 | 1.01 | -1.03 | 1.50 | 1.33 | -1.12 | 1.02 | -1.36 | 1.01 | -1.08 |
| miR-92b | 1.85 | 1.63 | 2.15 | 1.52 | 1.62 | 1.98 | 2.01 | 1.35 | 1.50 | 1.01 | 1.57 | 1.37 |
| miR-93 | 1.48 | 1.78 | 2.55 | 1.37 | 1.58 | 1.75 | 2.20 | 1.61 | 1.99 | 1.40 | -1.00 | 1.42 |
| miR-93* | -1.89 | -2.26 | -1.82 | -1.10 | -1.10 | 1.27 | 1.36 | -1.38 | 1.03 | -3.18 | -1.24 | -1.89 |
| miR-96 | 2.18 | 2.87 | 4.75 | 2.26 | 3.46 | 3.71 | 4.93 | 2.47 | 4.09 | -1.37 | 1.24 | 1.28 |
| miR-98 | 4.24 | 5.09 | 8.60 | 2.57 | 3.99 | 5.81 | 7.10 | 2.76 | 6.19 | 2.44 | 2.38 | 2.37 |
| miR-99a | 1.28 | 2.20 | 3.85 | 1.12 | 2.10 | 1.32 | 2.33 | 2.34 | 1.36 | -1.88 | -1.49 | -2.93 |
| miR-99b* | 1.55 | 1.59 | 1.89 | 1.44 | 1.58 | 2.44 | 1.85 | 1.15 | 1.18 | 1.69 | 1.87 | 1.54 |
| miR-101 | 3.45 | 4.15 | 5.94 | 3.57 | 3.54 | 4.09 | 5.12 | 3.75 | 4.64 | 1.59 | 2.32 | 3.02 |
| miR-101* | 6.52 | 5.19 | 10.22 | 7.76 | 10.59 | 11.79 | 13.72 | 6.18 | 11.12 | 1.52 | 3.22 | 2.84 |
| miR-103 | 2.83 | 3.40 | 4.87 | 2.92 | 3.03 | 3.35 | 4.19 | 3.08 | 3.81 | 2.13 | 1.90 | 2.34 |
| miR-106a | 2.26 | 2.72 | 3.90 | 2.34 | 2.42 | 2.68 | 3.36 | 2.46 | 3.05 | -1.41 | 1.50 | 1.34 |
| miR-106a* | -19.54 | ND | ND | 3.82 | 3.76 | 5.18 | 4.53 | 2.07 | 3.04 | ND | 1.62 | -5.21 |

| Hsa-miRNA | IS 24hr | IS 48hr | IS 168hr | LA 24hr | LA 48hr | LA 168hr | CE 24hr | CE 48hr | CE 168hr | SV 24hr | SV 48hr | SV 168hr |
|---|---|---|---|---|---|---|---|---|---|---|---|---|
| miR-106b | 1.44 | 1.73 | 2.48 | 1.49 | 1.54 | 1.71 | 2.11 | 1.57 | 1.94 | 1.18 | -1.03 | 1.17 |
| miR-106b* | 1.58 | 1.86 | 2.66 | 1.52 | 1.67 | 1.92 | 2.44 | 1.20 | 2.05 | -1.21 | 1.10 | -1.16 |
| miR-107 | 2.34 | 2.98 | 4.03 | 2.44 | 3.12 | 3.35 | 4.40 | 2.46 | 3.99 | 1.48 | 1.66 | 1.41 |
| miR-122 | -38.66 | ND | -2.02 | -2.36 | -3.21 | -1.37 | -2.20 | -2.86 | -3.39 | -2.80 | -1.98 | 1.12 |
| miR-122* | -1.48 | ND | ND | -1.35 | -1.11 | 1.24 | ND | -1.18 | ND | 1.00 | 1.71 | 1.27 |
| miR-124* | 2.47 | ND | ND | 5.21 | 1.19 | 6.93 | -1.46 | 3.19 | -1.33 | ND | 4.56 | 4.31 |
| miR-125a-5p | 1.02 | -1.12 | -1.33 | 1.00 | -1.30 | 1.18 | -1.42 | -1.40 | -1.41 | -1.76 | 1.02 | -1.41 |
| miR-125b | -2.21 | -1.34 | -1.65 | -1.02 | -1.25 | -1.23 | -1.21 | -1.34 | -1.11 | -27.06 | -2.51 | -6.13 |
| miR-125b-1* | 2.05 | 2.11 | 2.44 | 2.27 | 2.23 | 2.84 | 2.81 | 2.16 | 2.10 | 1.42 | 2.11 | 1.44 |
| miR-125b-2* | 4.19 | 3.06 | 2.25 | 6.58 | 5.48 | 7.20 | 5.01 | 6.17 | 4.69 | 2.44 | 4.62 | 3.34 |
| miR-126 | 1.23 | 1.48 | 2.36 | 1.42 | 1.78 | 1.96 | 2.27 | 1.18 | 2.29 | -1.86 | -1.58 | -1.89 |
| miR-126* | 4.04 | 4.99 | 9.20 | 5.29 | 6.27 | 7.27 | 8.10 | 4.38 | 7.61 | -1.19 | 1.57 | 1.93 |
| miR-128 | -1.12 | -1.36 | 1.93 | 1.80 | 2.12 | 2.58 | 3.30 | 1.77 | 3.15 | ND | 1.26 | -1.14 |
| miR-129* | 3.49 | -1.00 | -2.58 | 2.30 | 1.88 | 3.17 | -1.13 | 1.90 | 1.58 | 2.26 | 3.84 | 3.31 |
| miR-129-5p | 2.48 | 2.09 | 3.15 | 3.20 | 3.29 | 3.18 | 2.75 | 2.90 | 2.53 | 2.00 | 1.76 | 2.05 |
| miR-130a | 1.19 | 1.65 | 2.17 | 1.31 | 1.65 | 1.63 | 1.67 | 1.16 | 1.48 | -3.35 | -1.30 | -1.77 |
| miR-130b | 1.23 | 1.45 | 1.92 | 1.13 | 1.44 | 1.47 | 2.00 | 1.08 | 1.59 | -1.11 | 1.00 | -1.38 |
| miR-130b* | 1.57 | -1.47 | -1.09 | 1.89 | 1.96 | 3.25 | -1.81 | 1.25 | 1.15 | 2.63 | 2.57 | 1.57 |
| miR-132* | -1.71 | ND | ND | 1.62 | 1.38 | 1.94 | 1.67 | 1.82 | 1.44 | -1.25 | 1.82 | 2.29 |
| miR-135b | 1.90 | 1.96 | 3.39 | 3.87 | 4.88 | 7.02 | 6.78 | 3.62 | 4.58 | 1.58 | 2.21 | 2.07 |
| miR-138-1* | 1.74 | 1.82 | 1.91 | 1.35 | 1.83 | 2.41 | 2.50 | 1.30 | 1.24 | 2.18 | 1.70 | 1.43 |
| miR-138-2* | 2.01 | 1.87 | 1.42 | 1.52 | 1.55 | 3.19 | 2.42 | -1.18 | 1.11 | 1.69 | 2.53 | 1.43 |
| miR-140-3p | 1.11 | 1.53 | 2.12 | -1.01 | 1.39 | 1.31 | 2.10 | 1.13 | 1.74 | -2.31 | -1.24 | -1.52 |
| miR-140-5p | 7.27 | 9.12 | 17.60 | 6.50 | 9.30 | 14.93 | 15.41 | 7.08 | 13.24 | 3.44 | 4.52 | 4.63 |
| miR-142-3p | 1.73 | 2.07 | 2.97 | 1.78 | 1.85 | 2.04 | 2.56 | 1.88 | 2.32 | 1.80 | 1.16 | 1.97 |
| miR-142-5p | 1.86 | 2.17 | 3.32 | 1.98 | 2.06 | 2.29 | 2.86 | 1.74 | 2.60 | -1.54 | 1.05 | -1.18 |

| Hsa-miRNA | IS 24hr | IS 48hr | IS 168hr | LA 24hr | LA 48hr | LA 168hr | CE 24hr | CE 48hr | CE 168hr | SV 24hr | SV 48hr | SV 168hr |
|---|---|---|---|---|---|---|---|---|---|---|---|---|
| miR-143 | 3.08 | 4.00 | 8.47 | 3.75 | 5.36 | 8.24 | 5.52 | 4.47 | 6.23 | 1.15 | 2.88 | 4.83 |
| miR-144 | 1.19 | 1.43 | 2.04 | 1.23 | 1.27 | 1.41 | 1.76 | 1.29 | 1.60 | 1.61 | -1.25 | 1.36 |
| miR-144* | 2.93 | 3.52 | 5.05 | 3.03 | 3.14 | 3.47 | 4.35 | 3.19 | 3.95 | 2.76 | 1.97 | 2.59 |
| miR-145 | 2.58 | 2.08 | 2.79 | 2.54 | 3.34 | 6.70 | 2.25 | 2.17 | 1.58 | -1.01 | 3.55 | 4.88 |
| miR-145* | 1.54 | -1.99 | ND | 2.03 | 2.48 | 2.22 | 2.23 | 1.53 | 1.00 | 2.39 | 2.17 | 1.78 |
| miR-146a | 1.60 | 2.17 | 3.29 | 2.19 | 2.94 | 2.97 | 3.04 | 2.23 | 3.39 | -2.24 | 1.23 | -1.42 |
| miR-146b-3p | 1.30 | 1.38 | 1.19 | 1.61 | 1.45 | 1.63 | 1.25 | 9.76 | 1.32 | 1.49 | 1.72 | 1.50 |
| miR-146b-5p | 1.18 | 5.61 | 2.23 | 1.27 | 1.76 | 1.86 | 2.39 | 1.34 | 2.43 | -1.53 | -1.37 | -1.96 |
| miR-148a | 2.82 | 3.30 | 5.75 | 3.61 | 5.59 | 7.38 | 6.90 | 3.30 | 5.06 | 1.42 | 2.85 | 2.77 |
| miR-148b | -1.35 | -1.13 | 1.52 | -1.10 | 1.28 | 1.26 | 1.79 | -1.11 | 1.60 | -4.93 | -1.92 | -2.25 |
| miR-149* | -1.09 | 1.04 | 1.24 | 1.34 | 1.67 | 1.10 | 1.68 | 1.49 | 1.15 | 1.07 | -1.34 | -1.41 |
| miR-150 | -2.76 | -3.97 | -5.90 | -1.11 | -1.18 | -1.15 | -1.48 | -1.47 | -1.80 | -1.46 | -1.15 | -1.62 |
| miR-151-3p | 1.37 | 1.67 | 2.91 | 1.20 | 1.32 | 1.55 | 2.62 | 1.21 | 2.44 | -4.90 | -1.56 | -1.41 |
| miR-151-5p | 1.42 | 1.68 | 2.69 | 1.22 | 1.80 | 1.60 | 2.93 | 1.48 | 2.65 | -2.67 | -1.40 | -1.35 |
| miR-155 | -1.54 | -1.25 | -1.01 | 1.01 | 1.12 | 1.39 | 1.49 | -1.06 | 1.48 | -4.03 | -1.43 | -1.89 |
| miR-181a | 1.61 | 2.15 | 2.95 | 1.73 | 1.97 | 2.09 | 2.78 | 1.52 | 2.37 | -1.19 | 1.12 | -1.02 |
| miR-181a-2* | 3.58 | 2.67 | 3.60 | 2.47 | 1.65 | 6.07 | 1.02 | 1.17 | 1.29 | 2.85 | 3.75 | 3.02 |
| miR-181b | 1.62 | 1.43 | 3.52 | 3.09 | 2.77 | 4.03 | 3.59 | 2.38 | 3.61 | -1.21 | 2.10 | 1.71 |
| miR-182 | 1.10 | 1.42 | 2.37 | 1.08 | 1.50 | 1.44 | 2.59 | 1.13 | 2.27 | -5.10 | -1.61 | -1.92 |
| miR-183 | -1.05 | 1.13 | 1.69 | -1.17 | 1.09 | 1.14 | 1.60 | -1.33 | 1.49 | -1.72 | -1.38 | -2.08 |
| miR-183* | 1.96 | 2.46 | 2.86 | 1.75 | 1.77 | 1.90 | 2.42 | 2.19 | 1.80 | 1.83 | 1.59 | 1.43 |
| miR-184 | 2.71 | 2.86 | 3.31 | 2.42 | 2.50 | 3.71 | 2.08 | 2.20 | 1.93 | 2.17 | 2.56 | 2.36 |
| miR-185 | -1.07 | -1.18 | 1.58 | -1.52 | -1.19 | 1.01 | 1.83 | -1.58 | 1.58 | -3.07 | -2.36 | -3.25 |
| miR-185* | -1.27 | 1.12 | 1.43 | 1.07 | 1.20 | 1.10 | 1.14 | 1.07 | -1.04 | -1.39 | -1.82 | -2.02 |
| miR-186 | 1.46 | 1.69 | 2.72 | 1.42 | 1.75 | 1.61 | 2.68 | 1.28 | 2.35 | -1.42 | -1.31 | -1.28 |
| miR-187* | 3.92 | 4.40 | 3.55 | 3.21 | 2.68 | 6.70 | 3.59 | 3.44 | 2.80 | 2.65 | 4.10 | 3.53 |

| Hsa-miRNA | IS 24hr | IS 48hr | IS 168hr | LA 24hr | LA 48hr | LA 168hr | CE 24hr | CE 48hr | CE 168hr | SV 24hr | SV 48hr | SV 168hr |
|---|---|---|---|---|---|---|---|---|---|---|---|---|
| miR-188-5p | 4.24 | ND | 6.03 | 6.85 | 5.34 | 11.73 | 7.91 | 5.69 | 9.66 | ND | 3.69 | 3.82 |
| miR-190 | 6.71 | 7.13 | 15.10 | 7.27 | 8.35 | 12.52 | 15.48 | 7.11 | 13.34 | 2.06 | 2.71 | 2.47 |
| miR-191 | -1.01 | 1.36 | 1.93 | -1.07 | 1.18 | -1.00 | 1.90 | 1.08 | 1.82 | -2.60 | -1.57 | -1.83 |
| miR-192 | 1.81 | 2.21 | 3.92 | 1.81 | 2.30 | 2.83 | 3.88 | 1.69 | 3.11 | -1.48 | -1.09 | -1.39 |
| miR-193a-3p | -1.10 | -1.03 | 1.71 | 1.29 | 1.70 | 2.47 | 1.68 | -1.02 | 1.38 | ND | -1.14 | -1.54 |
| miR-193b* | 1.44 | 1.47 | 1.37 | 2.29 | 2.54 | 2.18 | 2.53 | 2.40 | 1.72 | 2.08 | 1.71 | 1.45 |
| miR-194 | 2.12 | 2.28 | 4.28 | 2.11 | 2.25 | 2.98 | 4.04 | 1.60 | 3.88 | -1.34 | -1.04 | -1.15 |
| miR-194* | 2.69 | -1.13 | -3.53 | 3.75 | 3.04 | 6.32 | 1.47 | 2.57 | 1.25 | 2.03 | 3.53 | 2.97 |
| miR-195 | 7.30 | 8.76 | 12.37 | 7.26 | 7.71 | 8.64 | 10.62 | 6.25 | 9.82 | 4.59 | 4.90 | 7.18 |
| miR-196a* | 2.34 | 2.09 | 2.50 | 1.67 | 1.70 | 2.20 | 1.85 | 1.65 | 1.62 | 1.84 | 2.51 | 2.17 |
| miR-196b | 3.20 | 3.56 | 6.66 | 4.86 | 4.70 | 6.70 | 5.31 | 3.53 | 6.00 | -14.05 | 2.34 | 1.94 |
| miR-197 | 2.00 | 1.45 | 1.76 | 1.67 | 1.64 | 2.08 | 1.80 | 1.42 | 1.65 | 1.49 | 1.86 | 1.94 |
| miR-198 | 19.03 | 3.93 | 1.75 | 4.79 | 5.72 | 3.01 | 1.87 | 1.75 | 1.38 | 2.60 | 2.49 | 3.03 |
| miR-199a-3p | 5.15 | 5.18 | 11.12 | 8.32 | 9.04 | 12.31 | 6.43 | 5.05 | 11.54 | 2.13 | 3.94 | 3.56 |
| miR-199a-5p | -5.63 | -10.61 | -2.45 | 1.08 | 1.43 | 1.63 | -7.33 | -1.11 | 1.71 | ND | -1.55 | -8.46 |
| miR-199b-5p | 1.01 | 3.32 | 5.41 | 3.08 | 3.75 | 5.58 | 4.58 | 2.70 | 3.87 | -2.26 | 3.03 | 3.79 |
| miR-200b | 2.00 | ND | ND | 1.37 | 1.68 | 2.20 | 1.28 | 1.16 | -1.40 | 1.82 | 2.99 | 1.98 |
| miR-200b* | 2.99 | 3.44 | 2.97 | 4.99 | 4.92 | 5.23 | 4.88 | 5.16 | 3.74 | 3.89 | 3.54 | 3.70 |
| miR-203 | 1.07 | 1.16 | -2.93 | -1.66 | -3.91 | 1.57 | -3.49 | -4.59 | -2.77 | ND | 1.74 | -2.36 |
| miR-206 | 3.87 | 2.88 | 2.59 | 3.51 | 3.33 | 5.77 | 3.83 | 2.74 | 3.09 | 2.60 | 4.33 | 3.27 |
| miR-208a | -1.73 | -1.67 | -2.89 | -2.47 | -2.72 | -1.52 | -2.82 | -2.79 | -4.08 | -2.14 | -1.44 | -2.23 |
| miR-208b | 3.86 | -7.39 | ND | 1.72 | 1.16 | 4.31 | ND | 3.13 | -1.10 | ND | 5.66 | 1.09 |
| miR-210 | 4.26 | 4.16 | 5.48 | 2.69 | 3.33 | 7.09 | 4.50 | 2.44 | 3.76 | 1.21 | 3.56 | 2.91 |
| miR-214 | 2.23 | 1.24 | -1.14 | 3.42 | 4.38 | 4.73 | 4.52 | 5.60 | 2.80 | 2.31 | 3.23 | 2.98 |
| miR-215 | 1.79 | 2.29 | 3.77 | 1.86 | 2.46 | 3.07 | 4.01 | 1.82 | 3.15 | -1.71 | 1.00 | -1.12 |
| miR-221 | 4.30 | 6.46 | 9.19 | 3.95 | 6.20 | 6.28 | 6.77 | 3.62 | 5.51 | 1.99 | 3.24 | 3.14 |

| Hsa-miRNA | IS 24hr | IS 48hr | IS 168hr | LA 24hr | LA 48hr | LA 168hr | CE 24hr | CE 48hr | CE 168hr | SV 24hr | SV 48hr | SV 168hr |
|---|---|---|---|---|---|---|---|---|---|---|---|---|
| miR-221* | -1.32 | ND | ND | 2.17 | -1.42 | 2.82 | -3.28 | 1.82 | 1.80 | ND | 2.71 | 1.26 |
| miR-222 | 1.49 | 2.00 | 3.03 | 1.30 | 1.68 | 1.84 | 2.01 | 1.03 | 1.90 | -2.58 | -1.03 | -1.20 |
| miR-223 | 3.19 | 4.17 | 6.18 | 2.86 | 3.84 | 4.21 | 5.16 | 3.24 | 4.76 | 2.77 | 2.41 | 3.89 |
| miR-299-3p | 1.31 | 1.11 | 1.20 | -1.11 | -1.34 | 1.25 | -1.16 | -1.49 | -1.43 | -1.21 | 1.26 | 1.03 |
| miR-300 | 1.85 | 1.93 | 3.10 | 2.06 | 2.23 | 2.51 | 2.17 | 1.83 | 1.62 | 1.95 | 1.44 | 1.42 |
| miR-301a | 2.47 | 2.68 | 5.26 | 2.05 | 2.64 | 3.47 | 6.03 | 2.46 | 5.40 | -2.15 | -1.12 | -1.07 |
| miR-301b | -4.39 | -17.04 | 1.85 | 3.16 | 2.93 | 5.32 | 8.13 | 3.10 | 8.75 | ND | 1.42 | -1.60 |
| miR-302c* | 1.31 | 1.68 | 1.01 | 2.98 | 2.77 | 4.08 | 2.63 | 3.08 | 1.45 | 3.28 | 3.17 | 2.44 |
| miR-302e | 1.41 | 1.46 | ND | -1.15 | 1.37 | 1.82 | -1.09 | -1.17 | -1.16 | 2.14 | 2.17 | 1.44 |
| miR-320a | -1.34 | -1.24 | 1.03 | -1.69 | -1.60 | -1.60 | 1.11 | -1.54 | -1.51 | -3.88 | -1.78 | -2.82 |
| miR-320b | -1.68 | -1.36 | -1.18 | -2.05 | -1.82 | -1.89 | -1.00 | -1.74 | -1.81 | -2.71 | -2.19 | -3.08 |
| miR-320c | -1.81 | -1.57 | -1.32 | -2.12 | -1.86 | -2.03 | -1.08 | -1.82 | -1.91 | -1.94 | -2.44 | -3.78 |
| miR-320d | -1.38 | -1.11 | 1.06 | -1.48 | -1.36 | -1.49 | 1.23 | -1.28 | -1.30 | -2.31 | -1.75 | -2.52 |
| miR-324-3p | -1.21 | -1.57 | 1.04 | 1.13 | -1.06 | 2.23 | 1.05 | -1.29 | 1.09 | 1.22 | 1.52 | 1.05 |
| miR-324-5p | -2.42 | -2.47 | -1.84 | -1.45 | -1.51 | -1.83 | 1.05 | -1.54 | 1.01 | -2.72 | -2.67 | -2.99 |
| miR-326 | 1.71 | 1.26 | 1.87 | 1.89 | 2.05 | 2.02 | 1.79 | 2.00 | 1.57 | 2.57 | 1.63 | 1.77 |
| miR-328 | -12.55 | ND | 1.41 | 1.41 | -1.37 | 1.81 | ND | -1.53 | -1.35 | -3.88 | 1.25 | -1.08 |
| miR-331-3p | 1.05 | 1.27 | 1.66 | 1.06 | 1.04 | 1.03 | 1.59 | 1.08 | 1.36 | -2.50 | -1.14 | -1.70 |
| miR-331-5p | -3.24 | -4.12 | -4.88 | -1.53 | -1.42 | -1.35 | -1.00 | -1.65 | -1.63 | -2.54 | -1.82 | -2.88 |
| miR-335 | -1.38 | 1.03 | 2.12 | 1.00 | 1.12 | 1.49 | 1.66 | -1.13 | 1.57 | -3.61 | -2.26 | -2.76 |
| miR-335* | -3.18 | ND | ND | -2.48 | -5.89 | 1.22 | -5.50 | -6.00 | ND | ND | -1.33 | -2.79 |
| miR-338-3p | 29.70 | 25.30 | 51.57 | 18.54 | 28.16 | 44.69 | 23.43 | 19.01 | 27.81 | 1.40 | 16.28 | 27.43 |
| miR-339-3p | -1.18 | -1.03 | 1.23 | 1.35 | 1.62 | 1.41 | 1.50 | -1.05 | 1.46 | -1.74 | -1.09 | -1.46 |
| miR-339-5p | -1.86 | -1.43 | -1.05 | -1.50 | -1.32 | -1.40 | -1.49 | -2.01 | -1.33 | -3.39 | -2.28 | -3.20 |
| miR-340 | 1.03 | -1.00 | 1.57 | 1.24 | 1.23 | 1.71 | 1.61 | 1.12 | 1.47 | -1.70 | 1.01 | -1.28 |
| miR-340* | 2.64 | 2.87 | 3.44 | 2.21 | 2.47 | 3.78 | 2.20 | 2.05 | 1.83 | 2.08 | 2.39 | 2.33 |

| Hsa-miRNA | IS 24hr | IS 48hr | IS 168hr | LA 24hr | LA 48hr | LA 168hr | CE 24hr | CE 48hr | CE 168hr | SV 24hr | SV 48hr | SV 168hr |
|---|---|---|---|---|---|---|---|---|---|---|---|---|
| miR-342-3p | -2.23 | -1.59 | -1.40 | -2.46 | -1.73 | -1.86 | -1.35 | -1.99 | -1.63 | -3.27 | -1.93 | -2.92 |
| miR-342-5p | -1.43 | -1.14 | -1.33 | -1.41 | -1.28 | -1.17 | -1.15 | -1.61 | -1.36 | -2.15 | -1.35 | -2.00 |
| miR-345 | 1.01 | -2.77 | -8.30 | -1.10 | 1.18 | 1.07 | 1.08 | -1.52 | -1.07 | -2.90 | -1.26 | -2.51 |
| miR-361-3p | 1.63 | 1.69 | 2.16 | 1.59 | 1.96 | 1.62 | 2.95 | 1.93 | 2.06 | 1.14 | 1.03 | -1.00 |
| miR-361-5p | -1.11 | 1.14 | 1.47 | -1.07 | 1.00 | 1.01 | 1.42 | -1.17 | 1.21 | -1.56 | -1.25 | -1.38 |
| miR-362-3p | 1.59 | 1.67 | 3.67 | 2.46 | 2.56 | 4.13 | 3.90 | 1.78 | 3.09 | ND | 1.00 | -3.88 |
| miR-362-5p | 1.02 | 1.31 | 1.83 | 1.01 | 1.40 | 1.37 | 2.35 | 1.10 | 1.83 | -1.96 | -1.55 | -1.76 |
| miR-363 | 1.63 | 2.16 | 3.33 | 2.11 | 2.30 | 2.26 | 2.76 | 1.57 | 3.02 | -1.99 | -1.37 | -1.56 |
| miR-363* | -2.07 | ND | 1.34 | 1.95 | -1.67 | 4.10 | ND | 1.52 | ND | -2.48 | 2.56 | 2.29 |
| miR-365 | -1.97 | -3.63 | ND | 1.45 | 1.71 | 2.42 | 1.46 | 1.28 | -1.23 | -2.57 | 1.70 | 1.38 |
| miR-370 | 1.40 | 1.74 | 2.59 | 1.21 | 1.37 | 1.71 | 1.83 | 1.33 | 1.39 | 1.80 | -1.02 | 1.42 |
| miR-374a | 1.88 | 2.51 | 4.77 | 2.21 | 2.76 | 3.43 | 4.25 | 2.04 | 3.71 | -2.52 | -1.07 | -1.22 |
| miR-374b | 3.86 | 4.47 | 7.53 | 3.93 | 5.08 | 6.87 | 7.94 | 3.25 | 6.87 | 1.27 | 2.39 | 2.13 |
| miR-374b* | 3.07 | 1.69 | 2.52 | 2.48 | 2.75 | 3.93 | 1.77 | 2.77 | 1.88 | 3.18 | 3.67 | 2.63 |
| miR-375 | -2.68 | ND | ND | -1.59 | -2.04 | 1.11 | -2.64 | -2.40 | ND | -4.00 | 1.02 | -1.53 |
| miR-378 | -1.33 | 1.01 | 1.59 | -1.24 | 1.08 | 1.01 | 1.66 | -1.18 | 1.30 | -3.62 | -2.20 | -2.52 |
| miR-381 | 1.99 | 2.10 | 2.27 | 2.47 | 1.91 | 2.86 | 1.98 | 2.62 | 1.86 | -1.10 | 1.84 | 1.13 |
| miR-382 | -1.06 | -1.94 | -2.53 | 1.47 | 1.70 | 1.88 | -1.06 | 1.36 | 1.03 | 1.38 | 1.43 | 1.07 |
| miR-412 | -11.46 | -18.44 | -35.56 | -1.11 | -1.57 | -1.23 | -4.66 | -5.19 | ND | -4.16 | -1.12 | -3.01 |
| miR-421 | 1.37 | 1.92 | 2.07 | 2.25 | 2.50 | 2.81 | 4.15 | 2.13 | 3.35 | -1.29 | 1.52 | 1.50 |
| miR-422a | 3.74 | 4.82 | 6.30 | 2.65 | 3.86 | 5.90 | 4.56 | 2.32 | 3.11 | 2.28 | 3.05 | 2.66 |
| miR-423-3p | -1.53 | -1.35 | -1.02 | -1.23 | -1.25 | -1.28 | -1.01 | -1.63 | -1.25 | -2.00 | -1.78 | -2.37 |
| miR-423-5p | -2.68 | -2.31 | -1.84 | -3.05 | -2.96 | -2.72 | -2.18 | -2.98 | -3.16 | -9.16 | -3.24 | -4.24 |
| miR-424 | 7.62 | 7.99 | 15.14 | 8.46 | 9.98 | 13.43 | 17.95 | 6.57 | 13.59 | 3.59 | 3.66 | 3.83 |
| miR-425 | 2.30 | 2.58 | 3.21 | 1.94 | 2.54 | 2.56 | 3.44 | 1.92 | 2.71 | 1.38 | 1.72 | 1.32 |
| miR-425* | -1.00 | 1.03 | 1.66 | 1.10 | 1.32 | 1.47 | 1.71 | 1.04 | 1.64 | -2.07 | -1.18 | -1.29 |

| Hsa-miRNA | IS 24hr | IS 48hr | IS 168hr | LA 24hr | LA 48hr | LA 168hr | CE 24hr | CE 48hr | CE 168hr | SV 24hr | SV 48hr | SV 168hr |
|---|---|---|---|---|---|---|---|---|---|---|---|---|
| miR-450a | ND | ND | ND | 3.16 | 3.13 | 5.43 | 4.58 | 3.47 | 4.27 | ND | 2.99 | 3.14 |
| miR-451 | 1.15 | 1.38 | 1.98 | 1.19 | 1.23 | 1.36 | 1.71 | 1.25 | 1.55 | 1.56 | -1.28 | 1.32 |
| miR-454 | 11.57 | 8.54 | 14.74 | 8.77 | 10.33 | 16.37 | 20.18 | 8.58 | 17.87 | 4.63 | 5.88 | 4.80 |
| miR-483-5p | 6.28 | 4.93 | 3.69 | 5.65 | 5.48 | 4.90 | 4.23 | 3.65 | 3.10 | 5.04 | 3.77 | 3.57 |
| miR-484 | 1.14 | 1.19 | 1.42 | 1.17 | 1.40 | 1.29 | 1.40 | 1.12 | 1.17 | -1.39 | 1.00 | -1.30 |
| miR-485-3p | 1.39 | 1.04 | 1.26 | 1.13 | 1.67 | 1.52 | 1.31 | 1.13 | -1.19 | 2.06 | 1.10 | 1.14 |
| miR-486-3p | ND | ND | ND | 1.02 | 1.64 | 1.71 | 1.06 | -1.28 | 1.09 | -9.67 | -1.31 | 1.10 |
| miR-486-5p | 1.15 | 1.38 | 1.99 | 1.19 | 1.23 | 1.36 | 1.71 | 1.25 | 1.55 | 1.56 | -1.28 | 1.32 |
| miR-487b | 5.03 | 5.30 | 5.00 | 3.41 | 3.51 | 6.35 | 4.73 | 2.41 | 3.03 | 3.81 | 6.50 | 4.89 |
| miR-488 | 3.30 | 2.34 | 2.19 | 5.81 | 3.88 | 6.71 | 3.72 | 5.18 | 3.14 | 1.47 | 4.71 | 3.65 |
| miR-489 | 1.63 | 1.32 | -3.09 | 2.42 | 2.25 | 3.46 | 2.94 | 2.26 | 1.15 | 1.45 | 2.73 | 2.48 |
| miR-490-3p | 5.14 | 2.51 | -1.12 | 3.11 | 3.34 | 4.88 | 3.53 | 3.92 | 2.70 | 2.96 | 5.93 | 3.61 |
| miR-491-3p | 2.35 | 1.75 | 2.25 | 1.45 | 1.39 | 2.19 | 1.90 | 1.12 | 1.15 | 1.79 | 2.24 | 2.02 |
| miR-492 | 2.66 | 2.18 | ND | 5.64 | 4.39 | 16.83 | 6.53 | 4.26 | 2.10 | 2.69 | 8.94 | 4.97 |
| miR-493* | 2.09 | 1.86 | 1.51 | 1.34 | 1.10 | 2.04 | 1.91 | -1.43 | 1.59 | -1.43 | 1.95 | -1.64 |
| miR-494 | 4.69 | 4.92 | 5.60 | 5.61 | 5.31 | 9.56 | 5.73 | 3.39 | 3.19 | 7.13 | 7.05 | 7.61 |
| miR-498 | 4.89 | 4.00 | 4.62 | 4.45 | 5.05 | 5.42 | 4.90 | 4.16 | 3.72 | 6.50 | 4.04 | 3.98 |
| miR-500 | 1.22 | 1.50 | 1.92 | 1.18 | 1.48 | 1.47 | 2.14 | 1.10 | 1.88 | -1.36 | -1.10 | -1.51 |
| miR-500* | -1.40 | -1.61 | -1.09 | -1.16 | 1.03 | 1.04 | 1.46 | -1.27 | 1.05 | -2.16 | -1.42 | -2.06 |
| miR-501-5p | -2.13 | -1.86 | -1.73 | -1.53 | -1.44 | -1.68 | 1.02 | -1.79 | -1.11 | -3.01 | -2.64 | -3.91 |
| miR-502-3p | -2.05 | -1.65 | -1.96 | -1.31 | -1.10 | -1.16 | 1.35 | -1.35 | -1.11 | -2.21 | -1.68 | -2.55 |
| miR-502-5p | -1.61 | 1.58 | -1.19 | -1.54 | -1.35 | 1.02 | 1.15 | -1.91 | -1.05 | -3.03 | -1.46 | -3.09 |
| miR-504 | -8.68 | -4.39 | -1.70 | -8.85 | -182.46 | ND | ND | -6.38 | -8.36 | ND | -5.40 | -9.86 |
| miR-505 | -1.14 | 1.27 | 2.69 | 1.88 | 3.02 | 3.22 | 3.91 | 2.10 | 3.54 | ND | 1.21 | -1.02 |
| miR-505* | -1.82 | -1.78 | -1.94 | -1.72 | -1.61 | -1.56 | -1.26 | -1.80 | -2.27 | -1.88 | 1.06 | -1.86 |
| miR-508-5p | 5.39 | 5.79 | 4.54 | 2.80 | 2.71 | 5.57 | 3.68 | 1.67 | 2.30 | 5.72 | 5.02 | 3.26 |

| Hsa-miRNA | IS 24hr | IS 48hr | IS 168hr | LA 24hr | LA 48hr | LA 168hr | CE 24hr | CE 48hr | CE 168hr | SV 24hr | SV 48hr | SV 168hr |
|---|---|---|---|---|---|---|---|---|---|---|---|---|
| miR-509-5p | -2.62 | -1.92 | ND | 1.10 | 1.17 | -1.24 | -1.08 | 3.02 | -1.32 | -1.84 | -1.21 | -1.75 |
| miR-510 | -1.66 | ND | ND | 2.56 | 3.06 | 1.80 | 2.47 | 2.53 | 1.33 | 1.50 | 1.83 | 1.59 |
| miR-513a-3p | 2.09 | 1.81 | 1.24 | 1.79 | 1.96 | 3.99 | 2.51 | 1.13 | -1.06 | 2.16 | 2.49 | 2.29 |
| miR-513a-5p | -1.74 | -1.58 | -1.33 | -1.39 | -1.24 | -1.33 | -1.74 | -1.26 | -1.70 | -1.27 | -1.84 | -2.16 |
| miR-516a-5p | -8.69 | -4.10 | ND | -2.52 | -1.53 | -3.96 | -4.34 | 1.68 | -5.40 | -4.66 | -2.79 | -4.67 |
| miR-516b | 1.82 | 1.50 | -2.60 | 2.37 | 2.04 | 3.63 | -1.13 | 2.07 | 1.35 | 1.94 | 3.39 | 2.67 |
| miR-518a-5p | -1.01 | 1.34 | 1.16 | 1.22 | 1.49 | 1.69 | 1.28 | 1.19 | -1.33 | 1.22 | 1.10 | -1.07 |
| miR-519c-5p | ND | -4.29 | ND | 2.13 | 2.43 | 2.19 | -2.77 | 6.14 | ND | 1.23 | 2.31 | 1.19 |
| miR-519d | -3.40 | -3.27 | -3.28 | -3.18 | -2.62 | -2.25 | -2.89 | -3.96 | -4.33 | -2.58 | -2.63 | -2.98 |
| miR-519e | 1.31 | 1.16 | 1.87 | 1.65 | 1.87 | 1.84 | 1.34 | 1.84 | 1.56 | 1.72 | 1.00 | 1.23 |
| miR-519e* | 2.51 | 2.90 | 2.86 | 2.11 | 2.41 | 2.67 | 2.59 | 1.83 | 1.54 | 2.95 | 2.54 | 2.09 |
| miR-520d-5p | 1.02 | 1.04 | -1.85 | 1.50 | 1.55 | 2.44 | 1.41 | 1.23 | -1.47 | 1.41 | 1.66 | 1.28 |
| miR-525-5p | 1.92 | 1.63 | 1.18 | 2.17 | 1.71 | 2.87 | 1.53 | 1.67 | 1.30 | 2.98 | 2.43 | 2.00 |
| miR-532-3p | -1.11 | -4.57 | -12.74 | -1.15 | -1.09 | 1.43 | -1.00 | -1.14 | -1.15 | -1.68 | 1.08 | -1.16 |
| miR-532-5p | 1.06 | 1.31 | 2.21 | 1.29 | 1.50 | 1.61 | 2.06 | 1.11 | 1.90 | -5.23 | -1.37 | -1.44 |
| miR-542-3p | 2.17 | 1.61 | 1.83 | 1.90 | 1.63 | 3.66 | 2.08 | 1.25 | 1.65 | -1.31 | 2.73 | 2.26 |
| miR-548e | 9.89 | 11.85 | 11.59 | 6.09 | 6.40 | 10.86 | 9.10 | 7.02 | 7.51 | 10.74 | 11.50 | 11.05 |
| miR-548n | 2.39 | 1.34 | 2.97 | 2.63 | 3.57 | 6.37 | 4.82 | 3.12 | 3.99 | 1.62 | 3.75 | 3.04 |
| miR-549 | 4.61 | 5.16 | 5.61 | 3.90 | 3.53 | 5.08 | 4.38 | 3.11 | 3.27 | 5.75 | 4.77 | 4.11 |
| miR-550 | -1.20 | -1.03 | 1.26 | -1.00 | 1.03 | -1.23 | 1.05 | 1.16 | 1.16 | -1.18 | -1.10 | -1.25 |
| miR-550* | 1.30 | 1.49 | 1.90 | 1.46 | 1.67 | 1.61 | 2.24 | 1.27 | 1.96 | -1.23 | 1.04 | -1.29 |
| miR-551a | 1.86 | -1.12 | -1.80 | 2.60 | 2.06 | 3.93 | 1.45 | 1.68 | 1.50 | 1.51 | 3.27 | 2.98 |
| miR-551b | -1.36 | -1.53 | -1.14 | -1.14 | -1.15 | -1.29 | -1.38 | -1.23 | -1.42 | -1.42 | -1.63 | -1.62 |
| miR-552 | 8.49 | 2.55 | 3.28 | 2.46 | 2.40 | 3.90 | 3.09 | 2.09 | 2.06 | 2.70 | 2.94 | 2.53 |
| miR-553 | 1.23 | 1.32 | -1.27 | 3.94 | 4.45 | 3.25 | 3.03 | 4.24 | 2.48 | 2.92 | 2.55 | 1.80 |
| miR-557 | 7.70 | 9.44 | 9.67 | 6.61 | 7.83 | 9.85 | 8.89 | 6.43 | 6.49 | 7.42 | 5.11 | 4.93 |

| Hsa-miRNA | IS 24hr | IS 48hr | IS 168hr | LA 24hr | LA 48hr | LA 168hr | CE 24hr | CE 48hr | CE 168hr | SV 24hr | SV 48hr | SV 168hr |
|---|---|---|---|---|---|---|---|---|---|---|---|---|
| miR-574-3p | -1.87 | -2.92 | -1.56 | 1.19 | 1.19 | 1.13 | 1.08 | 1.08 | -1.09 | -1.05 | 1.48 | 1.36 |
| miR-574-5p | -1.45 | -1.22 | 1.26 | -1.07 | -1.01 | -1.26 | 1.17 | -1.02 | -1.02 | -1.96 | -1.40 | -1.67 |
| miR-576-3p | 1.46 | 1.61 | 2.17 | 1.29 | 1.42 | 1.64 | 1.51 | 1.54 | 1.29 | 2.06 | 1.46 | 1.42 |
| miR-576-5p | 1.09 | 1.11 | 1.52 | 1.12 | 1.07 | 1.27 | 1.72 | -1.11 | 1.38 | -1.14 | -1.27 | -1.41 |
| miR-578 | ND | ND | ND | 2.35 | 1.18 | 2.11 | 1.78 | 1.92 | 1.96 | 1.24 | 1.73 | 2.04 |
| miR-581 | ND | ND | -1.72 | 2.32 | 1.03 | 2.46 | -2.12 | 1.89 | 1.95 | 1.29 | 1.36 | 1.88 |
| miR-583 | 1.41 | 1.89 | 1.58 | 1.55 | 2.02 | 1.57 | 1.57 | 1.43 | 1.07 | 1.34 | 1.15 | 1.10 |
| miR-584 | 6.31 | 6.02 | 6.70 | 4.79 | 4.56 | 7.33 | 6.67 | 4.75 | 4.20 | 6.33 | 6.66 | 6.85 |
| miR-585 | 7.40 | 7.55 | 10.33 | 7.70 | 8.16 | 10.01 | 7.48 | 6.67 | 5.91 | 6.77 | 5.40 | 6.37 |
| miR-589 | 4.32 | 5.46 | 4.30 | 2.46 | 2.75 | 4.51 | 4.02 | 1.95 | 2.96 | 3.22 | 4.64 | 3.33 |
| miR-590-5p | 10.78 | 12.65 | 25.93 | 10.18 | 14.47 | 21.69 | 25.69 | 11.58 | 19.80 | 1.65 | 5.47 | 4.88 |
| miR-597 | 5.01 | 5.61 | 4.02 | 3.86 | 3.78 | 7.85 | 4.98 | 2.23 | 3.36 | 3.21 | 7.45 | 5.18 |
| miR-600 | 4.58 | 3.13 | 2.85 | 3.44 | 2.59 | 4.66 | 2.29 | 2.63 | 2.65 | 4.48 | 5.12 | 4.31 |
| miR-601 | 1.19 | ND | -2.57 | 3.44 | 2.45 | 3.62 | 1.94 | 3.00 | 1.78 | 1.43 | 3.18 | 3.02 |
| miR-602 | 2.04 | 2.33 | 2.75 | 2.83 | 2.84 | 3.90 | 2.75 | 2.34 | 2.16 | 1.84 | 2.11 | 2.21 |
| miR-605 | -1.43 | -1.61 | -5.94 | -1.45 | 1.21 | 1.53 | -1.17 | -1.76 | -17.03 | 1.14 | 1.61 | 1.10 |
| miR-611 | 3.20 | 4.84 | 6.23 | 2.87 | 3.28 | 3.04 | 3.95 | 3.18 | 3.09 | 2.51 | 1.77 | 1.32 |
| miR-615-3p | -1.00 | -1.80 | -3.47 | 1.61 | -1.44 | 2.44 | -36.74 | -1.12 | -1.21 | 1.91 | 1.73 | -1.03 |
| miR-617 | 3.01 | 2.43 | 3.19 | 1.89 | 1.97 | 3.10 | 1.42 | 1.74 | 1.09 | 2.27 | 2.69 | 2.13 |
| miR-618 | ND | ND | -1.83 | 3.52 | 2.62 | 3.37 | ND | 1.58 | 1.55 | 3.36 | 3.11 | 4.36 |
| miR-620 | -1.00 | -1.21 | -1.20 | -1.32 | -1.19 | -1.06 | -1.61 | -1.09 | -1.34 | 1.04 | 1.13 | 1.02 |
| miR-622 | -3.24 | -1.74 | ND | -1.33 | -1.48 | 1.49 | -1.46 | -1.10 | -4.80 | -1.05 | 1.09 | -1.41 |
| miR-623 | 2.79 | 2.53 | 2.37 | 4.56 | 2.88 | 6.76 | 2.39 | 2.98 | 2.81 | 3.37 | 3.12 | 2.19 |
| miR-625 | -1.20 | 1.15 | 1.38 | 1.10 | 1.35 | 1.17 | 1.15 | -1.11 | 1.02 | -3.05 | -1.37 | -1.55 |
| miR-625* | -10.85 | -5.26 | ND | -1.38 | -1.76 | -1.15 | -2.66 | -1.76 | -2.48 | -1.26 | -1.32 | -1.44 |
| miR-627 | 3.78 | 4.39 | 5.75 | 4.52 | 5.34 | 6.48 | 6.35 | 4.02 | 6.77 | -2.33 | 3.72 | 1.80 |

| Hsa-miRNA | IS 24hr | IS 48hr | IS 168hr | LA 24hr | LA 48hr | LA 168hr | CE 24hr | CE 48hr | CE 168hr | SV 24hr | SV 48hr | SV 168hr |
|---|---|---|---|---|---|---|---|---|---|---|---|---|
| miR-628-3p | 1.22 | 1.51 | 2.04 | 1.56 | 1.52 | 1.34 | 1.48 | 1.67 | 1.30 | -1.50 | -1.10 | -1.27 |
| miR-629 | 1.01 | 1.27 | 1.73 | -1.13 | 1.17 | 1.35 | 1.61 | -1.03 | 1.12 | -2.29 | -1.42 | -1.82 |
| miR-629* | 2.94 | 3.78 | 3.97 | 2.93 | 3.25 | 6.77 | 2.96 | 1.86 | 1.58 | 2.77 | 4.91 | 4.82 |
| miR-630 | 1.22 | -7.02 | ND | 2.17 | 2.65 | 1.79 | -1.38 | 1.67 | -1.49 | 2.11 | 2.37 | 1.70 |
| miR-634 | -4.54 | -9.26 | -37.22 | -2.34 | -3.30 | -2.55 | -2.98 | -2.70 | -3.99 | -3.20 | -2.50 | -2.92 |
| miR-635 | 1.26 | 1.94 | ND | 1.93 | -1.15 | 3.69 | -2.87 | 1.12 | -4.67 | -2.09 | 2.26 | -2.52 |
| miR-636 | 1.07 | -1.10 | -1.20 | -1.11 | -1.20 | 1.30 | -1.25 | -1.35 | -1.04 | 1.11 | 1.16 | 1.04 |
| miR-637 | 3.03 | 3.37 | 4.44 | 3.59 | 3.59 | 3.98 | 2.97 | 3.22 | 2.64 | 2.37 | 2.05 | 1.85 |
| miR-638 | 5.28 | 3.59 | 4.41 | 4.59 | 5.17 | 5.90 | 5.07 | 4.12 | 3.33 | 4.40 | 3.83 | 4.88 |
| miR-642 | 1.24 | -1.34 | 1.19 | 1.47 | 1.40 | 1.38 | 1.71 | 1.35 | 1.24 | 1.53 | 1.08 | 1.21 |
| miR-647 | 1.87 | 1.33 | -1.37 | 1.89 | 2.02 | 2.29 | 4.17 | 1.64 | 2.90 | 2.14 | 2.37 | 1.44 |
| miR-652 | 1.78 | 1.83 | 2.30 | 2.00 | 1.89 | 1.85 | 2.47 | 1.87 | 2.15 | 1.38 | 1.45 | 1.23 |
| miR-659 | 2.95 | 3.42 | 2.31 | 4.45 | 5.82 | 3.56 | 2.77 | 2.42 | 2.23 | 2.56 | 3.25 | 3.00 |
| miR-660 | 2.29 | 2.58 | 4.62 | 2.51 | 3.12 | 3.73 | 5.02 | 2.32 | 4.61 | -1.21 | 1.04 | -1.04 |
| miR-664 | -5.12 | -68.14 | ND | 1.98 | 2.12 | 2.54 | 2.59 | 1.96 | 1.33 | 1.91 | 2.05 | 2.10 |
| miR-665 | -1.87 | -1.44 | -1.47 | -1.29 | -1.03 | -1.29 | -1.22 | -1.23 | -1.74 | -1.70 | -1.71 | -2.24 |
| miR-668 | 2.64 | 1.54 | 2.43 | 3.28 | 3.62 | 5.94 | 1.86 | 2.72 | 2.27 | 3.69 | 3.01 | 3.89 |
| miR-671-5p | 3.87 | 3.16 | 2.14 | 5.00 | 5.08 | 6.24 | 6.33 | 3.72 | 3.55 | 6.18 | 5.53 | 6.36 |
| miR-675 | 5.48 | 4.98 | 3.06 | 7.15 | 9.13 | 8.10 | 5.94 | 3.91 | 3.49 | 5.47 | 6.34 | 7.67 |
| miR-720 | -1.35 | -1.20 | 1.14 | -1.05 | 1.01 | -1.08 | 1.10 | -1.27 | -1.33 | -1.33 | -1.29 | -1.21 |
| miR-744 | 1.21 | 1.28 | 1.59 | 1.52 | 1.48 | 1.72 | 1.36 | 1.25 | 1.35 | -1.27 | -1.08 | -1.11 |
| miR-765 | 1.26 | 1.46 | 1.53 | 1.51 | 1.79 | 1.51 | 1.27 | 1.23 | 1.08 | 1.66 | 1.26 | 1.31 |
| miR-766 | -1.07 | -1.23 | -3.29 | 1.57 | 1.45 | 1.55 | 1.59 | 1.26 | -1.15 | 1.18 | 1.40 | 1.16 |
| miR-769-5p | -32.58 | ND | ND | 1.11 | 1.35 | 1.00 | -2.27 | -1.27 | -1.01 | ND | 1.25 | -1.86 |
| miR-874 | 1.64 | 1.08 | 1.55 | 2.69 | 2.62 | 3.86 | 2.41 | 2.36 | 1.90 | 1.78 | 2.83 | 2.65 |
| miR-876-3p | ND | 3.19 | 5.44 | -2.29 | -2.53 | -1.00 | ND | 1.69 | -1.01 | ND | -1.34 | -2.84 |

| Hsa-miRNA | IS 24hr | IS 48hr | IS 168hr | LA 24hr | LA 48hr | LA 168hr | CE 24hr | CE 48hr | CE 168hr | SV 24hr | SV 48hr | SV 168hr |
|---|---|---|---|---|---|---|---|---|---|---|---|---|
| miR-877 | -1.27 | -1.37 | -1.45 | -1.06 | -1.21 | 1.29 | 1.00 | -1.13 | -1.23 | -1.54 | 1.02 | -1.07 |
| miR-877* | ND | ND | ND | 2.60 | 2.48 | 3.91 | 2.28 | 1.75 | ND | 5.28 | 2.45 | 1.91 |
| miR-887 | 4.99 | 4.21 | 4.01 | 3.37 | 3.71 | 5.57 | 4.51 | 2.62 | 2.32 | 4.48 | 4.69 | 4.63 |
| miR-888* | 1.41 | 1.68 | 1.87 | 1.23 | 1.34 | 1.72 | 1.55 | 1.13 | 1.17 | 1.53 | 1.47 | 1.32 |
| miR-890 | 2.81 | 2.42 | 1.57 | 1.90 | 1.47 | 1.96 | 2.87 | 1.41 | 2.12 | 1.75 | 2.91 | 1.10 |
| miR-891a | 2.38 | 2.21 | 2.67 | 2.21 | 2.30 | 3.20 | 2.45 | 2.19 | 1.94 | 2.72 | 2.84 | 3.16 |
| miR-920 | 1.99 | -1.60 | ND | 2.91 | 2.54 | 3.34 | 2.54 | 3.16 | 1.74 | 3.07 | 3.78 | 3.45 |
| miR-923 | -5.93 | -4.23 | -2.95 | -4.49 | -3.73 | -4.63 | -4.03 | -3.96 | -5.27 | -4.86 | -7.63 | -8.18 |
| miR-933 | 3.04 | 3.22 | 4.30 | 2.22 | 2.32 | 3.15 | 2.45 | 1.73 | 1.56 | 3.22 | 2.64 | 2.72 |
| miR-934 | 2.95 | 1.64 | 1.62 | 2.01 | 2.08 | 3.04 | 1.63 | 2.54 | 1.73 | 2.74 | 3.12 | 2.34 |
| miR-937 | 2.19 | 2.09 | 1.41 | 1.75 | 1.48 | 3.26 | 2.41 | 1.14 | 2.08 | 3.49 | 3.47 | 2.13 |
| miR-939 | 1.07 | 1.26 | 1.46 | 1.42 | 1.95 | 1.28 | 1.65 | 1.61 | 1.29 | 1.45 | -1.04 | -1.31 |
| miR-941 | -2.70 | 1.73 | 1.73 | -4.10 | -1.76 | -1.63 | -1.36 | -2.25 | -5.10 | -1.62 | -3.19 | -13.67 |
| miR-942 | -14.09 | ND | 5.46 | 7.80 | 2.34 | 14.58 | 5.69 | 4.69 | ND | 4.40 | 6.04 | 8.88 |
| miR-943 | 2.13 | 1.10 | 1.28 | 3.90 | 3.76 | 3.37 | 3.16 | 2.91 | 2.14 | 3.62 | 2.29 | 2.93 |
| miR-944 | 2.87 | -6.62 | ND | 2.42 | -1.31 | 3.74 | 3.02 | 1.90 | 2.05 | 1.20 | 5.16 | 2.25 |
| miR-1184 | 1.12 | 1.99 | 2.69 | 1.25 | 1.29 | 2.05 | 1.05 | -1.13 | -1.13 | -1.59 | -1.04 | -1.35 |
| miR-1201 | 2.13 | 1.93 | 1.83 | 2.40 | 2.13 | 2.36 | 2.05 | 2.35 | 2.38 | 1.11 | 2.48 | 2.11 |
| miR-1224-3p | 2.79 | 4.39 | 4.17 | 1.12 | 2.11 | 2.14 | 2.32 | 1.70 | 1.47 | 1.43 | -1.08 | -1.21 |
| miR-1227 | ND | ND | ND | 3.99 | 3.76 | 4.49 | 4.19 | 2.06 | 1.35 | 3.29 | 3.24 | 2.45 |
| miR-1236 | -3.48 | -1.58 | 1.27 | 1.95 | 1.68 | 2.71 | -1.07 | 1.24 | 1.01 | 1.92 | 1.36 | 1.04 |
| miR-1246 | -1.03 | 1.23 | 1.76 | 1.08 | 1.76 | -1.03 | -1.04 | -1.24 | -1.20 | 1.18 | -1.56 | 1.08 |
| miR-1249 | -3.60 | -1.16 | -17.51 | 2.68 | 1.61 | 3.31 | -1.00 | 1.39 | 1.38 | 3.82 | 1.31 | 1.73 |
| miR-1255a | 1.24 | 1.33 | 1.58 | 1.41 | 1.48 | 1.55 | 1.40 | 1.50 | 1.26 | 1.37 | 1.25 | 1.29 |
| miR-1259 | 2.64 | 2.09 | 3.22 | 1.95 | 1.93 | 2.40 | 1.89 | 1.85 | 2.02 | 3.14 | 2.82 | 2.81 |
| miR-1260 | 1.71 | 1.37 | 1.17 | 1.73 | 1.17 | 2.73 | 1.39 | 1.16 | 1.09 | 1.17 | 2.40 | 1.79 |

| Hsa-miRNA | IS 24hr | IS 48hr | IS 168hr | LA 24hr | LA 48hr | LA 168hr | CE 24hr | CE 48hr | CE 168hr | SV 24hr | SV 48hr | SV 168hr |
|---|---|---|---|---|---|---|---|---|---|---|---|---|
| miR-1261 | 7.05 | 9.21 | 9.86 | 8.52 | 7.87 | 11.12 | 7.68 | 7.42 | 5.66 | 4.67 | 6.32 | 4.12 |
| miR-1264 | 1.79 | 2.01 | 3.31 | 1.50 | 1.71 | 2.26 | 1.68 | 1.74 | 1.55 | 2.09 | 1.91 | 2.10 |
| miR-1265 | -1.95 | -1.86 | -1.57 | -2.41 | -2.59 | -1.97 | -2.58 | -2.79 | -3.20 | -2.30 | -1.92 | -2.79 |
| miR-1274a | 4.32 | 4.30 | 4.97 | 5.34 | 5.17 | 12.29 | 5.11 | 2.90 | 2.99 | 4.18 | 7.63 | 7.84 |
| miR-1274b | 8.45 | 8.75 | 10.06 | 4.81 | 4.82 | 10.06 | 5.76 | 3.15 | 3.81 | 6.06 | 8.68 | 8.06 |
| miR-1275 | 1.10 | 1.17 | 1.06 | 1.36 | 1.29 | 1.50 | -1.03 | -1.34 | -1.43 | -1.09 | -1.05 | 1.29 |
| miR-1280 | -1.93 | -1.89 | -1.51 | -1.51 | -1.96 | -1.01 | -1.78 | -2.54 | -2.54 | -2.58 | -1.25 | -1.52 |
| miR-1284 | 1.62 | -1.61 | -1.15 | 2.95 | 3.18 | 1.74 | 2.76 | 3.77 | 2.54 | 2.10 | 1.64 | 2.18 |
| miR-1285 | -1.10 | -1.04 | 1.31 | -1.11 | -1.13 | 1.08 | -1.09 | -1.19 | -1.36 | -1.24 | -1.18 | -1.29 |
| miR-1290 | 1.30 | 1.89 | 1.93 | 1.43 | 3.48 | 1.03 | -1.01 | -1.57 | -1.49 | 1.61 | -1.35 | 2.09 |
| miR-1297 | 5.80 | 5.29 | 9.35 | 5.57 | 9.96 | 13.77 | 14.31 | 4.91 | 9.92 | 2.39 | 3.67 | 3.43 |
| miR-1299 | -1.70 | -1.64 | -1.23 | -1.49 | -1.32 | -1.18 | -1.59 | -1.17 | -1.62 | -2.02 | -1.42 | -1.77 |
| miR-1301 | 1.38 | 1.31 | 1.20 | 1.30 | 1.16 | 1.66 | 1.98 | 1.05 | 1.38 | 1.16 | 1.57 | 1.31 |
| miR-1304 | 1.29 | 1.20 | -1.30 | 2.25 | 2.45 | 2.28 | 1.91 | 1.99 | 1.50 | 1.58 | 2.60 | 1.92 |
| miR-1307 | 2.53 | 2.30 | 3.30 | 2.40 | 2.48 | 3.67 | 3.48 | 1.60 | 2.75 | 1.12 | 2.13 | 1.62 |
| miR-1308 | -1.00 | -1.13 | 1.31 | -1.00 | 1.26 | 1.17 | 1.03 | -1.03 | -1.18 | 1.85 | -1.28 | -1.03 |
| miR-1321 | 4.78 | 3.18 | 3.71 | 4.09 | 4.19 | 5.49 | 3.92 | 4.03 | 3.02 | 4.60 | 4.57 | 5.48 |
| miR-1826 | 1.15 | 1.38 | 1.98 | 1.19 | 1.23 | 1.36 | 1.71 | 1.25 | 1.55 | 1.56 | -1.28 | 1.32 |
| miR-1827 | 1.59 | 1.60 | 2.17 | 1.17 | 1.57 | 2.18 | 2.25 | 1.31 | 1.65 | 1.30 | -1.00 | -1.09 |

**Supplementary Table 2**: Expression of 352 miRNAs detected in low or no risk patients. MiRNAs were expressed as fold change compared with healthy controls. All miRNAs selected have positive raw intensity values and FDR < 0.05. ND represents not detected. LA: large artery stroke. CE: cardioembolic stroke. SV: small vessel stroke.

| Hsa-miRNA | LA1 >3mths (LC) | LA2 >3mths (LB) | LA3 >3mths (LX) | LA4 >3mths (E) | LA5 >3mths (BB) | LA6 >3mths (DB) | SV >3mths (LM) | CE >3mths (BE) |
|---|---|---|---|---|---|---|---|---|
| Let-7a | -1.75 | -1.01 | -1.78 | -2.55 | -2.06 | -3.09 | -2.04 | -5.00 |
| Let-7a* | 4.09 | 2.14 | 1.11 | 1.25 | 1.23 | 1.37 | 1.08 | -1.43 |
| Let-7b | -1.81 | -1.23 | -2.43 | -3.72 | -2.17 | -3.31 | -3.30 | -3.11 |
| Let-7b* | 2.68 | 1.96 | -1.33 | -1.75 | -1.17 | -1.57 | -1.35 | -2.02 |
| Let-7c | -1.36 | -1.02 | -2.39 | -3.34 | -1.91 | -3.22 | -2.88 | -3.22 |
| Let-7d | 1.49 | 2.52 | -1.11 | -1.46 | 1.23 | -1.59 | -1.24 | -2.69 |
| Let-7d* | -1.43 | -1.48 | -2.44 | -5.39 | -1.82 | -2.80 | -3.77 | -1.53 |
| Let-7e | 2.04 | 1.83 | 1.57 | 1.00 | 1.71 | -1.12 | -1.23 | 2.03 |
| Let-7f | -2.03 | -1.18 | -1.84 | -1.94 | -2.40 | -1.29 | -1.35 | -2.35 |
| Let-7g | -1.23 | 1.39 | -1.89 | -1.70 | -1.45 | -1.87 | -1.66 | -4.59 |
| Let-7i | 1.52 | 2.16 | -2.48 | -1.94 | -1.37 | -2.15 | -1.83 | -5.48 |
| miR-7 | 1.88 | 1.39 | -2.20 | -1.33 | -2.01 | -1.67 | -1.92 | -4.82 |
| miR-15a | -1.76 | -1.02 | -1.59 | -1.67 | -2.07 | -1.29 | -1.77 | -4.39 |
| miR-15b | -2.63 | -1.53 | -2.38 | -2.51 | -3.11 | -1.54 | -1.75 | -2.87 |
| miR-15b* | 4.33 | 1.88 | -1.65 | -1.27 | 1.15 | -1.31 | -3.09 | -8.28 |
| miR-16 | -2.64 | -1.53 | -2.38 | -2.51 | -3.11 | -1.54 | -1.76 | -2.87 |
| miR-16-2* | 3.96 | 4.34 | -1.74 | -2.86 | 1.20 | -2.07 | -3.06 | -3.38 |
| miR-17 | -1.58 | 1.08 | -2.03 | -2.82 | -1.86 | -2.52 | -2.98 | -5.23 |
| miR-17* | 3.02 | 2.07 | -1.34 | -1.88 | 1.36 | -1.12 | -2.29 | -1.59 |
| miR-18a | 1.49 | 1.22 | -2.20 | -2.65 | -1.53 | -1.72 | -3.86 | -4.90 |
| miR-18a* | -1.04 | -1.13 | -1.64 | -2.32 | -1.21 | -1.39 | -2.60 | -1.78 |
| miR-18b | 1.74 | 1.94 | -1.72 | -1.60 | -1.16 | -1.01 | -2.20 | -3.09 |

| Hsa-miRNA | LA1 >3mths (LC) | LA2 >3mths (LB) | LA3 >3mths (LX) | LA4 >3mths (E) | LA5 >3mths (BB) | LA6 >3mths (DB) | SV >3mths (LM) | CE >3mths (BE) |
|---|---|---|---|---|---|---|---|---|
| miR-19a | -1.62 | 1.05 | -1.47 | -1.55 | -1.91 | 1.05 | -1.08 | -1.77 |
| miR-19b | -1.15 | 1.48 | -1.04 | -1.10 | -1.36 | 1.48 | 1.29 | -1.26 |
| miR-20a | -1.53 | 1.11 | -1.39 | -1.46 | -1.81 | 1.11 | -1.02 | -1.67 |
| miR-20a* | 6.48 | 3.55 | -1.12 | -1.40 | 2.01 | -1.67 | -1.84 | -3.34 |
| miR-20b | 2.27 | 2.52 | -1.06 | -1.37 | 1.21 | -1.13 | -1.23 | -2.25 |
| miR-20b* | 1.19 | -1.17 | 1.05 | 1.03 | 1.10 | 1.07 | 1.03 | 1.18 |
| miR-21 | 1.21 | -3.32 | -5.15 | -3.66 | -4.19 | -4.44 | -5.59 | -27.05 |
| miR-22 | -2.60 | -1.51 | -2.35 | -2.48 | -3.07 | -1.52 | -1.73 | -2.83 |
| miR-22* | 3.11 | 1.82 | -1.10 | -1.28 | 1.25 | 1.07 | -1.62 | -1.52 |
| miR-23a | 1.64 | -1.09 | -2.38 | -3.27 | -1.53 | -2.86 | -2.41 | -5.81 |
| miR-23b | 2.30 | 1.66 | -1.51 | -2.20 | 1.05 | -1.47 | -1.75 | -2.84 |
| miR-24 | 1.65 | 1.98 | -1.41 | -1.43 | 1.40 | -1.28 | -1.29 | -2.02 |
| miR-24-1* | 1.46 | 1.59 | 1.16 | -1.10 | 1.41 | 1.04 | 1.05 | 1.08 |
| miR-25 | 1.58 | 2.42 | -1.34 | -1.37 | 1.16 | -1.54 | -1.54 | -2.69 |
| miR-25* | -1.01 | 1.58 | 1.18 | 1.29 | -1.15 | 1.53 | 1.64 | 1.16 |
| miR-26a | -1.18 | 1.11 | -2.25 | -3.22 | -1.40 | -3.60 | -3.69 | -7.01 |
| miR-26a-2* | 2.40 | 1.16 | -1.50 | -1.55 | 1.09 | -1.78 | -3.12 | -3.99 |
| miR-26b | -1.71 | 1.00 | -1.60 | -1.80 | -2.01 | -2.11 | -2.00 | -4.84 |
| miR-26b* | 2.14 | 1.66 | 1.43 | 1.40 | 1.64 | 1.50 | 1.06 | 1.51 |
| miR-27a | 4.08 | 2.14 | -1.56 | -1.06 | 1.59 | -1.19 | -1.28 | -2.08 |
| miR-27a* | 2.82 | 2.89 | 1.86 | 1.17 | -1.69 | 1.00 | 1.93 | -1.41 |
| miR-28-5p | 4.05 | 2.01 | -1.18 | -1.13 | 1.59 | -1.20 | -1.18 | -1.97 |
| miR-29a | 2.47 | -1.05 | -2.55 | -2.12 | -1.20 | -2.57 | -2.50 | -3.65 |
| miR-29a* | 4.12 | 3.88 | 3.09 | 3.39 | 2.52 | 4.22 | 1.98 | 2.04 |
| miR-29b | 4.09 | 2.50 | -1.02 | 1.38 | 1.48 | 1.20 | 1.09 | 2.41 |
| miR-29b-2* | 2.13 | 1.47 | 1.51 | 1.33 | 1.73 | 1.30 | 1.01 | 1.02 |

| Hsa-miRNA | LA1 >3mths (LC) | LA2 >3mths (LB) | LA3 >3mths (LX) | LA4 >3mths (E) | LA5 >3mths (BB) | LA6 >3mths (DB) | SV >3mths (LM) | CE >3mths (BE) |
|---|---|---|---|---|---|---|---|---|
| miR-29c | 3.47 | 1.10 | -2.06 | -1.86 | -1.04 | -1.74 | -2.37 | -3.28 |
| miR-29c* | 1.97 | -1.43 | -1.35 | -1.48 | 1.06 | -1.20 | -2.02 | -2.40 |
| miR-30a | -1.98 | -1.15 | -1.79 | -1.89 | -2.33 | -1.29 | -1.87 | -2.16 |
| miR-30b | -1.16 | 1.47 | -1.24 | -1.95 | -1.37 | -1.53 | -1.52 | -2.61 |
| miR-30c | -1.10 | 1.55 | -1.57 | -2.42 | -1.30 | -1.82 | -2.05 | -3.08 |
| miR-30d | 1.23 | 1.07 | -1.21 | -2.75 | 1.02 | -2.40 | -3.10 | -2.02 |
| miR-30e | 1.40 | 2.41 | -1.12 | -1.18 | 1.18 | 1.07 | -1.16 | -2.30 |
| miR-30e* | 2.42 | 1.30 | -2.98 | -3.52 | -1.13 | -4.04 | -4.58 | -6.04 |
| miR-32 | 3.99 | 1.96 | -1.91 | -2.36 | -2.16 | -1.85 | -2.63 | -5.21 |
| miR-32* | -1.44 | -1.31 | -1.18 | -2.16 | -1.20 | -1.80 | -2.05 | -1.26 |
| miR-33a | 11.98 | 1.53 | 1.76 | 4.78 | 1.08 | 2.81 | -1.74 | -1.65 |
| miR-34b | -1.06 | 1.32 | -1.49 | -1.04 | -1.24 | 1.10 | -1.28 | -1.15 |
| miR-92a | 1.09 | 1.08 | -1.19 | -1.44 | -1.07 | -1.21 | -1.40 | -1.09 |
| miR-92b | -1.19 | -1.16 | -1.42 | -2.20 | -1.24 | -1.45 | -1.68 | -1.34 |
| miR-93 | -2.05 | -1.19 | -1.86 | -2.16 | -2.42 | -2.06 | -2.78 | -2.74 |
| miR-93* | 1.68 | 1.68 | -1.08 | -1.67 | 1.19 | -1.25 | -2.94 | -1.82 |
| miR-96 | -1.26 | 1.82 | -3.52 | -1.78 | -2.26 | -3.94 | -3.10 | -4.72 |
| miR-98 | 2.78 | 1.59 | -2.14 | -1.75 | -1.50 | -1.94 | -1.48 | -5.48 |
| miR-99a | 2.16 | 2.40 | -1.01 | 1.10 | -1.15 | -1.01 | 1.20 | 1.35 |
| miR-99b* | -1.06 | 1.04 | -1.17 | -1.12 | -1.28 | 1.09 | -1.17 | -1.54 |
| miR-101 | 1.13 | 1.94 | -1.42 | -1.54 | -1.04 | -1.37 | -1.83 | -3.30 |
| miR-101* | 6.36 | 1.76 | -1.66 | -1.53 | 1.59 | -1.40 | -2.24 | -3.10 |
| miR-103 | -1.07 | -1.21 | -1.90 | -3.41 | -1.33 | -2.97 | -3.72 | -6.31 |
| miR-106a | -1.34 | 1.27 | -1.65 | -2.51 | -1.58 | -2.29 | -2.57 | -4.43 |
| miR-106a* | 8.66 | 2.91 | 1.18 | -1.21 | 1.61 | -12.29 | ND | -2.46 |
| miR-106b | -2.11 | -1.23 | -1.91 | -2.01 | -2.49 | -1.27 | -1.47 | -2.30 |

| Hsa-miRNA | LA1 >3mths (LC) | LA2 >3mths (LB) | LA3 >3mths (LX) | LA4 >3mths (E) | LA5 >3mths (BB) | LA6 >3mths (DB) | SV >3mths (LM) | CE >3mths (BE) |
|---|---|---|---|---|---|---|---|---|
| miR-106b* | 1.74 | 1.07 | -1.81 | -2.43 | -1.20 | -2.34 | -3.49 | -2.80 |
| miR-107 | -1.02 | 1.24 | -1.68 | -2.87 | -1.21 | -2.71 | -3.27 | -4.40 |
| miR-122 | -2.20 | -2.07 | -1.97 | -2.15 | -3.32 | -1.86 | -1.70 | -2.79 |
| miR-122* | -1.14 | -1.19 | 1.58 | 2.00 | 1.14 | 1.79 | 2.45 | -1.02 |
| miR-124* | 2.79 | 1.97 | 2.20 | 2.02 | 1.75 | 2.25 | 2.90 | 1.84 |
| miR-125a-5p | 1.41 | 1.27 | 1.43 | -1.02 | -1.06 | -1.04 | 1.25 | -1.16 |
| miR-125b | 1.10 | 2.03 | 1.43 | 1.82 | 2.35 | -1.39 | -2.38 | 1.48 |
| miR-125b-1* | -1.19 | 1.46 | -1.06 | -2.37 | -2.10 | -2.08 | 1.16 | -2.66 |
| miR-125b-2* | 1.72 | 1.41 | 1.99 | 1.05 | 1.09 | -1.23 | 2.04 | 1.20 |
| miR-126 | -1.32 | 1.29 | -1.46 | -1.72 | -1.55 | -2.40 | -1.64 | -5.43 |
| miR-126* | 3.26 | -1.26 | -3.15 | -2.45 | -1.58 | -4.06 | -3.25 | -15.58 |
| miR-128 | 2.11 | 1.02 | -1.45 | -1.76 | -1.10 | -1.80 | -6.01 | -3.02 |
| miR-129* | 1.28 | -1.18 | 1.71 | 1.35 | 1.46 | 1.33 | 1.48 | 1.43 |
| miR-129-5p | 1.05 | 2.42 | 1.31 | 1.01 | -1.64 | 1.28 | 1.88 | -1.56 |
| miR-130a | 1.34 | 2.29 | -1.61 | -2.67 | 1.13 | -1.46 | -1.70 | -2.13 |
| miR-130b | 1.31 | -1.08 | -1.70 | -3.63 | -1.66 | -3.94 | -2.97 | -3.49 |
| miR-130b* | 1.96 | 2.00 | 2.40 | 1.67 | 2.01 | 1.63 | 1.93 | 2.24 |
| miR-132* | 7.17 | 1.95 | 1.40 | 1.42 | -1.12 | 1.62 | 1.66 | 1.03 |
| miR-135b | 2.90 | 1.82 | 1.31 | 1.30 | 1.30 | 2.14 | 1.03 | -1.25 |
| miR-138-1* | -1.16 | -1.03 | -1.10 | -1.33 | -1.37 | -1.14 | -1.65 | -1.50 |
| miR-138-2* | 2.75 | 2.85 | 1.90 | 1.34 | 1.27 | -1.02 | -1.85 | -5.57 |
| miR-140-3p | -1.46 | 1.13 | -1.60 | -2.30 | -1.72 | -1.75 | -2.67 | -1.88 |
| miR-140-5p | 1.79 | -1.16 | -2.71 | -2.38 | -1.91 | -2.32 | -4.25 | -7.40 |
| miR-142-3p | -1.76 | -1.02 | -2.05 | -1.68 | -2.07 | -1.19 | -1.79 | -6.45 |
| miR-142-5p | -1.57 | 1.08 | -1.42 | -1.50 | -1.86 | -1.22 | -1.27 | -2.26 |
| miR-143 | 7.67 | 4.85 | 1.38 | 1.45 | 2.34 | 2.18 | 2.02 | -1.21 |

| Hsa-miRNA | LA1 >3mths (LC) | LA2 >3mths (LB) | LA3 >3mths (LX) | LA4 >3mths (E) | LA5 >3mths (BB) | LA6 >3mths (DB) | SV >3mths (LM) | CE >3mths (BE) |
|---|---|---|---|---|---|---|---|---|
| miR-144 | -2.56 | -1.49 | -2.31 | -2.44 | -3.02 | -1.49 | -1.70 | -2.79 |
| miR-144* | -1.04 | 1.64 | -1.42 | -1.34 | -1.22 | -1.85 | -1.29 | -6.55 |
| miR-145 | 2.70 | 2.19 | 1.80 | 2.52 | 2.77 | 5.20 | 3.17 | 2.58 |
| miR-145* | 1.12 | 1.18 | 1.67 | 1.19 | 1.33 | 1.53 | 1.07 | 1.12 |
| miR-146a | 2.51 | 1.48 | -1.95 | -1.75 | -1.27 | -1.66 | -1.45 | -4.97 |
| miR-146b-3p | 1.29 | 1.57 | 1.86 | 1.35 | 1.74 | 1.27 | 1.16 | 1.57 |
| miR-146b-5p | 2.97 | 1.73 | -1.80 | -1.54 | -1.19 | -1.83 | -1.47 | -4.25 |
| miR-148a | 5.65 | 2.92 | -1.41 | -1.11 | 1.43 | -1.20 | 1.01 | -2.64 |
| miR-148b | 4.48 | 3.02 | -1.32 | -1.57 | 1.88 | -1.09 | -1.32 | -1.50 |
| miR-149* | -1.09 | 1.53 | 1.14 | -2.42 | -1.71 | -2.12 | -1.23 | -1.27 |
| miR-150 | 2.39 | 1.54 | 1.48 | 1.32 | 2.14 | -1.74 | -1.20 | -1.91 |
| miR-151-3p | 1.43 | -1.88 | -3.28 | -3.68 | -1.61 | -3.03 | -4.41 | -4.27 |
| miR-151-5p | 2.73 | 1.39 | -1.74 | -2.60 | 1.06 | -1.98 | -1.97 | -2.39 |
| miR-155 | 1.06 | -1.36 | -1.54 | -1.49 | -1.56 | -1.53 | -1.69 | -1.44 |
| miR-181a | 1.37 | -1.88 | -2.73 | -3.39 | -1.37 | -7.63 | -6.27 | -2.26 |
| miR-181a-2* | 2.48 | 2.63 | 1.47 | 1.10 | 1.11 | -1.37 | 2.69 | -1.12 |
| miR-181b | 1.52 | 2.26 | -1.13 | 1.04 | -1.08 | -1.08 | -1.38 | -1.53 |
| miR-182 | 1.25 | 2.76 | -2.33 | -1.82 | -1.35 | -4.01 | -3.28 | -4.46 |
| miR-183 | -1.41 | 1.96 | -1.94 | -1.95 | -1.16 | -3.35 | -3.75 | -2.15 |
| miR-183* | -1.13 | 1.23 | 1.10 | -1.55 | -1.43 | -1.57 | -1.18 | -1.19 |
| miR-184 | -1.05 | 1.43 | -1.01 | 1.12 | -1.35 | 1.12 | 1.42 | -1.04 |
| miR-185 | -1.53 | 1.07 | -2.16 | -2.70 | -1.80 | -1.18 | -2.90 | -3.03 |
| miR-185* | 1.04 | 2.06 | -1.03 | -1.84 | -2.34 | -1.28 | 1.44 | -2.36 |
| miR-186 | -1.15 | -2.02 | -3.77 | -5.11 | -2.43 | -2.92 | -7.72 | -5.19 |
| miR-187* | 1.40 | 1.86 | 1.32 | -1.13 | -1.02 | 1.07 | 1.44 | -1.05 |
| miR-188-5p | 1.64 | -1.39 | 1.23 | 1.52 | 1.24 | 1.66 | -2.26 | -1.37 |

| Hsa-miRNA | LA1 >3mths (LC) | LA2 >3mths (LB) | LA3 >3mths (LX) | LA4 >3mths (E) | LA5 >3mths (BB) | LA6 >3mths (DB) | SV >3mths (LM) | CE >3mths (BE) |
|---|---|---|---|---|---|---|---|---|
| miR-190 | 1.04 | -2.33 | -5.35 | -3.09 | -5.34 | -3.86 | -5.55 | -26.35 |
| miR-191 | -2.09 | -1.22 | -1.89 | -2.02 | -2.47 | -1.73 | -1.83 | -2.28 |
| miR-192 | 1.76 | -1.02 | -3.23 | -4.40 | -2.16 | -4.23 | -8.17 | -10.90 |
| miR-193a-3p | 2.09 | 1.45 | -1.16 | -1.57 | 1.18 | -1.19 | -1.64 | -2.09 |
| miR-193b* | -1.17 | 1.27 | 1.13 | -1.28 | -1.07 | -1.15 | -1.12 | -1.06 |
| miR-194 | 3.34 | 1.48 | -1.86 | -1.58 | 1.39 | -1.00 | -2.24 | -2.38 |
| miR-194* | 1.58 | 1.79 | 1.46 | 1.34 | -1.41 | 1.50 | 1.84 | 1.16 |
| miR-195 | 3.44 | 1.84 | 1.04 | 1.13 | 2.04 | -2.02 | -1.93 | -9.85 |
| miR-196a* | 1.48 | 1.13 | 1.39 | 1.90 | 1.50 | 1.45 | 1.94 | 1.29 |
| miR-196b | 2.82 | -1.00 | -1.26 | -1.23 | -1.72 | 1.47 | -1.42 | -2.30 |
| miR-197 | 1.03 | 1.05 | 1.05 | -1.51 | 1.06 | 1.05 | -1.11 | 1.18 |
| miR-198 | 1.02 | -1.04 | 1.18 | 1.06 | 1.02 | 1.26 | 1.18 | 1.06 |
| miR-199a-3p | 7.12 | 1.91 | 1.20 | -1.04 | 1.34 | 1.16 | 1.09 | -39.42 |
| miR-199a-5p | 4.30 | 2.65 | 1.14 | -1.19 | 1.20 | 1.44 | -1.00 | -1.39 |
| miR-199b-5p | 3.70 | 2.31 | 1.50 | 2.02 | 1.72 | 1.74 | 2.11 | 1.26 |
| miR-200b | 1.28 | -1.21 | 1.63 | 1.35 | 1.46 | 1.48 | 1.08 | 1.00 |
| miR-200b* | 1.40 | 1.52 | 1.51 | 1.05 | 1.12 | -1.36 | 2.00 | 1.52 |
| miR-203 | -3.58 | ND | -2.76 | -3.79 | -3.78 | -11.80 | ND | -10.10 |
| miR-206 | 1.49 | 3.46 | 1.43 | 1.07 | 1.19 | -1.48 | 2.55 | -2.18 |
| miR-208a | -1.15 | -1.11 | -1.36 | -1.41 | -1.58 | 1.10 | -1.65 | -2.01 |
| miR-208b | 1.87 | 1.54 | 1.60 | 1.08 | -1.00 | ND | 2.29 | 1.35 |
| miR-210 | 3.16 | 1.49 | -1.28 | 1.11 | 1.99 | 3.00 | -1.22 | 1.09 |
| miR-214 | 1.84 | 1.58 | 1.77 | 1.04 | 1.86 | -1.49 | -1.10 | 1.24 |
| miR-215 | 2.85 | 2.01 | -1.62 | -1.46 | -1.17 | -1.36 | -1.92 | -3.26 |
| miR-221 | 3.28 | 1.39 | 1.30 | 1.07 | 1.66 | -1.26 | -1.18 | -3.73 |
| miR-221* | 2.07 | 1.61 | 1.82 | 1.19 | 1.59 | -1.45 | 1.20 | 1.13 |

| Hsa-miRNA | LA1 >3mths (LC) | LA2 >3mths (LB) | LA3 >3mths (LX) | LA4 >3mths (E) | LA5 >3mths (BB) | LA6 >3mths (DB) | SV >3mths (LM) | CE >3mths (BE) |
|---|---|---|---|---|---|---|---|---|
| miR-222 | 1.06 | -1.49 | -1.77 | -3.52 | -1.53 | -2.96 | -2.38 | -4.65 |
| miR-223 | 1.17 | 2.01 | -1.13 | -1.13 | -1.00 | 1.46 | 1.24 | -1.97 |
| miR-299-3p | 1.14 | 1.28 | 1.59 | 1.28 | 1.54 | 2.20 | 1.58 | 1.37 |
| miR-300 | -1.22 | 1.30 | -1.46 | -2.62 | -1.60 | -2.09 | -2.00 | -1.32 |
| miR-301a | 2.89 | 1.54 | -1.94 | -3.34 | -1.60 | -2.22 | -2.80 | -9.31 |
| miR-301b | 5.82 | 1.42 | -1.00 | -1.08 | -1.25 | -4.60 | ND | ND |
| miR-302c* | 1.84 | 1.77 | 1.86 | 1.54 | 1.20 | 1.78 | 1.21 | 1.26 |
| miR-302e | 2.09 | 2.24 | 1.71 | 1.36 | 1.42 | 1.41 | 1.70 | 1.03 |
| miR-320a | -1.75 | -2.06 | -1.76 | -4.26 | -2.06 | -2.90 | -4.80 | -2.22 |
| miR-320b | -1.64 | -2.16 | -1.92 | -4.07 | -1.88 | -3.03 | -5.01 | -2.27 |
| miR-320c | -1.76 | -1.15 | -1.60 | -2.37 | -2.08 | -1.68 | -2.35 | -1.92 |
| miR-320d | -1.11 | -1.44 | -1.42 | -2.89 | -1.32 | -2.06 | -3.24 | -1.66 |
| miR-324-3p | 1.62 | 1.40 | 1.13 | 1.14 | 1.60 | 1.34 | -1.07 | 1.06 |
| miR-324-5p | 1.11 | -1.01 | -1.36 | -2.66 | 1.20 | -2.30 | -2.87 | -1.72 |
| miR-326 | -2.23 | 1.04 | -1.12 | -1.13 | -1.53 | -1.33 | -2.07 | -3.33 |
| miR-328 | 1.71 | 1.47 | 1.61 | 1.46 | 2.02 | 2.14 | 1.11 | 1.50 |
| miR-331-3p | 1.01 | -1.09 | -1.41 | -2.42 | 1.00 | -1.40 | -2.35 | -1.22 |
| miR-331-5p | -1.55 | -2.90 | -2.96 | -4.27 | -1.93 | -4.85 | -9.51 | -4.45 |
| miR-335 | 5.06 | 3.81 | -1.29 | -1.88 | 1.45 | -1.51 | -1.51 | -2.89 |
| miR-335* | -1.04 | 1.41 | -1.18 | -1.35 | -2.53 | -1.04 | 1.08 | -2.86 |
| miR-338-3p | 2.37 | 1.29 | 1.19 | 1.90 | 1.34 | 2.87 | 1.51 | -1.44 |
| miR-339-3p | 1.75 | -1.08 | -2.05 | -2.10 | 1.65 | -2.14 | -2.44 | -1.05 |
| miR-339-5p | 1.60 | 1.22 | -1.75 | -2.72 | 1.69 | -1.53 | -2.05 | 1.60 |
| miR-340 | 3.27 | 1.69 | -1.09 | -1.37 | 1.05 | -1.12 | -1.71 | -1.97 |
| miR-340* | 1.76 | 2.37 | 1.54 | 1.31 | 1.07 | 1.58 | 2.09 | -1.18 |
| miR-342-3p | 1.55 | 1.10 | -1.12 | -1.09 | 1.51 | -1.62 | -1.29 | -2.14 |

| Hsa-miRNA | LA1 >3mths (LC) | LA2 >3mths (LB) | LA3 >3mths (LX) | LA4 >3mths (E) | LA5 >3mths (BB) | LA6 >3mths (DB) | SV >3mths (LM) | CE >3mths (BE) |
|---|---|---|---|---|---|---|---|---|
| miR-342-5p | 1.17 | -1.95 | -1.53 | -1.39 | 1.02 | -2.46 | -2.28 | -2.38 |
| miR-345 | 2.72 | 2.96 | 1.47 | 1.51 | 2.50 | 2.12 | 1.40 | 1.27 |
| miR-361-3p | 1.08 | 1.22 | -1.37 | -1.39 | -1.49 | -1.50 | -1.56 | -1.47 |
| miR-361-5p | 2.03 | 1.14 | 1.29 | 1.26 | 1.73 | -1.19 | -2.89 | -3.60 |
| miR-362-3p | 5.99 | 2.04 | -1.23 | -2.29 | -1.00 | -3.04 | -4.63 | -5.20 |
| miR-362-5p | 1.32 | -1.23 | -2.46 | -3.92 | -1.84 | -3.99 | -5.69 | -5.50 |
| miR-363 | 1.16 | -1.00 | -1.57 | -3.02 | -1.13 | -2.93 | -3.59 | -2.90 |
| miR-363* | 1.37 | 1.23 | 2.24 | 2.74 | 1.64 | 2.03 | 1.91 | 1.52 |
| miR-365 | 2.10 | 2.54 | 1.31 | 1.46 | 2.51 | 1.90 | 1.21 | 1.03 |
| miR-370 | -1.08 | 1.40 | -1.08 | -1.01 | -1.31 | 1.59 | 1.35 | -1.15 |
| miR-374a | 1.09 | 1.81 | -1.56 | -1.98 | -1.11 | -2.02 | -2.34 | -8.06 |
| miR-374b | 3.46 | 1.57 | -1.64 | -1.99 | 1.07 | -2.26 | -2.38 | -6.46 |
| miR-374b* | 1.74 | 1.43 | 1.79 | 1.60 | 1.69 | 1.39 | 1.40 | 1.73 |
| miR-375 | 1.00 | -1.00 | 1.15 | 1.03 | -1.28 | 1.02 | -1.35 | -1.40 |
| miR-378 | 2.11 | 1.34 | -1.16 | -1.86 | 1.19 | -1.45 | -1.75 | -1.02 |
| miR-381 | -1.14 | 1.36 | -1.01 | -2.30 | -1.72 | -1.76 | 1.01 | -1.35 |
| miR-382 | 1.41 | 1.66 | 1.51 | 1.19 | 1.18 | 1.29 | 1.88 | 1.65 |
| miR-412 | -1.26 | -1.48 | -1.23 | -1.81 | -1.34 | -1.94 | -1.85 | -1.38 |
| miR-421 | -1.33 | -2.60 | -1.92 | -2.15 | -1.72 | -2.73 | -2.60 | -3.42 |
| miR-422a | 1.15 | -1.66 | -1.26 | -1.41 | -1.22 | -1.45 | -1.71 | -1.84 |
| miR-423-3p | -1.35 | -1.30 | -1.76 | -2.78 | -1.31 | -1.25 | -3.27 | -1.22 |
| miR-423-5p | -2.05 | -1.87 | -1.99 | -4.06 | -2.41 | -2.24 | -3.88 | -2.23 |
| miR-424 | 3.07 | -1.41 | -1.74 | -1.29 | -2.01 | -4.71 | -2.30 | -3.53 |
| miR-425 | 1.35 | 1.02 | -1.27 | -2.38 | 1.03 | -2.42 | -2.35 | -3.30 |
| miR-425* | 1.48 | 1.16 | -1.22 | -1.79 | 1.06 | -1.57 | -1.70 | -1.44 |
| miR-450a | 1.57 | 1.50 | 1.88 | 2.63 | 1.69 | 2.59 | 2.19 | 1.28 |

| Hsa-miRNA | LA1 >3mths (LC) | LA2 >3mths (LB) | LA3 >3mths (LX) | LA4 >3mths (E) | LA5 >3mths (BB) | LA6 >3mths (DB) | SV >3mths (LM) | CE >3mths (BE) |
|---|---|---|---|---|---|---|---|---|
| miR-451 | -2.63 | -1.53 | -2.38 | -2.51 | -3.11 | -1.54 | -1.75 | -2.87 |
| miR-454 | 3.51 | 1.45 | -1.13 | 1.17 | 1.20 | -1.19 | -1.36 | ND |
| miR-483-5p | -1.26 | 3.90 | 1.15 | 1.01 | 1.04 | 1.24 | 1.19 | 1.18 |
| miR-484 | 1.47 | 1.45 | -1.03 | -1.91 | 1.31 | 1.22 | -1.21 | 1.05 |
| miR-485-3p | -1.28 | 1.43 | 1.22 | 1.22 | -1.07 | 1.10 | -1.21 | -1.42 |
| miR-486-3p | 3.52 | 4.67 | -1.17 | 1.31 | 1.00 | 2.90 | 2.29 | -3.04 |
| miR-486-5p | -2.64 | -1.53 | -2.38 | -2.51 | -3.11 | -1.54 | -1.75 | -2.87 |
| miR-487b | -1.10 | -1.56 | -1.26 | -1.65 | -1.31 | -1.14 | -2.12 | -2.83 |
| miR-488 | 2.75 | 2.82 | 2.30 | 1.23 | 1.21 | 1.30 | 2.15 | 1.02 |
| miR-489 | 2.10 | 2.92 | 1.59 | 1.13 | -1.01 | 1.31 | 2.32 | 1.17 |
| miR-490-3p | 2.20 | 1.34 | 3.01 | 1.77 | 3.15 | 1.71 | 1.09 | 3.03 |
| miR-491-3p | -1.04 | -1.94 | -1.08 | 1.46 | 1.27 | 1.99 | -1.84 | 1.56 |
| miR-492 | 1.15 | ND | 2.36 | 1.20 | -1.48 | ND | -1.23 | -1.86 |
| miR-493* | -1.47 | 1.49 | -1.89 | -3.03 | -2.94 | -3.29 | -1.14 | -5.52 |
| miR-494 | 1.76 | 1.69 | 1.61 | 1.64 | 1.39 | 2.16 | 1.47 | 1.35 |
| miR-498 | 1.30 | 1.62 | 1.64 | 1.37 | 1.25 | 1.66 | 1.77 | 1.50 |
| miR-500 | 1.00 | -1.98 | -2.29 | -4.55 | -1.45 | -3.55 | -6.09 | -4.29 |
| miR-500* | 1.01 | -1.35 | -1.85 | -2.81 | -1.49 | -3.49 | -3.97 | -3.38 |
| miR-501-5p | -1.19 | -1.79 | -1.80 | -3.54 | -1.59 | -2.84 | -5.25 | -2.89 |
| miR-502-3p | 1.20 | -1.14 | -1.61 | -2.48 | -1.22 | -3.02 | -4.13 | -2.60 |
| miR-502-5p | -1.26 | -1.10 | -1.66 | -2.82 | -2.17 | -2.35 | -1.81 | -3.77 |
| miR-504 | -7.13 | -8.12 | -4.50 | -4.06 | -4.40 | -4.53 | -5.74 | -4.43 |
| miR-505 | 1.43 | -1.60 | -2.14 | -2.86 | -1.45 | -3.86 | ND | -3.57 |
| miR-505* | -1.22 | -1.30 | -1.42 | -2.12 | -1.34 | -1.96 | -2.07 | -1.72 |
| miR-508-5p | -1.09 | -1.49 | -1.08 | -1.53 | -1.70 | -2.38 | -1.26 | -2.40 |
| miR-509-5p | 2.07 | 1.86 | 2.22 | 1.21 | 2.03 | -1.30 | -1.35 | 1.24 |

| Hsa-miRNA | LA1 >3mths (LC) | LA2 >3mths (LB) | LA3 >3mths (LX) | LA4 >3mths (E) | LA5 >3mths (BB) | LA6 >3mths (DB) | SV >3mths (LM) | CE >3mths (BE) |
|---|---|---|---|---|---|---|---|---|
| miR-510 | 1.61 | 2.15 | 2.14 | -1.10 | 1.38 | -1.28 | 1.42 | 1.57 |
| miR-513a-3p | 2.19 | 2.71 | 1.39 | 1.13 | 1.17 | 1.34 | 1.51 | 1.18 |
| miR-513a-5p | -1.21 | 1.70 | 1.24 | 1.19 | -1.13 | 1.59 | 1.92 | 1.75 |
| miR-516a-5p | -2.17 | -2.73 | -2.00 | -3.10 | -2.35 | -3.38 | -3.71 | -2.07 |
| miR-516b | 1.61 | 1.60 | 1.98 | 2.01 | 1.70 | 1.79 | 1.81 | 1.77 |
| miR-518a-5p | 1.09 | 1.04 | -1.02 | -1.84 | -1.15 | -1.46 | -1.87 | -1.56 |
| miR-519c-5p | 1.77 | -1.16 | 1.97 | 1.50 | 1.54 | 1.09 | -1.22 | 1.49 |
| miR-519d | 1.10 | -1.00 | 1.08 | -1.37 | -1.15 | 1.18 | -2.07 | -1.70 |
| miR-519e | -1.01 | 1.68 | 1.08 | 1.03 | -1.19 | 1.68 | 1.47 | -1.10 |
| miR-519e* | 1.89 | 1.15 | 2.27 | 1.11 | 1.91 | -1.09 | -2.21 | -1.59 |
| miR-520d-5p | 2.02 | 1.50 | 1.86 | 1.13 | 1.59 | 1.44 | -1.11 | 1.19 |
| miR-525-5p | 1.30 | -1.07 | 1.54 | 1.14 | 1.33 | 1.28 | 1.13 | 1.51 |
| miR-532-3p | 1.78 | 1.28 | 1.42 | -1.28 | 1.92 | 1.19 | -1.28 | 1.68 |
| miR-532-5p | 2.33 | 1.55 | -1.47 | -2.53 | -1.02 | -2.15 | -3.12 | -2.61 |
| miR-542-3p | -1.35 | -1.48 | -1.55 | -1.46 | -2.01 | -1.72 | -1.33 | -1.82 |
| miR-548e | 1.73 | -1.03 | 1.49 | 2.17 | 1.44 | 1.31 | 1.35 | -1.06 |
| miR-548n | -1.05 | 1.02 | 1.33 | 1.65 | 1.24 | 1.65 | 1.19 | -1.04 |
| miR-549 | 1.13 | 1.02 | 1.29 | -1.09 | 1.29 | -1.13 | -1.15 | 1.11 |
| miR-550 | 1.00 | -1.16 | 1.03 | -1.59 | 1.15 | -1.64 | -1.99 | -1.00 |
| miR-550* | -1.03 | -1.45 | -1.54 | -3.39 | -1.10 | -2.20 | -3.20 | -1.77 |
| miR-551a | 1.58 | 2.02 | 1.52 | 1.48 | 1.57 | 2.05 | 1.57 | 1.24 |
| miR-551b | 1.13 | 2.04 | 1.41 | 1.03 | -1.01 | 1.84 | 1.16 | 1.11 |
| miR-552 | 1.05 | 1.06 | -1.06 | -1.14 | -1.41 | 1.16 | 1.26 | 1.81 |
| miR-553 | 2.56 | 3.11 | 3.09 | 1.42 | 1.45 | 1.39 | 2.42 | 1.39 |
| miR-557 | 1.33 | 1.30 | 1.02 | -1.51 | -1.45 | -1.55 | -1.02 | -1.27 |
| miR-574-3p | 1.68 | 1.20 | 1.62 | 1.01 | 1.73 | -1.06 | -1.18 | 1.10 |

| Hsa-miRNA | LA1 >3mths (LC) | LA2 >3mths (LB) | LA3 >3mths (LX) | LA4 >3mths (E) | LA5 >3mths (BB) | LA6 >3mths (DB) | SV >3mths (LM) | CE >3mths (BE) |
|---|---|---|---|---|---|---|---|---|
| miR-574-5p | -1.02 | 1.02 | -1.03 | -1.80 | -1.05 | -1.36 | -1.80 | -1.35 |
| miR-576-3p | 1.21 | 1.32 | 1.59 | 1.43 | 1.77 | 1.55 | 1.50 | 1.89 |
| miR-576-5p | 1.09 | 1.03 | -2.45 | -2.52 | -1.93 | -1.36 | -2.28 | -2.72 |
| miR-578 | 1.34 | 1.94 | 1.86 | 2.34 | 1.33 | 3.57 | 2.81 | 1.60 |
| miR-581 | 1.07 | 1.08 | 1.55 | 1.84 | 1.20 | 2.72 | 1.92 | 1.35 |
| miR-583 | 1.00 | 1.02 | 1.11 | -1.39 | -1.02 | -1.28 | -1.23 | 1.03 |
| miR-584 | -1.27 | -2.27 | -1.64 | -2.27 | -1.21 | -1.70 | -2.97 | -1.95 |
| miR-585 | 1.76 | 3.34 | 2.19 | 2.85 | 1.26 | 3.23 | 3.88 | 1.35 |
| miR-589 | 1.10 | -1.11 | -1.07 | -1.17 | -1.03 | -1.13 | -1.16 | -1.19 |
| miR-590-5p | 2.61 | -1.26 | -2.03 | -1.98 | -2.07 | -2.59 | -19.55 | ND |
| miR-597 | 1.03 | -1.91 | -1.23 | -1.47 | -1.42 | -2.61 | -2.08 | -5.38 |
| miR-600 | 1.57 | 1.34 | 2.20 | 2.23 | 1.77 | 2.81 | 2.51 | -2.97 |
| miR-601 | 2.26 | 1.97 | 2.46 | 2.70 | 2.21 | 3.48 | 2.10 | 2.26 |
| miR-602 | 1.55 | 2.61 | 1.39 | 1.25 | -1.09 | 1.71 | 2.05 | 1.46 |
| miR-605 | 1.01 | -1.24 | 1.30 | -1.20 | -1.02 | 1.04 | -1.85 | -1.72 |
| miR-611 | 1.53 | 2.25 | 1.32 | 1.12 | -1.24 | 1.46 | 1.32 | 1.18 |
| miR-615-3p | 2.14 | 2.04 | 2.36 | 2.01 | 1.78 | 2.38 | 1.90 | 1.66 |
| miR-617 | -1.56 | -1.24 | -1.12 | -1.57 | -1.46 | -1.89 | -1.21 | -1.53 |
| miR-618 | 1.78 | 1.84 | 1.92 | 1.99 | 1.77 | 2.68 | 2.63 | 1.95 |
| miR-620 | 1.42 | 1.38 | 1.93 | 1.46 | 1.91 | 1.51 | 1.57 | 2.42 |
| miR-622 | 1.70 | -1.24 | 1.00 | -1.27 | -1.19 | 1.06 | -3.31 | 1.18 |
| miR-623 | 1.62 | 1.61 | 1.35 | -1.17 | -1.15 | -1.00 | 1.36 | 1.28 |
| miR-625 | 1.09 | 1.00 | -1.58 | -2.11 | -1.30 | 1.17 | -2.81 | -1.35 |
| miR-625* | -1.29 | -1.48 | -1.30 | -1.38 | -1.50 | -1.10 | -1.51 | -1.52 |
| miR-627 | 2.61 | 1.04 | -1.60 | 1.30 | 2.58 | -1.73 | -2.19 | -2.27 |
| miR-628-3p | -1.08 | 1.83 | 1.12 | -1.47 | -1.58 | -1.38 | 1.21 | -1.25 |

| Hsa-miRNA | LA1 >3mths (LC) | LA2 >3mths (LB) | LA3 >3mths (LX) | LA4 >3mths (E) | LA5 >3mths (BB) | LA6 >3mths (DB) | SV >3mths (LM) | CE >3mths (BE) |
|---|---|---|---|---|---|---|---|---|
| miR-629 | -1.02 | -1.46 | -2.57 | -2.36 | -1.02 | -2.05 | -2.84 | -2.15 |
| miR-629* | -1.19 | -1.33 | 1.04 | -1.12 | -1.30 | 1.01 | -1.78 | -1.70 |
| miR-630 | 1.11 | 1.31 | 1.88 | 1.15 | 1.62 | 1.24 | 1.29 | 1.69 |
| miR-634 | -1.17 | 1.02 | -1.09 | -1.44 | -1.38 | -1.18 | -1.73 | -1.88 |
| miR-635 | 2.02 | 2.75 | 2.06 | 1.09 | 1.05 | -3.06 | 1.95 | -1.23 |
| miR-636 | -1.02 | -1.37 | -1.16 | -1.15 | -1.01 | 1.27 | -1.04 | -1.44 |
| miR-637 | 1.73 | 2.75 | 1.71 | -1.17 | -1.96 | -1.01 | 2.27 | -1.93 |
| miR-638 | 1.39 | 1.81 | 2.00 | 1.38 | -1.04 | 1.68 | 2.08 | 1.22 |
| miR-642 | -1.41 | -1.08 | -1.15 | -1.56 | -1.33 | -1.23 | -1.46 | -1.23 |
| miR-647 | 1.19 | 1.55 | -1.19 | -1.29 | 1.07 | -1.10 | 1.15 | -1.08 |
| miR-652 | 1.07 | -1.36 | -1.33 | -2.66 | -1.21 | -2.98 | -3.91 | -2.18 |
| miR-659 | 1.46 | 1.41 | 1.70 | 1.38 | 1.55 | 1.55 | 1.53 | 1.55 |
| miR-660 | 5.06 | 2.71 | -1.32 | -1.66 | 1.00 | -1.61 | -1.67 | -3.16 |
| miR-664 | 1.73 | 2.28 | 1.90 | 1.64 | 1.69 | 2.08 | 1.71 | 1.44 |
| miR-665 | 1.61 | 1.62 | 1.93 | -1.01 | 1.85 | 1.23 | -1.80 | 2.80 |
| miR-668 | 1.19 | 2.77 | 2.38 | 2.55 | 1.51 | 2.77 | 2.76 | 1.68 |
| miR-671-5p | -1.02 | -1.36 | 1.03 | 1.25 | 1.32 | -1.27 | -4.22 | 1.71 |
| miR-675 | 1.40 | 1.26 | 1.21 | -1.20 | -1.14 | -1.19 | -1.30 | 1.05 |
| miR-720 | -2.26 | -1.31 | -2.04 | -2.15 | -2.66 | -1.32 | -1.52 | -2.46 |
| miR-744 | -1.02 | 1.47 | -1.07 | -2.07 | -1.55 | -1.15 | -1.09 | -1.56 |
| miR-765 | -1.34 | -1.09 | 1.00 | -1.29 | 1.00 | -1.12 | -1.38 | 1.24 |
| miR-766 | 1.09 | -1.01 | 1.05 | -1.44 | 1.08 | -1.11 | -1.60 | 1.16 |
| miR-769-5p | -1.13 | -4.27 | -1.69 | -2.19 | -1.05 | -1.81 | -16.31 | -2.36 |
| miR-874 | 1.94 | 1.40 | 1.75 | 1.11 | 1.93 | -1.32 | -1.41 | 1.06 |
| miR-876-3p | 1.59 | -1.83 | 1.19 | 1.14 | 1.09 | 1.30 | -1.25 | -1.63 |
| miR-877 | -2.27 | -2.79 | -2.11 | -2.43 | -1.93 | -1.69 | -2.77 | -1.85 |

| Hsa-miRNA | LA1 >3mths (LC) | LA2 >3mths (LB) | LA3 >3mths (LX) | LA4 >3mths (E) | LA5 >3mths (BB) | LA6 >3mths (DB) | SV >3mths (LM) | CE >3mths (BE) |
|---|---|---|---|---|---|---|---|---|
| miR-877* | 2.40 | 2.77 | 2.41 | 2.56 | 1.59 | 3.79 | 2.62 | 2.03 |
| miR-887 | -1.72 | -3.23 | -1.61 | -2.49 | -2.20 | -2.25 | -4.29 | -2.57 |
| miR-888* | 1.13 | 1.24 | 1.10 | -1.30 | -1.23 | 1.37 | -1.34 | -1.15 |
| miR-890 | -1.25 | -1.27 | 1.00 | -1.67 | -1.13 | -1.53 | -1.20 | -1.57 |
| miR-891a | -1.28 | 1.26 | 1.16 | 1.35 | 1.06 | 1.22 | -1.20 | -1.20 |
| miR-920 | 1.77 | 1.58 | 2.15 | 1.94 | 2.29 | 1.68 | 1.75 | 2.34 |
| miR-923 | -1.81 | -2.22 | -1.64 | -4.71 | -2.14 | -3.84 | -3.36 | -1.98 |
| miR-933 | 1.08 | 1.11 | 1.46 | 1.16 | 1.22 | 1.40 | -1.04 | -1.03 |
| miR-934 | 1.35 | 1.21 | 1.98 | 1.39 | 1.70 | 1.17 | 1.32 | 1.60 |
| miR-937 | 1.90 | 1.65 | 1.14 | 1.13 | 1.44 | -1.19 | 1.92 | -1.03 |
| miR-939 | -1.07 | 1.26 | 1.04 | -2.52 | -1.42 | -2.17 | -1.62 | -1.00 |
| miR-941 | -1.81 | -2.47 | -5.79 | -2.20 | -4.17 | -3.87 | -2.95 | -2.60 |
| miR-942 | 3.02 | 1.45 | 3.37 | 4.37 | 2.71 | 4.45 | 2.93 | 2.64 |
| miR-943 | 2.30 | 3.89 | 2.27 | 1.84 | 1.34 | 2.66 | 3.34 | 1.22 |
| miR-944 | 6.78 | -1.13 | 1.40 | 1.19 | 1.26 | -2.37 | -1.46 | -1.54 |
| miR-1184 | -1.13 | 2.07 | -1.12 | -1.96 | -2.41 | -1.52 | -1.31 | -2.78 |
| miR-1201 | 1.44 | -1.03 | 1.22 | 1.09 | 1.38 | -1.54 | 1.05 | 1.11 |
| miR-1224-3p | 2.11 | 3.50 | 1.26 | 1.95 | -1.27 | 1.94 | 2.48 | 1.40 |
| miR-1227 | 1.98 | 2.41 | 2.57 | 2.37 | 1.78 | 3.12 | 2.53 | 1.59 |
| miR-1236 | 1.08 | 1.58 | 1.13 | -1.32 | -1.41 | 1.09 | -1.00 | -1.34 |
| miR-1246 | -1.09 | 1.45 | -1.04 | -1.01 | 1.02 | 1.26 | 1.24 | 1.11 |
| miR-1249 | 2.00 | 2.43 | 1.56 | 1.66 | 1.23 | 2.50 | 2.07 | 1.22 |
| miR-1255a | 1.03 | 1.43 | 1.52 | 1.38 | 1.50 | 1.37 | 1.16 | 1.50 |
| miR-1259 | 1.05 | -1.01 | 1.17 | 1.60 | 1.08 | 1.26 | 1.52 | -1.00 |
| miR-1260 | 1.18 | 1.02 | 1.09 | -1.50 | -1.22 | -1.04 | -1.48 | -1.46 |
| miR-1261 | 1.65 | 2.71 | 2.41 | -1.47 | -1.07 | 1.35 | 2.37 | -1.71 |

| Hsa-miRNA | LA1 >3mths (LC) | LA2 >3mths (LB) | LA3 >3mths (LX) | LA4 >3mths (E) | LA5 >3mths (BB) | LA6 >3mths (DB) | SV >3mths (LM) | CE >3mths (BE) |
|---|---|---|---|---|---|---|---|---|
| miR-1264 | -1.32 | 1.32 | 1.21 | 1.32 | -1.02 | 1.52 | -1.25 | -1.59 |
| miR-1265 | -1.21 | -1.01 | 1.14 | -1.03 | 1.01 | 1.31 | -1.29 | -1.18 |
| miR-1274a | 1.84 | 1.31 | 1.31 | 1.14 | 1.01 | 1.61 | -1.21 | -1.08 |
| miR-1274b | -1.08 | -1.59 | -1.14 | -1.32 | -1.51 | 1.01 | -1.58 | -2.00 |
| miR-1275 | -1.67 | -1.44 | -2.07 | -2.29 | -2.37 | -2.64 | -1.90 | -2.21 |
| miR-1280 | 1.47 | 1.28 | 1.39 | -1.12 | 1.15 | 1.36 | -1.39 | -1.03 |
| miR-1284 | -2.52 | 1.15 | 1.04 | -1.31 | -1.07 | -1.14 | -1.64 | -1.50 |
| miR-1285 | 1.44 | 2.44 | 1.61 | 1.34 | 1.23 | 1.84 | 1.72 | 1.34 |
| miR-1290 | -1.55 | -1.62 | -1.96 | -1.92 | 1.01 | -1.76 | -2.16 | 1.90 |
| miR-1297 | 7.57 | 8.35 | 1.32 | 2.43 | 2.63 | 2.26 | 2.98 | -2.25 |
| miR-1299 | -1.41 | -1.33 | -1.02 | -2.10 | -1.08 | -1.61 | -2.05 | -1.24 |
| miR-1301 | -1.07 | -1.21 | -1.56 | -1.97 | -1.40 | -1.94 | -1.86 | -1.82 |
| miR-1304 | 2.07 | 1.22 | 2.28 | 1.65 | 3.48 | -1.08 | 1.22 | 2.01 |
| miR-1307 | 1.43 | -1.69 | -1.80 | -1.55 | 1.11 | 1.05 | -3.74 | -1.03 |
| miR-1308 | -1.34 | 1.47 | -1.04 | -1.10 | -1.36 | 1.48 | 1.29 | -1.25 |
| miR-1321 | 1.18 | 1.29 | 1.51 | 1.32 | 1.42 | 1.24 | 1.28 | 1.48 |
| miR-1826 | -2.64 | -1.53 | -2.39 | -2.51 | -3.11 | -1.54 | -1.75 | -2.87 |
| miR-1827 | 2.53 | 2.21 | 1.71 | 1.05 | 2.00 | -1.01 | 1.09 | 1.81 |

**Supplementary Table 3**: Expression of 250 miRNAs detected at various time-points (12hr, 24hr, 48hr, 72hr, 120hr and 168hr). MiRNAs were expressed as fold change compared with normal control. All miRNAs selected have positive raw intensity values and FDR < 0.05. ND represents not detected.

| Rno-miRNA | 12hr | 24hr | 48hr | 72hr | 120hr | 168hr | Rno-miRNA | 12hr | 24hr | 48hr | 72hr | 120hr | 168hr |
|---|---|---|---|---|---|---|---|---|---|---|---|---|---|
| let-7a | -1.46 | -1.39 | -1.46 | -2.14 | -2.08 | -2.81 | miR-22* | -3.87 | -3.10 | -2.67 | -4.94 | -4.26 | -5.20 |
| let-7b | -1.34 | -1.23 | -1.42 | -1.87 | -2.12 | -2.44 | miR-23a | -2.55 | -1.64 | -1.59 | -2.42 | -1.70 | -2.30 |
| let-7b* | -1.47 | -1.47 | -1.33 | -1.81 | -1.71 | -2.66 | miR-23b | -2.96 | -2.50 | -2.53 | -3.35 | -2.92 | -4.00 |
| let-7c | -1.07 | -1.03 | -1.14 | -1.62 | -1.87 | -2.15 | miR-24 | -5.62 | -3.42 | -3.15 | -4.98 | -3.80 | -5.85 |
| let-7d | -2.26 | -2.18 | -2.16 | -2.98 | -2.79 | -3.40 | miR-24-1* | -2.92 | -2.27 | -2.20 | -3.57 | -3.29 | -3.61 |
| let-7d* | -1.80 | -1.47 | -1.45 | -2.18 | -1.65 | -2.02 | miR-24-2* | -1.68 | -1.21 | -1.38 | -2.24 | -2.27 | -2.29 |
| let-7e | -2.24 | -2.28 | -2.75 | -4.29 | -4.42 | -6.19 | miR-25 | -3.01 | -2.65 | -3.48 | -3.07 | -1.64 | -1.82 |
| let-7e* | -1.66 | -1.33 | -1.54 | -1.90 | -1.22 | -1.41 | miR-26a | -1.52 | -1.52 | -1.57 | -2.23 | -2.49 | -3.18 |
| let-7f | -1.31 | -1.51 | ND | -2.27 | -2.65 | ND | miR-26b | -1.96 | -1.95 | -2.08 | -3.05 | -3.13 | -3.86 |
| let-7i | -2.33 | -2.36 | -2.11 | -3.46 | -3.28 | -4.07 | miR-27a | -3.48 | -2.56 | -2.67 | -3.08 | -3.25 | -4.34 |
| let-7i* | 3.07 | 2.13 | -2.10 | 1.59 | 4.73 | -2.82 | miR-27a* | 3.87 | 5.30 | 5.18 | 7.39 | 21.97 | 7.03 |
| miR-7a | 1.61 | -1.77 | -2.00 | -2.78 | -7.87 | -6.84 | miR-27b | -2.12 | -2.31 | -2.08 | -2.93 | -1.85 | -3.38 |
| miR-7b | -1.66 | -1.94 | -2.24 | -2.72 | -2.75 | -2.89 | miR-28 | -2.75 | -2.46 | -2.55 | -3.51 | -3.36 | -3.95 |
| miR-9 | -4.57 | -3.64 | -4.18 | -6.01 | -6.43 | -9.35 | miR-29a | -2.82 | -2.35 | -2.76 | -3.26 | -3.38 | -4.70 |
| miR-9* | -3.63 | -5.24 | -3.65 | -7.00 | -8.83 | -14.97 | miR-29a* | -2.97 | -2.42 | -2.37 | -2.93 | -2.68 | -3.04 |
| miR-10b | 1.30 | 1.85 | 1.31 | 1.44 | 2.64 | 1.44 | miR-29b | -8.11 | -9.82 | -7.48 | -14.78 | -17.73 | -26.20 |
| miR-15b | -2.54 | -2.58 | -1.88 | -1.94 | -1.01 | -1.12 | miR-29c | -4.12 | -4.32 | -5.29 | -7.45 | -12.44 | -13.83 |
| miR-16 | -2.99 | -2.35 | -2.54 | -4.51 | -3.50 | -3.60 | miR-29c* | -2.68 | -3.73 | -3.09 | -3.43 | -4.21 | -3.04 |
| miR-19a | -3.80 | -4.97 | -2.56 | -3.00 | -5.13 | -5.62 | miR-30a | -3.01 | -2.65 | -3.17 | -4.36 | -5.41 | -6.41 |
| miR-19b | -7.39 | -7.06 | -5.94 | -8.39 | -8.96 | -13.68 | miR-30b-3p | -2.43 | -2.79 | ND | -3.04 | -4.32 | -4.67 |
| miR-21 | -1.76 | -1.80 | -1.11 | -1.71 | -1.36 | -1.92 | miR-30b-5p | -1.62 | -1.29 | -1.97 | -2.51 | -2.70 | -3.21 |
| miR-21* | -1.10 | -1.06 | -1.83 | -3.85 | -4.45 | -7.98 | miR-30c | -1.83 | -1.51 | -1.76 | -2.22 | -2.44 | -3.07 |
| miR-22 | -4.35 | -4.05 | -2.41 | -4.12 | -2.64 | -4.16 | miR-30d* | 2.44 | 3.50 | 2.23 | 11.17 | 4.67 | 3.89 |

| Rno-miRNA | 12hr | 24hr | 48hr | 72hr | 120hr | 168hr | Rno-miRNA | 12hr | 24hr | 48hr | 72hr | 120hr | 168hr |
|---|---|---|---|---|---|---|---|---|---|---|---|---|---|
| miR-30e | -5.60 | -5.65 | -4.21 | -7.77 | -8.96 | -13.45 | miR-125b-5p | -3.75 | -3.30 | -2.90 | -3.94 | -3.23 | -4.42 |
| miR-30e* | -3.58 | -3.41 | -3.18 | -4.22 | -4.15 | -5.43 | miR-126 | -1.63 | -1.64 | -1.64 | -2.60 | -2.28 | -3.32 |
| miR-31 | -2.22 | -4.20 | -2.70 | -4.36 | -3.81 | -4.51 | miR-126* | -3.68 | -3.78 | -3.55 | -5.49 | -6.34 | -7.88 |
| miR-32 | -2.36 | -3.00 | -3.69 | -4.74 | -5.29 | -9.53 | miR-127 | -2.93 | -3.24 | -3.45 | -4.74 | -4.56 | -5.37 |
| miR-33 | -3.94 | -6.02 | -4.69 | -6.53 | -9.07 | -4.61 | miR-128 | -4.80 | -2.82 | -3.04 | -4.27 | -3.83 | -5.98 |
| miR-34a | -3.52 | -3.23 | -2.38 | -4.20 | -3.95 | -5.12 | miR-129 | -1.47 | -1.19 | -1.45 | -1.93 | -2.01 | -2.48 |
| miR-34b | -2.77 | -6.44 | -6.52 | -7.87 | -18.97 | -15.29 | miR-129* | -2.83 | -2.80 | -2.61 | -2.81 | -3.13 | -4.37 |
| miR-34c | -2.97 | -4.17 | -5.67 | -5.86 | -5.41 | -8.16 | miR-130a | -1.07 | -1.27 | -1.92 | -2.65 | -3.31 | -3.93 |
| miR-34c* | -4.60 | -5.16 | -4.11 | -5.06 | -7.60 | -7.97 | miR-132 | -5.16 | -2.22 | -3.30 | -3.60 | -3.94 | -3.76 |
| miR-92b | -1.58 | -1.73 | -1.83 | -2.42 | -2.76 | -3.42 | miR-135a | -2.60 | -5.07 | -4.27 | -5.44 | -9.26 | -13.13 |
| miR-93 | -2.30 | -2.24 | -2.35 | -2.31 | -1.84 | -2.26 | miR-135b | -2.75 | -2.60 | -2.94 | -3.82 | -3.83 | -4.06 |
| miR-98 | -1.72 | -1.94 | -1.94 | -3.09 | -4.24 | -5.10 | miR-136 | -2.78 | -4.11 | -4.65 | -7.43 | -9.61 | -12.87 |
| miR-99a | -2.39 | -3.04 | -2.79 | -4.30 | -3.25 | -5.02 | miR-136* | -1.33 | -1.63 | -2.09 | -2.79 | -5.45 | -7.26 |
| miR-99b | -1.14 | -1.19 | -1.15 | -1.51 | -1.44 | -2.07 | miR-137 | -2.62 | -4.19 | -7.58 | -8.22 | -18.23 | -20.12 |
| miR-99b* | -3.72 | -2.89 | -2.52 | -2.86 | -2.86 | -3.39 | miR-138 | -7.92 | -7.83 | -5.30 | -8.46 | -7.06 | -10.13 |
| miR-100 | -2.58 | -2.72 | -2.43 | -3.64 | -3.20 | -4.60 | miR-138* | -3.08 | -2.59 | -2.27 | -3.94 | -4.27 | -5.17 |
| miR-101a | -3.19 | -3.71 | -3.07 | -5.69 | -9.45 | -12.08 | miR-139-3p | 3.45 | 3.16 | 1.56 | 1.73 | 2.81 | -1.02 |
| miR-101a* | 9.45 | 12.82 | 9.90 | 7.07 | 11.98 | 16.60 | miR-139-5p | -2.31 | -1.66 | -2.17 | -2.42 | -1.78 | -2.34 |
| miR-101b | -2.91 | -3.80 | -3.38 | -5.34 | -7.93 | -9.36 | miR-140 | -2.40 | -2.85 | -3.39 | -4.27 | -4.76 | -4.66 |
| miR-103 | -2.54 | -2.66 | -3.26 | -3.89 | -3.89 | -4.47 | miR-140* | -1.13 | -1.26 | -1.44 | -1.76 | -1.94 | -2.16 |
| miR-106b | -1.21 | -1.45 | -1.33 | -1.83 | -1.81 | -2.19 | miR-142-3p | -2.40 | -2.34 | -1.38 | -2.01 | -1.47 | -1.21 |
| miR-107 | -3.66 | -4.76 | -5.53 | -7.11 | -7.12 | -8.13 | miR-142-5p | -1.35 | -1.39 | 1.30 | -1.20 | 1.17 | 1.26 |
| miR-124 | -2.69 | -2.25 | -2.02 | -2.74 | -2.20 | -3.58 | miR-143 | -1.27 | -1.89 | -1.46 | -2.36 | -2.18 | -2.75 |
| miR-124* | -2.67 | -2.57 | -2.08 | -3.54 | -2.58 | -4.07 | miR-144 | -2.27 | -1.37 | -4.33 | -9.06 | -5.14 | -9.14 |
| miR-125a-5p | -1.67 | -1.82 | -2.05 | -2.23 | -2.21 | -3.06 | miR-145 | -3.04 | -4.46 | -3.99 | -4.46 | -4.62 | -5.21 |
| miR-125b* | -2.00 | -1.91 | -2.58 | -4.02 | -5.58 | -6.24 | miR-146a | 1.02 | -1.07 | -1.09 | -1.24 | 1.20 | 2.60 |
| miR-125b-3p | -1.75 | -1.44 | -1.75 | 1.60 | -2.73 | -3.18 | miR-146b | -1.59 | -1.28 | -1.44 | -1.97 | -1.70 | -1.79 |

| Rno-miRNA | 12hr | 24hr | 48hr | 72hr | 120hr | 168hr | Rno-miRNA | 12hr | 24hr | 48hr | 72hr | 120hr | 168hr |
|---|---|---|---|---|---|---|---|---|---|---|---|---|---|
| miR-147 | 3.00 | 4.53 | 3.54 | 2.83 | 4.71 | 3.88 | miR-204 | -5.26 | -5.17 | -6.68 | -5.29 | -4.31 | -5.16 |
| miR-148b-3p | -1.74 | -1.77 | -1.84 | -2.48 | -2.58 | -3.33 | miR-204* | -3.44 | -3.05 | -3.35 | -5.40 | -5.71 | -6.79 |
| miR-148b-5p | 5.39 | 2.40 | -2.10 | 3.69 | 6.54 | 3.36 | miR-206 | -1.39 | 1.79 | 1.09 | -2.27 | -2.08 | -2.99 |
| miR-150 | -4.89 | -5.11 | -1.31 | -3.97 | -7.41 | -8.65 | miR-207 | -6.21 | -7.45 | -4.34 | -11.95 | -13.50 | -18.53 |
| miR-151 | -2.25 | -2.06 | -2.23 | -3.16 | -3.01 | -3.56 | miR-208 | -2.97 | -1.83 | -1.17 | -4.60 | -3.53 | -3.50 |
| miR-181a | -5.54 | -4.57 | -5.07 | -5.56 | -6.90 | -8.42 | miR-212 | -2.87 | -1.73 | -2.34 | -3.58 | -4.22 | -5.82 |
| miR-181a* | -3.71 | -3.23 | -3.04 | -3.65 | -4.04 | -6.74 | miR-214 | -1.67 | -1.77 | -2.10 | -3.01 | -1.28 | -1.46 |
| miR-181b | -2.96 | -2.77 | ND | -4.39 | -5.22 | -6.07 | miR-217 | 4.59 | 8.06 | 3.55 | -1.56 | 2.92 | 1.94 |
| miR-181c | -7.88 | -5.42 | -7.99 | -10.57 | -8.01 | -9.67 | miR-218 | -5.14 | -3.94 | -5.40 | -7.52 | -11.06 | -14.12 |
| miR-181d | ND | -1.87 | -2.25 | ND | -1.97 | -2.03 | miR-219-2-3p | -4.73 | -4.93 | -4.44 | -7.01 | -8.14 | -10.04 |
| miR-183 | -8.45 | -4.40 | -2.72 | -7.08 | -9.54 | -5.25 | miR-219-5p | -5.57 | -12.61 | -6.33 | -12.65 | -21.97 | -34.81 |
| miR-184 | -1.91 | -2.61 | -2.59 | -1.70 | -3.95 | -4.42 | miR-221 | -6.73 | -4.86 | -5.57 | -6.85 | -5.45 | -6.99 |
| miR-185 | 1.08 | -1.21 | -1.17 | -1.75 | -2.04 | -2.73 | miR-222 | -2.20 | -1.85 | -2.17 | -3.05 | -2.91 | -3.96 |
| miR-186 | -3.00 | -2.64 | -3.29 | -3.89 | -4.79 | -4.87 | miR-223 | -1.35 | -1.12 | 1.52 | 1.12 | 1.61 | 1.01 |
| miR-190 | -2.68 | -4.02 | -2.57 | -5.13 | -6.92 | -8.60 | miR-290 | -1.04 | -1.45 | -1.28 | -3.24 | -3.81 | -4.82 |
| miR-191 | -1.20 | -1.31 | -1.27 | -1.67 | -1.68 | -1.86 | miR-291a-3p | -2.70 | -3.05 | -2.40 | -3.71 | -3.52 | -2.36 |
| miR-192 | -1.19 | -1.17 | -1.68 | -2.01 | -1.04 | -12.88 | miR-291a-5p | 2.59 | 3.01 | 1.05 | -1.46 | -1.76 | -2.08 |
| miR-193 | -1.13 | -1.28 | -1.04 | -1.68 | -1.68 | -2.58 | miR-292-3p | 5.29 | 4.43 | 12.75 | 5.26 | 4.59 | 3.50 |
| miR-194 | -3.66 | -3.55 | -4.51 | -3.80 | -4.37 | -9.73 | miR-298 | 2.38 | 1.03 | -1.07 | -1.22 | -1.79 | -2.28 |
| miR-195 | -1.82 | -1.30 | -1.62 | -2.31 | -2.88 | -3.46 | miR-300-3p | -1.01 | -1.39 | -1.89 | -2.32 | -4.05 | -4.18 |
| miR-196a* | -4.96 | -4.41 | -4.20 | -4.86 | -6.67 | -7.87 | miR-300-5p | -1.24 | -1.26 | -2.06 | -3.26 | -4.26 | -5.73 |
| miR-199a-3p | -1.10 | -1.21 | -1.84 | -1.36 | 1.53 | 2.25 | miR-320 | 1.67 | 1.29 | 1.18 | 1.00 | -1.10 | -1.26 |
| miR-199a-5p | -1.05 | 1.09 | -2.38 | -1.29 | 1.73 | 1.53 | miR-322 | -1.95 | -1.93 | -2.62 | -3.17 | -3.46 | -3.57 |
| miR-200a | 4.55 | 16.03 | 1.12 | 3.10 | 7.77 | 8.23 | miR-322* | 8.29 | 3.68 | -2.10 | -1.56 | 5.20 | -2.25 |
| miR-200b | -1.27 | 1.44 | -1.05 | -1.22 | -1.46 | 1.03 | miR-323 | -3.45 | -3.75 | -3.80 | -5.36 | -6.37 | -8.05 |
| miR-200c | 1.59 | 2.42 | 2.62 | 1.38 | 1.49 | 1.56 | miR-324-5p | -2.39 | -3.49 | -4.78 | -5.04 | -3.85 | -4.77 |
| miR-203 | -2.50 | -2.54 | -1.51 | -5.04 | -4.72 | -5.37 | miR-325-3p | -3.01 | -2.99 | -2.94 | -3.89 | -4.26 | -5.89 |

| Rno-miRNA | 12hr | 24hr | 48hr | 72hr | 120hr | 168hr | Rno-miRNA | 12hr | 24hr | 48hr | 72hr | 120hr | 168hr |
|---|---|---|---|---|---|---|---|---|---|---|---|---|---|
| miR-325-5p | -1.44 | -1.67 | -1.52 | -2.25 | -2.82 | -3.44 | miR-365 | -1.95 | -2.11 | -2.24 | -2.33 | -2.62 | -3.68 |
| miR-326 | -1.50 | -1.33 | -1.99 | -3.48 | -3.32 | -3.98 | miR-369-3p | -1.95 | -2.99 | -2.84 | -4.43 | -8.80 | -9.42 |
| miR-328 | -3.02 | -2.29 | -2.38 | -2.88 | -2.36 | -2.64 | miR-369-5p | -2.09 | -2.57 | -3.81 | -3.26 | -4.60 | -4.69 |
| miR-329 | -1.53 | -1.78 | -1.81 | -2.32 | -2.74 | -3.23 | miR-370 | -2.49 | -2.03 | -1.67 | -2.30 | -1.70 | -2.26 |
| miR-330 | -2.54 | -2.89 | -2.43 | -2.94 | -2.95 | -3.48 | miR-374 | -6.95 | -7.25 | -8.48 | -8.10 | -3.92 | -4.72 |
| miR-330* | -1.81 | -2.33 | -2.44 | -2.82 | -4.09 | -5.31 | miR-375 | -2.84 | -1.83 | -2.68 | -2.31 | -1.82 | -1.87 |
| miR-331 | -3.61 | -3.70 | -3.59 | -5.18 | -6.48 | -7.13 | miR-376a | -1.53 | -2.57 | -2.74 | -4.08 | -6.36 | -10.50 |
| miR-335 | -1.18 | -1.74 | -1.48 | -2.74 | -4.42 | -6.22 | miR-376a* | -1.40 | -1.55 | -2.41 | -2.84 | -2.30 | -2.49 |
| miR-336 | -4.77 | -2.85 | -2.42 | -3.50 | -3.57 | -3.35 | miR-376b-3p | -2.00 | -2.74 | -2.63 | -3.77 | -6.35 | -7.85 |
| miR-337 | 1.14 | -1.18 | -1.40 | -1.82 | -2.01 | -2.04 | miR-376b-5p | -2.25 | -2.27 | -2.53 | -3.13 | -3.16 | -3.26 |
| miR-338* | -2.11 | -2.27 | -2.28 | -3.19 | -3.83 | ND | miR-376c | -2.12 | -2.07 | -2.29 | -2.71 | -4.31 | -4.85 |
| miR-339-5p | -2.21 | -2.22 | -1.62 | -1.76 | 1.12 | 1.38 | miR-377 | -4.28 | -3.38 | -2.78 | -3.88 | -4.56 | -4.70 |
| miR-340-3p | -4.37 | -3.92 | -3.98 | -5.06 | -5.07 | -5.45 | miR-378 | -2.06 | -1.89 | -2.05 | -2.19 | -1.42 | -1.67 |
| miR-340-5p | -4.76 | -8.33 | -5.37 | -10.12 | -17.39 | -24.20 | miR-378* | 22.21 | 40.77 | 36.12 | 14.66 | 30.69 | 19.92 |
| miR-341 | 1.11 | -1.46 | -2.22 | -2.63 | -6.17 | -5.36 | miR-379 | -1.24 | -1.55 | -1.72 | -2.53 | -3.66 | -5.58 |
| miR-342-3p | -2.20 | -2.09 | -2.39 | -2.86 | -2.60 | -2.61 | miR-381 | -1.19 | -1.58 | -1.94 | -2.54 | -3.66 | -3.98 |
| miR-342-5p | -1.11 | -1.39 | -2.13 | -1.38 | -1.59 | -1.43 | miR-382 | -2.32 | -2.33 | -2.33 | -3.37 | -3.36 | -4.13 |
| miR-344-3p | -1.26 | -1.96 | -3.24 | -1.94 | -1.38 | -4.51 | miR-382* | -3.41 | -1.57 | -1.99 | -4.09 | -2.67 | -4.21 |
| miR-345-5p | -1.30 | -1.59 | -1.55 | -1.91 | -1.62 | -3.20 | miR-383 | -1.13 | -1.11 | -1.47 | -1.75 | -1.77 | -1.81 |
| miR-346 | -1.48 | -1.64 | -1.58 | -1.47 | -1.04 | 1.23 | miR-384-3p | -2.97 | -3.30 | -3.00 | -5.53 | -9.88 | -17.06 |
| miR-347 | -4.09 | -3.78 | -2.55 | -4.51 | 1.28 | -1.34 | miR-384-5p | -2.22 | ND | ND | -4.63 | -7.78 | -13.52 |
| miR-350 | -1.70 | -1.90 | -1.51 | -2.13 | -2.31 | -3.50 | miR-409-3p | -1.97 | -1.77 | -2.53 | -2.69 | -3.15 | -4.03 |
| miR-351 | -1.10 | -1.43 | -1.50 | -3.06 | -4.19 | -5.07 | miR-409-5p | -1.78 | -2.01 | -2.09 | -2.83 | -3.22 | -3.47 |
| miR-352 | -4.11 | -4.31 | -5.09 | -4.97 | -5.02 | -9.11 | miR-410 | -1.40 | -2.09 | -3.74 | -3.80 | -5.75 | -8.48 |
| miR-361 | -1.05 | -1.17 | -1.22 | -1.59 | -2.14 | -2.20 | miR-411 | -2.73 | -3.04 | 2.13 | -3.96 | -4.70 | -6.83 |
| miR-363 | 8.78 | 12.82 | 10.44 | 8.86 | 10.87 | 21.38 | miR-412 | -1.67 | -1.69 | -1.53 | -2.18 | -2.01 | -2.41 |
| miR-363* | -3.79 | -2.61 | -3.27 | -3.54 | -2.54 | -2.35 | miR-423 | -2.17 | -2.03 | -1.87 | -2.79 | -1.78 | -2.29 |

| Rno-miRNA | 12hr | 24hr | 48hr | 72hr | 120hr | 168hr | Rno-miRNA | 12hr | 24hr | 48hr | 72hr | 120hr | 168hr |
|---|---|---|---|---|---|---|---|---|---|---|---|---|---|
| miR-425 | -2.69 | -5.95 | -2.96 | -1.06 | -2.06 | -3.40 | miR-540 | 17.08 | 19.37 | 7.36 | 9.99 | 10.22 | 8.48 |
| miR-429 | 5.30 | -2.33 | -2.10 | 4.47 | 6.19 | 4.25 | miR-541 | 1.17 | -1.03 | -1.58 | -1.84 | -1.98 | -2.58 |
| miR-431 | -1.27 | -1.84 | 1.07 | -1.36 | 1.11 | 1.44 | miR-542-3p | -2.34 | -2.56 | -2.27 | -3.42 | -4.95 | -3.52 |
| miR-433 | -1.71 | -2.55 | -3.07 | -3.73 | -4.66 | -5.10 | miR-542-5p | 1.82 | 2.89 | 1.38 | -1.16 | 1.23 | -1.00 |
| miR-434 | -1.18 | -1.23 | -1.25 | -1.70 | -1.72 | -2.36 | miR-551b | -4.58 | -4.07 | -3.93 | -5.87 | -5.68 | -7.22 |
| miR-448 | -1.44 | -1.46 | -2.35 | -1.48 | 1.34 | -1.13 | miR-598-3p | -2.61 | -2.58 | -3.26 | -3.50 | -3.11 | -2.91 |
| miR-451 | -5.41 | -2.49 | -4.83 | -19.32 | -16.53 | -6.85 | miR-598-5p | 8.74 | 16.56 | 6.16 | 7.49 | 14.61 | 26.61 |
| miR-466b | -1.01 | -1.15 | -1.56 | -2.12 | -2.65 | -2.29 | miR-652 | -2.67 | -3.82 | -3.34 | -4.84 | -5.53 | -3.98 |
| miR-466c | -1.41 | -1.82 | ND | -2.26 | ND | ND | miR-664 | -1.69 | -1.71 | ND | -2.79 | -2.97 | -3.84 |
| miR-471 | -2.62 | -3.31 | -1.69 | -3.81 | -3.38 | -5.44 | miR-673 | 2.40 | 3.63 | -2.10 | 7.17 | 5.49 | 18.15 |
| miR-485 | -1.88 | -2.43 | -2.51 | -2.48 | -2.76 | -2.37 | miR-674-3p | -1.46 | 1.08 | 1.21 | -1.05 | -1.09 | -1.18 |
| miR-487b | -3.65 | -4.30 | -3.33 | -7.28 | -7.79 | -8.49 | miR-674-5p | -1.46 | -1.08 | -1.13 | -1.46 | -1.54 | -1.89 |
| miR-488 | -1.84 | -1.91 | -2.26 | -3.27 | -2.10 | -2.07 | miR-708 | -1.56 | -1.56 | -2.29 | -3.10 | -4.68 | -5.68 |
| miR-489 | 13.16 | 1.28 | -2.10 | 5.07 | -2.13 | -2.82 | miR-742 | -1.84 | -2.56 | -1.68 | -3.32 | -3.75 | -5.02 |
| miR-493 | 9.76 | 8.87 | 10.38 | 14.52 | 27.01 | 14.83 | miR-743b | -2.95 | -4.43 | -2.53 | -4.39 | -6.52 | -6.51 |
| miR-494 | -4.89 | -4.83 | -4.65 | -11.34 | -12.01 | -19.76 | miR-872 | -2.15 | -1.71 | -2.48 | -2.81 | -3.11 | -2.47 |
| miR-495 | -2.14 | -2.81 | -3.33 | -4.42 | -7.23 | -8.38 | miR-872* | -1.95 | -2.35 | -1.85 | -3.97 | -4.87 | -6.29 |
| miR-497 | -4.23 | -4.36 | -3.83 | -4.97 | -5.03 | -10.45 | miR-873 | -1.61 | -1.36 | -2.99 | -3.12 | -3.47 | -2.88 |
| miR-503 | -1.38 | -1.67 | -1.63 | -3.31 | -3.90 | -4.23 | miR-877 | -1.29 | -1.51 | -1.60 | -2.40 | -2.85 | -2.69 |
| miR-505 | -1.83 | -1.45 | -1.66 | -1.98 | -2.30 | -1.88 | miR-879 | -3.58 | -3.53 | -6.29 | -3.98 | -4.90 | -5.42 |
| miR-539 | -1.64 | -2.03 | -2.52 | -3.14 | -3.36 | -4.02 | miR-881 | -2.80 | 3.95 | -2.10 | 3.01 | 19.35 | 4.73 |

**Supplementary Table 4**: List of 857 miRNA predicted to target *CD46* 3'UTR.

| Hsa-miRNA | Number of databases | Hsa-miRNA | Number of databases | Hsa-miRNA | Number of databases |
|---|---|---|---|---|---|
| let-7a | 3 | miR-1231 | 1 | miR-1279 | 2 |
| let-7a* | 2 | miR-1233 | 1 | miR-128 | 1 |
| let-7b | 3 | miR-1234 | 1 | miR-1281 | 1 |
| let-7b* | 3 | miR-1236 | 1 | miR-1283 | 4 |
| let-7c | 3 | miR-1237 | 1 | miR-1284 | 3 |
| let-7d | 3 | miR-1238 | 1 | miR-1285 | 1 |
| let-7e | 3 | miR-124 | 1 | miR-1286 | 1 |
| let-7f | 3 | miR-124* | 3 | miR-1288 | 1 |
| let-7f-1* | 2 | miR-1243 | 1 | miR-1289 | 1 |
| let-7f-2* | 2 | miR-1244 | 1 | miR-1290 | 1 |
| let-7g | 3 | miR-1245 | 1 | miR-1292 | 1 |
| let-7i | 3 | miR-1246 | 1 | miR-1293 | 1 |
| miR-1 | 1 | miR-1247 | 1 | miR-1294 | 1 |
| miR-101 | 1 | miR-1248 | 2 | miR-129-5p | 4 |
| miR-103 | 1 | miR-1250 | 1 | miR-1297 | 1 |
| miR-103-2* | 3 | miR-1251 | 1 | miR-1298 | 1 |
| miR-105 | 4 | miR-1252 | 1 | miR-1299 | 1 |
| miR-106a | 6 | miR-1253 | 1 | miR-1300 | 1 |
| miR-106b | 6 | miR-1255a | 1 | miR-1301 | 6 |
| miR-107 | 1 | miR-1255b | 1 | miR-1302 | 1 |
| miR-10a | 1 | miR-1256 | 3 | miR-1303 | 6 |
| miR-10b | 1 | miR-1257 | 1 | miR-1304 | 1 |
| miR-1178 | 1 | miR-1258 | 1 | miR-1305 | 2 |
| miR-1179 | 2 | miR-1259 | 1 | miR-1306 | 2 |
| miR-1180 | 1 | miR-125a-3p | 1 | miR-1308 | 1 |
| miR-1182 | 1 | miR-125a-5p | 1 | miR-130a | 1 |
| miR-1184 | 2 | miR-125b | 1 | miR-130b | 1 |
| miR-1185 | 1 | miR-1261 | 1 | miR-132 | 2 |
| miR-1185-1* | 1 | miR-1262 | 1 | miR-1321 | 1 |
| miR-1185-2* | 1 | miR-1263 | 2 | miR-1322 | 1 |
| miR-1197 | 1 | miR-1264 | 1 | miR-1323 | 2 |
| miR-1200 | 3 | miR-1265 | 1 | miR-1324 | 1 |
| miR-1201 | 1 | miR-1266 | 1 | miR-133a | 1 |
| miR-1202 | 2 | miR-1267 | 1 | miR-133b | 1 |
| miR-1203 | 1 | miR-1268 | 1 | miR-134 | 2 |
| miR-1204 | 1 | miR-1269 | 1 | miR-135a | 7 |
| miR-1205 | 1 | miR-1270 | 1 | miR-135b | 7 |
| miR-1206 | 2 | miR-1271 | 1 | miR-136 | 1 |
| miR-1207-3p | 1 | miR-1272 | 1 | miR-137 | 1 |
| miR-1207-5p | 1 | miR-1273 | 1 | miR-138 | 1 |
| miR-1208 | 1 | miR-1273c | 1 | miR-139-3p | 1 |
| miR-122 | 1 | miR-1274a | 2 | miR-139-5p | 6 |
| miR-1224-5p | 1 | miR-1274b | 1 | miR-140-3p | 1 |
| miR-1225-3p | 1 | miR-1275 | 1 | miR-140-5p | 2 |
| miR-1225-5p | 1 | miR-127-5p | 1 | miR-141 | 1 |
| miR-1227 | 1 | miR-1276 | 1 | miR-141-5p | 3 |
| miR-1228 | 1 | miR-1277 | 1 | miR-142-3p | 1 |
| miR-1229 | 1 | miR-1278 | 1 | miR-142-5p | 3 |

| Hsa-miRNA | Number of databases | Hsa-miRNA | Number of databases | Hsa-miRNA | Number of databases |
|---|---|---|---|---|---|
| miR-143 | 4 | miR-193a-5p | 1 | miR-220a | 1 |
| miR-144 | 5 | miR-193b | 1 | miR-220b | 1 |
| miR-145 | 1 | miR-194 | 3 | miR-220c | 1 |
| miR-146a | 1 | miR-195 | 1 | miR-221 | 2 |
| miR-146b-3p | 1 | miR-195* | 2 | miR-222 | 1 |
| miR-146b-5p | 1 | miR-196a | 1 | miR-222* | 1 |
| miR-147 | 1 | miR-196b | 1 | miR-223 | 1 |
| miR-147b | 1 | miR-197 | 1 | miR-224 | 1 |
| miR-148a | 1 | miR-198 | 1 | miR-2278 | 1 |
| miR-148b | 1 | miR-199a-3p | 2 | miR-23a | 1 |
| miR-149 | 3 | miR-199a-5p | 1 | miR-23b | 1 |
| miR-150* | 1 | miR-199b-3p | 2 | miR-24 | 1 |
| miR-151-3p | 1 | miR-199b-5p | 1 | miR-25 | 1 |
| miR-152 | 1 | miR-19a | 5 | miR-26a | 1 |
| miR-153 | 1 | miR-19a* | 1 | miR-26a-2* | 1 |
| miR-154 | 5 | miR-19b | 5 | miR-26b | 1 |
| miR-155 | 1 | miR-19b-1* | 1 | miR-27a | 1 |
| miR-15a | 1 | miR-19b-2* | 1 | miR-27b | 1 |
| miR-15a* | 1 | miR-200a | 1 | miR-28-3p | 1 |
| miR-15b | 1 | miR-200b | 1 | miR-28-5p | 2 |
| miR-15b* | 1 | miR-200c | 1 | miR-296-3p | 1 |
| miR-16 | 1 | miR-202 | 3 | miR-297 | 1 |
| miR-16-1* | 3 | miR-203 | 4 | miR-298 | 1 |
| miR-16-2* | 2 | miR-204 | 1 | miR-299-3p | 1 |
| miR-17 | 5 | miR-205 | 1 | miR-299-5p | 1 |
| miR-17* | 1 | miR-2053 | 1 | miR-29a | 1 |
| miR-181a | 5 | miR-206 | 1 | miR-29b | 1 |
| miR-181b | 5 | miR-208a | 1 | miR-29b-2* | 1 |
| miR-181c | 5 | miR-208b | 1 | miR-29c | 1 |
| miR-181d | 4 | miR-20a | 6 | miR-300 | 7 |
| miR-182 | 1 | miR-20b | 5 | miR-301a | 1 |
| miR-1825 | 1 | miR-2113 | 4 | miR-301b | 1 |
| miR-1826 | 1 | miR-2114 | 1 | miR-302a | 4 |
| miR-1827 | 1 | miR-2116 | 1 | miR-302b | 4 |
| miR-183 | 1 | miR-2117 | 4 | miR-302b* | 1 |
| miR-184 | 1 | miR-21 | 1 | miR-302c | 4 |
| miR-185 | 5 | miR-21* | 2 | miR-302c* | 2 |
| miR-186 | 6 | miR-210 | 1 | miR-302d | 4 |
| miR-187 | 1 | miR-211 | 1 | miR-302d* | 1 |
| miR-188-3p | 1 | miR-212 | 2 | miR-302e | 4 |
| miR-188-5p | 4 | miR-214 | 2 | miR-302f | 2 |
| miR-18a | 5 | miR-215 | 1 | miR-3064-3p | 2 |
| miR-18b | 3 | miR-216a | 1 | miR-30a | 1 |
| miR-190 | 4 | miR-216b | 1 | miR-30a* | 2 |
| miR-190b | 3 | miR-217 | 2 | miR-30b | 1 |
| miR-191 | 1 | miR-218 | 5 | miR-30c | 1 |
| miR-1911* | 3 | miR-219 | 1 | miR-30d | 1 |
| miR-192 | 1 | miR-219-1* | 1 | miR-30d* | 2 |
| miR-192* | 5 | miR-219-2* | 1 | miR-30e | 1 |
| miR-193a-3p | 1 | miR-22 | 1 | miR-30e* | 2 |

| Hsa-miRNA | Number of databases | Hsa-miRNA | Number of databases | Hsa-miRNA | Number of databases |
|---|---|---|---|---|---|
| miR-31 | 2 | miR-33a* | 2 | miR-376c | 4 |
| miR-3118 | 1 | miR-33b | 1 | miR-377 | 1 |
| miR-3119 | 5 | miR-340 | 5 | miR-378 | 1 |
| miR-3120 | 3 | miR-342-3p | 1 | miR-379* | 1 |
| miR-3121 | 2 | miR-342-5p | 1 | miR-380 | 1 |
| miR-3122 | 1 | miR-346 | 1 | miR-380-5p | 1 |
| miR-3123 | 4 | miR-34a | 2 | miR-381 | 7 |
| miR-3125 | 1 | miR-34a* | 1 | miR-382 | 1 |
| miR-3128 | 2 | miR-34b | 1 | miR-383 | 1 |
| miR-3129-5p | 1 | miR-34c-3p | 1 | miR-384 | 1 |
| miR-3133 | 3 | miR-34c-5p | 2 | miR-3909 | 1 |
| miR-3136-3p | 3 | miR-3545-3p | 1 | miR-3913-5p | 1 |
| miR-3140-3p | 1 | miR-3591-3p | 3 | miR-3919 | 1 |
| miR-3143 | 1 | miR-3607-5p | 2 | miR-3920 | 1 |
| miR-3145 | 1 | miR-3609 | 1 | miR-3922-5p | 1 |
| miR-3153 | 2 | miR-361-5p | 1 | miR-3925-5p | 2 |
| miR-3158 | 3 | miR-3611 | 1 | miR-3938 | 1 |
| miR-3160-5p | 1 | miR-3613-3p | 3 | miR-3942-5p | 1 |
| miR-3162-5p | 1 | miR-3616-3p | 1 | miR-3972 | 1 |
| miR-3163 | 4 | miR-362-3p | 1 | miR-3973 | 1 |
| miR-3164 | 2 | miR-362-5p | 1 | miR-3976 | 2 |
| miR-3173 | 2 | miR-3646 | 1 | miR-409-3p | 1 |
| miR-3180-5p | 3 | miR-3647-5p | 1 | miR-409-5p | 1 |
| miR-3182 | 2 | miR-365 | 1 | miR-410 | 2 |
| miR-3183 | 3 | miR-3662 | 2 | miR-411 | 1 |
| miR-3190 | 1 | miR-3663-5p | 1 | miR-411* | 1 |
| miR-3190* | 1 | miR-3664-5p | 1 | miR-412 | 1 |
| miR-32 | 3 | miR-3667-3p | 1 | miR-421 | 5 |
| miR-3200-5p | 1 | miR-367 | 1 | miR-422a | 1 |
| miR-320a | 1 | miR-3672 | 2 | miR-423-5p | 1 |
| miR-320b | 1 | miR-3675-3p | 2 | miR-424 | 3 |
| miR-320c | 1 | miR-3682-5p | 2 | miR-425 | 1 |
| miR-320d | 1 | miR-3683 | 3 | miR-4253 | 3 |
| miR-323-3p | 5 | miR-3688-5p | 1 | miR-4255 | 3 |
| miR-323-5p | 1 | miR-3689a | 1 | miR-4259 | 2 |
| miR-323b-3p | 1 | miR-3689b | 1 | miR-4262 | 2 |
| miR-323b-5p | 1 | miR-3689e | 1 | miR-4263 | 1 |
| miR-324-5p | 1 | miR-3689f | 1 | miR-4266 | 1 |
| miR-325 | 1 | miR-369-3p | 2 | miR-4273 | 3 |
| miR-326 | 1 | miR-370 | 3 | miR-4275 | 1 |
| miR-328 | 3 | miR-371-3p | 2 | miR-4276 | 2 |
| miR-329 | 1 | miR-371-5p | 6 | miR-4279 | 3 |
| miR-330-3p | 2 | miR-372 | 5 | miR-4280 | 1 |
| miR-330-5p | 1 | miR-373 | 4 | miR-4282 | 3 |
| miR-331-5p | 1 | miR-374a | 5 | miR-4288 | 1 |
| miR-335 | 4 | miR-374b | 5 | miR-4289 | 3 |
| miR-337-3p | 1 | miR-374c | 1 | miR-429 | 1 |
| miR-337-5p | 1 | miR-375 | 3 | miR-4302 | 2 |
| miR-338-3p | 1 | miR-376a | 3 | miR-4306 | 2 |
| miR-33a | 1 | miR-376b | 3 | miR-4307 | 2 |

| Hsa-miRNA | Number of databases | Hsa-miRNA | Number of databases | Hsa-miRNA | Number of databases |
|---|---|---|---|---|---|
| miR-431 | 1 | miR-4660 | 1 | miR-4796-3p | 1 |
| miR-4311 | 1 | miR-4661-5p | 1 | miR-4797-3p | 1 |
| miR-432 | 1 | miR-4662a | 1 | miR-4797-5p | 1 |
| miR-4324 | 2 | miR-4666-3p | 2 | miR-4799-5p | 1 |
| miR-4325 | 1 | miR-4668-5p | 1 | miR-4802-3p | 1 |
| miR-433 | 2 | miR-4670-3p | 1 | miR-4803 | 1 |
| miR-4419a | 1 | miR-4673 | 1 | miR-4804-3p | 1 |
| miR-4422 | 3 | miR-4677-5p | 1 | miR-483-3p | 3 |
| miR-4428 | 1 | miR-4684-5p | 1 | miR-483-5p | 1 |
| miR-4446-3p | 1 | miR-4686 | 3 | miR-485-3p | 4 |
| miR-4452 | 2 | miR-4687-3p | 1 | miR-486-3p | 1 |
| miR-4458 | 1 | miR-4690-5p | 1 | miR-487a | 1 |
| miR-4464 | 1 | miR-4693-3p | 3 | miR-487b | 1 |
| miR-4470 | 1 | miR-4694-3p | 1 | miR-488 | 6 |
| miR-4475 | 1 | miR-4698 | 1 | miR-489 | 1 |
| miR-4477b | 1 | miR-4699-5p | 2 | miR-490-3p | 1 |
| miR-448 | 4 | miR-4703-5p | 1 | miR-490-5p | 1 |
| miR-4480 | 2 | miR-4709-3p | 1 | miR-491-3p | 4 |
| miR-4481 | 1 | miR-4709-5p | 1 | miR-491-5p | 2 |
| miR-4495 | 1 | miR-4712-3p | 1 | miR-492 | 1 |
| miR-449a | 2 | miR-4714-3p | 1 | miR-493 | 1 |
| miR-449b | 2 | miR-4714-5p | 1 | miR-494 | 5 |
| miR-449b* | 1 | miR-4715-5p | 2 | miR-495 | 7 |
| miR-4500 | 1 | miR-4720-3p | 1 | miR-496 | 2 |
| miR-4501 | 1 | miR-4721 | 1 | miR-497 | 1 |
| miR-4502 | 2 | miR-4723-3p | 2 | miR-497* | 1 |
| miR-4520a | 1 | miR-4724-3p | 1 | miR-498 | 7 |
| miR-450a | 1 | miR-4729 | 1 | miR-499-3p | 1 |
| miR-450b-3p | 1 | miR-4735-5p | 1 | miR-499-5p | 2 |
| miR-450b-5p | 2 | miR-4738-3p | 3 | miR-500 | 1 |
| miR-451 | 1 | miR-4742-5p | 2 | miR-500* | 1 |
| miR-4510 | 1 | miR-4745-5p | 1 | miR-5002-5p | 2 |
| miR-452 | 3 | miR-4748 | 1 | miR-5007-5p | 1 |
| miR-4520a | 2 | miR-4752 | 1 | miR-5008-3p | 1 |
| miR-4520b | 1 | miR-4753-3p | 2 | miR-501-3p | 2 |
| miR-4529-3p | 1 | miR-4760-3p | 3 | miR-501-5p | 1 |
| miR-453 | 1 | miR-4761-3p | 1 | miR-5011-5p | 2 |
| miR-454 | 1 | miR-4762-3p | 1 | miR-502-3p | 2 |
| miR-455-3p | 1 | miR-4766-5p | 1 | miR-502-5p | 1 |
| miR-455-5p | 1 | miR-4768-5p | 1 | miR-502-5p | 1 |
| miR-4635 | 2 | miR-4770 | 1 | miR-5047 | 3 |
| miR-4642 | 1 | miR-4775 | 1 | miR-505 | 1 |
| miR-4643 | 1 | miR-4776-3p | 1 | miR-506 | 1 |
| miR-4644 | 1 | miR-4778-3p | 2 | miR-507 | 4 |
| miR-4645-3p | 1 | miR-4779 | 2 | miR-508-3p | 1 |
| miR-4645-5p | 1 | miR-4780 | 1 | miR-508-5p | 1 |
| miR-4656 | 1 | miR-4786-3p | 1 | miR-509-3-5p | 1 |
| miR-4659a | 1 | miR-4789-3p | 3 | miR-509-3p | 1 |
| miR-4659b | 1 | miR-4789-5p | 3 | miR-509-5p | 1 |
| miR-466 | 4 | miR-4795-5p | 1 | miR-510 | 1 |

| Hsa-miRNA | Number of databases | Hsa-miRNA | Number of databases | Hsa-miRNA | Number of databases |
|---|---|---|---|---|---|
| miR-511 | 3 | miR-526b | 3 | miR-556-5p | 1 |
| miR-512-3p | 1 | miR-526b* | 5 | miR-557 | 2 |
| miR-512-5p | 1 | miR-527 | 1 | miR-558 | 1 |
| miR-513a-3p | 5 | miR-532-5p | 1 | miR-5580-3p | 1 |
| miR-513a-5p | 1 | miR-539 | 1 | miR-5586-3p | 1 |
| miR-513b | 1 | miR-539-3p | 2 | miR-559 | 2 |
| miR-513c | 1 | miR-541 | 1 | miR-561 | 1 |
| miR-513c-3p | 1 | miR-542-3p | 1 | miR-562 | 2 |
| miR-514 | 3 | miR-542-5p | 1 | miR-563 | 2 |
| miR-514b-3p | 2 | miR-543 | 1 | miR-564 | 1 |
| miR-515-5p | 5 | miR-544 | 3 | miR-567 | 1 |
| miR-516a-3p | 1 | miR-545 | 3 | miR-568 | 4 |
| miR-516b | 1 | miR-545* | 1 | miR-5688 | 2 |
| miR-517a | 1 | miR-548a-3p | 4 | miR-5692b | 2 |
| miR-517b | 1 | miR-548a-5p | 3 | miR-5692c | 2 |
| miR-517c | 1 | miR-548aa | 1 | miR-569 | 1 |
| miR-518a-3p | 2 | miR-548ab | 1 | miR-5696 | 1 |
| miR-518a-5p | 1 | miR-548ah | 1 | miR-570 | 3 |
| miR-518b | 1 | miR-548ak | 1 | miR-571 | 5 |
| miR-518c | 2 | miR-548av-3p | 1 | miR-572 | 1 |
| miR-518d-3p | 1 | miR-548b-3p | 4 | miR-573 | 2 |
| miR-518d-5p | 1 | miR-548b-5p | 2 | miR-574-3p | 1 |
| miR-518e | 1 | miR-548c-3p | 4 | miR-574-5p | 1 |
| miR-518f | 1 | miR-548c-5p | 2 | miR-575 | 1 |
| miR-519a | 2 | miR-548d-3p | 1 | miR-576-3p | 1 |
| miR-519b-3p | 2 | miR-548d-5p | 2 | miR-576-5p | 3 |
| miR-519b-5p | 1 | miR-548e | 3 | miR-577 | 1 |
| miR-519c-3p | 2 | miR-548f | 3 | miR-578 | 6 |
| miR-519c-5p | 1 | miR-548g | 1 | miR-579 | 1 |
| miR-519d | 4 | miR-548h | 2 | miR-580 | 2 |
| miR-519e | 1 | miR-548i | 2 | miR-581 | 1 |
| miR-519e* | 3 | miR-548j | 2 | miR-582-3p | 3 |
| miR-520a-3p | 5 | miR-548k | 2 | miR-582-5p | 1 |
| miR-520a-5p | 5 | miR-548l | 6 | miR-583 | 1 |
| miR-520b | 6 | miR-548m | 1 | miR-584 | 1 |
| miR-520c-3p | 6 | miR-548n | 1 | miR-585 | 1 |
| miR-520c-5p | 1 | miR-548o | 2 | miR-586 | 1 |
| miR-520d-3p | 5 | miR-548p | 3 | miR-587 | 1 |
| miR-520d-5p | 7 | miR-548t | 2 | miR-588 | 1 |
| miR-520e | 5 | miR-548v | 1 | miR-589 | 1 |
| miR-520f | 1 | miR-548w | 1 | miR-590-3p | 7 |
| miR-520g | 1 | miR-548y | 1 | miR-590-5p | 1 |
| miR-520h | 1 | miR-549 | 1 | miR-591 | 1 |
| miR-521 | 1 | miR-550 | 1 | miR-592 | 1 |
| miR-522 | 2 | miR-551a | 1 | miR-593 | 1 |
| miR-524-3p | 1 | miR-551b* | 2 | miR-595 | 2 |
| miR-524-5p | 7 | miR-552 | 1 | miR-597 | 1 |
| miR-525-3p | 1 | miR-553 | 1 | miR-599 | 1 |
| miR-525-5p | 4 | miR-555 | 1 | miR-600 | 1 |
| miR-526a | 1 | miR-556-3p | 1 | miR-601 | 1 |

| Hsa-miRNA | Number of databases | Hsa-miRNA | Number of databases | Hsa-miRNA | Number of databases |
|---|---|---|---|---|---|
| miR-602 | 1 | miR-643 | 1 | miR-769-5p | 1 |
| miR-603 | 1 | miR-644 | 1 | miR-802 | 5 |
| miR-604 | 1 | miR-645 | 1 | miR-873 | 1 |
| miR-605 | 1 | miR-646 | 2 | miR-875-3p | 1 |
| miR-606 | 1 | miR-648 | 1 | miR-875-5p | 1 |
| miR-607 | 2 | miR-649 | 2 | miR-876-3p | 1 |
| miR-608 | 1 | miR-650 | 1 | miR-876-5p | 1 |
| miR-609 | 1 | miR-651 | 2 | miR-877 | 2 |
| miR-610 | 2 | miR-653 | 1 | miR-885-5p | 1 |
| miR-612 | 1 | miR-654-3p | 1 | miR-887 | 1 |
| miR-613 | 1 | miR-655 | 3 | miR-888 | 2 |
| miR-614 | 1 | miR-656 | 1 | miR-889 | 1 |
| miR-615-5p | 1 | miR-657 | 1 | miR-890 | 1 |
| miR-616 | 2 | miR-658 | 1 | miR-891a | 1 |
| miR-617 | 1 | miR-659 | 2 | miR-891b | 2 |
| miR-618 | 1 | miR-660 | 1 | miR-892a | 1 |
| miR-619 | 1 | miR-661 | 1 | miR-892b | 1 |
| miR-620 | 1 | miR-662 | 1 | miR-9 | 4 |
| miR-621 | 1 | miR-663b | 1 | miR-920 | 1 |
| miR-622 | 1 | miR-664 | 1 | miR-921 | 1 |
| miR-623 | 4 | miR-665 | 1 | miR-922 | 1 |
| miR-624 | 1 | miR-668 | 1 | miR-923 | 1 |
| miR-625 | 1 | miR-671-3p | 1 | miR-924 | 1 |
| miR-626 | 1 | miR-671-5p | 1 | miR-92a | 1 |
| miR-627 | 1 | miR-676-5p | 1 | miR-92b | 1 |
| miR-628-3p | 1 | miR-7 | 1 | miR-93 | 5 |
| miR-628-5p | 3 | miR-7-1* | 3 | miR-93* | 1 |
| miR-629 | 1 | miR-7-2* | 3 | miR-934 | 1 |
| miR-630 | 1 | miR-708 | 3 | miR-935 | 2 |
| miR-631 | 1 | miR-720 | 1 | miR-936 | 3 |
| miR-632 | 1 | miR-758 | 1 | miR-940 | 1 |
| miR-633 | 2 | miR-759 | 2 | miR-942 | 1 |
| miR-635 | 1 | miR-765 | 2 | miR-943 | 1 |
| miR-636 | 2 | miR-767-3p | 1 | miR-944 | 1 |
| miR-639 | 1 | miR-767-5p | 5 | miR-95 | 1 |
| miR-640 | 1 | miR-768-3p | 1 | miR-96 | 1 |
| miR-641 | 4 | miR-768-5p | 1 | miR-98 | 3 |
| miR-642 | 1 | miR-769-3p | 1 | | |

**Supplementary Table 5**: List of 66 miRNA predicted to target *Ccl2* 3'UTR.

| Hsa-miRNA | Number of databases | Hsa-miRNA | Number of databases | Hsa-miRNA | Number of databases |
|---|---|---|---|---|---|
| miR-1 | 1 | miR-27b | 2 | miR-3564 | 1 |
| miR-101a | 1 | miR-290 | 3 | miR-3570 | 1 |
| miR-105 | 1 | miR-291a-3p | 1 | miR-3592 | 1 |
| miR-122 | 1 | miR-292-5p | 5 | miR-362 | 1 |
| miR-124 | 3 | miR-293 | 3 | miR-369-3p | 3 |
| miR-130a | 1 | miR-295 | 2 | miR-369-5p | 1 |
| miR-130b | 1 | miR-299 | 1 | miR-374 | 1 |
| miR-137 | 2 | miR-301a | 1 | miR-375 | 1 |
| miR-139-5p | 1 | miR-301b | 1 | miR-376a | 1 |
| miR-181a | 1 | miR-30a | 1 | miR-376b-3p | 1 |
| miR-181b | 1 | miR-30b-5p | 1 | miR-377 | 1 |
| miR-181c | 1 | miR-30c | 1 | miR-384-5p | 2 |
| miR-181d | 1 | miR-30d | 1 | miR-409-5p | 1 |
| miR-190 | 1 | miR-30e | 1 | miR-431 | 1 |
| miR-1912-3p | 1 | miR-323 | 4 | miR-434 | 4 |
| miR-19a | 1 | miR-325-5p | 2 | miR-488 | 2 |
| miR-19b | 1 | miR-327 | 1 | miR-539 | 4 |
| miR-203 | 1 | miR-33 | 3 | miR-543* | 1 |
| miR-222 | 1 | miR-338* | 3 | miR-653 | 1 |
| miR-23a | 4 | miR-342-3p | 1 | miR-664 | 4 |
| miR-23b | 4 | miR-344-3p | 1 | miR-673 | 1 |
| miR-27a | 2 | miR-350 | 1 | miR-876 | 2 |

**Supplementary Table 6**: List of 419 miRNA predicted to target *CCL2* 3'UTR.

| Hsa-miRNA | Number of databases | Hsa-miRNA | Number of databases | Hsa-miRNA | Number of databases |
|---|---|---|---|---|---|
| let-7c-3p | 1 | miR-1322 | 1 | miR-2110 | 3 |
| let-7e | 1 | miR-1323 | 3 | miR-216a | 1 |
| miR-1 | 7 | miR-134 | 1 | miR-216b | 1 |
| miR-101 | 2 | miR-140-5p | 1 | miR-219-2-3p | 2 |
| miR-106a | 1 | miR-141 | 2 | miR-22 | 3 |
| miR-106a* | 1 | miR-142-3p | 2 | miR-220c | 1 |
| miR-10a* | 2 | miR-142-5p | 2 | miR-223* | 1 |
| miR-10b* | 3 | miR-143 | 1 | miR-224 | 1 |
| miR-1179 | 1 | miR-144 | 1 | miR-23a | 5 |
| miR-1182 | 1 | miR-146a | 1 | miR-23b | 5 |
| miR-1184 | 1 | miR-146b-5p | 1 | miR-23c | 1 |
| miR-1205 | 2 | miR-148a | 1 | miR-26a | 2 |
| miR-1206 | 1 | miR-148b | 1 | miR-26b | 2 |
| miR-122 | 5 | miR-149-3p | 1 | miR-28-3p | 1 |
| miR-1225-3p | 1 | miR-151-3p | 1 | miR-296-3p | 1 |
| miR-1231 | 4 | miR-152 | 1 | miR-297 | 1 |
| miR-124 | 5 | miR-153 | 1 | miR-298 | 1 |
| miR-124* | 1 | miR-154 | 1 | miR-29a | 1 |
| miR-1246 | 1 | miR-17 | 1 | miR-29b | 1 |
| miR-1252 | 1 | miR-17* | 1 | miR-29c | 1 |
| miR-1253 | 1 | miR-181a | 1 | miR-301a | 1 |
| miR-1255a | 1 | miR-181b | 1 | miR-301b | 1 |
| miR-1255b | 1 | miR-181c | 1 | miR-302a | 1 |
| miR-1257 | 1 | miR-181d | 1 | miR-302a* | 3 |
| miR-125a-5p | 1 | miR-182 | 1 | miR-302b | 1 |
| miR-125b | 1 | miR-183* | 1 | miR-302c | 1 |
| miR-126 | 2 | miR-1825 | 1 | miR-302c* | 3 |
| miR-1262 | 1 | miR-1826 | 1 | miR-302d | 1 |
| miR-1263 | 1 | miR-185 | 1 | miR-302e | 1 |
| miR-1264 | 1 | miR-186 | 2 | miR-302f | 1 |
| miR-1266 | 1 | miR-190 | 1 | miR-30a | 1 |
| miR-1267 | 1 | miR-190b | 1 | miR-30b | 1 |
| miR-1272 | 1 | miR-1911 | 1 | miR-30c | 1 |
| miR-1276 | 1 | miR-1915 | 3 | miR-30d | 1 |
| miR-1277 | 1 | miR-193a-5p | 1 | miR-30e | 1 |
| miR-1278 | 1 | miR-196a | 1 | miR-3065-5p | 2 |
| miR-1283 | 2 | miR-196b | 1 | miR-31 | 1 |
| miR-1285 | 1 | miR-19a | 3 | miR-3125 | 3 |
| miR-1290 | 1 | miR-19b | 4 | miR-3132 | 2 |
| miR-1291 | 1 | miR-200a | 2 | miR-3143 | 3 |
| miR-129-5p | 1 | miR-203 | 2 | miR-3145 | 1 |
| miR-1297 | 2 | miR-2053 | 1 | miR-3149 | 2 |
| miR-1304 | 1 | miR-2054 | 2 | miR-3153 | 2 |
| miR-1306 | 1 | miR-206 | 6 | miR-3158-5p | 1 |
| miR-1308 | 1 | miR-208a | 1 | miR-3163 | 2 |
| miR-130a | 1 | miR-208b | 1 | miR-3170 | 1 |
| miR-130a* | 3 | miR-20a | 1 | miR-3174 | 2 |
| miR-130b | 1 | miR-20b | 1 | miR-3189 | 1 |

| Hsa-miRNA | Number of databases | Hsa-miRNA | Number of databases | Hsa-miRNA | Number of databases |
|---|---|---|---|---|---|
| miR-320a | 1 | miR-424 | 1 | miR-503 | 1 |
| miR-320b | 1 | miR-424* | 1 | miR-504 | 2 |
| miR-320c | 1 | miR-429 | 1 | miR-505 | 3 |
| miR-320d | 1 | miR-4271 | 1 | miR-506 | 4 |
| miR-323-3p | 6 | miR-4282 | 1 | miR-509-3-5p | 1 |
| miR-323b-5p | 1 | miR-4307 | 1 | miR-509-5p | 1 |
| miR-324-5p | 2 | miR-431 | 2 | miR-512-3p | 1 |
| miR-328 | 1 | miR-4318 | 2 | miR-513a-3p | 2 |
| miR-330-3p | 1 | miR-432 | 1 | miR-513a-5p | 1 |
| miR-335 | 3 | miR-4327 | 1 | miR-513c | 1 |
| miR-338-5p | 1 | miR-433 | 1 | miR-514 | 1 |
| miR-33a | 6 | miR-4471 | 1 | miR-515-3p | 1 |
| miR-33a* | 3 | miR-450a | 3 | miR-515-5p | 1 |
| miR-33b | 6 | miR-450b-5p | 2 | miR-516b | 1 |
| miR-340 | 1 | miR-4507 | 1 | miR-518a-3p | 1 |
| miR-34a-5p | 1 | miR-452 | 1 | miR-518a-5p | 5 |
| miR-34b | 1 | miR-4528 | 2 | miR-518b | 3 |
| miR-34c-3p | 1 | miR-454 | 1 | miR-518c | 1 |
| miR-361-3p | 1 | miR-455-3p | 1 | miR-518d-3p | 1 |
| miR-361-5p | 1 | miR-4635 | 1 | miR-518d-5p | 2 |
| miR-362-5p | 1 | miR-4646-3p | 1 | miR-518e | 2 |
| miR-3659 | 1 | miR-4650-3p | 1 | miR-518f | 2 |
| miR-3667-5p | 1 | miR-4658 | 1 | miR-518f* | 1 |
| miR-3673 | 1 | miR-4664-5p | 1 | miR-519a | 1 |
| miR-3679-3p | 1 | miR-4667-5p | 2 | miR-519b-3p | 1 |
| miR-3691-3p | 1 | miR-4668-5p | 1 | miR-519b-5p | 1 |
| miR-3692 | 2 | miR-4685-5p | 1 | miR-519c-3p | 1 |
| miR-369-3p | 4 | miR-4690-3p | 1 | miR-519c-5p | 1 |
| miR-3714 | 1 | miR-4700-5p | 2 | miR-520a-3p | 1 |
| miR-371b-5p | 2 | miR-4701-5p | 1 | miR-520a-5p | 1 |
| miR-373 | 2 | miR-4703-5p | 1 | miR-520b | 1 |
| miR-373* | 3 | miR-4704-5p | 1 | miR-520c-3p | 1 |
| miR-374a | 6 | miR-4725-3p | 1 | miR-520c-5p | 1 |
| miR-374b | 6 | miR-4726-3p | 1 | miR-520d-3p | 1 |
| miR-374b* | 1 | miR-4742-3p | 1 | miR-520d-5p | 4 |
| miR-377 | 2 | miR-4752 | 1 | miR-520e | 1 |
| miR-378a-5p | 1 | miR-4760-3p | 1 | miR-520f | 1 |
| miR-379 | 4 | miR-486-3p | 1 | miR-520g | 1 |
| miR-380 | 2 | miR-488 | 1 | miR-520h | 1 |
| miR-382 | 1 | miR-489 | 2 | miR-522 | 1 |
| miR-383 | 1 | miR-491-3p | 1 | miR-524-3p | 1 |
| miR-3908 | 2 | miR-491-5p | 1 | miR-524-5p | 3 |
| miR-3910 | 2 | miR-493* | 2 | miR-525-3p | 1 |
| miR-3916 | 2 | miR-494 | 4 | miR-525-5p | 1 |
| miR-3923 | 1 | miR-495 | 6 | miR-526a | 1 |
| miR-3940-5p | 1 | miR-496 | 1 | miR-526b | 1 |
| miR-3942-5p | 1 | miR-499-3p | 3 | miR-527 | 4 |
| miR-409-3p | 4 | miR-499-5p | 1 | miR-532-5p | 1 |
| miR-410 | 1 | miR-5002-5p | 1 | miR-539 | 1 |
| miR-421 | 5 | miR-501-5p | 1 | miR-541* | 1 |

| Hsa-miRNA | Number of databases | Hsa-miRNA | Number of databases | Hsa-miRNA | Number of databases |
|---|---|---|---|---|---|
| miR-542-3p | 1 | miR-579 | 4 | miR-653 | 1 |
| miR-543 | 4 | miR-580 | 1 | miR-655 | 1 |
| miR-544 | 1 | miR-581 | 1 | miR-656 | 1 |
| miR-545 | 2 | miR-583 | 1 | miR-657 | 1 |
| miR-548a-3p | 1 | miR-584 | 1 | miR-659 | 1 |
| miR-548a-5p | 2 | miR-586 | 5 | miR-662 | 1 |
| miR-548b-3p | 1 | miR-587 | 1 | miR-664 | 5 |
| miR-548b-5p | 1 | miR-588 | 1 | miR-665 | 1 |
| miR-548c-3p | 3 | miR-589 | 1 | miR-671-3p | 1 |
| miR-548c-5p | 2 | miR-590-3p | 1 | miR-675 | 1 |
| miR-548d-3p | 1 | miR-591 | 2 | miR-6783-5p | 1 |
| miR-548d-5p | 1 | miR-592 | 1 | miR-6824-5p | 1 |
| miR-548f | 1 | miR-593 | 4 | miR-6844 | 1 |
| miR-548g | 1 | miR-598 | 1 | miR-6859-5p | 1 |
| miR-548h | 1 | miR-599 | 1 | miR-7 | 1 |
| miR-548i | 1 | miR-600 | 1 | miR-7-1* | 2 |
| miR-548j | 1 | miR-601 | 1 | miR-7-2* | 2 |
| miR-548k | 1 | miR-603 | 1 | miR-767-5p | 1 |
| miR-548l | 1 | miR-605 | 1 | miR-768-3p | 1 |
| miR-548m | 1 | miR-607 | 1 | miR-769-3p | 1 |
| miR-548n | 1 | miR-608 | 1 | miR-770-5p | 1 |
| miR-548o | 2 | miR-609 | 3 | miR-802 | 1 |
| miR-548p | 1 | miR-610 | 1 | miR-8089 | 1 |
| miR-551b* | 1 | miR-611 | 1 | miR-873 | 1 |
| miR-552 | 1 | miR-612 | 1 | miR-875-3p | 1 |
| miR-553 | 1 | miR-613 | 7 | miR-876-3p | 2 |
| miR-554 | 1 | miR-615-3p | 1 | miR-877 | 1 |
| miR-555 | 1 | miR-616* | 3 | miR-885-5p | 1 |
| miR-556-3p | 1 | miR-617 | 1 | miR-886-5p | 1 |
| miR-557 | 1 | miR-624* | 3 | miR-888 | 1 |
| miR-5572 | 1 | miR-625 | 1 | miR-891a | 2 |
| miR-559 | 2 | miR-626 | 1 | miR-891b | 2 |
| miR-5591-5p | 1 | miR-632 | 1 | miR-892a | 1 |
| miR-561 | 1 | miR-633 | 5 | miR-9 | 3 |
| miR-562 | 1 | miR-635 | 2 | miR-9* | 1 |
| miR-568 | 1 | miR-636 | 1 | miR-924 | 1 |
| miR-569 | 3 | miR-637 | 2 | miR-93 | 1 |
| miR-570 | 2 | miR-639 | 1 | miR-935 | 2 |
| miR-574-5p | 2 | miR-641 | 1 | miR-944 | 1 |
| miR-576-3p | 1 | miR-643 | 1 | miR-95 | 1 |
| miR-577 | 5 | miR-647 | 1 | miR-96 | 1 |
| miR-578 | 1 | miR-651 | 1 | | |

```
gi|299522993:1352-3402      TGAGAAGGAGAGATGAGAGAAAGGTTTGCTTTTATCATTAAAAGGAAAGCAGATGGTGGA 60
gi|299523000:1328-3264      ------------------------------------------------------------ 0
gi|299523007:1223-3155      ------------------------------------------------------------ 0
gi|299522998:1307-3357      TGAGAAGGAGAGATGAGAGAAAGGTTTGCTTTTATCATTAAAAGGAAAGCAGATGGTGGA 60
gi|299523001:1262-3312      TGAGAAGGAGAGATGAGAGAAAGGTTTGCTTTTATCATTAAAAGGAAAGCAGATGGTGGA 60
gi|299523003:1283-3219      ------------------------------------------------------------ 0
gi|299522996:1373-3309      ------------------------------------------------------------ 0
gi|299523006:1241-3177      ------------------------------------------------------------ 0


gi|299522993:1352-3402      GCTGAATATGCCACTTACCAGACTAAATCAACCACTCCAGCAGAGCAGAGAGGCTGAATA 120
gi|299523000:1328-3264      ----------------------------------------------------TGAATA 6
gi|299523007:1223-3155      ------------------------------------------------------------TA 2
gi|299522998:1307-3357      GCTGAATATGCCACTTACCAGACTAAATCAACCACTCCAGCAGAGCAGAGAGGCTGAATA 120
gi|299523001:1262-3312      GCTGAATATGCCACTTACCAGACTAAATCAACCACTCCAGCAGAGCAGAGAGGCTGAATA 120
gi|299523003:1283-3219      ----------------------------------------------------TGAATA 6
gi|299522996:1373-3309      ----------------------------------------------------TGAATA 6
gi|299523006:1241-3177      ----------------------------------------------------TGAATA 6
                                                                                    **

gi|299522993:1352-3402      GATTCCACAACCTGGTTTGCCAGTTCATCTTTTGACTCTATTAAAATCTTCAATAGTTGT 180
gi|299523000:1328-3264      GATTCCACAACCTGGTTTGCCAGTTCATCTTTTGACTCTATTAAAATCTTCAATAGTTGT 66
gi|299523007:1223-3155      GATTCCACAACCTGGTTTGCCAGTTCATCTTTTGACTCTATTAAAATCTTCAATAGTTGT 62
gi|299522998:1307-3357      GATTCCACAACCTGGTTTGCCAGTTCATCTTTTGACTCTATTAAAATCTTCAATAGTTGT 180
gi|299523001:1262-3312      GATTCCACAACCTGGTTTGCCAGTTCATCTTTTGACTCTATTAAAATCTTCAATAGTTGT 180
gi|299523003:1283-3219      GATTCCACAACCTGGTTTGCCAGTTCATCTTTTGACTCTATTAAAATCTTCAATAGTTGT 66
gi|299522996:1373-3309      GATTCCACAACCTGGTTTGCCAGTTCATCTTTTGACTCTATTAAAATCTTCAATAGTTGT 66
gi|299523006:1241-3177      GATTCCACAACCTGGTTTGCCAGTTCATCTTTTGACTCTATTAAAATCTTCAATAGTTGT 66
                            ************************************************************
```

```
gi|299522993:1352-3402      TATTCTGTAGTTTCACTCTCATGAGTGCAACTGTGGCTTAGCTAATATTGCAATGTGGCT 240
gi|299523000:1328-3264      TATTCTGTAGTTTCACTCTCATGAGTGCAACTGTGGCTTAGCTAATATTGCAATGTGGCT 126
gi|299523007:1223-3155      TATTCTGTAGTTTCACTCTCATGAGTGCAACTGTGGCTTAGCTAATATTGCAATGTGGCT 122
gi|299522998:1307-3357      TATTCTGTAGTTTCACTCTCATGAGTGCAACTGTGGCTTAGCTAATATTGCAATGTGGCT 240
gi|299523001:1262-3312      TATTCTGTAGTTTCACTCTCATGAGTGCAACTGTGGCTTAGCTAATATTGCAATGTGGCT 240
gi|299523003:1283-3219      TATTCTGTAGTTTCACTCTCATGAGTGCAACTGTGGCTTAGCTAATATTGCAATGTGGCT 126
gi|299522996:1373-3309      TATTCTGTAGTTTCACTCTCATGAGTGCAACTGTGGCTTAGCTAATATTGCAATGTGGCT 126
gi|299523006:1241-3177      TATTCTGTAGTTTCACTCTCATGAGTGCAACTGTGGCTTAGCTAATATTGCAATGTGGCT 126
                            ************************************************************

gi|299522993:1352-3402      TGAATGTAGGTAGCATCCTTTGATGCTTCTTTGAAACTTGTATGAATTTGGGTATGAACA 300
gi|299523000:1328-3264      TGAATGTAGGTAGCATCCTTTGATGCTTCTTTGAAACTTGTATGAATTTGGGTATGAACA 186
gi|299523007:1223-3155      TGAATGTAGGTAGCATCCTTTGATGCTTCTTTGAAACTTGTATGAATTTGGGTATGAACA 182
gi|299522998:1307-3357      TGAATGTAGGTAGCATCCTTTGATGCTTCTTTGAAACTTGTATGAATTTGGGTATGAACA 300
gi|299523001:1262-3312      TGAATGTAGGTAGCATCCTTTGATGCTTCTTTGAAACTTGTATGAATTTGGGTATGAACA 300
gi|299523003:1283-3219      TGAATGTAGGTAGCATCCTTTGATGCTTCTTTGAAACTTGTATGAATTTGGGTATGAACA 186
gi|299522996:1373-3309      TGAATGTAGGTAGCATCCTTTGATGCTTCTTTGAAACTTGTATGAATTTGGGTATGAACA 186
gi|299523006:1241-3177      TGAATGTAGGTAGCATCCTTTGATGCTTCTTTGAAACTTGTATGAATTTGGGTATGAACA 186
                            ************************************************************

gi|299522993:1352-3402      GATTGCCTGCTTTCCCTTAAATAACACTTAGATTTATTGGACCAGTCAGCACAGCATGCC 360
gi|299523000:1328-3264      GATTGCCTGCTTTCCCTTAAATAACACTTAGATTTATTGGACCAGTCAGCACAGCATGCC 246
gi|299523007:1223-3155      GATTGCCTGCTTTCCCTTAAATAACACTTAGATTTATTGGACCAGTCAGCACAGCATGCC 242
gi|299522998:1307-3357      GATTGCCTGCTTTCCCTTAAATAACACTTAGATTTATTGGACCAGTCAGCACAGCATGCC 360
gi|299523001:1262-3312      GATTGCCTGCTTTCCCTTAAATAACACTTAGATTTATTGGACCAGTCAGCACAGCATGCC 360
gi|299523003:1283-3219      GATTGCCTGCTTTCCCTTAAATAACACTTAGATTTATTGGACCAGTCAGCACAGCATGCC 246
gi|299522996:1373-3309      GATTGCCTGCTTTCCCTTAAATAACACTTAGATTTATTGGACCAGTCAGCACAGCATGCC 246
gi|299523006:1241-3177      GATTGCCTGCTTTCCCTTAAATAACACTTAGATTTATTGGACCAGTCAGCACAGCATGCC 246
                            ************************************************************
```

```
gi|299522993:1352-3402      TGGTTGTATTAAAGCAGGGATATGCTGTATTTTATAAAATTGGCAAAATTAGAGAAATAT 420
gi|299523000:1328-3264      TGGTTGTATTAAAGCAGGGATATGCTGTATTTTATAAAATTGGCAAAATTAGAGAAATAT 306
gi|299523007:1223-3155      TGGTTGTATTAAAGCAGGGATATGCTGTATTTTATAAAATTGGCAAAATTAGAGAAATAT 302
gi|299522998:1307-3357      TGGTTGTATTAAAGCAGGGATATGCTGTATTTTATAAAATTGGCAAAATTAGAGAAATAT 420
gi|299523001:1262-3312      TGGTTGTATTAAAGCAGGGATATGCTGTATTTTATAAAATTGGCAAAATTAGAGAAATAT 420
gi|299523003:1283-3219      TGGTTGTATTAAAGCAGGGATATGCTGTATTTTATAAAATTGGCAAAATTAGAGAAATAT 306
gi|299522996:1373-3309      TGGTTGTATTAAAGCAGGGATATGCTGTATTTTATAAAATTGGCAAAATTAGAGAAATAT 306
gi|299523006:1241-3177      TGGTTGTATTAAAGCAGGGATATGCTGTATTTTATAAAATTGGCAAAATTAGAGAAATAT 306
                            ************************************************************

gi|299522993:1352-3402      AGTTCACAATGAAATTATATTTTCTTTGTAAAGAAAGTGGCTTGAAATCTTTTTTGTTCA 480
gi|299523000:1328-3264      AGTTCACAATGAAATTATATTTTCTTTGTAAAGAAAGTGGCTTGAAATCTTTTTTGTTCA 366
gi|299523007:1223-3155      AGTTCACAATGAAATTATATTTTCTTTGTAAAGAAAGTGGCTTGAAATCTTTTTTGTTCA 362
gi|299522998:1307-3357      AGTTCACAATGAAATTATATTTTCTTTGTAAAGAAAGTGGCTTGAAATCTTTTTTGTTCA 480
gi|299523001:1262-3312      AGTTCACAATGAAATTATATTTTCTTTGTAAAGAAAGTGGCTTGAAATCTTTTTTGTTCA 480
gi|299523003:1283-3219      AGTTCACAATGAAATTATATTTTCTTTGTAAAGAAAGTGGCTTGAAATCTTTTTTGTTCA 366
gi|299522996:1373-3309      AGTTCACAATGAAATTATATTTTCTTTGTAAAGAAAGTGGCTTGAAATCTTTTTTGTTCA 366
gi|299523006:1241-3177      AGTTCACAATGAAATTATATTTTCTTTGTAAAGAAAGTGGCTTGAAATCTTTTTTGTTCA 366
                            ************************************************************

gi|299522993:1352-3402      AAGATTAATGCCAACTCTTAAGATTATTCTTTCACCAACTATAGAATGTATTTTATATAT 540
gi|299523000:1328-3264      AAGATTAATGCCAACTCTTAAGATTATTCTTTCACCAACTATAGAATGTATTTTATATAT 426
gi|299523007:1223-3155      AAGATTAATGCCAACTCTTAAGATTATTCTTTCACCAACTATAGAATGTATTTTATATAT 422
gi|299522998:1307-3357      AAGATTAATGCCAACTCTTAAGATTATTCTTTCACCAACTATAGAATGTATTTTATATAT 540
gi|299523001:1262-3312      AAGATTAATGCCAACTCTTAAGATTATTCTTTCACCAACTATAGAATGTATTTTATATAT 540
gi|299523003:1283-3219      AAGATTAATGCCAACTCTTAAGATTATTCTTTCACCAACTATAGAATGTATTTTATATAT 426
gi|299522996:1373-3309      AAGATTAATGCCAACTCTTAAGATTATTCTTTCACCAACTATAGAATGTATTTTATATAT 426
gi|299523006:1241-3177      AAGATTAATGCCAACTCTTAAGATTATTCTTTCACCAACTATAGAATGTATTTTATATAT 426
                            ************************************************************
```

```
gi|299522993:1352-3402      CGTTCATTGTAAAAAGCCCTTAAAAATATGTGTATACTACTTTGGCTCTTGTGCATAAAA 600
gi|299523000:1328-3264      CGTTCATTGTAAAAAGCCCTTAAAAATATGTGTATACTACTTTGGCTCTTGTGCATAAAA 486
gi|299523007:1223-3155      CGTTCATTGTAAAAAGCCCTTAAAAATATGTGTATACTACTTTGGCTCTTGTGCATAAAA 482
gi|299522998:1307-3357      CGTTCATTGTAAAAAGCCCTTAAAAATATGTGTATACTACTTTGGCTCTTGTGCATAAAA 600
gi|299523001:1262-3312      CGTTCATTGTAAAAAGCCCTTAAAAATATGTGTATACTACTTTGGCTCTTGTGCATAAAA 600
gi|299523003:1283-3219      CGTTCATTGTAAAAAGCCCTTAAAAATATGTGTATACTACTTTGGCTCTTGTGCATAAAA 486
gi|299522996:1373-3309      CGTTCATTGTAAAAAGCCCTTAAAAATATGTGTATACTACTTTGGCTCTTGTGCATAAAA 486
gi|299523006:1241-3177      CGTTCATTGTAAAAAGCCCTTAAAAATATGTGTATACTACTTTGGCTCTTGTGCATAAAA 486
                            ************************************************************

gi|299522993:1352-3402      ACAAGAACACTGAAAATTGGGAATATGCACAAACTTGGCTTCTTTAACCAAGAATATTAT 660
gi|299523000:1328-3264      ACAAGAACACTGAAAATTGGGAATATGCACAAACTTGGCTTCTTTAACCAAGAATATTAT 546
gi|299523007:1223-3155      ACAAGAACACTGAAAATTGGGAATATGCACAAACTTGGCTTCTTTAACCAAGAATATTAT 542
gi|299522998:1307-3357      ACAAGAACACTGAAAATTGGGAATATGCACAAACTTGGCTTCTTTAACCAAGAATATTAT 660
gi|299523001:1262-3312      ACAAGAACACTGAAAATTGGGAATATGCACAAACTTGGCTTCTTTAACCAAGAATATTAT 660
gi|299523003:1283-3219      ACAAGAACACTGAAAATTGGGAATATGCACAAACTTGGCTTCTTTAACCAAGAATATTAT 546
gi|299522996:1373-3309      ACAAGAACACTGAAAATTGGGAATATGCACAAACTTGGCTTCTTTAACCAAGAATATTAT 546
gi|299523006:1241-3177      ACAAGAACACTGAAAATTGGGAATATGCACAAACTTGGCTTCTTTAACCAAGAATATTAT 546
                            ************************************************************

gi|299522993:1352-3402      TGGAAAATTCTCTAAAAGTTAATAGGGTAAATTCTCTATTTTTTGTAATGTGTTCGGTGA 720
gi|299523000:1328-3264      TGGAAAATTCTCTAAAAGTTAATAGGGTAAATTCTCTATTTTTTGTAATGTGTTCGGTGA 606
gi|299523007:1223-3155      TGGAAAATTCTCTAAAAGTTAATAGGGTAAATTCTCTATTTTTTGTAATGTGTTCGGTGA 602
gi|299522998:1307-3357      TGGAAAATTCTCTAAAAGTTAATAGGGTAAATTCTCTATTTTTTGTAATGTGTTCGGTGA 720
gi|299523001:1262-3312      TGGAAAATTCTCTAAAAGTTAATAGGGTAAATTCTCTATTTTTTGTAATGTGTTCGGTGA 720
gi|299523003:1283-3219      TGGAAAATTCTCTAAAAGTTAATAGGGTAAATTCTCTATTTTTTGTAATGTGTTCGGTGA 606
gi|299522996:1373-3309      TGGAAAATTCTCTAAAAGTTAATAGGGTAAATTCTCTATTTTTTGTAATGTGTTCGGTGA 606
gi|299523006:1241-3177      TGGAAAATTCTCTAAAAGTTAATAGGGTAAATTCTCTATTTTTTGTAATGTGTTCGGTGA 606
                            ************************************************************
```

```
gi|299522993:1352-3402      TTTCAGAAAGCTAGAAAGTGTATGTGTGGCATTTGTTTTCACTTTTTAAAACATCCCTAA 780
gi|299523000:1328-3264      TTTCAGAAAGCTAGAAAGTGTATGTGTGGCATTTGTTTTCACTTTTTAAAACATCCCTAA 666
gi|299523007:1223-3155      TTTCAGAAAGCTAGAAAGTGTATGTGTGGCATTTGTTTTCACTTTTTAAAACATCCCTAA 662
gi|299522998:1307-3357      TTTCAGAAAGCTAGAAAGTGTATGTGTGGCATTTGTTTTCACTTTTTAAAACATCCCTAA 780
gi|299523001:1262-3312      TTTCAGAAAGCTAGAAAGTGTATGTGTGGCATTTGTTTTCACTTTTTAAAACATCCCTAA 780
gi|299523003:1283-3219      TTTCAGAAAGCTAGAAAGTGTATGTGTGGCATTTGTTTTCACTTTTTAAAACATCCCTAA 666
gi|299522996:1373-3309      TTTCAGAAAGCTAGAAAGTGTATGTGTGGCATTTGTTTTCACTTTTTAAAACATCCCTAA 666
gi|299523006:1241-3177      TTTCAGAAAGCTAGAAAGTGTATGTGTGGCATTTGTTTTCACTTTTTAAAACATCCCTAA 666
                            ************************************************************

gi|299522993:1352-3402      CTGATCGAATATATCAGTAATTTCAGAATCAGATGCATCCTTTCATAAGAAGTGAGAGGA 840
gi|299523000:1328-3264      CTGATCGAATATATCAGTAATTTCAGAATCAGATGCATCCTTTCATAAGAAGTGAGAGGA 726
gi|299523007:1223-3155      CTGATCGAATATATCAGTAATTTCAGAATCAGATGCATCCTTTCATAAGAAGTGAGAGGA 722
gi|299522998:1307-3357      CTGATCGAATATATCAGTAATTTCAGAATCAGATGCATCCTTTCATAAGAAGTGAGAGGA 840
gi|299523001:1262-3312      CTGATCGAATATATCAGTAATTTCAGAATCAGATGCATCCTTTCATAAGAAGTGAGAGGA 840
gi|299523003:1283-3219      CTGATCGAATATATCAGTAATTTCAGAATCAGATGCATCCTTTCATAAGAAGTGAGAGGA 726
gi|299522996:1373-3309      CTGATCGAATATATCAGTAATTTCAGAATCAGATGCATCCTTTCATAAGAAGTGAGAGGA 726
gi|299523006:1241-3177      CTGATCGAATATATCAGTAATTTCAGAATCAGATGCATCCTTTCATAAGAAGTGAGAGGA 726
                            ************************************************************

gi|299522993:1352-3402      CTCTGACAGCCATAACAGGAGTGCCACTTCATGGTGCGAAGTGAACACTGTAGTCTTGTT 900
gi|299523000:1328-3264      CTCTGACAGCCATAACAGGAGTGCCACTTCATGGTGCGAAGTGAACACTGTAGTCTTGTT 786
gi|299523007:1223-3155      CTCTGACAGCCATAACAGGAGTGCCACTTCATGGTGCGAAGTGAACACTGTAGTCTTGTT 782
gi|299522998:1307-3357      CTCTGACAGCCATAACAGGAGTGCCACTTCATGGTGCGAAGTGAACACTGTAGTCTTGTT 900
gi|299523001:1262-3312      CTCTGACAGCCATAACAGGAGTGCCACTTCATGGTGCGAAGTGAACACTGTAGTCTTGTT 900
gi|299523003:1283-3219      CTCTGACAGCCATAACAGGAGTGCCACTTCATGGTGCGAAGTGAACACTGTAGTCTTGTT 786
gi|299522996:1373-3309      CTCTGACAGCCATAACAGGAGTGCCACTTCATGGTGCGAAGTGAACACTGTAGTCTTGTT 786
gi|299523006:1241-3177      CTCTGACAGCCATAACAGGAGTGCCACTTCATGGTGCGAAGTGAACACTGTAGTCTTGTT 786
                            ************************************************************
```

```
gi|299522993:1352-3402      GTTTTCCCAAAGAGAACTCCGTATGTTCTCTTAGGTTGAGTAACCCACTCTGAATTCTGG 960
gi|299523000:1328-3264      GTTTTCCCAAAGAGAACTCCGTATGTTCTCTTAGGTTGAGTAACCCACTCTGAATTCTGG 846
gi|299523007:1223-3155      GTTTTCCCAAAGAGAACTCCGTATGTTCTCTTAGGTTGAGTAACCCACTCTGAATTCTGG 842
gi|299522998:1307-3357      GTTTTCCCAAAGAGAACTCCGTATGTTCTCTTAGGTTGAGTAACCCACTCTGAATTCTGG 960
gi|299523001:1262-3312      GTTTTCCCAAAGAGAACTCCGTATGTTCTCTTAGGTTGAGTAACCCACTCTGAATTCTGG 960
gi|299523003:1283-3219      GTTTTCCCAAAGAGAACTCCGTATGTTCTCTTAGGTTGAGTAACCCACTCTGAATTCTGG 846
gi|299522996:1373-3309      GTTTTCCCAAAGAGAACTCCGTATGTTCTCTTAGGTTGAGTAACCCACTCTGAATTCTGG 846
gi|299523006:1241-3177      GTTTTCCCAAAGAGAACTCCGTATGTTCTCTTAGGTTGAGTAACCCACTCTGAATTCTGG 846
                            ************************************************************

                                        miR-185 seed region
gi|299522993:1352-3402      TTACATGTGTTTTTCTCTCCCTCCTTAAATAAAGAGAGGGGTTAAACATGCCCTCTAAAA 1020
gi|299523000:1328-3264      TTACATGTGTTTTTCTCTCCCTCCTTAAATAAAGAGAGGGGTTAAACATGCCCTCTAAAA 906
gi|299523007:1223-3155      TTACATGTGTTTTTCTCTCCCTCCTTAAATAAAGAGAGGGGTTAAACATGCCCTCTAAAA 902
gi|299522998:1307-3357      TTACATGTGTTTTTCTCTCCCTCCTTAAATAAAGAGAGGGGTTAAACATGCCCTCTAAAA 1020
gi|299523001:1262-3312      TTACATGTGTTTTTCTCTCCCTCCTTAAATAAAGAGAGGGGTTAAACATGCCCTCTAAAA 1020
gi|299523003:1283-3219      TTACATGTGTTTTTCTCTCCCTCCTTAAATAAAGAGAGGGGTTAAACATGCCCTCTAAAA 906
gi|299522996:1373-3309      TTACATGTGTTTTTCTCTCCCTCCTTAAATAAAGAGAGGGGTTAAACATGCCCTCTAAAA 906
gi|299523006:1241-3177      TTACATGTGTTTTTCTCTCCCTCCTTAAATAAAGAGAGGGGTTAAACATGCCCTCTAAAA 906
                            ************************************************************

gi|299522993:1352-3402      GTAGGTGGTTTTGAAGAGAATAAATTCATCAGATAACCTCAAGTCACATGAGAATCTTAG 1080
gi|299523000:1328-3264      GTAGGTGGTTTTGAAGAGAATAAATTCATCAGATAACCTCAAGTCACATGAGAATCTTAG 966
gi|299523007:1223-3155      GTAGGTGGTTTTGAAGAGAATAAATTCATCAGATAACCTCAAGTCACATGAGAATCTTAG 962
gi|299522998:1307-3357      GTAGGTGGTTTTGAAGAGAATAAATTCATCAGATAACCTCAAGTCACATGAGAATCTTAG 1080
gi|299523001:1262-3312      GTAGGTGGTTTTGAAGAGAATAAATTCATCAGATAACCTCAAGTCACATGAGAATCTTAG 1080
gi|299523003:1283-3219      GTAGGTGGTTTTGAAGAGAATAAATTCATCAGATAACCTCAAGTCACATGAGAATCTTAG 966
gi|299522996:1373-3309      GTAGGTGGTTTTGAAGAGAATAAATTCATCAGATAACCTCAAGTCACATGAGAATCTTAG 966
gi|299523006:1241-3177      GTAGGTGGTTTTGAAGAGAATAAATTCATCAGATAACCTCAAGTCACATGAGAATCTTAG 966
                            ************************************************************
```

```
gi|299522993:1352-3402      TCCATTTACATTGCCTTGGCTAGTAAAAGCCATCTATGTATATGTCTTACCTCATCTCCT 1140
gi|299523000:1328-3264      TCCATTTACATTGCCTTGGCTAGTAAAAGCCATCTATGTATATGTCTTACCTCATCTCCT 1026
gi|299523007:1223-3155      TCCATTTACATTGCCTTGGCTAGTAAAAGCCATCTATGTATATGTCTTACCTCATCTCCT 1022
gi|299522998:1307-3357      TCCATTTACATTGCCTTGGCTAGTAAAAGCCATCTATGTATATGTCTTACCTCATCTCCT 1140
gi|299523001:1262-3312      TCCATTTACATTGCCTTGGCTAGTAAAAGCCATCTATGTATATGTCTTACCTCATCTCCT 1140
gi|299523003:1283-3219      TCCATTTACATTGCCTTGGCTAGTAAAAGCCATCTATGTATATGTCTTACCTCATCTCCT 1026
gi|299522996:1373-3309      TCCATTTACATTGCCTTGGCTAGTAAAAGCCATCTATGTATATGTCTTACCTCATCTCCT 1026
gi|299523006:1241-3177      TCCATTTACATTGCCTTGGCTAGTAAAAGCCATCTATGTATATGTCTTACCTCATCTCCT 1026
                            ************************************************************

gi|299522993:1352-3402      AAAAGGCAGAGTACAAAGTAAGCCATGTATCTCAGGAAGGTAACTTCATTTTGTCTATTT 1200
gi|299523000:1328-3264      AAAAGGCAGAGTACAAAGTAAGCCATGTATCTCAGGAAGGTAACTTCATTTTGTCTATTT 1086
gi|299523007:1223-3155      AAAAGGCAGAGTACAAAGTAAGCCATGTATCTCAGGAAGGTAACTTCATTTTGTCTATTT 1082
gi|299522998:1307-3357      AAAAGGCAGAGTACAAAGTAAGCCATGTATCTCAGGAAGGTAACTTCATTTTGTCTATTT 1200
gi|299523001:1262-3312      AAAAGGCAGAGTACAAAGTAAGCCATGTATCTCAGGAAGGTAACTTCATTTTGTCTATTT 1200
gi|299523003:1283-3219      AAAAGGCAGAGTACAAAGTAAGCCATGTATCTCAGGAAGGTAACTTCATTTTGTCTATTT 1086
gi|299522996:1373-3309      AAAAGGCAGAGTACAAAGTAAGCCATGTATCTCAGGAAGGTAACTTCATTTTGTCTATTT 1086
gi|299523006:1241-3177      AAAAGGCAGAGTACAAAGTAAGCCATGTATCTCAGGAAGGTAACTTCATTTTGTCTATTT 1086
                            ************************************************************
                                                                        miR-20a seed region
gi|299522993:1352-3402      GCTGTTGATTGTACCAAGGGATGGAAGAAGTAAATATAGCTCAGGTAGCACTTTATACTC 1260
gi|299523000:1328-3264      GCTGTTGATTGTACCAAGGGATGGAAGAAGTAAATATAGCTCAGGTAGCACTTTATACTC 1146
gi|299523007:1223-3155      GCTGTTGATTGTACCAAGGGATGGAAGAAGTAAATATAGCTCAGGTAGCACTTTATACTC 1142
gi|299522998:1307-3357      GCTGTTGATTGTACCAAGGGATGGAAGAAGTAAATATAGCTCAGGTAGCACTTTATACTC 1260
gi|299523001:1262-3312      GCTGTTGATTGTACCAAGGGATGGAAGAAGTAAATATAGCTCAGGTAGCACTTTATACTC 1260
gi|299523003:1283-3219      GCTGTTGATTGTACCAAGGGATGGAAGAAGTAAATATAGCTCAGGTAGCACTTTATACTC 1146
gi|299522996:1373-3309      GCTGTTGATTGTACCAAGGGATGGAAGAAGTAAATATAGCTCAGGTAGCACTTTATACTC 1146
gi|299523006:1241-3177      GCTGTTGATTGTACCAAGGGATGGAAGAAGTAAATATAGCTCAGGTAGCACTTTATACTC 1146
                            ************************************************************
```

```
gi|299522993:1352-3402      AGGCAGATCTCAGCCCTCTACTGAGTCCCTTAGCCAAGCAGTTTCTTTCAAAGAAGCCAG 1320
gi|299523000:1328-3264      AGGCAGATCTCAGCCCTCTACTGAGTCCCTTAGCCAAGCAGTTTCTTTCAAAGAAGCCAG 1206
gi|299523007:1223-3155      AGGCAGATCTCAGCCCTCTACTGAGTCCCTTAGCCAAGCAGTTTCTTTCAAAGAAGCCAG 1202
gi|299522998:1307-3357      AGGCAGATCTCAGCCCTCTACTGAGTCCCTTAGCCAAGCAGTTTCTTTCAAAGAAGCCAG 1320
gi|299523001:1262-3312      AGGCAGATCTCAGCCCTCTACTGAGTCCCTTAGCCAAGCAGTTTCTTTCAAAGAAGCCAG 1320
gi|299523003:1283-3219      AGGCAGATCTCAGCCCTCTACTGAGTCCCTTAGCCAAGCAGTTTCTTTCAAAGAAGCCAG 1206
gi|299522996:1373-3309      AGGCAGATCTCAGCCCTCTACTGAGTCCCTTAGCCAAGCAGTTTCTTTCAAAGAAGCCAG 1206
gi|299523006:1241-3177      AGGCAGATCTCAGCCCTCTACTGAGTCCCTTAGCCAAGCAGTTTCTTTCAAAGAAGCCAG 1206
                            ************************************************************

gi|299522993:1352-3402      CAGGCGAAAAGCAGGGACTGCCACTGCATTTCATATCACACTGTTAAAAGTTGTGTTTTG 1380
gi|299523000:1328-3264      CAGGCGAAAAGCAGGGACTGCCACTGCATTTCATATCACACTGTTAAAAGTTGTGTTTTG 1266
gi|299523007:1223-3155      CAGGCGAAAAGCAGGGACTGCCACTGCATTTCATATCACACTGTTAAAAGTTGTGTTTTG 1262
gi|299522998:1307-3357      CAGGCGAAAAGCAGGGACTGCCACTGCATTTCATATCACACTGTTAAAAGTTGTGTTTTG 1380
gi|299523001:1262-3312      CAGGCGAAAAGCAGGGACTGCCACTGCATTTCATATCACACTGTTAAAAGTTGTGTTTTG 1380
gi|299523003:1283-3219      CAGGCGAAAAGCAGGGACTGCCACTGCATTTCATATCACACTGTTAAAAGTTGTGTTTTG 1266
gi|299522996:1373-3309      CAGGCGAAAAGCAGGGACTGCCACTGCATTTCATATCACACTGTTAAAAGTTGTGTTTTG 1266
gi|299523006:1241-3177      CAGGCGAAAAGCAGGGACTGCCACTGCATTTCATATCACACTGTTAAAAGTTGTGTTTTG 1266
                            ************************************************************
                                              miR-19a seed region
gi|299522993:1352-3402      AAATTTTATGTTTAGTTGCACAAATTGGGCCAAAGAAACATTGCCTTGAGGAAGATATGA 1440
gi|299523000:1328-3264      AAATTTTATGTTTAGTTGCACAAATTGGGCCAAAGAAACATTGCCTTGAGGAAGATATGA 1326
gi|299523007:1223-3155      AAATTTTATGTTTAGTTGCACAAATTGGGCCAAAGAAACATTGCCTTGAGGAAGATATGA 1322
gi|299522998:1307-3357      AAATTTTATGTTTAGTTGCACAAATTGGGCCAAAGAAACATTGCCTTGAGGAAGATATGA 1440
gi|299523001:1262-3312      AAATTTTATGTTTAGTTGCACAAATTGGGCCAAAGAAACATTGCCTTGAGGAAGATATGA 1440
gi|299523003:1283-3219      AAATTTTATGTTTAGTTGCACAAATTGGGCCAAAGAAACATTGCCTTGAGGAAGATATGA 1326
gi|299522996:1373-3309      AAATTTTATGTTTAGTTGCACAAATTGGGCCAAAGAAACATTGCCTTGAGGAAGATATGA 1326
gi|299523006:1241-3177      AAATTTTATGTTTAGTTGCACAAATTGGGCCAAAGAAACATTGCCTTGAGGAAGATATGA 1326
                            ************************************************************
```

```
gi|299522993:1352-3402      TTGGAAAATCAAGAGTGTAGAAGAATAAATACTGTTTTACTGTCCAAAGACATGTTTATA 1500
gi|299523000:1328-3264      TTGGAAAATCAAGAGTGTAGAAGAATAAATACTGTTTTACTGTCCAAAGACATGTTTATA 1386
gi|299523007:1223-3155      TTGGAAAATCAAGAGTGTAGAAGAATAAATACTGTTTTACTGTCCAAAGACATGTTTATA 1382
gi|299522998:1307-3357      TTGGAAAATCAAGAGTGTAGAAGAATAAATACTGTTTTACTGTCCAAAGACATGTTTATA 1500
gi|299523001:1262-3312      TTGGAAAATCAAGAGTGTAGAAGAATAAATACTGTTTTACTGTCCAAAGACATGTTTATA 1500
gi|299523003:1283-3219      TTGGAAAATCAAGAGTGTAGAAGAATAAATACTGTTTTACTGTCCAAAGACATGTTTATA 1386
gi|299522996:1373-3309      TTGGAAAATCAAGAGTGTAGAAGAATAAATACTGTTTTACTGTCCAAAGACATGTTTATA 1386
gi|299523006:1241-3177      TTGGAAAATCAAGAGTGTAGAAGAATAAATACTGTTTTACTGTCCAAAGACATGTTTATA 1386
                            ************************************************************

gi|299522993:1352-3402      GTGCTCTGTAAATGTTCCTTTCCTTTGTAGTCTCTGGCAAGATGCTTTAGGAAGATAAAA 1560
gi|299523000:1328-3264      GTGCTCTGTAAATGTTCCTTTCCTTTGTAGTCTCTGGCAAGATGCTTTAGGAAGATAAAA 1446
gi|299523007:1223-3155      GTGCTCTGTAAATGTTCCTTTCCTTTGTAGTCTCTGGCAAGATGCTTTAGGAAGATAAAA 1442
gi|299522998:1307-3357      GTGCTCTGTAAATGTTCCTTTCCTTTGTAGTCTCTGGCAAGATGCTTTAGGAAGATAAAA 1560
gi|299523001:1262-3312      GTGCTCTGTAAATGTTCCTTTCCTTTGTAGTCTCTGGCAAGATGCTTTAGGAAGATAAAA 1560
gi|299523003:1283-3219      GTGCTCTGTAAATGTTCCTTTCCTTTGTAGTCTCTGGCAAGATGCTTTAGGAAGATAAAA 1446
gi|299522996:1373-3309      GTGCTCTGTAAATGTTCCTTTCCTTTGTAGTCTCTGGCAAGATGCTTTAGGAAGATAAAA 1446
gi|299523006:1241-3177      GTGCTCTGTAAATGTTCCTTTCCTTTGTAGTCTCTGGCAAGATGCTTTAGGAAGATAAAA 1446
                            ************************************************************

gi|299522993:1352-3402      GTTTGAGGAGAACAAACAGGAATTCTGAATTAAGCACAGAGTTGAAGTTTATACCCGTTT 1620
gi|299523000:1328-3264      GTTTGAGGAGAACAAACAGGAATTCTGAATTAAGCACAGAGTTGAAGTTTATACCCGTTT 1506
gi|299523007:1223-3155      GTTTGAGGAGAACAAACAGGAATTCTGAATTAAGCACAGAGTTGAAGTTTATACCCGTTT 1502
gi|299522998:1307-3357      GTTTGAGGAGAACAAACAGGAATTCTGAATTAAGCACAGAGTTGAAGTTTATACCCGTTT 1620
gi|299523001:1262-3312      GTTTGAGGAGAACAAACAGGAATTCTGAATTAAGCACAGAGTTGAAGTTTATACCCGTTT 1620
gi|299523003:1283-3219      GTTTGAGGAGAACAAACAGGAATTCTGAATTAAGCACAGAGTTGAAGTTTATACCCGTTT 1506
gi|299522996:1373-3309      GTTTGAGGAGAACAAACAGGAATTCTGAATTAAGCACAGAGTTGAAGTTTATACCCGTTT 1506
gi|299523006:1241-3177      GTTTGAGGAGAACAAACAGGAATTCTGAATTAAGCACAGAGTTGAAGTTTATACCCGTTT 1506
                            ************************************************************
```

```
gi|299522993:1352-3402      CACATGCTTTTCAAGAATGTCGCAATTACTAAGAAGCAGATAATGGTGTTTTTTAGAAAC 1680
gi|299523000:1328-3264      CACATGCTTTTCAAGAATGTCGCAATTACTAAGAAGCAGATAATGGTGTTTTTTAGAAAC 1566
gi|299523007:1223-3155      CACATGCTTTTCAAGAATGTCGCAATTACTAAGAAGCAGATAATGGTGTTTTTTAGAAAC 1562
gi|299522998:1307-3357      CACATGCTTTTCAAGAATGTCGCAATTACTAAGAAGCAGATAATGGTGTTTTTTAGAAAC 1680
gi|299523001:1262-3312      CACATGCTTTTCAAGAATGTCGCAATTACTAAGAAGCAGATAATGGTGTTTTTTAGAAAC 1680
gi|299523003:1283-3219      CACATGCTTTTCAAGAATGTCGCAATTACTAAGAAGCAGATAATGGTGTTTTTTAGAAAC 1566
gi|299522996:1373-3309      CACATGCTTTTCAAGAATGTCGCAATTACTAAGAAGCAGATAATGGTGTTTTTTAGAAAC 1566
gi|299523006:1241-3177      CACATGCTTTTCAAGAATGTCGCAATTACTAAGAAGCAGATAATGGTGTTTTTTAGAAAC 1566
                            ************************************************************

                                                                    miR-374b seed region
gi|299522993:1352-3402      CTAATTGAAGTATATTCAACCAAATACTTTAATGTATAAAATAAATATTATACAATATAC 1740
gi|299523000:1328-3264      CTAATTGAAGTATATTCAACCAAATACTTTAATGTATAAAATAAATATTATACAATATAC 1626
gi|299523007:1223-3155      CTAATTGAAGTATATTCAACCAAATACTTTAATGTATAAAATAAATATTATACAATATAC 1622
gi|299522998:1307-3357      CTAATTGAAGTATATTCAACCAAATACTTTAATGTATAAAATAAATATTATACAATATAC 1740
gi|299523001:1262-3312      CTAATTGAAGTATATTCAACCAAATACTTTAATGTATAAAATAAATATTATACAATATAC 1740
gi|299523003:1283-3219      CTAATTGAAGTATATTCAACCAAATACTTTAATGTATAAAATAAATATTATACAATATAC 1626
gi|299522996:1373-3309      CTAATTGAAGTATATTCAACCAAATACTTTAATGTATAAAATAAATATTATACAATATAC 1626
gi|299523006:1241-3177      CTAATTGAAGTATATTCAACCAAATACTTTAATGTATAAAATAAATATTATACAATATAC 1626
                            ************************************************************

gi|299522993:1352-3402      TTGTATAGCAGTTTCTGCTTCACATTTGATTTTTTCAAATTTAATATTTATATTAGAGAT 1800
gi|299523000:1328-3264      TTGTATAGCAGTTTCTGCTTCACATTTGATTTTTTCAAATTTAATATTTATATTAGAGAT 1686
gi|299523007:1223-3155      TTGTATAGCAGTTTCTGCTTCACATTTGATTTTTTCAAATTTAATATTTATATTAGAGAT 1682
gi|299522998:1307-3357      TTGTATAGCAGTTTCTGCTTCACATTTGATTTTTTCAAATTTAATATTTATATTAGAGAT 1800
gi|299523001:1262-3312      TTGTATAGCAGTTTCTGCTTCACATTTGATTTTTTCAAATTTAATATTTATATTAGAGAT 1800
gi|299523003:1283-3219      TTGTATAGCAGTTTCTGCTTCACATTTGATTTTTTCAAATTTAATATTTATATTAGAGAT 1686
gi|299522996:1373-3309      TTGTATAGCAGTTTCTGCTTCACATTTGATTTTTTCAAATTTAATATTTATATTAGAGAT 1686
gi|299523006:1241-3177      TTGTATAGCAGTTTCTGCTTCACATTTGATTTTTTCAAATTTAATATTTATATTAGAGAT 1686
                            ************************************************************
```

```
gi|299522993:1352-3402      CTATATATGTATAAATATGTATTTTGTCAAATTTGTTACTTAAATATATAGAGACCAGTT 1860
gi|299523000:1328-3264      CTATATATGTATAAATATGTATTTTGTCAAATTTGTTACTTAAATATATAGAGACCAGTT 1746
gi|299523007:1223-3155      CTATATATGTATAAATATGTATTTTGTCAAATTTGTTACTTAAATATATAGAGACCAGTT 1742
gi|299522998:1307-3357      CTATATATGTATAAATATGTATTTTGTCAAATTTGTTACTTAAATATATAGAGACCAGTT 1860
gi|299523001:1262-3312      CTATATATGTATAAATATGTATTTTGTCAAATTTGTTACTTAAATATATAGAGACCAGTT 1860
gi|299523003:1283-3219      CTATATATGTATAAATATGTATTTTGTCAAATTTGTTACTTAAATATATAGAGACCAGTT 1746
gi|299522996:1373-3309      CTATATATGTATAAATATGTATTTTGTCAAATTTGTTACTTAAATATATAGAGACCAGTT 1746
gi|299523006:1241-3177      CTATATATGTATAAATATGTATTTTGTCAAATTTGTTACTTAAATATATAGAGACCAGTT 1746
                            ************************************************************

gi|299522993:1352-3402      TTCTCTGGAAGTTTGTTTAAATGACAGAAGCGTATATGAATTCAAGAAAATTTAAGCTGC 1920
gi|299523000:1328-3264      TTCTCTGGAAGTTTGTTTAAATGACAGAAGCGTATATGAATTCAAGAAAATTTAAGCTGC 1806
gi|299523007:1223-3155      TTCTCTGGAAGTTTGTTTAAATGACAGAAGCGTATATGAATTCAAGAAAATTTAAGCTGC 1802
gi|299522998:1307-3357      TTCTCTGGAAGTTTGTTTAAATGACAGAAGCGTATATGAATTCAAGAAAATTTAAGCTGC 1920
gi|299523001:1262-3312      TTCTCTGGAAGTTTGTTTAAATGACAGAAGCGTATATGAATTCAAGAAAATTTAAGCTGC 1920
gi|299523003:1283-3219      TTCTCTGGAAGTTTGTTTAAATGACAGAAGCGTATATGAATTCAAGAAAATTTAAGCTGC 1806
gi|299522996:1373-3309      TTCTCTGGAAGTTTGTTTAAATGACAGAAGCGTATATGAATTCAAGAAAATTTAAGCTGC 1806
gi|299523006:1241-3177      TTCTCTGGAAGTTTGTTTAAATGACAGAAGCGTATATGAATTCAAGAAAATTTAAGCTGC 1806
                            ************************************************************

gi|299522993:1352-3402      AAAAATGTATTTGCTATAAAATGAGAAGTCTCACTGATAGAGGTTCTTTATTGCTCATTT 1980
gi|299523000:1328-3264      AAAAATGTATTTGCTATAAAATGAGAAGTCTCACTGATAGAGGTTCTTTATTGCTCATTT 1866
gi|299523007:1223-3155      AAAAATGTATTTGCTATAAAATGAGAAGTCTCACTGATAGAGGTTCTTTATTGCTCATTT 1862
gi|299522998:1307-3357      AAAAATGTATTTGCTATAAAATGAGAAGTCTCACTGATAGAGGTTCTTTATTGCTCATTT 1980
gi|299523001:1262-3312      AAAAATGTATTTGCTATAAAATGAGAAGTCTCACTGATAGAGGTTCTTTATTGCTCATTT 1980
gi|299523003:1283-3219      AAAAATGTATTTGCTATAAAATGAGAAGTCTCACTGATAGAGGTTCTTTATTGCTCATTT 1866
gi|299522996:1373-3309      AAAAATGTATTTGCTATAAAATGAGAAGTCTCACTGATAGAGGTTCTTTATTGCTCATTT 1866
gi|299523006:1241-3177      AAAAATGTATTTGCTATAAAATGAGAAGTCTCACTGATAGAGGTTCTTTATTGCTCATTT 1866
                            ************************************************************
```

```
gi|299522993:1352-3402      TTTAAAAAATGGACTCTTGAAATCTGTTAAAATAAAATTGTACATTTGGAGATGTTTCAT 2040
gi|299523000:1328-3264      TTTAAAAAATGGACTCTTGAAATCTGTTAAAATAAAATTGTACATTTGGAGATGTTTCAT 1926
gi|299523007:1223-3155      TTTAAAAAATGGACTCTTGAAATCTGTTAAAATAAAATTGTACATTTGGAGATGTTTCAT 1922
gi|299522998:1307-3357      TTTAAAAAATGGACTCTTGAAATCTGTTAAAATAAAATTGTACATTTGGAGATGTTTCAT 2040
gi|299523001:1262-3312      TTTAAAAAATGGACTCTTGAAATCTGTTAAAATAAAATTGTACATTTGGAGATGTTTCAT 2040
gi|299523003:1283-3219      TTTAAAAAATGGACTCTTGAAATCTGTTAAAATAAAATTGTACATTTGGAGATGTTTCAT 1926
gi|299522996:1373-3309      TTTAAAAAATGGACTCTTGAAATCTGTTAAAATAAAATTGTACATTTGGAGATGTTTCAT 1926
gi|299523006:1241-3177      TTTAAAAAATGGACTCTTGAAATCTGTTAAAATAAAATTGTACATTTGGAGATGTTTCAT 1926
                            ************************************************************

gi|299522993:1352-3402      GAAAAAAAAAA 2051
gi|299523000:1328-3264      GAAAAAAAAAA 1937
gi|299523007:1223-3155      GAAAAAAAAAA 1933
gi|299522998:1307-3357      GAAAAAAAAAA 2051
gi|299523001:1262-3312      GAAAAAAAAAA 2051
gi|299523003:1283-3219      GAAAAAAAAAA 1937
gi|299522996:1373-3309      GAAAAAAAAAA 1937
gi|299523006:1241-3177      GAAAAAAAAAA 1937
                            ***********
```

**Supplementary Figure 1:** 3'UTR alignment of *CD46* mRNA variants. Region bound by forward primer is highlighted in green while region bound by reverse primer is highlighted in blue. Seed regions of respective miRNAs are highlighted in yellow. gi|299522993: transcript variant a. gi|299523000: transcript variant d. gi|299523007: transcript variant n. gi|299522998: transcript variant c. gi|299523001: transcript variant e. gi|299523003: transcript variant f. gi|299522996: transcript variant b. gi|299523006: transcript variant l.